

Sheffield Hallam University

Electrochemical Biosensor Arrays Utilising Bacteria and Aptamer Nano-bioreceptors for Toxic Chemicals Detection

ABU-ALI, Hisham Faiadh Mohammad

Available from the Sheffield Hallam University Research Archive (SHURA) at:

<http://shura.shu.ac.uk/25595/>

A Sheffield Hallam University thesis

This thesis is protected by copyright which belongs to the author.

The content must not be changed in any way or sold commercially in any format or medium without the formal permission of the author.

When referring to this work, full bibliographic details including the author, title, awarding institution and date of the thesis must be given.

Please visit <http://shura.shu.ac.uk/25595/> and <http://shura.shu.ac.uk/information.html> for further details about copyright and re-use permissions.



**Electrochemical Biosensor Arrays Utilising
Bacteria and Aptamer Nano-bioreceptors for
Toxic Chemicals Detection**

By

Hisham Faiadh Mohammad Abu-Ali

**Thesis submitted in partial fulfillment of the
requirements of Sheffield Hallam University for the degree of
Doctor of Philosophy**

Supervision Team: Prof. Alexei Nabok¹ & Prof. Thomas Smith²

¹ Materials and Engineering Research Institute, Sheffield Hallam University, UK

² Biomolecular Research Centre, Sheffield Hallam University, UK

2019

DECLARATION

I hereby declare that this thesis submitted for the degree of PhD is the result of my own research and that this thesis has not been submitted for a higher degree to any other university or institution

Signed

DEDICATION

*To my parents, specially my dearest father
To my mother soul your sacrifices shan 't be forgotten
To my beloved and soulmate wife (Hala), and my angels
(Um Al-Baneen and Mohammad)
Without your support and patience throughout my study,
This work would never has seen light*

Hisham

ABSTRACT

This work was dedicated to development of novel biosensing technologies for detection of toxic chemicals, such as heavy metals, pesticides and petrochemicals, which possess a serious threat to humans and all living organisms in our planet nowadays. This was the main motivation for research in such important field. In the present work a novel approach in detection of heavy metal salts (HgCl_2 , PbCl_2 , ZnCl_2 and CdCl_2), pesticides (atrazine, simazine, DDVP), and petro-chemicals (hexane, octane, pentane, toluene, pyrene and ethanol) dissolved in water was proposed. It is based on a concept of inhibition sensor array utilising different whole bacteria cells. The main aim of this project is to develop novel, simple and cost-effective biosensing technologies for in-field detection of the above pollutants in water which effectively reduce the time and cost of analysis. Electrochemical detection appeared to be the most suitable for such task.

In this project, three types of bacteria, e.g. *Escherichia coli*, *Methylococcus capsulatus* (Bath) or *Methylosinus trichosporium* (OB3b) and *Shewanella oneidensis*, were selected because of their different inhibition patterns. The concentration of live bacteria (which is an indicator of the presence of pollutants) was first characterised by the optical analytical methods of optical density OD_{600} , fluorescence microscopy and flow cytometry. The main findings of this study were the facts that *E. coli* (K12 strain, gram-negative bacteria) are very sensitive to all above mentioned pollutants; methanotrophic bacteria (*Mc. capsulatus* Bath & *Ms. trichosporium* OB3b) appeared to be more resistant to petrochemicals; while *S. oneidensis* (MR-1 strain, gram negative bacteria) are more tolerant to heavy metals. A series of AC and DC electrochemical measurements were carried out on the same bacteria samples. As a first step, a correlation between optical and electrochemical characteristics of bacteria concentration in solution was established. The study of the effect of heavy metals, pesticides and petrochemicals on DC and electrical characteristics of bacteria in suspension revealed a similar inhibition pattern as was found in optical study. Then a similar study was carried out on samples of bacteria immobilized on the surface of screen-printed electrodes, which is more suitable for sensing applications. The results of DC (cyclic voltammograms) and AC (impedance spectroscopy) measurements were consistent with previous studies. A possibility of pattern recognition of pollutants by their inhibition effects on the selected bacteria was found. The classes of pollutants, e.g. heavy metals, pesticides, and petrochemicals, can be identified from pseudo-3D graphs of responses of the three sensing channels, e.g. electrodes with different immobilized bacteria. Much more accurate assessment of pollutants was achieved with Artificial Neural Network (ANN) software which was developed using MatLab. ANN programme was capable of both the identification of pollutants with 91% accuracy and rough estimation of their concentrations in five bands from 0.01 ng/ml to 1000 ng/ml (ppb). The developed bacteria sensor array could be suitable for simple, inexpensive, and quick preliminary in-field detection (screening) of water samples. The suspected highly contaminated samples could be easily identified and passed to specialized laboratories for further more detailed testing. In such way, the time and cost of analysis could be substantially reduced.

In addition to the inhibition sensor array utilising non-specific bio-receptors such as bacteria, the electrochemical detection of heavy metal ions (Hg^{2+} and Pb^{2+}) was attempted using novel highly specific aptamer bio-receptors labelled with redox groups. Such experiments were successful; the above metal ions in very low concentrations down to 1 pg/ml (or 1 ppt) were detected using both cyclic voltammograms and impedance spectroscopy. The affinity of the aptamers used was found to be very high and similar to that of antibodies. Additional advantages of aptamers were their high stability and simple recovery by thermo-cycling. Considering fast evolvement of aptamer research, their advantages and low cost, the development of aptasensor arrays for accurate detection of large number of pollutants is possible in near future.

ACKNOWLEDGEMENTS

It is a difficult task to thank all the people who made this PhD thesis possible with so few words. However, I will try to do my best to extend my great appreciation to everyone who helped me scientifically and emotionally throughout this study. First of all, I would like to thank my god (Allah) for giving me the patience and stamina to overcome the difficulties that faced me during my PhD study. Secondly, I would like to acknowledge my country (Iraq) and the financial sponsor, Ministry of Higher Education and Scientific Research in Iraq and University of Basrah, Faculty of Science, Biology Department. Also I gratefully acknowledge the Iraqi Cultural Attaché in London for their support during my PhD research. I would like to express my sincere gratitude and thanks to my director of studies in Materials Engineering Research Institute (MERI), Professor Alexei V. Nabok for his excellent supervision, guidance and support during the study period, and for his discussion and interpretation of various aspects of science, experimental procedures and the results analysis. Without his support and encouragement, this work would not have been possible. My deepest appreciations and huge thanks go to my gorgeous supervisor, Professor Thomas J. Smith the head of research group of Molecular Microbiology in BioMolecular Research Centre (BMRC), for his advice, help, discussion and suggestion. My special thanks and love go to lovely wife and my children. My sincere thanks must go to Dr. Jim Yong (BMRC), for his help with fluorescence microscope measurements. Many thanks are also due to Dr. Sarah Small (BMRC) for her essential help and discussion about flow cytometer measurements. In addition, I would like to thank Dr. Tim Nichol (BMRC), for his help and advice with molecular microbiology laboratory and bacteria samples preparation. Also big thanks go to Dr. Mohammad Akram Khan, for his essential help about the chemicals preparation. Many thanks must go to MERI reception staff for the help and assistance especially Corrie Houton, Amy McNally, Gail Hallewell and Rachael Toogood. I would also like to thank all technical staff of Sheffield Hallam University (MERI) and (BMRC) training team and workshop, especially Mr. Paul Allender for training and preparing the SEM and AFM imaging process measurements and Mr. Michael Cox for ICP-MS training and measurements. Finally I would like to thank all my brilliant Iraqi and English friends, PhD students at MERI and BMRC also my colleagues from University of Sheffield.

LIST of ABBREVIATIONS

<i>E. coli</i>	<i>Escherichia coli</i> bacteria
<i>S. oneidensis</i>	<i>Shewanella oneidensis</i> bacteria
<i>Mc. Capsulatus</i>	<i>Methylococcus capsulatus</i> bacteria
<i>Ms. trichosporium</i>	<i>Methylosinus trichosporium</i> bacteria
OD600	Optical Density at 600nm wavelength of light
UV/Vis	UltraViolet /Visible (spectroscopy)
MTB	Methanotrophic bacteria
K12	Strain of <i>E. coli</i> bacteria
MR-1	Strain of <i>S. oneidensis</i> bacteria
Bath	Strain of methanotrophic bacteria
OB3b	Strain of methanotrophic bacteria
DC	Direct Current
AC	Alternative Current
DNA	Deoxyribonucleic Acid
BTEX	Benzene, Toluene, Ethylbenzene and Xylene
PAHs	Polycyclic Aromatic Hydrocarbons
PAH	Poly Allyamine Hydrochloride
pH	Measure of the acidity of an aqueous solution
DDVP	Dichlorvos (commercial pesticide)
ANN	Artificial Neural Network
PCA	Principal Component Analysis
LbL	layer-by-layer (deposition)
CV	Cyclic Voltammogram
EIS	Electrochemical Impedance Spectroscopy
GLC	Gas Liquid Chromatography

IDAM	Interdigitated Array Microelectrodes
NMS	Nitrate Mineral Salts
PEM	Poly Electrolyte Multilayers
ROS	Reactive Oxygen Species
LPO	Lipid Per Oxidation
H ₂ O ₂	Hydrogen Peroxide
dsDNA	double strand DNA
ssDNA	single strand DNA
SPGEs	Screen printed gold electrodes
BESs	Bio-electrochemical systems
AAS	Atomic Absorption Spectroscopy
AES	Atomic Emission Spectroscopy
ICP-MS	Inductively Coupled Plasma Mass Spectroscopy
CVAFS	Cold Vapours Atomic Fluorescence Spectroscopy
HPLC	High-Performance Liquid Chromatography
GC-MS	Gas Chromatography–Mass Spectrometry
LC-MS	Liquid Chromatography–Mass Spectrometry
IFM	Infinite Focus Microscopy
AFM	Atomic Force Microscopy
SEM	Scanning Electron Microscopy
TEM	Transmission Electron Microscopy
US EPA	U.S. Environmental Protection Agency
IARC	International Agency for Research on Cancer
SELEX	Systematic Evolution of Ligands by Exponential Enrichment
QCM	Quartz Crystal Microbalance and
SAW	Surface Acoustic Wave

LIST of PUBLICATIONS

Journals Publication

- ❖ **Abu-Ali, H., Nabok, A., & Smith, T. J. (2019). Electrochemical inhibition bacterial sensor array for detection of water pollutants: artificial neural network (ANN) approach. *Analytical and bioanalytical chemistry*, 1-10.**
- ❖ **Abu-Ali, H., Nabok, A., Smith, T. J., & Al-Shanawa, M. (2019). Development of a novel electrochemical inhibition sensor array based on bacteria immobilized on modified screen-printed gold electrodes for water pollution detection. *BioNanoScience*, 9(2), 345-355.**
- ❖ **Abu-Ali, H., Nabok, A., & Smith, T. J. (2019). Development of novel and highly specific ssDNA-Aptamer-based electrochemical biosensor for rapid detection of Mercury (II) and Lead (II) ions in water. *Chemosensors*, 7(2), 27.**
- ❖ **Al-Jawdah, A., Nabok, A., Abu-Ali, H., Catanante, G., Marty, J. L., & Szekacs, A. (2019). Highly sensitive label-free in vitro detection of aflatoxin B1 in an aptamer assay using optical planar waveguide operating as a polarization interferometer. *Analytical and Bioanalytical Chemistry*, 1-8.**
- ❖ **Abu-Ali, H. F., Nabok, A., Smith, T., & Al-Shanawa, M. A. (2018). Electrochemical inhibition biosensor array for rapid detection of water pollutions based on bacteria immobilized on screen-printed gold electrodes. *European Chemical Bulletin*, 7(10), 307-314.**
- ❖ **Abu-Ali, H., Nabok, A., Smith, T., & Al-Shanawa, M. (2017). Inhibition biosensor based on DC and AC electrical measurements of bacteria samples. *Procedia technology*, 27, 129-130.**
- ❖ **Abu-Ali, H., Nabok, A., Smith, T., & Al-Shanawa, M. (2017). Development of electrochemical inhibition biosensor based on bacteria for detection of environmental pollutants. *Sensing and Bio-Sensing Research*, 13, 109-114.**
- ❖ **Al-Rubaye, A., Nabok, A., Abu-Ali, H., Szekacs, A., & Takacs, E. (2017). LSPR/TIRE bio-sensing platform for detection of low molecular weight toxins. *IEEE SENSORS* (pp. 1-3). IEEE.**
- ❖ **Hisham Abu-Ali, A. Nabok, T. Smith Novel inhibition electrochemical biosensor array based on bacteria for toxic chemicals detection: Review and recent achievements, *Biosensors*. (in submission process).**
- ❖ **Alexei Nabok, Cansu Ozkaya, Hisham Abu-Ali, Frank Davis, Nik Walch, Deborah Hammond, Seamus P.J. Higson, Rifat Capan, Metal sulphide sub-nanometre clusters formed within calix[8]arene LB films, *Langmuir Journal*. (in submission process)**

- ❖ Alexei Nabok, **Hisham Abu-Ali**, Cansu Ozkaya, Frank Davis, Nik Walch, Seamus P.J. Higson. **Electrochemical Aptasensor for Detection of Dopamine**, *Sensors and Actuators: B Chemical Journal*. (in submission process).

Conference Publications

- ❖ **Hisham Abu-Ali**, A. Nabok, T. Smith and M. Al-Shanawa, Inhibition Biosensor Based on Bacteria for Environmental Pollution Detection Using Optical and Electrochemical Measurements (Poster), 18-20 May 2016, **MERI Student Symposium**, Sheffield Hallam University, Sheffield, **UK**.
- ❖ **Hisham Abu-Ali**, A. Nabok, T. Smith and M. Al-Shanawa Inhibition Biosensor Based on DC and AC Electrical Measurements of Bacteria Samples, **Biosensor 2016 Congress** (Poster), 25-27 May 2016, Gothenburg - **Sweden**.
- ❖ **Hisham Abu-Ali**, A. Nabok, T. Smith and M. Al-Shanawa, Using Optical and Electrochemical Measurements for Development Inhibition Biosensor Based on Bacteria for Environmental Pollution Detection (Poster), 16 December 2016, **MERI and BMRC Student Symposium**, Sheffield Hallam University, Sheffield, **UK**.
- ❖ **Hisham Abu-Ali**, A. Nabok, T. Smith and M. Al-Shanawa,(2017) Development of Novel Inhibition Biosensor Based on Bacteria for Environmental Pollutants Detection , **MERI Proceeding** , 16th -17th May (1), 6-8. Sheffield Hallam University, Sheffield, **UK**.
- ❖ **Hisham Abu-Ali**, A. Nabok, T. Smith Development of Novel Inhibition Biosensor Based on Bacteria for Environmental Pollution Detection (Oral), 23-24 May 2017, **MERI Student Symposium**, Sheffield Hallam University, Sheffield, **UK**.
- ❖ **Hisham Abu-Ali**, A. Nabok, T. Smith and M. Al-Shanawa, Development of a Novel Inhibition Biosensor Based on Immobilized Bacteria for Environmental Pollution Detection Using Optical and Electrochemical Measurements (Poster), **Biosensing Technology Congress**, 05-11 May 2017, Riva Del Garda - **Italy**.
- ❖ **Hisham Abu-Ali**, A. Nabok, T. Smith Nano-Bioreceptors DNA-Aptamer-Based Electrochemical Biosensor for Heavy Metal ions Detection in Water Samples (Oral), **Aptamer in Bordeaux Conference**, 21-23 September 2017, Bordeaux- **France**.
- ❖ **Hisham Abu-Ali**, A. Nabok, T. Smith, The First Iraqi Student Conference in UK, Sheffield, University of Sheffield, 29 September 2017, Sheffield - **UK**.

- ❖ **Hisham Abu-Ali**, A. Nabok, T. Smith Novel ssDNA-Aptamer-Based Electrochemical Nanobiosensor for Rapid Detection of Heavy metal Ions in Water (Poster), **NanoToday Conference**, 6-10 December 2017, Hawaii - **USA**.
- ❖ **Hisham Abu-Ali**, A. Nabok, T. Smith and M. Al-Shanawa Using Immobilized Bacteria as a Novel Inhibition Biosensor for Environmental Pollutants Detection (Oral), **Applied Molecular Microbiology Techniques Conference**, 15-16 January 2018, Zurich - **Switzerland**.
- ❖ **Hisham Abu-Ali**, A. Nabok, T. Smith Using double strand DNA Based Electrochemical Biosensor for Hg^{2+} and Pb^{2+} Detection in Water (Oral), **Applied Molecular Bionanotechnology Conference**, 23-24 January 2018, Amsterdam - **Netherlands**.
- ❖ **Hisham Abu-Ali**, A. Nabok, T. Smith Using novel ssDNA-Aptamer-Based Electrochemical Biosensor for Rapid Detection of Heavy metal Ions in Real Water Samples (Oral), **Biosensor 2018 Congress**, 23-25 Jun 2018. Miami - **USA**.
- ❖ **Hisham Abu-Ali**, A. Nabok, T. Smith Application of artificial neural network for preliminary detection of water pollution using inhibition electrochemical sensor array based on immobilized bacteria and modified screen-printed gold electrodes (Poster), 14 December 2018, **MERI and BMRC Student Symposium**, Sheffield Hallam University, Sheffield, **UK**.
- ❖ **Hisham Abu-Ali**, A. Nabok, T. Smith ssDNA-Aptamer-Based Biosensor for Rapid Detection of Heavy metal Ions in Real Water Samples (Oral). **The 21st International Conference of Lab on a chip device, system and technology**, 23-24 May 2019, Barcelona - **Spain**.
- ❖ A. Nabok, **H. Abu-Ali**, A. Al-Rubaye, A. Al-Jawdah, C. Ozkaya, G. Catanante, F. Davis, **The use of aptamers immobilized on the surface of transducers for detection of low molecular weight analytes** (Oral) **16th European Conference on Organized Films, ECOF 16**, 8-12 July 2019, Paris - **France**.
- ❖ Cansu Ozkaya, Alexei Nabok, **Hisham Abu-Ali**, Frank Davis, Nik Walch, Deborah Hammond, Seamus P.J. Higson, Rifat Capan, **Metal sulphide sub-nanometre clusters formed within calix[8]arene LB films** (Oral) **16th European Conference on Organized Films, ECOF 16**, 8-12 July 2019, Paris - **France**.

PRIZES and AWARDS

1. The best presentation and paper placing in The 20th International Conference of Environmental Microbiology, (Zurich, 15th-16th January 2018, Switzerland).
2. The best poster and paper placing in The 21st International Conference of Lab on a chip device, system and technology (Barcelona, 23th-24th May 2019, Spain).
3. Award from the Iraqi Cultural Attaché as one of excellence organizers in the First Iraqi Student Conference in UK, Sheffield, University of Sheffield (Sheffield, 29th September 2017, UK).
4. Award from the Iraqi Minister of Higher Education and Scientific Research as one of the best 20 student in the UK during the PhD study period. (London, 18th January 2018, UK).

LIST of FIGURES

Figure 1-1. The schematic diagram of biosensor application areas.....	3
Figure 1-2. Scheme of electrochemical biosensor.....	6
Figure 2-1. The sources and products containing heavy metals.....	23
Figure 2-2. Common commercial petrochemicals.....	25
Figure 2-3. Types of pesticides and herbicides used.....	27
Figure 2-4. Schematic diagram of Atomic absorption spectroscopy	35
Figure 2-5. Schematic diagram of inductively coupled plasma mass spectrometry.....	37
Figure 2-6. Schematic diagram of Chromatography Measuring process.....	38
Figure 2-7. Typical biosensor elements.....	40
Figure 2-8. Schematic of whole-cell-based biosensors.....	44
Figure 2-9. Schematic of electrochemical DNA biosensor.....	45
Figure 2-10. Schematic of aptamer-based biosensors.....	46
Figure 2-11. SELEX process.....	47
Figure 2-12. Aptamer secondary structures.....	48
Figure 2-13. The schematic structural image of a typical Gram-positive and Gram-negative bacteria cell.....	61
Figure 2-14. <i>E. coli</i> bacteria cells (Gram-Negative) and their colonies.....	63
Figure 2-15. <i>S.oneidensis</i> bacteria cells (Gram-Negative) and their colonies.....	64
Figure 2-16. <i>Mc. Capsulatus</i> bacteria cells (Gram-Negative) and their colonies....	65
Figure 3-1. Fluorescence microscope Olympus-BX60 (A), and its schematic diagra.	85
Figure 3-2. (A) 6715 UV/Vis spectrophotometer; (B) Schematic of optical process...	85
Figure 3-3. (A) Flow cytometry instrument (B);Schematic diagram of measurements	88
Figure 3-4. (A) Scanning Electron Microscope FEI-Nova (B) Schematic diagram.....	89

Figure 3-5. (A) Atomic force microscope (B) Schematic diagram.....	91
Figure 3-6. Charges exchanges on metal electrodes in contact with electrolyte.....	93
Figure 3-7. Electrical double layer (EDL) at metal-electrolyte interface and the resulted distribution of surface potential in EDL.....	94
Figure 3-8. Two-electrode system (a) and potential distribution in it (b); three-electrode (c) and four-electrode systems (d).....	95
Figure 3-9. Circuit for voltammetry in three-electrode cell (a), the same circuit with potentiostat (b).....	96
Figure 3-10. Typical cyclic voltammogram of redox reaction.....	98
Figure 3-11. Clark oxygen electrode (a), Glucose sensor (b).....	99
Figure 3-12. The scheme of mediated enzyme reaction.....	100
Figure 3-13. (A) Four-channel C.V experimental set-up; (B) Typical voltammogram and screen-printed three electrode assemblies	103
Figure 3-14. (A) Typical plot of C.V; and (B) Dependence of scan rate (a) and rate constant of electron-transfer process in the cyclic voltammogram (b).....	105
Figure 3-15. (A) PARSTAT 4000A impedance analyzer instrument; (B) Schematic diagram of impedance measurements, and DropSens interdigitated electrode used....	108
Figure 3-16. Design of interdigitated electrodes and AC measurements	109
Figure 3-17. Equivalent circuit for impedance measurement in electrolyte-metal system (a) simplified equivalent circuit (b).....	110
Figure 3-18. Nyquist plot Z'' vs Z' ; Dotted line indicate the outcome of binding an analyte to receptor (a) schematic graph of the affinity (b).....	111
Figure 4-1. Fluorescence microscopy images of <i>E. coli</i> before (A) and after (B) treatment with $HgCl_2$ salt (1M).....	117
Figure 4-2. Fluorescence microscopy images of <i>Ms. trichosporium</i> (OB3b) before (A) and after (B) treatment with $HgCl_2$ salt (1M).....	117
Figure 4-3. Fluorescence microscopy images of <i>S. oneidensis</i> before (A) and after (B) treatment with $HgCl_2$ salt (1M).....	118
Figure 4-4. Flow cytometry results for <i>E. coli</i> (A) , <i>S. oneidensis</i> (B) and <i>Ms. trichosporium</i> (OB3b) (C) ; (a) and (b) were obtained, respectively, before and after treatment with $HgCl_2$ (1M).....	119

Figure 4-5. CV recorded on <i>S. oneidensis</i> (A), <i>E. coli</i> (B) of different dilutions (1:10, 1:5, 1:2, 1:1, and stock solutions) and <i>M. capsulatus</i> (C) treated with different of HgCl_2 ; CV curves for clear LB broth are shown on all graphs.....	122
Figure 4-6. CV of <i>E.coli</i> (A) <i>S. oneidensis</i> (B) and <i>Ms. trichosporium</i> (OB3b) (C) treated with of HgCl_2	124
Figure 4-7. The dependence of relative changes in cathode current at -0.5V for <i>S. oneidensis</i> , <i>Ms. trichosporium</i> (OB3b) and <i>E. coli</i> treated with HgCl_2	125
Figure 4-8. The Nyquist plots ($-Z_{im}$ vs Z_{re}) for interdigitated electrodes with bacteria suspension treated with Hg^{2+} ions (A); equivalent circuit (B).....	126
Figure 5-1. DropSens three-electrode assembly (a), DropSens interdigitated electrodes (b), Schematic diagram of bacteria immobilization procedure (c).....	129
Figure 5-2. Fluorescence microscopy images of immobilized <i>Shewanella oneidensis</i> bacteria before (A) and after (B) treatment with PbCl_2 salt (1 M) for 2 hr.....	132
Figure 5-3. Fluorescence microscopy images of immobilized <i>Shewanella oneidensis</i> before (A) and after (B) treatment with ZnCl_2 salt (1M) for 2 hr	132
Figure 5-4. SEM images of <i>E. coli</i> after treatment with pentane (1M) (A), <i>S. oneidensis</i> after treatment with ZnCl_2 (1M) (B) and <i>Mc. capsulatus</i> Bath after treatment with ZnCl_2 salt (1M) (C) for 2 hr	134
Figure 5-5. AFM images of modified SPGE with immobilized bacteria before (A) and after (B) treated bacteria with poly -L-lysine.....	135
Figure 5-6. Cyclic voltammograms in the selected voltage range from (-0.5 V to $+0.5\text{ V}$) for: <i>E.coli</i> in solution (A) and immobilized <i>E.coli</i> (B) treated with hexane; <i>M. capsulatus</i> in solution (C) and immobilized <i>M. capsulatus</i> (D) treated with atrazine; and <i>Shewanella oneidensis</i> in solution (E) and immobilized <i>Shewanella oneidensis</i> (F) treated with PbCl_2	137
Figure 5-7. Comparison of relative changes of anodic current (I_A) at $+0.5\text{V}$ of all three types immobilized bacteria samples on modified electrodes exposure to PbCl_2 (A), Atrazine (B), and Hexane (C).....	140
Figure 5-8. 3D plot of relative changes in anodic current for <i>E.coli</i> , <i>M. capsulatus</i> , and <i>S. oneidensis</i> caused by different pollutants. Arrows show the direction of the pollutants' concentration increase from 0.1-100mM	143

Figure 5-9. The Nyquist plots (-Z _{im} vs Z _{re}) for interdigitated electrodes modified with immobilized bacteria treated with Hg ²⁺ ions of different concentrations (A); equivalent circuit (B).....	144
Figure 6-1. Schematic diagram of ANN.....	149
Figure 6-2. The strategy of ANN development for water pollutants identification.....	151
Figure 6-3. The ANN design used in the work for data analysis of bacteria sensor array.....	153
Figure 6-4. ANN training: Reduction of MSE during the 250,000 epochs of data feeding.....	156
Figure 7-1. PCR activation process; (A) SPGEs functionalized with Hg ²⁺ and Pb ²⁺ -specific aptamers; (B) heating up to 95 °C and (C) cooling aptamers at (4 °C).....	166
Figure 7-2. Schematic diagram of electrochemical detection of heavy metal ions Hg ²⁺ (A) and Pb ²⁺ (B) using redox-labelled aptamers.....	167
Figure 7-3. Cyclic voltammograms of screen-printed electrodes with immobilized anti Hg ²⁺ (A) and anti-Pb ²⁺ (B) aptamers in HBB solutions with different concentrations of HgCl ₂ and PbCl ₂ salts. The reference curves were recorded in pure HBB without heavy metal salts added.....	169
Figure 7-4. Cyclic voltammograms of screen-printed electrodes without immobilized aptamers in HBB solutions with different concentrations of HgCl ₂ and PbCl ₂ salts. ..	170
Figure 7-5. The concentration dependences of changes in anodic current at 0.2V upon binding of Hg ²⁺ (A) and Pb ²⁺ (B) ions to respective aptamers. Insets show the zoomed-in calibration curves with the data of five real samples of water (marked as star points).....	171
Figure 7-6. The cross-sensitivity tests: responses of anti-Hg ²⁺ aptamer (blue) and anti-Pb ²⁺ aptamer (red) to Zn ²⁺ , Cu ²⁺ , Cd ²⁺ , Hg ²⁺ , and Pb ²⁺ ions in 100 ng/ml concentrations.....	172
Figure 7-7. The Nyquist plots (-Z _{im} vs Z _{re}) for interdigitated electrodes with immobilized anti-Hg ²⁺ aptamers binding Hg ²⁺ ions of different concentrations (A); the	

Nyquist plot for bare interdigitated electrodes in solutions with different concentrations of HgCl₂ (B).....175

Figure 7-8. Typical kinetics for anti-Hg²⁺ aptamers binding Hg²⁺ ions of different concentrations. Inset shows the dependence of 1/ τ against the concentration of Hg²⁺ ions.....177

LIST of TABLES

Table 1-1. Historical overview of biosensors development.....	7
Table 2-1. Bacterial biosensors for different pollutants detection.....	53
Table 4-1. The results of OD ₆₀₀ after exposure to HgCl ₂ for 2 hr.....	120
Table 4-2. Values for the EIS parameters obtained from fitting the Nyquist plots shown in Figure 4-9 to the equivalent circuit model.....	127
Table 5-1. The numbers of live and dead bacteria immobilized on microscopic images of modified screen printed gold electrodes for all three bacteria before and after treatment with 1M solutions of the three pollutants for 2 hr.....	133
Table 5-2. Values for the EIS parameters obtained from fitting the Nyquist plots shown in Figure 5-9 to the Randles' circuit.....	145
Table 6-1. Data set of the neural network training	154
Table 6-2. The results of ANN identification of pollutants and estimation their concentration.....	156
Table 7-1. ICP-MS testing results of real samples.....	173
Table 7-2. Values for the EIS parameters obtained from fitting the Nyquist plots shown in Figure 7-6A to the equivalent circuit model.....	176

TABLE of CONTENTS

DECLARATION	I
DEDICATION	II
ABSTRACT.....	III
ACKNOWLEDGEMENTS	IV
LIST OF ABBREVIATION	V
LIST OF PUBLICATIONS	VII
PRIZES AND AWARDS	X
LIST OF FIGURES	XI
LIST OF TABLES	XVI
TABLE of CONTENTS.....	XII
CHAPTER 1 INTRODUCTION	1
1.1 The need of biosensors	1
1.2 Sensing and biosensing system	2
1.3 Biosensors and sensor arrays.....	4
1.4 The history of electrochemical biosensors	5
1.5 Bio-electrochemical systems (BESs)	8
1.6 Inhibition electrochemical biosensor principles	9
1.7 Aims and objectives	10
References	12

CHAPTER 2 LITERATURE REVIEW	18
2.1 Toxic chemicals and environmental pollution	18
2.2 Detection of toxic chemical pollutants	19
2.3 Classification of toxic chemical pollutants.....	22
2.3.1 Heavy metals.....	22
2.3.2 Petrochemicals and BTEX compounds.....	24
2.3.3 Pesticide and herbicides	26
2.4 Effects of toxic chemical pollutants on living organisms	29
2.5 Detection and remediation of toxic pollutants	33
2.5.1 Atomic absorption spectroscopy (AAS)	34
2.5.2 Inductively coupled plasma mass spectrometry (ICP-MS).....	36
2.5.3 Chromatography.....	37
2.6 Biosensors and sensor array.....	38
2.6.1 Classification of Biosensors	41
2.6.2 Whole-cell bacterial Sensor array	43
2.6.3 DNA Biosensors and Microarrays	44
2.6.4 Apta-sensors.....	45
2.6.4.1 Aptamer selection process (SELEX).....	46
2.6.4.2 Structure and types of aptamers.....	47
2.6.5 Immobilization strategy of bioreceptors	48

2.6.6	Methods of immobilization	49
2.6.7	Inhibition bacterial sensor array.....	52
2.6.8	Electrochemical sensor based on immobilized bacteria cells	54
2.7	Bacteria as sensing elements and pollutants remediators.....	56
2.7.1	General description of bacteria	57
2.7.2	Bacterial cell wall structure.....	59
2.7.3	Growth of bacteria.....	62
2.8	Types of bacteria used as sensing elements in this work	63
2.8.1	<i>Escherichia coli</i> (K-12 strain).....	63
2.8.2	<i>Shewanella oneidensis</i> (MR-1 strain)	64
2.8.3	Methanotrophic bacteria <i>Mc. capsulatus</i> (Bath)& <i>Ms. Trichosporium</i> (OB3b)..	65
References		66
 CHAPTER 3 EXPERIMENTAL METHODOLOGY		83
3.1	Experimental equipment used in this work.....	83
3.1.1	Optical methods	83
3.1.1.1	Olympus-BX60 Fluorescence microscopy.....	84
3.1.1.2	UV/Vis spectra measurements using 6715spectrophotometer	85
3.1.1.3	Flow cytometry using Becton-Dickinson FACSCalibur	86
3.1.1.4	Scanning Electron Microscopy using FEI- Nova SEM.....	88
3.1.1.5	Atomic Force Microscopy (AFM) using Nanoscope AFM.....	90

3.2	Electrochemical DC and AC methods for biosensing approaches	92
3.2.1	DC electrochemical measurements	92
3.2.1.1	Cyclic voltammetry using μ STAT4000.....	101
3.2.1.2	Cyclic voltammograms analysis.....	103
3.2.2	AC electrochemical measurements	105
3.2.2.1	Electrochemical Impedance Spectroscopy (PARSTAT 4000A).....	105
3.2.2.2	Electrochemical impedance analysis.....	108
	References.....	113
	 CHAPTER 4 Optical and electrochemical results of bacteria in suspension samples.....	116
4.1	Bacterial culture conditioning	116
4.2	Preparation of analyte samples	116
4.3	Optical Measurements of bacteria suspension samples.....	117
4.4	Electrochemical measurements of bacteria suspension samples.....	120
4.4.1	CV measurements	120
4.4.2	Electrochemical Impedance Spectroscopy measurements.....	126
	References	128
	 CHAPTER 5 Optical and electrochemical results of immobilized bacteria samples.....	129
5.1	Bacterial immobilization process	129
5.2	Preparation of analyte solutions	130

5.3	Optical and SEM characterization of immobilized bacteria.....	130
5.3.1	Fluorescent microscopy study of immobilized bacteria.....	130
5.3.2	SEM study of immobilized bacteria.....	130
5.3.3	Fixation of immobilized bacteria samples for SEM measurements.....	131
5.3.4	AFM imaging of immobilized live bacteria.....	131
5.4	Electrochemical measurements of immobilized bacteria samples	135
5.4.1	Cyclic voltammograms (CVs) measurements.....	135
5.5	Sensor array data analysis	141
5.5.1	Identification of water pollutants using pseudo 3D graphs of sensor responses.....	141
5.5.2	Electrochemical Impedance Spectroscopy (EIS) measurements	143
5.6	Discussion of the optical and electrochemical measurements results	145
	References	147
	CHAPTER 6 Analysis of Environmental Pollutants using Artificial Neural (ANN) Network Algorithm.....	148
6.1	Statistical analysis of sensor array data.....	148
6.2	The concept of artificial neural network	163
6.3	The design strategy of ANN for data analysis of bacteria sensor array.....	164
6.4	The ANN design	165
6.5	ANN training.....	166
6.6	ANN testing (simulation).....	179

6.7 Summary.....	158
References	180
CHAPTER 7 Detection of heavy metals using aptamer-based assays.....	163
7.1 Experimental Methodology.....	163
7.1.1 Aptamers and other chemicals used.....	163
7.1.2 Immobilization of aptamers.....	164
7.2 ICP-MS measurements.....	164
7.3 Electrochemical measurements.....	165
7.4 Results and discussion.....	166
7.4.1 Design strategy of the apta-sensor.....	166
7.4.2 Cyclic Electrochemical measurements.....	167
7.4.3 Impedance spectroscopy measurements.....	174
7.4.4 The kinetics of aptamers (Hg ²⁺ and Pb ²⁺) binding.....	178
7.5 Discussion.....	179
References	181
CHAPTER 8 Conclusion and future work	181
8.1 Thesis conclusions	181
8.2 Suggestions for future work.....	185
Appendix A-C.....	187

CHAPTER 1 INTRODUCTION

The need of biosensors and the use of sensing and biosensing technology approach are outlined in this chapter, also the invention history of electrochemical biosensor and classification of biosensors are covered in this chapter. The concept of the proposed inhibition biosensor based on bacteria, and inhibition biosensor array, has been outlined. At the end of this chapter, the aims and objectives of this research are given.

1.1 The needs of biosensors

The explosive development of industrial and agricultural activities contaminated the environment with large number of toxic chemicals, particularly, heavy metals, pesticides, petro-chemicals and BTEX compounds (which refer to benzene, toluene, ethylbenzene and xylene). High concentrations of these toxic chemical were observed at industrial and agricultural areas. The above chemicals considered among the most abundantly produced chemicals in the world spread in the atmosphere and aquatic environment, and have negative impacts on all the living organisms which led to call for fast and cost-effective analytical techniques to be used for extensive in field monitoring programs [1-5]. The detection of the above toxic chemicals in low concentrations is a quite difficult task, though not impossible and can be achieved with the existing advanced analytical methods such as atomic absorption or atomic emission spectroscopies (AAS, AES), inductively coupled plasma mass spectroscopy (ICP-MS), cold vapours atomic fluorescence spectroscopy (CVAFS) and high-performance liquid chromatography (HPLC). These methods are extremely sensitive but expensive, requiring specialized laboratory conditions and highly trained personnel [6-9]. As a result, both the time and cost of analysis become very high.

An alternative approach to those sophisticated methods is based on the use of biosensors, which could be much simpler, easy-to-use, and inexpensive. The main problem of biosensors, however, is the selection of bio-receptors which actually provide the function of recognition of target analyte molecules. Typical bio-receptors used in biosensors, i.e. enzymes, antibodies, aptamers, nucleic acids and peptides, can easily provide such functionality [10-14]. However the traditional biosensing approach may

struggle with a difficult task of detecting a large number of these toxic chemicals in a complex natural environment because every analyte may require a specific receptor. In this context, inhibition biosensors and biosensor array appear as suitable alternative to traditional biosensors.

1.2 Sensing and biosensing systems

Sensing and biosensing technologies have been expanded since 1962, when Clark and Lyons' invented the first electrochemical biosensor for blood glucose detection [15], Chen and Chzo, were differentiated between sensor and biosensor, depending on their active recognizing material immobilized on the surface of electrode which was used. Selecting this material differs with respect to the nature of the target analyte and the kind of effective reaction between both of them [16]. A sensor is a device that responds to a physical stimulus (such as heat, light, sound, pressure, magnetism, or a particular motion) and transmits a resulting impulse (as for measurement or operating a control) [17]. While, biosensor is an analytical device which uses living bioreceptors or biological elements such as tissue, microorganisms, organelles, whole cell, enzymes, antibodies, nucleic acids to measure the presence of chemical substance by generating signals proportional to detect the concentration of an analyte in the specimens [18]. Figure (1-1) presents the scheme of biosensor application areas.

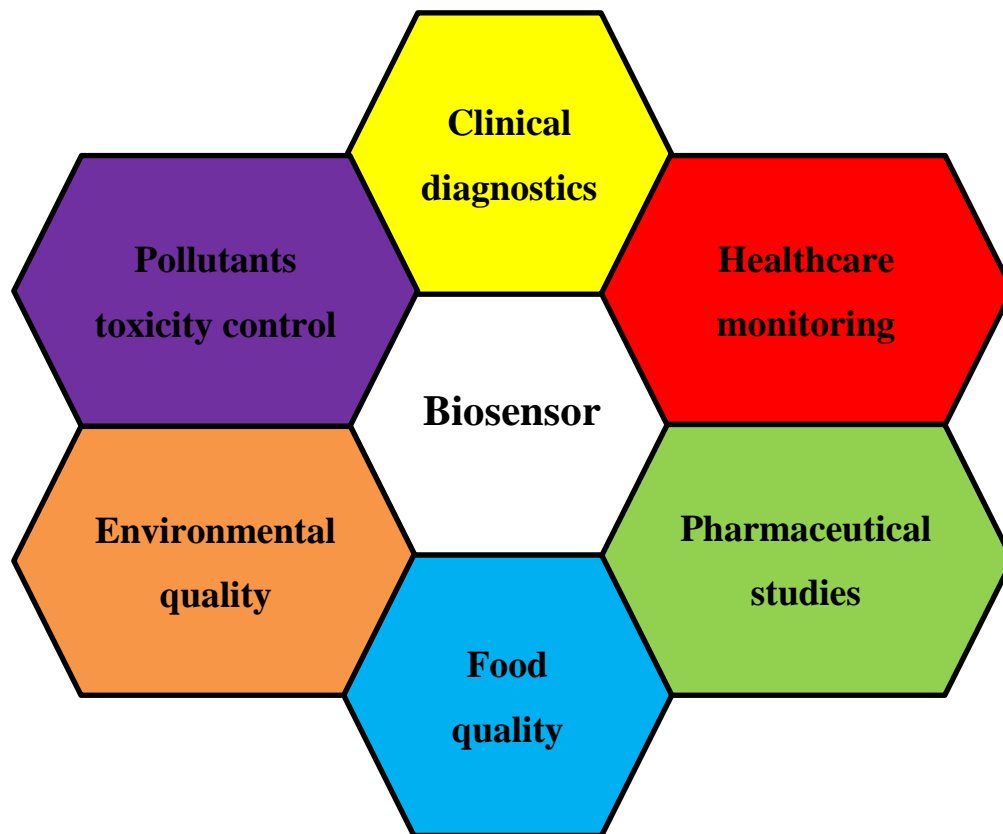


Figure1-1: The schematic diagram of biosensor application areas.

Heavy metals, pesticides, and petrochemicals possessing serious threat to humans and living organisms are of the main concern for the environmental security, nowadays. The most common sources of environmental pollution are manufacturing, automotive, agricultural, chemical, and medical industries. For instance, three of the most common heavy metals released from road travel are zinc, copper, and lead, accounting for at least 90% of the total metals in road runoff [19, 20].

These analytes do not remain where they originate. They can be transported to different locations in a number of different ways. Some of these toxic compounds (e.g. heavy metals, pesticides and hydrocarbons) can evaporate and drift away by winds before precipitating as rainfall. In addition, runoff from agricultural and urban areas into drainage pipes and sewers also contributes to significant pollution of surface and ground water with this kind of pollutants. The rain droplets included soluble heavy metal salts with the highest concentrations were zinc (Zn, 200 $\mu\text{g L}^{-1}$), iron (Fe, 88 $\mu\text{g L}^{-1}$), and

lead (Pb, $77 \mu\text{g L}^{-1}$). TEM reveals that 76% of cloud drops include metal particles that range from 50 nm to 1 μm diameter with a median diameter of 250 nm [21, 22]. A study from Switzerland revealed that much of the rain in Europe contains high levels of dissolved pesticides, actually 4 $\mu\text{g/l}$ of 2,4-dinitrophenol, that it would be illegal to supply this water for drinking purposes [23]. A field conditions study in Hungary revealed the presence of 154 $\mu\text{g/l}$ of atrazine, 89.1 $\mu\text{g/l}$ of acetochlor, 47.4 $\mu\text{g/l}$ of propisochlor, and 0.139 $\mu\text{g/l}$ of chlorpyrifos in runoff water [24].

1.3 Biosensors and biosensor arrays

The emergent needs for a portable, rapid, sensitive, and specific screening instrument for multiple pollutants detection at the site of sample collection in the field could be solved via biosensors and biosensor arrays. Perumal and Hashim (2014), were defined biosensor array as a device composed of three elements (biological molecules, bioreceptors and transducers) which are intimately associated [25]. There are five of the most important features that must be available in the biosensor array which are (i), sensitivity; (ii), reproducibility; (iii), repeatability; (iv), stability and (v), simplicity in the procedure of surface modification and biological molecule immobilization [26]. The use of biosensor arrays have several very significant advantages over using a single biosensor for such applications lie in the following fact (1) Biosensor array adds new dimensions to the observation, helping to estimate more parameters and improve the estimation performance [27]. (2) The number of analyte which can be detected simultaneously can be expanded as need dictates and specific analyte become available (3) The biosensor arrays and tracer reagents are reusable if no target agent binds to the array surface. This feature significantly decreases the cost and operational burden for the user and simplifies automation for extended monitoring applications [28]. (4) The biosensor array is simple to use. It is easily portable for first responder applications. The insertion of the sensor array, tracer reagents and samples is very simple with no requirement for alignment operations by the user [29]. (5) The biosensor array is a low-cost system which can be made even more cost effective with mass production. (6) The biosensor array can be easily adapted for continuous monitoring operations by integration with a computer-controlled sampler to format automatic analytical system.

Because of these advantages, more and more biosensor arrays are applied in varied areas including environmental monitoring [30]. (7) The identification of many types of pollutants in the environment and the evaluation of their concentration is a much more difficult task which is impossible to solve using a single type of biosensor. However, the biosensor array approach utilising several types of biological materials being inhibited differently by different types of pollutants could solve the problem of environmental pollution detection.

1.4 The history of electrochemical biosensor

Electrochemical biosensors comprise potentiometric, amperometric, and impedimetric sensing techniques, with amperometric sensors which being the first type of biosensors described in 1953. Electrochemical biosensors have subsequently become the most developed group with greatest commercial success, largely due to amperometric glucose detection in diabetes monitoring. Their key advantages are low cost, point-of-care testing, and miniaturization capacity [31]. Electrochemical biosensor is a device composed of two intimately associated elements, a bio-receptor and transducer as shown in Figure (1-2) which presents this scheme. The electrochemical biosensor is the first form of all biosensor types and started to be common in labs of chemical industries, and many other searching fields, the history of electrochemical biosensor began when the pH thin glass electrode invented by Max Cremer, which was the oldest electrochemical sensor in 1906. After that, Søren Peder Lauritz Sørensen demonstrated the concept of pH (hydrogen ion concentration) in 1909, and the first electrode for pH measurements was brought to the world in 1922 by W.S. Hughes [32]. During the period from 1909 to 1922, Griffin and Nelson, demonstrated the first immobilisation of the enzyme invertase on aluminium hydroxide and charcoal [33], and then Leland Clark, was inventioned the first electrochemical biosensor for detection of blood oxygen in 1956. He is known as the ‘father of biosensors’, and his invention of the oxygen electrode bears his name: “Clark electrode” [34].

The feasibility and their recognition ability make electrochemical sensors a good candidate for application in many disciplines such as food, biomedical, environmental,

agricultural, and industrial fields. That is owing to their precise, cost effective, fast, and reliable detection of many organic and inorganic compounds. However, further development of these biosensors requires multidisciplinary research in the fields of material science, electronics, and computer science to meet the emergent needs in different fields [35].

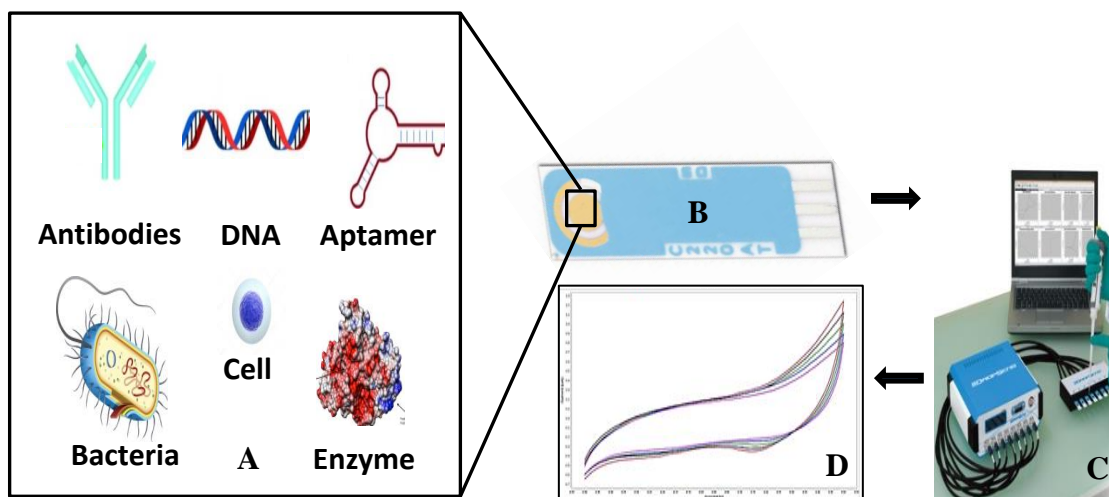


Figure 1-2: Scheme of electrochemical biosensor: (A) bio-receptors, (B) modified SPGE, (C) DropSens μ Stat equipment (D) cyclic voltammogram.

The demonstration of an amperometric enzyme electrode for the detection of glucose by Leland Clark in 1962 was followed by the discovery of the first potentiometric biosensor to detect urea in 1969 by Guilbault and Montalvo Jr [36]. Eventually, in 1975 the first commercial electrochemical biosensor was developed by Yellow Spring Instruments (YSI). Table 1-1 shows the historical overview of biosensors in the period 1916 till 2018.

Table 1-1: Historical overview of biosensors development.

Year	The invention and development event
1916	First report on the immobilization of proteins [37].
1922	First glass pH electrode [38].
1956	Invention of the (Clark) oxygen electrode [39].
1962	First description of a biosensor: an amperometric enzyme electrode for glucose (Clark) [40].
1969	First potentiometric biosensor: urease immobilized on an ammonia electrode to detect urea [41].
1970	Discovery of ion-sensitive field-effect transistor (ISFET) by Bergveld [42].
1975	Fibre-optic biosensor being carbon dioxide and oxygen detection by Lubbers and Opitz [43].
1975	First commercial biosensor for glucose detection by YSI [44].
1975	First microbe-based immunosensor by Suzuki et al. [45].
1982	Fibre-optic biosensor for glucose detection by [46].
1983	Surface plasmon resonance (SPR) immunosensor by Liedberg et al. [47].
1984	First mediated amperometric biosensor: ferrocene used with glucose oxidase for glucose detection [48].
1990	SPR-based biosensor by Pharmacia Biacore [49]
1992	Handheld blood biosensor by i-STAT [50].
1996	Glucocard launched [51].
1996	Abbott acquires MediSense for \$867 million [52].
1998	Launch of LifeScan FastTake blood glucose biosensor [53].
1998	Merger of Roche and Boehringer Mannheim to form Roche Diagnostics [54].
1999- 2018	BioNMES, Quantum dots, Nanoparticles, Nanocantilever, Nanowire and Nanotube [55].

Ever since the development of the i-STAT sensor for glucose remarkable progress has been achieved in the field of biosensors. The field is now a multidisciplinary area of research that bridges the principles of basic sciences (physics, chemistry and biology) with fundamentals of micro/nanotechnology, electronics and applicatory medicine. The database ‘Web of Science’ has indexed over 84 000 reports on the topic of ‘biosensors’ in the last ten years. According to the categories typically used, the “enzyme electrode” introduced by Clark and Lyons in 1962 [56, 57] was an amperometric biosensor. This milestone in biosensor development was followed by other electrochemical biosensors, but it was not until ten years later that biosensors based on other transduction principles were published. Electrochemical biosensors, for instance, are meanwhile comparatively easy to miniaturize, which is one of the reasons for their widespread availability. In fact, detectors for biosensors used today depend mainly on electrochemical transduction, followed by optical and acoustic effects [58]. Thermal transduction is less frequently used, as are magnetic effects. However, the latter is increasingly employed as a separation tool in bioanalytical assays [59, 60].

1.5 Bio-electrochemical systems (BESs)

Electrochemical properties of biomaterials, such as whole cells and bacteria, were studied extensively in the past [61]. Recently, the subject of electrochemical characterisation of cells came back because of recent development in bio-cell sensors [62]. The electrochemical bio-cell sensor is a relatively young field, but is now achieving substantial success in science, engineering, and technology. There are several advantages of electrochemical techniques: (i), the measurements can be made quickly, which refer to the environment activities and can be easily transmitted, amplified and digitized, (ii), the measurements can be carried out in the laboratory, as a portable device (portable detector). Bio-electrochemical systems (BESs) take advantage of biological objects (enzymes, microbes, plants) for the catalysis of electrochemical reactions [63]. Some examples of BES are: Microbial Fuel Cells, Plant-Microbial Fuel Cells, Enzymatic Fuel Cells, Microbial Electrolysis Cells, Microbial Electro-synthesis Cells and Microbial Desalination.

BESs have recently emerged as a promising technology for energy recovery and for providing valuable products, such as hydrogen, ethanol and other organic molecules [64]. BES appears as a promising alternative for treating different types of wastewater. BESs use whole cell biocatalysts to drive oxidation and reduction reactions at solid-state electrodes. The most widespread application is presently the microbial fuel cell, which aims to generate power or at least decrease the usage of power associated with wastewater treatment. In the slipstream of microbial fuel cells, microbial electrolysis cells have emerged recently. The versatility of the latter has notably expanded the range of applications of BESs. Key applications are wastewater treatment, sediment-based electrical power generation, value added product generation, bioremediation and detecting of the biomass (biological elements concentration).

The electrical properties of biological material have been studied using suitable instrumentation. In addition, impedance techniques have been used to study and monitoring the growth rate of organs *in-vivo*, whole blood and erythrocytes, cultured cell suspensions and bacterial growth [65]. The integration of impedance with biological

recognition technology for detection of bacteria has led to the development of impedance biosensors that have come to be widely used in recent years. In addition, DC and AC properties of bacteria cell have been studied and monitored.

1.6 Inhibition electrochemical biosensor scenario

In the last 20 years many researchers described the realization of inhibition biosensors for environmental pollution detection. This study has focused on the development of inhibition bacteria based electrochemical biosensors for the determination of environmental pollutants. We have indeed designed, realized and applied inhibitor bacteria based bio-sensors.

Electrochemical devices are the most common in commercial sensor development because of their simplicity of construction and therefore low cost, reliability of performance, high sensitivity with minimal concentrations of analytes down to 10^{-8}M , and wide dynamic range (up to 4 orders of magnitude in analyte concentration). The first biosensor, i.e. the glucose sensor based on Clark's electrode, was actually electrochemical.

Electrochemical and electrical sensors are clearly distinguishable. Electrochemical sensors are based on detection of electrochemical reactions on electrodes in solutions, while electrical sensors detect variations in electrical parameters of materials or devices (current, voltage, conductance, resistance, impedance) during molecular adsorption, most-likely in a gaseous environment (gas sensors) as well as in liquids (ion sensors). These devices will be outlined in more detail in the sections below. However, before going into analysis of different electrical and electrochemical sensors, the physico-chemical processes in the electrolyte-solid state system have to be discussed first.

In this study the bio-cell sensor that included the microorganisms (bacteria) was employed for detection of heavy metals, pesticides and petrochemicals which is considered to be a cheap (cost effective), simple (easy to use), powerless (portable) and sensitive technique. Other and more sophisticated techniques, like HPLC, GC-MS and/or LC-MS should be used as confirmation techniques whenever a "positive" sample

is detected. The use of this and analogous inhibition biosensors in environmental field can represent an important tool for environmental monitoring activity. In particular inhibition based bio- sensors, for their simplicity of realization. In recent years the research in the field of the biosensors was directed to the development of highly selective and sensitive devices, but it is our personal opinion that in environmental analysis, as well as in food analysis, the use of biosensor is not going to be “exclusive” (like it may be for instance in the case of biocompatible implantable devices to be used in clinical chemistry). The role of biosensors in the determination of environmental pollutants is in our opinion not to completely replace the traditional, more sophisticated instrumental techniques, but to represent a valid complement to them, especially in all those situations where it is necessary to carry out measures “on the spot”, reducing the overall times of analysis and minimizing the sample pre-treatment process. In such situations a biosensor (or better an array of biosensors) would be the analytical tool supplying all the necessary information to monitor, in real time, the state of pollution of the matrix under investigation. In the case of a positive response of one or more biosensors “traditional” sampling procedure will be activated to carry out more specific assays aimed to confirm and quantify more precisely the extent of each case of environmental contamination. In this field the development of inhibition based biosensors would be a very powerful tool for the screening of huge populations of samples for different classes of pollutants, thus detecting any compound belonging to the same class on the basis of the common biological effects, and representing an effective and powerful aid for the early detection of environmental contamination.

1.7 Aims and objectives

The main aim of this project is the development of novel inhibition biosensing array for the detection of environmental pollution. The study utilizes three types of bacteria samples (*Escherichia coli*, *Methylococcus capsulatus* (Bath) or *Methylosinus trichosporium* (OB3b) and *Shewanella oneidensis*) for the study of their optical and electrochemical properties under effects of petrochemicals, pesticides and heavy metals. One of the main reasons of using bacteria is their versatility in detecting different pollutants. Another reason is the cost-effectiveness of bacterial inhibition sensors.

Potentially, this work may lead to the development of novel, inexpensive, low power, and portable sensor array for early detection (preliminary screening) of petrochemicals, pesticides and heavy metals.

These aims can be achieved through the following objectives:

1. To select the suitable bacteria species and use poly-L-lysine for their immobilization protocol.
2. To utilise several optical techniques, such as Optical Density (O.D600), Fluorescence microscopy, and flow cytometry for counting the bacteria number and percentage which is affected by the environmental pollutants such as petrochemicals, pesticides and heavy metals, also establishing a correlation between optical properties of bacteria (in suspension and immobilized forms).
3. To utilize AC and DC electrochemical measurements for detection of these pollutants and to establish a correlation between optical and electrochemical properties and bacteria concentration.
4. To study the effect of heavy metal salts (HgCl_2 , PbCl_2 , ZnCl_2 and CdCl_2), pesticides (atrazine, simazine, DDVP), and petro-chemicals (hexane, octane, pentane, toluene, pyrene and ethanol) on optical and electrochemical properties of bacteria suspension and immobilized bacteria.
5. To develop an inhibition bacterial biosensor array prototype suitable for identification and concentration evaluation of petrochemicals, pesticides and heavy metals in water using Artificial Neural Network (ANN) data processing. This study includes a possibility of using aptamers for electrochemical detection of (Hg^{2+} and Pb^{2+}) ions analysis of real samples of water from different sources.

References

1. Cristaldi, A., Conti, G. O., Jho, E. H., Zuccarello, P., Grasso, A., Copat, C., & Ferrante, M. (2017). Phytoremediation of contaminated soils by heavy metals and PAHs. A brief review. *Environmental Technology & Innovation*, 8, 309-326.
2. El-Shahawi, M. S., Hamza, A., Bashammakh, A. S., & Al-Saggaf, W. T. (2010). An overview on the accumulation, distribution, transformations, toxicity and analytical methods for the monitoring of persistent organic pollutants. *Talanta*, 80(5), 1587-1597.
3. Förstner, U., & Wittmann, G. T. (2012). *Metal pollution in the aquatic environment*. Springer Science & Business Media.
4. Schwarzenbach, R. P., Egli, T., Hofstetter, T. B., Von Gunten, U., & Wehrli, B. (2010). Global water pollution and human health. *Annual Review of Environment and Resources*, 35, 109-136.
5. Arias-Estévez, M., López-Periago, E., Martínez-Carballo, E., Simal-Gándara, J., Mejuto, J. C., & García-Río, L. (2008). The mobility and degradation of pesticides in soils and the pollution of groundwater resources. *Agriculture, Ecosystems & Environment*, 123(4), 247-260.
6. Evans, E. H., Day, J. A., Palmer, C. D., Price, W. J., Smith, C. M., Tyson, J. F. (2005). Atomic spectrometry update. Advances in atomic emission, absorption and fluorescence spectrometry, and related techniques. *Journal of Analytical Atomic Spectrometry*, 20(6), 562-590.
7. Montes-Bayon, M., DeNicola, K., Caruso, J.A. (2003) Liquid chromatography-inductively coupled plasma mass spectrometry. *J. Chromatography A*, 1000, 457–476.
8. Zhang, Y., Adeloju, S.B. (2015). Coupling of non-selective adsorption with selective elution for novel in-line separation and detection of cadmium by vapour generation atomic absorption spectrometry. *Talanta* , 137, 148–155.
9. Harrington, C.F., Clough, R., Drennan-Harris, L.R., Hill, S.J., Tyson, J.F. (2011). Atomic spectrometry update. Elemental speciation. *J. Anal. At. Spectrom.* 26, 1561–1595.

10. Walcarius, A., Minter, S. D., Wang, J., Lin, Y., & Merkoçi, A. (2013). Nanomaterials for bio-functionalized electrodes: recent trends. *Journal of Materials Chemistry B*, 1(38), 4878-4908.
11. March, G., Nguyen, T. D., Piro, B. (2015). Modified electrodes used for electrochemical detection of metal ions in environmental analysis. *Biosensors*, 5(2), 241-275.
12. Zamora-Galvez, A., Morales-Narváez, E., Mayorga-Martinez, C. C., & Merkoçi, A. (2017). Nanomaterials connected to antibodies and molecularly imprinted polymers as bio/receptors for bio/sensor applications. *Applied Materials Today*, 9, 387-401.
13. Ansari, M. H., Hassan, S., Qurashi, A., & Khanday, F. A. (2016). Microfluidic-integrated DNA nanobiosensors. *Biosensors and Bioelectronics*, 85, 247-260.
14. Palchetti, I., & Mascini, M. (2011). Biosensor techniques for environmental monitoring (pp. 1-16). The Royal Society of Chemistry: Cambridge.
15. Caygill, R. L., Blair, G. E., & Millner, P. A. (2010). A review on viral biosensors to detect human pathogens. *Analytica Chimica Acta*, 681(1-2), 8-15.
16. Chen, S. M., & Chzo, W. Y. (2006). Simultaneous voltammetric detection of dopamine and ascorbic acid using didodecyldimethylammonium bromide (DDAB) film-modified electrodes. *Journal of Electroanalytical Chemistry*, 587(2), 226-234.
17. Fraden, J. (2004). *Handbook of modern sensors: physics, designs, and applications*. Springer Science & Business Media.
18. Sharma, H., Agarwal, M., Goswami, M., Sharma, A., Roy, S. K., Rai, R., & Murugan, M. S. (2013). Biosensors: tool for food borne pathogen detection. *Veterinary world*, 6(12), 968.
19. Philp, J. C., Bamforth, S., Singleton, I., & Atlas, R. M. (2005). Environmental pollution and restoration: a role for bioremediation. In *Bioremediation* (pp. 1-48). American Society of Microbiology.
20. Rathoure, A. K. (2016). Heavy metal pollution and its management: Bioremediation of heavy metal. In *Toxicity and waste management using bioremediation* (pp. 27-50). IGI Global.

21. Li, W., Wang, Y., Collett Jr, J. L., Chen, J., Zhang, X., Wang, Z., & Wang, W. (2013). Microscopic evaluation of trace metals in cloud droplets in an acid precipitation region. *Environmental science & technology*, 47(9), 4172-4180.
22. Walter, I., Martinez, F., Cala, V. (2006). Heavy metal speciation and phytotoxic effects of three representative sewage sludges for agricultural uses. *Environmental pollution*, 139(3), 507-514.
23. Pearce, F., Mackenzie, D. (1999). It's raining pesticides. *New Scientist*, 162(2180), 23.
24. Nabok, A., Haron, S. (2004). Registration of heavy metal ions and pesticides with ATR planar waveguide enzyme sensors. *Applied Surface Science*, 238(1), 423-428.
25. Perumal, V., & Hashim, U. (2014). Advances in biosensors: Principle, architecture and applications. *Journal of applied biomedicine*, 12(1), 1-15.
26. Hunt, H. K., & Armani, A. M. (2010). Label-free biological and chemical sensors. *Nanoscale*, 2(9), 1544-1559.
27. Yogeswaran, U., & Chen, S. M. (2008). A review on the electrochemical sensors and biosensors composed of nanowires as sensing material. *Sensors*, 8(1), 290-313.
28. Ronkainen, N. J., Halsall, H. B., & Heineman, W. R. (2010). Electrochemical biosensors. *Chemical Society Reviews*, 39(5), 1747-1763.
29. Shriver-Lake, L. C., & Ligler, F. S. (2005). The array biosensor for counterterrorism. *IEEE Sensors journal*, 5(4), 751-756.
30. Turner, A. P. (2013). Biosensors: sense and sensibility. *Chemical Society Reviews*, 42(8), 3184-3196.
31. Ahmed, A., Rushworth, J. V., Hirst, N. A., & Millner, P. A. (2014). Biosensors for whole-cell bacterial detection. *Clinical microbiology reviews*, 27(3), 631-646.
32. Camoes, M. F. (2010). A Century of pH Measurements. *Chemistry international*, 32(2), 3-7.
33. Bhalla, N., Jolly, P., Formisano, N., & Estrela, P. (2016). Introduction to biosensors. *Essays in biochemistry*, 60(1), 1-8.
34. Arya, R. (2014). Biosensors. In *Advances in Biotechnology* (pp. 179-194). Springer, New Delhi.

35. O'Mara, P., Farrell, A., Bones, J., & Twomey, K. (2018). Staying alive! Sensors used for monitoring cell health in bioreactors. *Talanta*, 176, 130-139.
36. Dhawan, G., Sumana, G., & Malhotra, B. D. (2009). Recent developments in urea biosensors. *Biochemical Engineering Journal*, 44(1), 42-52.
37. Krishnamoorthi, S., Banerjee, A., & Roychoudhury, A. (2015). Immobilized enzyme technology: potentiality and prospects. *J Enzymol Metabol*, 1(1), 010-104.
38. Anker, P., Ammann, D., & Simon, W. (1983). Blood pH measurement with a solvent polymeric membrane electrode in comparison with a glass electrode. *Microchimica Acta*, 79(3-4), 237-242.
39. Severinghaus, J. W. (2002). The invention and development of blood gas analysis apparatus. *Anesthesiology: The Journal of the American Society of Anesthesiologists*, 97(1), 253-256.
40. Wang, J. (2001). Glucose biosensors: 40 years of advances and challenges. *Electroanalysis: An International Journal Devoted to Fundamental and Practical Aspects of Electroanalysis*, 13(12), 983-988.
41. Kuralay, F., Özyörük, H., & Yıldız, A. (2005). Potentiometric enzyme electrode for urea determination using immobilized urease in poly (vinylferrocenium) film. *Sensors and Actuators B: Chemical*, 109(2), 194-199.
42. Bergveld, P. (1970). Development of an ion-sensitive solid-state device for neurophysiological measurements. *IEEE Transactions on Biomedical Engineering*, (1), 70-71.
43. Mun'delanji, C. V., Kerman, K., Hsing, I. M., & Tamiya, E. (Eds.). (2015). *Nanobiosensors and Nanobioanalyses*. New York: Springer.
44. Yoo, E. H., & Lee, S. Y. (2010). Glucose biosensors: an overview of use in clinical practice. *Sensors*, 10(5), 4558-4576.
45. Suzuki, S., Takahashi, F., Satoh, I., & Sonobe, N. (1975). Ethanol and Lactic Acid Sensors Using Electrodes Coated with Dehydrogenase—Collagen Membranes. *Bulletin of the Chemical Society of Japan*, 48(11), 3246-3249.
46. Goldstick, T. K., Ciuryla, V. T., & Zuckerman, L. (1976). Diffusion of oxygen in plasma and blood. In *Oxygen Transport to Tissue—II* (pp. 183-190). Springer, Boston, MA.

47. Liedberg, B., Nylander, C., & Lunström, I. (1983). Surface plasmon resonance for gas detection and biosensing. *Sensors and actuators*, 4, 299-304.
48. Cass, A. E., Davis, G., Francis, G. D., Hill, H. A. O., Aston, W. J., Higgins, I. J., & Turner, A. P. (1984). Ferrocene-mediated enzyme electrode for amperometric determination of glucose. *Analytical chemistry*, 56(4), 667-671.
49. Wang, J. (2006). Electrochemical biosensors: towards point-of-care cancer diagnostics. *Biosensors and Bioelectronics*, 21(10), 1887-1892.
50. Ekonomou, A. (2014). Enzymatic biosensors. Portable biosensing of food toxicants and environmental pollutants. CRC Press, Boca Raton, 123-160.
51. Atta, N. F., Galal, A., & Ali, S. (2011). Nanobiosensors for health care. In *Biosensors for Health, Environment and Biosecurity*. IntechOpen.
52. Feldman, B., McGarraugh, G., Heller, A., Bohannon, N., Skyler, J., DeLeeuw, E., & Clarke, D. (2000). FreeStyle™: a small-volume electrochemical glucose sensor for home blood glucose testing. *Diabetes technology & therapeutics*, 2(2), 221-229.
53. Crismore, W. F., Surridge, N. A., McMinn, D. R., Bodensteiner, R. J., Diebold, E. R., Delk, R. D., & Heald, B. A. (2001). U.S. Patent No. 6,270,637. Washington, DC: U.S. Patent and Trademark Office.
54. Atta, N. F., Galal, A., & Ali, S. (2011). Nanobiosensors for health care. In *Biosensors for Health, Environment and Biosecurity*. IntechOpen.
55. Singh, B. (2018). *NanoBioMaterials: Nanobiomaterials*. CRC Press.
56. Mishra, N., Kadam, Y., & Malek, N. (2018). Overview of enzyme based biosensors and their applications. *Current Trends in Biotechnology and Pharmacy*, 12(1), 108-117.
57. Zhu, Y. C., Mei, L. P., Ruan, Y. F., Zhang, N., Zhao, W. W., Xu, J. J., & Chen, H. Y. (2019). Enzyme-Based Biosensors and Their Applications. In *Advances in Enzyme Technology* (pp. 201-223). Elsevier.
58. Cooper, M. A., & Singleton, V. T. (2007). A survey of the 2001 to 2005 quartz crystal microbalance biosensor literature: applications of acoustic physics to the analysis of biomolecular interactions. *Journal of Molecular Recognition: An Interdisciplinary Journal*, 20(3), 154-184.

59. Gruhl, F. J., Rapp, B. E., & Länge, K. (2011). Biosensors for diagnostic applications. In *Molecular Diagnostics* (pp. 115-148). Springer, Berlin, Heidelberg.
60. Thakur, M. S., & Ragavan, K. V. (2013). Biosensors in food processing. *Journal of food science and technology*, 50(4), 625-641.
61. Busalmen, J. P., Esteve-Nuñez, A., & Feliu, J. M. (2008). Whole cell electrochemistry of electricity-producing microorganisms evidence an adaptation for optimal exocellular electron transport. *Environmental science & technology*, 42(7), 2445-2450.
62. Liu, X., Li, L., & Mason, A. J. (2014). High-throughput impedance spectroscopy biosensor array chip. *Philosophical Transactions of the Royal Society A: Mathematical, Physical and Engineering Sciences*, 372(2012), 20130107.
63. Hamelers, H. V., Ter Heijne, A., Sleutels, T. H., Jeremiasse, A. W., Strik, D. P., & Buisman, C. J. (2010). New applications and performance of bioelectrochemical systems. *Applied microbiology and biotechnology*, 85(6), 1673-1685.
64. Bajracharya, S., Sharma, M., Mohanakrishna, G., Benneton, X. D., Strik, D. P., Sarma, P. M., & Pant, D. (2016). An overview on emerging bioelectrochemical systems (BESs): technology for sustainable electricity, waste remediation, resource recovery, chemical production and beyond. *Renewable Energy*, 98, 153-170.
65. Rabaey, K., & Rozendal, R. A. (2010). Microbial electrosynthesis revisiting the electrical route for microbial production. *Nature reviews microbiology*, 8(10), 706.

CHAPTER 2 LITERATURE REVIEW

This chapter covers the toxic chemicals which cause the environmental pollution, classification of environmental pollutants i.e. heavy metals, pesticides, petrochemicals and BTEX compounds) and their spread of these toxic chemicals and their impact on the environment as well and the methods for detection of these pollutants, and the effect of these pollutants on living organisms and bacteria mass in particular. Also the more detailed description of the sensing material (bacteria) is given at the end of this chapter.

1.2 Toxic chemicals and environmental pollution

Environmental security is one of the important requirements for protecting living organisms in our planet. However, it still remains a major global challenge [1, 2]. The environmental pollution with toxic chemicals is considered as a main and the vital issue of the global biosphere. The evolution in agriculture, pharmaceutical, and chemical manufacturing is essential to fulfill the requirements and demands of the growing human population. However, such developments often caused additional pollution of environment [3]. These pollutants are spread into the different parts of the environment and have negative impacts on the living organisms [4]. Environmental pollution has been described as any natural or industrial release of the chemical, thermal, biological or radioactive elements to some part of the environment which makes a threat to the health and wellbeing of the living species [5]. Today, environmental pollution has become a significant problem which threatening the wellbeing of the living organisms. There are so many other sources of hazardous and pollutants, such as chemical plants, roads which release heavy metals, agriculture which use pesticides and chemical industry using petrochemicals and other toxic components. These sites pose a serious threat to the human being, animals, plants and microorganisms [6].

Pollutants might cause either destruction with direct visible effects on the environment, or minor destruction in the system of living organism life cycle due to disturbance of a delicate balance of the biological nutrition which are noticeable after a certain time [7]. Water pollution is of particular concern nowadays, and the needs of the methods of detecting and eliminating pollutants is growing. There are many different pollutants with petrochemicals, heavy metals, and pesticides being the most common ones. Water pollution can be defined as the presence of any chemical or microbial objects in the fresh or seawater which reduce the water quality and affect the living bodies in it. [8]. A large number of unregulated chemicals are consistently introduced into watercourses. Furthermore, several of the mining processes cause discharges of chemical waste which damages the surrounding environment. Non-conventional waste product varies from naturally inactive substances, for instance, clay and ferrous remains [9].

2.2 Detection of toxic chemical pollutants

Removal of toxic pollutants from the environment, i.e. air, soil and water should start with the detection of these harmful elements. Ecological monitoring is all about sensing the pollution which currently occurs in the air, soil and in water. The treatment of environmental pollution with toxic chemicals problem needs sequence of processes, firstly, to have reliable methods of detection and identification of pollutants and secondly, adequate remediation procedures which can be applied.

The environmental pollutants detection and monitoring in air, water and soil is very important in the overall safety and security of humans, other animals and plants. Highly sensitive traditional analytical techniques such as chromatography and inductively coupled plasma mass spectroscopy are considered time consuming, expensive and require a lot of expertise. Many of analytical techniques for the detection of toxic pollutants and chemical pollutions have been established in the last 40-50 years, [10]. Powerful analytical tools such as gas liquid chromatography (GLC) and inductively coupled plasma mass spectrometry mass (ICP-MS) can identify any chemical contamination in very low concentrations down to the part per billion (ppb). However,

very often these methods are expensive, require the use of sophisticated equipment, specialized laboratories, and highly trained personnel, and thus cannot be used for in-field trials. At the present time, the needs for low-cost, portable, easy-to-use sensor devices, which can be used even by non-specialists in field conditions, is increasing.

Therefore, there is need for simple, rapid, none expensive, highly sensitive, specific and portable device for analysing environmental pollutants.

There are many methods of toxic chemical environmental pollution detection, but this study focuses on the development of novel, portable and cost-effective inhibition biosensor array for preliminary analysis (screening) of the presence of petrochemicals, heavy metals, and pesticides in water and mostly on the development of simple and rapid method of their detection.

The main problem of sensor development, however, is the synthesis of specific receptors for a huge variety of pollutants. The use of natural bio-receptors such as enzymes and antibodies or their artificial analogs such as aptamers could be the way forward, though such bio receptors are quite expensive. The idea of using bio-objects (such as enzymes, whole cell, and microorganisms) which can be inhibited by pollutants is a new trend in bio-sensing. The inhibition sensor arrays are capable of differentiation and quantification of pollutants [11].

The highly sensitive electrochemical sensors dominate biosensing market, and they are the most common biosensors for detection of different analytes [12]. In addition, the inexpensive, simple design and small size make them excellent candidates for the development of portable biosensors [13]. The new idea which recently appeared is the use of microorganisms which can resist the high concentrations of petrochemicals, pesticides and heavy metals. There are several reports about biosensing applications of microorganisms such as *Escherichia coli*, *Pseudomonas putida*, *Shewanella oneidensis* bacteria and *Anabaena algae* which have the ability to pollution resistivity [14].

Recently, the utilize of whole bacteria cell as a biosensor to detect the toxins in the environment was reported with *Shewanella oneidensis* MR-1 which is a

Gammaproteobacterium, that is mean it has the ability to detoxify many kinds of heavy metals and some organic solvent [15, 16].

In this project, it was proposed to use some of these microorganisms for detection of the presence of toxic chemicals (heavy metals, hydrocarbons, and pesticides) by monitoring live and dead bacteria count. The pollution detection processes of above pollutants were developing by discovering optical and electrochemical microbial biosensors [17, 18]. A number of experimental techniques will be used in this project, such as electrochemical methods such of cyclic voltammograms using three-electrode assemblies and DropSens potentiostat, also electrochemical impedance spectroscopy, optical methods such as fluorescence microscopy, optical density and flow cytometry. These measurements will be carried out before and after exposure of the bacteria in suspension as well as immobilized bacteria on the modified screen printed gold electrode to detect the above mentioned toxic compounds. The most favourable methods will be selected to provide the dependable response and high sensitivity. Other criteria for selection of experimental methods are the cost and the sensor development suitability. The new trend of the sensor array in this project will be explored about using different types of bacteria in the same sensor chip, for example, a screen printed gold electrode containing different immobilized bacteria colonies could be used. For this purpose, the bacterial responses such as anode or cathode current, AC impedance analysis and DC cyclic voltammograms could be utilized from each well. Different levels of different pollutants concentrations will be recorded and provide a database for pattern recognition. Such sensor array approach based on ANN (Artificial Neuro Network) will be applied for recognition of pollutants and evaluation of their concentration [19- 22]. For this work three strains of bacteria were selected, namely *Escherichia coli* (*E. coli*), Methanotrophic bacteria (*Methylococcus capsulatus* (Bath) and *Methylosinus trichosporium* (OB3b) and *Shewanella oneidensis* MR-1 (*S.oneidensis*). *E.coli* and (*M. capsulatus* (Bath) or *M. trichosporium* (OB3b) being quite sensitive to heavy metal and pesticides, and could be suitable for monitoring the contamination at a low concentration. While *S. oneidensis* is known by its resistance to these kinds of

pollutants [23, 24]. In the meantime, preliminary results were obtained by Al-Shanawa et al (2013, 2014) [25, 26], and this study is a further development of the concept of the inhibition bacterial sensor array, so these bacterial samples will be tested under treatment with heavy metals, pesticides and hydrocarbons. In order to acquire the fundamental knowledge and understanding of the mechanism of bacteria inhibition by different pollutants, the correlation between the bacterial concentration with the optical and electrochemical properties of liquid and immobilized bacteria samples have to be established. For this purpose, several optical methods, including fluorescent microscopy, optical density, and flow cytometry will be used in this study, along with electrochemical AC and DC measurements, in order to study the effect of heavy metal salts (HgCl_2 , PbCl_2 , ZnCl_2 and CdCl_2), pesticides (atrazine, simazine, DDVP), and petro-chemicals (hexane, octane, pentane, toluene, pyrene and ethanol) on the above bacteria. Electrochemical measurements are considered promising for the development of simple inhibition bacteria-based biosensors for the detection of these pollutants. The use of three (or more) types of bacteria will lead to the development of sensor arrays utilizing the principles of pattern recognition such as (ANN) for inhibition elements detection.

2.3 Classification of toxic chemical pollutants

2.3.1 Heavy metals

Heavy metal pollution is a serious global environmental problem and among the most abundant, toxic and persistent inorganic toxic chemicals which adversely affect living organisms and cause genetic mutation [27, 28]. Due to their high atomic weight and high density they are commonly referred to trace metals; many of these trace metals (e.g. Hg, Pb, Cd and Ni) are highly toxic to humans and other living organisms, and their presence in surface water at above background concentrations is undesirable [29]. The detection of toxic metal ions in aquatic environment is an important global issue because these contaminants may have severe effects on microorganisms, plants, animals

elements that exhibit metallic properties. These mainly include transition metals, some metalloids, lanthanides, and actinides. Several definitions have been proposed, some based on density, some on atomic number or atomic weight, and some on chemical properties or toxicity. Heavy metals occur naturally in ecosystems, with large variations in concentration [34]. During precipitation on road surfaces, most heavy metals become bound to the road dust or other particulates or become soluble. In either case, the metals enter the soil or water resources. Whether in the soil or aquatic environment, metals can be transported by several processes, which are governed by the chemical nature of metals, soil and sediment particles, and the pH of the surrounding environment. Other common sources of metal contaminants in the environment are mining and smelting activities; other industrial emissions and effluents; urban development; vehicle emissions; dumped waste materials; contaminated dust and rainfall [35]. In conclusion, there are seven major categories of sources of metals contamination of the environment.

1. Natural sources, such as surface mineralization, volcanic gasses, spontaneous combustions or forest fires.
2. Metal containing agricultural sprays or soil amendments.
3. Emissions from large industrial sources, such as metal smelters and refineries, chemical and pharmaceutical industries.
4. The disposal of wastes from mines or mills.
5. Emissions from municipal utilities, such as coal or power stations or municipal incinerators.
6. Emissions from transport automobiles.
7. Other relatively minor sources of contamination, such as smaller scale industries that process metals.

2.3.2 Petrochemicals and BTEX compounds

The extensive use of petrochemicals and hydrocarbon products such as (hexane, octane, pentane, pyrene and ethanol) and BTEX compounds (e.g. benzene, toluene,

ethylbenzene and xylene) leads to the contamination of almost all environmental resources. Particularly in the zones of petrochemical production, the surface soils and water environments are exposed to contamination by the industrial products. Nowadays, the growths of urban industry process lead to greater than before release of the petrochemical products into the eco-system. Petroleum production process is distribute many of environmental pollutants which enter the water environment due to releases of manufacturing products such as urban effluents, shipping activities, offshore oil production, oil spills, fossil fuel combustion, and natural seeps [36]. Petroleum production is costly and globally degrading; most of the petroleum oil sources are associated with visible large escapes, and many oil fields are found due to natural outflows. In addition to the main use of oil as a fuel, oil is extensively used in chemical industry for production of large varieties of chemicals. Figure (2-2) shows the number of petrochemical products. To make a full assessment of the petroleum extraction processes impact on the environment, the detailed characterization of the environment, such as water, air, vegetation, and soil, is required. For this reason, the detection of petrochemical pollution is vital to give information on environmental quality.



Figure 2-2: Common commercial petrochemicals.

It was described by some researchers that petroleum extraction processes commonly mount up heavy metal release from many sources, for instance rocks, sea salt intrusion, during migration to its present reservoir, refining, transportation, and handling [37].

Wastewater of some petrochemical plants, in addition to hydrocarbons, contains chlorinated chemicals. The biological treatment; particularly by the activated sludge process has been widely used for removal of organic compounds from petrochemical wastewater. The microbial composition of the activated sludge and its activity depends on the nature and availability of petroleum hydrocarbons, nutrient composition, and other environmental conditions (pH, temperature, dissolved oxygen, mixing system, plant configuration). The microbial degraders of organopollutants of contaminated areas are normally chemoorganotrophic species, which are able to use a huge number of natural and xenobiotic compounds as carbon sources and as electron donors for the generation of energy. Numerous microorganisms, including bacteria, fungi and yeasts, predominantly aerobics, are known for their ability to degrade these organopollutants [38, 39]. The typical aerobic degrading bacteria in organopolluted site belong to a spectrum of genera and species including, *Pseudomonas sp.*, *Acinetobacter sp.*, *Alcaligenes sp.*, *Flavobacterium cytophaga* group, *Xanthomonas sp.*, *Nocardia sp.*, *Mycobacterium sp.*, *Corynebacterium sp.*, *Arthrobacter sp.*, *Comamonas sp.*, and *Bacillus sp.* [40].

2.3.3 Pesticides and herbicides

The environmental impacts of pesticides and herbicides depend on their toxicity, solubility, distribution and the concentration in the environment. During the 1940s, the first synthetic pesticides come to be available, making huge benefits and increasing the food manufacture. Negative effect of pesticides on the eco-system and on the life cycle of living organisms started being noticed in the early 1960s [41]. Since then, the debate on the risks and benefits of pesticides has not ceased, and a large amount of research has been conducted into the impact of pesticides on the environment. 2.5 million tons of

pesticides have been estimated and applied to the crops agriculture worldwide yearly, the amount of pesticide coming in direct contact with or consumed by target pests is an extremely small percentage of the amount applied. In most studies the proportion of applied pesticides reaching the target pest has been found to be less than 0.3%, and 99.7% went 'somewhere else' in the environment [42]. The use of pesticides and herbicides in agriculture inevitably affects non-target organisms (including humans). Undesirable side-effects may occur in some species, communities or on ecosystems as a whole. The environmental effect of pesticide applications is increasing, and it has been taken into account by regulatory bodies, leading to increased restrictions on the use of pesticides or their complete ban. Although some of these pesticides have been eliminated the most harmful agents environmentally. The inputs of fertilisers and agrochemicals were reduced since the late 1970s and there has been considerable interest in 'integrated' arable farming systems, which attempt to reduce the use of pesticides [43]. Figure (2-3) shows the types of commercial pesticides and herbicides.



Figure 2-3: Types of pesticides and herbicides used.

In traditional cultivation farming systems, there are several reasons interfering with the farmer's choice to make use of a specific pesticide such as the anticipated effectiveness against the pest, the risk of phytotoxicity to the crop and the cost of the application. In combined agricultural, the ecological influence of the pesticide has to be a most important condition to take into account. Several approaches were planned to assist

agriculturalists in estimating the environmental impact of pesticides in the last few years [44].

Manuel, et al (2008) [45] defined pesticides and herbicides as any substance or mixture of substances intended for preventing, destroying, repelling, or mitigating of any pest or weed. Frank, et al (1991) [46] reported that pesticides and herbicides are the most cost-effective means of pest and weed control known to contain numerous geno-toxic compounds. Pesticides can be classified according to their target, their mode or period of action, or their chemical structure. There are different types of pesticides which are herbicides, insecticides, fungicides and nematocides. More than 500 different pesticide formulations are being used in our environment, mostly in agriculture, although the control of biological public health hazards also continues to be an important field of application. In the last 50 years, the use of pesticides has greatly increased the quantity and improved the quality of food for the growing world population. Below, the three compounds used in this work are described in more details.

Atrazine (6-Chloro-N-ethyl-N-1-methylethyl-triazine-2,4,-diamine) is one of the herbicides discovered in 1958 and used first to control the agricultural weeds in 1960 and it is still in use, occupying 83% of U.S pesticides market.

An atrazine monitoring program has been established in water systems due to atrazine being discovered and treated in polluted water. In addition, the program investigated the metabolites of atrazine derivatives which have the same poisonous effect as the parent compound [47]. Several studies in the U.S on the role of atrazine in causing cancer in human and animals have been performed but they concluded this program need to regulate the using of this pesticide rather than prevent it [48].

Simazine, (6-chloro-N₂, N₄-diethyl-1,3,5-triazine-2,4-diamine), was one of the first compound of atrazines [49], registered in 1957. From 1990 to 1993 it was among the most widely used herbicides in the US for pre and post-emergence weed control. It is a white crystalline solid with a melting point of 226 °C, slightly soluble in water (5 mg l⁻¹) and highly soluble in organic solvents. When applied to the soil it is absorbed

by leaves and roots, causing inhibition of photosynthesis in the entire plant [50] and [51]. It is biodegradable, metabolized in plants and soil through both chemical and microbial processes.

Simazine was used to prevent and control the growth of any unwanted plant and algae in water resources. Due to these negative impacts simazine use is banned in the countries of the European Union and currently simazine is considered dangerous for the environment.

Dichlorvos or 2, 2-dichlorovinyl dimethyl phosphate (commonly abbreviated as a DDVP) is an organophosphate widely used as an insecticide to control household pests, and protecting stored product from insects [52]. The compound has been commercially available since 1961 and has become controversial because of its prevalence in urban waterways and the fact that its toxicity extends well beyond insects. The insecticide has been banned in European Union since 1998 [53].

2.4 Effects of toxic chemical pollutants on living organisms

Heavy metals are one of the toxic and non-biodegradable pollutants released into the environment by industrial, mining and agricultural activities [54]. The density of heavy metals is 6.0 g/cm^3 while the soils density is 2.65 g/cm^3 but concentrations are frequently elevated; because of the contamination of soil which occurs naturally. The most important heavy metals have potential hazards and occurrences in contaminated soils are cadmium (Cd), chromium (Cr), mercury (Hg), lead (Pb), nickel (Ni) and zinc (Zn).

Cadmium's (Cd) toxicity has been linked to reproductive disorder by affecting the number, shape and activity of sperm, in addition reducing the weight of the neonate. Moreover it is causing possible carcinogenic anomalies and seems to be a causal factor in cardiovascular diseases and hypertension [55].

Chromium (Cr) in inorganic systems occurs in several chemical forms. Only Cr (III) and Cr (VI) are significant in biological systems. Trivalent chromium is an essential nutrient component [56]. Chromium is required for carbohydrate and lipid metabolism and the utilization of amino acids [57]. The biological function of Cr is also closely associated with that of insulin and most Cr-stimulated reactions depend on insulin [58]. However, excess of Cr (VI) in biological process has been implicated in specific forms of cancer.

Lead (Pb) is known to be toxic. It is a widespread contaminant in soils and water. Lead poisoning is one of the most prevalent public health problems in many parts of the world [59]. It was the first metal to be linked with failures in reproduction due to its penetration the placenta easily, and it also affects the brain, causing damaging brain development in infants [60].

Mercury (Hg) is toxic even at low concentrations to a wide range of organisms, including humans, the organic form of mercury can be particularly toxic [61].

Zinc (Zn) is essential micronutrient in plants, animals and human [62]. However, the excessive amount of zinc salts affects several organs simultaneously as exemplified by zinc phosphide. When this rodenticide is ingested, it reacts with water and stomach juice to release phosphine gas which can enter the blood stream and affect the lungs, liver, kidney, heart and central nervous system [63].

Nickel (Ni) occurs in the environment only at very low levels. Foodstuffs have a low natural content of nickel but high amounts can occur in food crops grown in polluted soils. Uptake of high quantities of nickel can cause cancer, respiratory failure, birth defects, allergies, and heart failure [64].

Recent research showed the ability of microorganism to survive in the presence of different types of heavy metals in a wide range of concentrations [65].

On the other hand, the possibility of using metal resistant bacteria as bio-indicators of polluted environment has been shown to be a sensitive and reliable tool in detecting the sub-lethal toxicity of these toxic compounds [66].

Saturated noncyclic hydrocarbons, cyclic hydrocarbons, olefinic hydrocarbons, aromatic hydrocarbons, sulphur compounds, nitrogen–oxygen compounds and heavy metals are considered the main contains of the petrochemical products. On the other hand, the chemical structures and the physical features were widely varies of any crude oil or refined product depending of its origin for production [67]. As a result of the petrochemical entrance to the marine environment, these pollutants may possibly suffer physical, chemical and biological changes due to the weathering processes, which could be considered as one of the main causes which inducing the toxicity and the potential eco-toxicological impacts of these ecological pollutants [68].

The most toxic components of petroleum products are polycyclic aromatic hydrocarbons (PAHs), alcohols, ketones, benzene derivatives or (BTEX), etc. Considering the adverse effects of the above pollutants on humans, animals, and wild life, the environmental agencies and World Health Organization set quite low limits (from 0.1 to 0.5 mg/l) for heavy metals, pesticides and some petrochemical (i.e. methyl alcohol and BTEX) pollutants in drinking water, food and feed. Aquatic organisms have the ability to take up these hydrophobic compounds due to their ability to connect with cellular molecules after binding to the lipophilic sites on organism cell wall. If the target substance is an important molecule of a cellular process, a toxic response may be induced, and, at the extreme, the integrity of the organism can be seriously compromised [69]. After being taken up by an organism, hydrocarbons and their metabolic products may enhance the production of reactive oxygen species (ROS) by several mechanisms that can lead to cellular damage through protein oxidation, lipid peroxidation (LPO) and DNA damage [70].

Reactive oxygen species (ROS) are generated in all living organisms mainly during mitochondrial metabolism [71]. ROS may include superoxide anion (O_2^-), hydroxyl radical (OH^-), hydrogen peroxide (H_2O_2) and nitric oxide (NO). Excessive amounts of ROS may overwhelm natural antioxidant defences promoting DNA, lipid and protein oxidative damage and oxidative stress, which may lead to cell apoptosis and death [72]. ROIs play a central role in the defence of plant and animal cell against pathogen attack [73].

Enhancement of DNA damage was due to oxidative stress, indicating that ROS accumulation in tissues caused subsequent DNA damage,. A number of studies have shown that ROS are the major source of DNA damage by causing strand breaks, removal of nucleotides, and various modifications of the nucleotide bases [74]. There are many environmental factors which cause or induce the DNA damage and there are differences in DNA repair capacity [75].

Pesticides and herbicides usually cause unplanned ecological impacts, when they are not completely selective to the target organism. Living species possibly will uptake the pesticides during the digestion of contaminated supplements both food and water or by respiration of contaminated air and through direct skin contact. Agriculturalists and farmland workers suffer more than other people from higher dermal and respiratory up take and genetic disorders due to direct contact with mixed and sprayed pesticides causing exposure [76]. Although the majority of pesticides were used to control pests in above-ground plant parts, they can reach the soil directly. The soil biological population consist of different types of micro and macro organisms such as bacteria, fungi, algae, earthworms and insects [77], which can be affected by pesticides.

Death of animals may be related to feeding on sources contaminated with pesticides and herbicides. Widespread mortality of wild animals in association with major pest control programmes was reported, when organochlorine pesticides were used in particular [78]. Peri and neonatal animals exposed to pesticides such as aldrin, atrazine, chlordane and

dieldrin, has shown these substances can elicit a variety of perturbations in the sexual differentiation. Birth defects in the male reproductive tract [79] and reductions in sperm count have been associated with the presence of endocrine disrupting chemicals in the environment [80].

In the assessment of pesticide toxicity to living species (humans and animals), the phenomena of carcinogenesis, immuno-disfunction, mutagenesis, neurotoxicity, endometriosis and teratogenesis should be considered along with toxicity in the restricted sense [81]. A recent report shows that toxic chemicals such as pesticides may damage the immune system [82], and can mimic hormones thus disrupting the endocrine system in both humans and animals, causing a variety of disorders [83]. Human health issues such as increased incidences of breast cancer, prostate cancer, testicular cancer, due to the highly toxicity of atrazine and simazine pesticides to human and other living organisms [84, 85].

2.5 Detection and remediation of toxic pollutants

There are many techniques used for detection of environmental pollutants as toxic chemicals, for example heavy metals, pesticides and hydrocarbons. A number of analytical methods, such as atomic absorption or atomic emission spectroscopies (AAS, AES), inductively coupled plasma mass spectroscopy (ICP-MS), cold vapour atomic fluorescence spectroscopy (CVAFS), and high pressure liquid chromatography (HPLC) are capable of detecting traces of toxic pollutants. However, these methods require sophisticated analytical equipment, specialised laboratories and highly qualified personnel, which make such analysis very expensive and time consuming. Conventional analytical techniques such as atomic absorption spectroscopy (AAS), inductively coupled plasma mass spectroscopy (ICP-MS) and chromatography are very sensitive and reliable [86]. However, they also suffer from the disadvantages of high cost, being time consuming, the need for highly trained technicians and the fact that they are mostly laboratory based [87]. Therefore, the development of alternative detection technologies,

for example, simple and inexpensive biosensor devices, capable of rapid detection of environmental pollutions, is urgently needed.

2.5.1 Atomic absorption spectroscopy (AAS)

Atomic absorption spectrometry has been described as a spectral analytical procedure for the quantitative determination of chemical elements employing the absorption of light by free atoms in a gaseous state. AAS is one of the most important instrumental techniques for both quantitative and qualitative analysis of metallic and non-metallic elements in organic or inorganic chemicals [88]. The atomic absorption phenomenon has been noticed firstly in 1802 with Wollaston's observation when he detected the dark bands in the emission spectrum of sunlight [89]. In 1859, Kirchoff and Bunsen correctly explained Wollaston's observation by showing that the dark bands were due to the absorption of solar radiation by ground-state gas-phase atoms [90]. However, the process of absorption by atomic vapours would not be used as a quantitative analytical tool for nearly a century until Alan Walsh fabricated the first analytical atomic absorption spectrophotometer in 1953 [91]. Since its invention, atomic absorption spectroscopy (AAS) has gained acceptance as a standard method for the analysis of both metallic and non-metallic elements. AAS is widely accepted because of its high sensitivity at the parts-per-million level and below. Examples of application of AAS as a routine method of chemical analysis include various forms of industrial manufacturing, geology, medicine, and agriculture. The AAS technique has been divided into two stages: the conversion of an analyte molecule into its constituent atoms (atomization), and the subsequent absorption of radiation by these free atoms. AAS quantization is accomplished by measuring the amount of absorbing species at a given wavelength. AAS quantitation principles are based on the Beer-Lambert law, which establishes a linear relationship between the absorbance and the concentration of gas-phase atoms. The AAS instrumentation is similar to other high-resolution spectroscopic techniques, with the main difference in the radiation sources and the need of heating to vapourise materials. The atomic spectrometer schematically shown in Figure (2-4)

which operates as the follows radiation source. In short, electrons of atoms in the atomizer can be promoted to higher orbitals (excited state) for a short period of time (typically in nanoseconds) by absorbing a defined quantity of energy (radiation of a given wavelength). This amount of energy, i.e., wavelength, is specific to a particular electron transition in a particular element. In general, each wavelength corresponds to only one element, and the width of an absorption line is only of the order of a few picometers (pm), which gives the technique its elemental selectivity. The radiation flux without a sample and with a sample in the atomizer is measured using a detector, and the ratio between the two values (the absorbance) is converted to analyte concentration or mass using the Beer-Lambert Law [92]. Usually, this requirement is met by using a spectral source, such as the hollow cathode lamp [93]. AAS can be used to determine over 70 different elements in solution or directly in solid samples employed in pharmacology, biophysics and toxicology research. The technique makes use of absorption spectrometry to assess the concentration of an analyte in a sample. It requires standards with known analyte content to establish the relation between the measured absorbance and the analyte concentration [94].

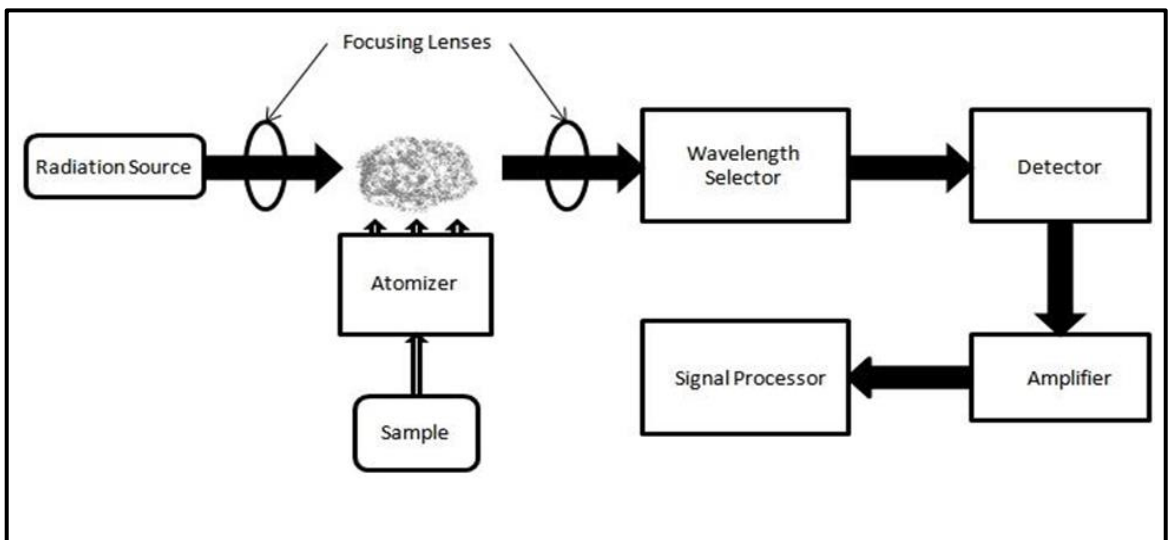


Figure 2-4: Schematic diagram of atomic absorption spectroscopy (AAS) [92].

2.5.2 Inductively coupled plasma mass spectrometry (ICP-MS)

The quantitative analysis of priority hazardous substances in the environment becomes more and more challenging because new legislation often requires more sensitive methods, or even completely new approaches, for the determination at very low concentrations (pg/L levels) of already defined priority compounds or newly emerging contaminants that show up in the environment as substitutes for already banned substances or as a result of changing industrial processes [95]. Since its introduction in the 1980s, inductively coupled plasma mass spectrometry (ICP-MS) has evolved to become arguably the most versatile, element-specific detection technique [96].

In parallel, because of the fast developments in the field of elemental speciation, the utilization concept of ICP-MS has undergone a significant change. It is a type of mass spectrometry which is capable of detecting metals and several non-metals at concentrations as low as one part in 10^{12} ppt (parts per trillion). Inductively coupled plasma-mass spectrometry (ICP-MS) is a very sensitive analytical technique with a high linear dynamic range (ultra-trace to main components). It is capable of analysing all elements from Li to U and can be applied to solutions, solids and gasses [97]. ICP-MS sampled material is transferred by an argon flow as shown in Figure 2-5 into inductively coupled plasma in which an effective temperature of 7000°K results in atomisation and ionisation of the material. Subsequently, the ions are extracted into a mass spectrometer, with which the elemental composition of the material is determined [98]. This is achieved by ionizing the sample with inductively coupled plasma and then using a mass spectrometer to separate and quantify those ions. Compared to atomic absorption techniques, ICP-MS has greater speed, precision, and sensitivity [99].

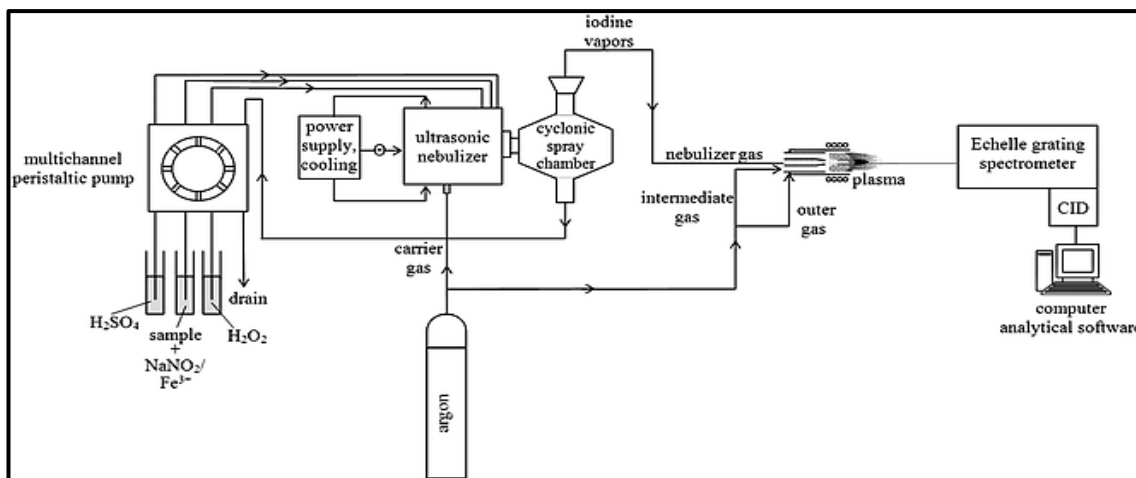


Figure 2-5: Schematic diagram of inductively coupled plasma mass spectrometry (ICP-MS) [100].

2.5.3 Chromatography

Chromatography is one of the most important analytical techniques used in pollutants residue analysis. It has two advantages which are, firstly, the sensitivity and specificity of the detection systems, secondly, the ability to separate the mixture of analytes in the column. Until recently gas/liquid chromatography (GLC) of pesticides was conducted using packed columns containing a variety of liquid phases and supports [101]. A wide range of volatilities and specific responses of pesticides necessitated numerous analytical conditions in order to chromatograph several classes of pesticides in a single sample. Many pesticides are too polar or do not respond on a packed column while others are thermally unstable and degrade during the chromatographic analysis. Electron capture is equipped to determine low amounts of residues from small samples of various substrates. Although total reliance should not be placed on the analytical data obtained from GLC for the identification of a pesticide residue, there is a need to compare it with other methods like GC-MS and LC-MS also using alternate column packings.

GLC deploys a physical method of separation of two phases, one stationary phase and the other mobile phase moving in a particular direction. Chromatography is the collective term for a set of laboratory techniques for the separation of mixtures. The

mixture is dissolved in a fluid, the mobile phase (as it shown in Figure 2-6), which carries it through a structure holding another material called as the stationary phase. The different components of the mixture travel at different speeds, causing them to separate. The separation is based on differential partitioning between the mobile and stationary phases. A subtle difference in a compound's adsorption coefficient results in differential retention in the stationary phase and thus in the separation of compounds. Chromatography may be preparative or analytical.

The purpose of preparative chromatography is to separate the components of a mixture for more advanced use (this is a form of purification) [102]. Analytical chromatography is done normally using small amounts of material and it measures the relative proportions of the analytes in a mixture. The two are not mutually exclusive. The above mentioned techniques are very expensive in both the actual equipment cost and exploitation cost which requires special laboratories and highly qualified personnel.

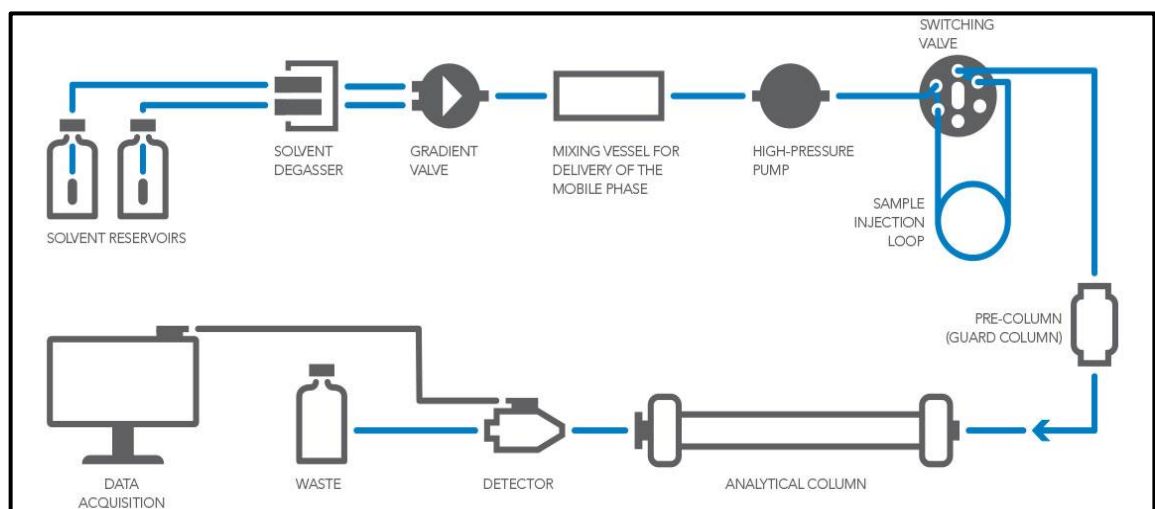


Figure 2-6: Schematic diagram of the chromatographic measuring process [103].

2.6 Biosensors and sensor arrays

Much more affordable option of pollution detection is the use of chemical sensors or biosensors which involves integration of recognition elements with transducing

materials for identifying the analyte activity or concentration which present in the sample. Since the mid-1980s there has been a continuous growth in the use of biosensors for environmental analysis owing to their advantages, such as screening of various contaminants in environmental matrices, minimizing sample pre-treatment, reducing the cost and time of analysis, and displaying sufficient sensitivity and selectivity [104]. Biosensors are formed by a combining molecular recognition, (such as an enzyme, an antibody, a microorganism, whole plant cell and tissue) and physicochemical transducer which convert chemical reaction into physical measurable parameter such as the signal (for example: an electrochemical, optical, piezoelectric and so on). A particular subclass of biosensors is represented by the electrochemical biosensors or bio-electrodes, in which combined enzymes and electrochemical transducer.

The general mechanism on which all bio-electrodes are based depends on the interaction between the analyte, present in the sample, and the biochemical component (typically enzyme) immobilized on the surface of the electrode: the consequent formation of one or more electro active species generates an electrical signal or a variation of the existing electrical signal, such signal can be easily recorded using suitable electrochemical apparatus and therefore it is proportional to the concentration or the activity of the chemical species to be determined.

Inhibition biosensors have been used for indirect monitoring of organic (e.g., pesticides) or inorganic substances (e.g., heavy metals) which inhibit its bio-catalytic properties of enzyme. The problem with these types of biosensors based in enzymatic inhibition is that only a few enzymes are sensitive to heavy metals [105] and majority of enzymes are extremely sensitive to environmental conditions such as temperature and pH and thus can not function for long.

The development and research of (bio) sensors is becoming one of the most popular scientific areas at the intersection of the biological and the engineering sciences. Semiconducting technology has developed so much that we see now a rapid infiltration

of new nanotechnology-based approaches in the field of sensors. The resulting new discipline of nanobiosensing is a good example of how engineering sciences, biosensor-related research has experienced an explosive growth over the last two decades. A biosensor is generally defined as an analytical device which converts a biological response into a quantifiable and processable signal [106]. Figure (2-7) shows schematically the following parts comprising a typical biosensor: (a), bioreceptor that specifically binds the analyte; (b), an interface architecture where a specific biological event takes place and gives rise to a signal picked up by (c), the transducer element. The transducer signal which could be anything from the in-coupling angle of a laser beam to the current produced at an electrode, is converted to an electronic signal and amplified by a detector circuit using the appropriate reference and sent for processing to (d), computer software which converts a physical parameter describing the process to electrical signals. Finally, the resulting signals are presented through (e), an interface to the human operator.

Biosensors can be applied to a large variety of samples including body fluids, food samples, cell cultures and be used to analyse environmental samples.

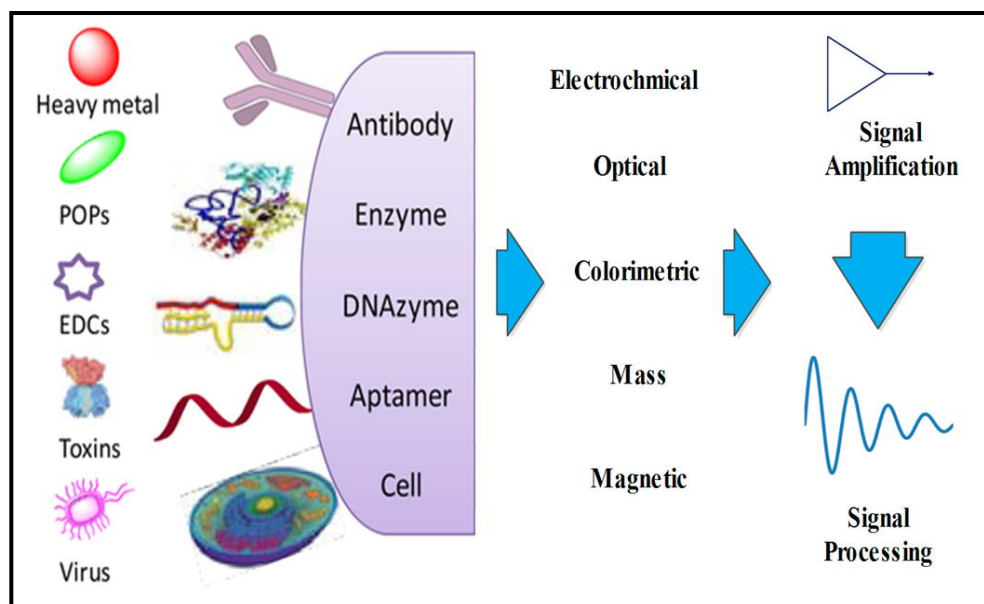


Figure 2-7: Typical biosensor elements [107].

In order to construct a reliable biosensor suitable the use by general public a number of conditions must be met:

1. The biocatalyst (i.e. enzyme, antibody and whole cell) must be highly specific for particular analyte of interest, be stable under normal storage conditions and show a low variation of performance between batches.
2. The reaction should be independent from variations of basic such physical parameters of the environment as temperature, pH and highly controlled stirring. This will allow the analysis of samples with minimal pre-treatment. If the reaction involves co-factors or co-enzymes these should be also immobilized on the surface of transducer
3. The response should be accurate, precise, reproducible and linear over the concentration range of interest, without dilution or concentration of samples. It should also be free from electrical or other transducer induced noise.
4. If the biosensor is to be used for invasive monitoring in the clinical environment, the probe must be tiny and biocompatible, not causing toxic or antigenic effects. Furthermore, the biosensor should not be prone to inactivation or proteolysis.
5. For rapid measurements of analytes from human samples it is desirable that the biosensor can provide real-time analysis.
6. The complete biosensor should be cheap, small, portable and capable of being used by semi-skilled operators.

2.6.1 Classification of biosensors

Biosensors can be broadly classified on the basis of bioreceptors types and transducing elements used:

I) On the basis of biological elements

- a) Enzyme biosensors: enzymes having high selectivity and activity towards specific substrata are the best candidates to be used as bio-receptors. Most of the enzymes used in biosensor are oxidizes but there are certain limitations as their activity is susceptible to pH, temperature, ionic strength etc.
- b) Microbial biosensors: they use either cell or microorganisms as biological element .The metabolism of cell or microorganism is used as a basis of their activity. They are cheaper and more versatile as compared to other sensor elements.
- c) Immune biosensors: they use antibodies as a bioreceptors which are immobilized on the surfaces of transducer
- d) Chemical biosensors: they use aptamers or DNA oligomers or synthetic binding proteins named affimers as a bioreceptors which are immobilized on the surfaces of transducer.

II) On the basis of transducing elements

- a) Electrochemical transducers: the three common types of electrochemical transducers are impedimetric, amperometric and potentiometric transducers. In amperometric transducers the potential between the two electrodes is set, and the current produced by oxidation / reduction of the electro - active species is measured and correlated with the concentration of the analyte of interest. Potentiometric sensors measure the potential of electrochemical cell with zero current. Impedimetric sensors are based on AC measurements of impedance.
- b) Optical transducers: they are used for determining the concentration of analyte on the basis of change in optical density or other optical parameters at appropriate wavelength of light, for example absorption, reflection , polarization, interference Photodetector as a function of incident angle. The examples are optical biosensors based on SPR surface plasmon resonance, wave guide interferometers and optical fibres
- c) Calorimetric transducers: they used for calculating the heat of biochemical reactions by measuring the temperature difference between the reaction vessel and isothermal heat sink surrounding it [108].

d) Gravimetric transducers: they are based on measurements of resonance frequency of piezoelectric materials which depends on the mass of adsorbed analyte. Typical examples are QCM quartz crystal microbalance and SAW surface acoustic wave sensors [109].

2.6.2 Whole-cell bacterial sensor array

Whole-cell bacterial biosensors have recently been used in environmental studies to quantify heavy metals and xenobiotic and antibiotic compounds [110]. Bacteria display many surface epitopes that can lead to nonspecific interactions with the sensor surface [111].

In the last few years, there have been dramatic advances in new analytical formats such as microarrays which have revolutionized our ability to characterize and quantify biologically relevant molecules [112]. The principle in all cases is the same. A large family of well-defined reactive molecules is fixed onto a mapped solid surface grid and exposed to a multi-component analyte mixture. Sites on the chip in which a recognition event has occurred (e.g. by a complementary nucleic acid sequence) are identified by one of several possible detection techniques, for example fluorescence. The characteristics of the sample can then be recognized from the nature of the bioreceptor molecules which binding to these sites. Using this principle, an increasingly large number of applications are being developed in medicine, biology, toxicology, drug screening and more. The idea of whole-cell arrays has been advanced by Van Dyk and co-workers [113].

A whole-cell-based biosensor is an analytical device that assimilates a whole cell as the biological component of the sensor. It gives high selectivity and has a physical transducer to generate an assessable signal relative to the concentration of the analyte [11]. Whole-cell biosensors are very specific in nature and the cost of such devices is generally low. They have many advantages such as the ease of use, transferability, and

the capacity to provide constant real-time signals [114]. The concept of synthetic biology offers a platform for redesigning of novel gene composition of a cell. This can be done by pairing a reporter gene that generates a signal with a contaminant-sensing component that responds to chemical or physical change to exposure to a specific analyte. A schematic of whole-cell biosensor is given in Figure (2-8)

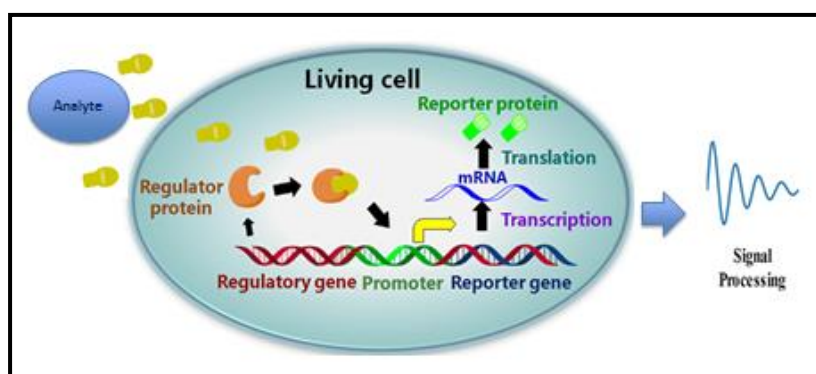


Figure 2-8: Schematic of whole-cell-based biosensor [115].

2.6.3 DNA Biosensors and microarrays

In recent years, there has been an enormous increase in the utilization of nucleic acids to recognize toxic compounds, specifically metal ions, because many toxic chemicals such as pollutants show a high affinity toward DNA/RNA. Metal ions exhibit a very high affinity toward DNA, as the interaction between DNA and metal ions either gives favourable or adverse effects such as DNA damage and gene mutation. For this reason, nucleic acid-based biosensors have been developed and used. DNA biosensors exploit the preferential binding of complementary single-stranded nucleic acid sequences. They usually rely on the immobilization of a single-stranded DNA probe onto a surface able to recognize its complementary DNA target sequence by hybridization [116].

Recently, an electrochemical DNA biosensor was developed to study DNA damage caused by several pesticides, such as atrazine, 2,4-D, glufosinate ammonium, carbofuran, paraoxonethyl and difluorobenzuron [117]. A biotinylated DNA probe was immobilized on a streptavidin-modified electrode surface. This DNA probe was hybridized with biotinylated complementary DNA target analyte. Streptavidin labelled

with ferrocene was further attached to the hybridized biotinylated DNA. The close proximity of ferrocene to the electrode surface induced a current signal. The presence of pesticides caused an un-winding of the DNA and thus a decrease of the ferrocene oxidation current which was observed (see Figure 2-9) in voltammetry experiments. Paraoxonethyl and atrazine caused the fastest and most severe damage to DNA.

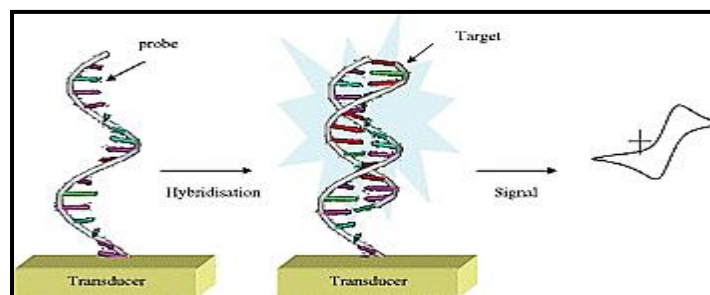


Figure 2-9: Schematic of electrochemical DNA biosensor [118].

2.6.4 Apta-sensors

In 1990, Ellington's group [119] reported the development of an *in vitro* selection technique which allowed the discovery of specific nucleic acid sequences that bind non-nucleic acid targets with high affinity and specificity. The technique was called SELEX (systematic evolution of ligands by exponential enrichment) and the resulting DNA or RNA oligonucleotides are referred to as aptamers [120].

Aptamers show high affinity towards a wide range of target analytes, including proteins, metal ions, and various organic and pathogenic microorganisms. Aptamers possess several competitive advantages over antibodies, first of all, their accurate and reproducible chemical production [121]. The selected nucleic acids bind their targets with affinity and specificity comparable to those of anti-bodies. Aptamers are more stable than antibodies. They can be selected in extreme conditions whereas antibodies are only stable in physiological conditions. Aptamers can undergo reversible denaturation and they can be easily modified with new functional groups without affecting their activity. Also aptamers are able to change their secondary structure by

engulfing the target. Such transformations can be detected using either ferrocene or electrochemical labels as shown in Figure (2-10). Because of these advantages, numerous aptamer-based biosensors have been developed for the detection of a wide range of targets [122]. There is little information for the detection of pesticides using aptamers. However, a single strand DNA aptamer with specific binding to acetamiprid was described [123]. The potential of aptamers for the pesticide and petrochemical detection has not been exploited yet but aptamer-based biosensors could be an alternative to the conventional methods of pollutants analysis.

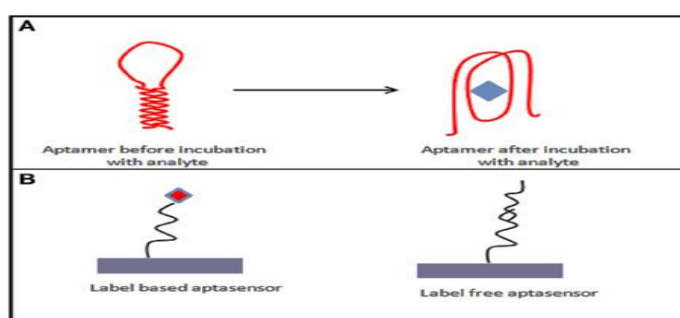


Figure 2-10: Schematic of aptamer-based biosensors, (A) hairpin and quadruplex shapes; (B) linear labelled and label free aptmer [124].

2.6.4.1 Aptamer selection process (SELEX)

Much of the success of nucleic acid aptamers is due to SELEX (systematic evolution of ligands by exponential enrichment; an elegant process by which aptamers can be generated for a given target (e.g protein) [125]. In SELEX, a single-stranded DNA library is first generated and exposed to the target. Any oligonucleotides within the library that bind to the target are retained, while the non-binding sequences are washed away [126]. Typically, the sequences in the library that bind to the target will be a small fraction of the total library so, after this first step, most of the library will have been washed away, and the overall concentration of DNA will be significantly reduced. The remaining (bound) sequences are then eluted and retained. In the next step, the

remaining (binding) sequences are amplified by polymerase chain reaction (PCR). This increases the concentration of DNA in preparation for the next round of SELEX. The library is now biased, or enriched, towards sequences that bind to the target [127].

The process is repeated many times. Often, the binding conditions are made more stringent as SELEX proceeds through each round, increasing the selection pressure. Successive selection and amplification result in a library that, at the end of the SELEX process (typically 8-15 rounds), contains only sequences that bind strongly to the target. After SELEX is complete, the binding sequences need to be identified, which is done by sequencing [128]. Figure (2-11), shows the SELEX process.

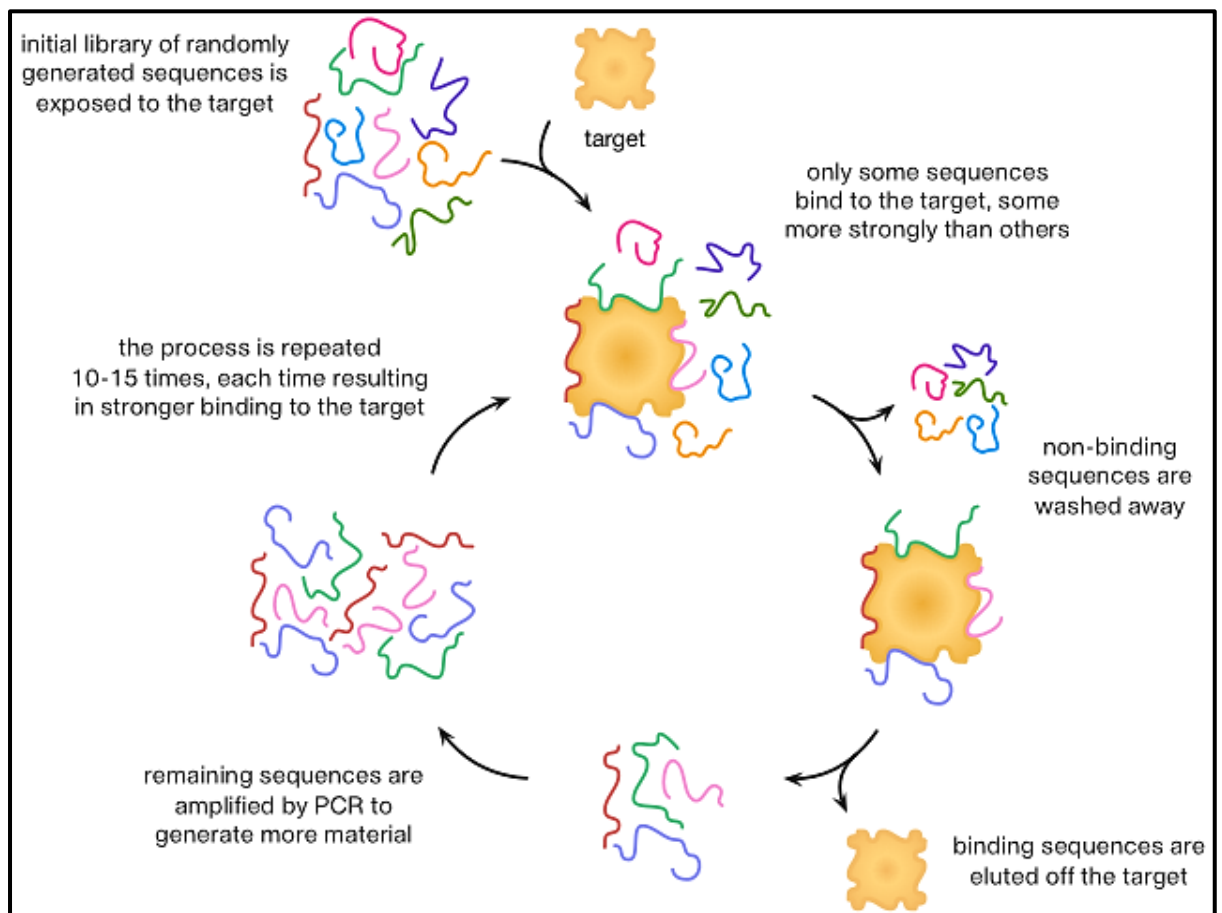


Figure 2-11: SELEX process [129].

2.6.4.2 Structure and types of aptamers

Aptamers have different types of secondary structure which depends on the nucleotide sequence used to accommodate particular targets. Typical 3D secondary structures are shown below and illustrated in Figure (2-12)

1. Hairpin (or stem-loop) occurs when two regions of the same strand are complementary to one another and can form Watson-Crick base pairs.
2. Quadruplex occurs in guanine-rich sequences, when four guanine bases can associate through hydrogen bonding.
3. Kissing complex formed when the unpaired nucleotides in one hairpin loop base pair with the unpaired nucleotides in another hairpin loop. Usually occurs in RNA.

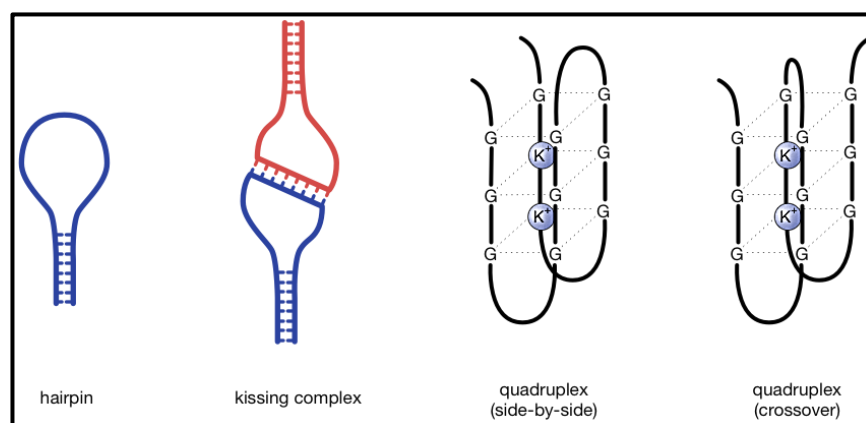


Figure 2-12: Aptamer secondary structures [130].

2.6.5 Immobilization of bioreceptors

The basic requirement of a biosensor is that the biological material should bring the physicochemical changes in close proximity to the transducer. In this sense, the immobilization technology has played a major role to get the solution [131]. Immobilization not only helps in forming the required close proximity between the biomaterial and the transducer, but also helps in stabilising it for reuse. The biological

material has been immobilised directly on the transducer or in most cases, in membranes, which can subsequently be mounted on the transducer. Biomaterials can be immobilised either through adsorption, entrapment, covalent or electrostatic binding, cross-linking or a combination of these techniques.

Several immobilization techniques such as covalent binding, physical entrapment, adsorption, cross-linking, and encapsulation have been reported in literature but not a single technique can be considered as a universal method of immobilization to achieve the better biosensor response. The most important factor to be considered while designing a biosensor is to attain higher sensitivity, and functional stability. For immobilization of whole bacteria as bio-sensitive cells on the sensor surface, a bio-receiving membrane was coated using an electrostatic layer-by-layer (LbL) deposition method. In recent years indeed, polyelectrolyte multilayers (PEM) represented a new attractive way for creating bio-functionalized surface coatings. The LbL assembly technique consists in the alternate deposition of polyanions and polycations from aqueous solutions to build ultrathin multi-layered films on flat substrates [132]. It was first introduced to immobilize biomacromolecules such as doxorubicin [133].

2.6.6 Methods of immobilization

Immobilization of bioreceptors in biological processes can occur either as a natural phenomenon or through artificial process [134]. Different immobilization types have been defined: covalent coupling/cross linking, capture behind semi-permeable membrane or encapsulation, entrapment and adsorption [135]. The types of immobilization can be grouped as “passive” (using the natural tendency of molecules to attach to surfaces-natural or synthetic, and grow on them) and “active” (flocculants agents, chemical attachment and gel encapsulation) [136].

2.6.6.1 Covalent binding/cross linking processes

The mechanism involved in this method is based on covalent bonds formation between activated inorganic support and the cell in the presence of a binding (crosslinking)

agent. For covalent linking, chemical modification of the surface is necessary. Covalent attachment and cross-linking are effective and durable to enzymes and antibodies, but it is rarely applied for immobilization of cells. It is caused mainly by the fact that agents used for covalent bonds formation are usually cytotoxic and it is difficult to find conditions when cells can be immobilized without any damage [134]. There are few reports of successful covalent binding of cells and most of them are related to yeast. Navarro and Durand (1977) [137], published an article describing a successful way of covalent binding of *Saccharomyces carlsbergensis* on porous silica beads. Two years later, there was another publication concerning yeast (*Saccharomyces cerevisiae*, *Saccharomyces amurcea*) immobilization with this method on borosilicate glass and zirconia ceramics [138].

2.6.6.2 Entrapment process

Entrapment is an irreversible method, where immobilized cells are entrapped in a support matrix or inside fibres. This technique creates a protective barrier around the immobilized microbes, ensuring their prolonged viability during processing and storage in polymers [139]. Entrapment is the most extensively studied method in cell immobilization. The matrices used are agar, alginate, carrageenan, cellulose and its derivatives, collagen, gelatine, epoxy resin, photo cross-linkable resins, polyacrylamide, polyester, polystyrene and polyurethane [134]. Entrapment of the microorganisms in porous polymer carrier was often used to capture the microorganisms from suspended solution and then obtain the immobilized microorganisms. As a rule, the entrapment methods are based on the inclusion of cells within a rigid network to prevent the cells from diffusing into surrounding medium while still allowing penetration of the analyte. Entrapment of cells in alginate gel is popular because of the requirement for mild conditions and the simplicity of the used procedure. Entrapment allows high mechanical strength, but has some disadvantages, such as, cell leakage, costs of immobilization, diffusion limitations, and deactivation during immobilization and abrasion of support material during usage. Another disadvantage is low loading capacity as biocatalysts have to be incorporated into the support matrix [140].

2.6.6.3 Encapsulation process

Encapsulation is another irreversible immobilization method, similar to entrapment. In this process, bioreceptors are restricted by the membrane walls (usually in a form of a capsule), but free-floating within the core space [139]. The membrane itself is semi-permeable, allowing for free flow of substrates and nutrients (when cells are used as a biocatalyst), yet keeping the biocatalyst inside. The factor determining this phenomenon is the proper pore size of the membrane, attuned to the size of core material. This limited access to the microcapsule interior is one of the main advantages of microencapsulation, for it protects the biocatalyst from the harsh environmental conditions. As most immobilization method, it prevents biocatalyst leakage, increasing the process efficiency as a result [141]. However, even though in encapsulation, high cell loading can be achieved, but the capsules are still very weak [142]. The diffusion limitation is one of the inevitable drawbacks associated with encapsulation method [143].

2.6.6.4 Adsorption process

Cell immobilization is probably the simplest method of reversible immobilization [144]. This technique is based on the physical interaction between the microorganism and the carrier surfaces, simple, cheap and effective. The immobilization of microorganisms on properly chosen adsorbents stimulates microbial metabolism, protects cells from unfavorable agents, and preserves their physiological activity [145]. This cell immobilization technique involves the transport of the cells from the bulk phase to the surface of support (porous and inert support materials), followed by the adhesion of cells, and subsequent colonization of the support surface [146].

Adsorption is based on weak forces. However, it still enables efficient binding process. Usually in bonds formation, several forces are involved: van der Waals forces, ionic and hydrophobic interactions and hydrogen bonds. Both electrostatic and hydrophobic interactions govern the cell-support adhesion, which is the key step in controlling the cell immobilization on the support [139].

Due to their high specific surface area, void volume, mechanical and permeability, low pressure drop, diffusion problems and toxicity, maximum loading, biodegradability and durability and low cost and high availability, they are widely applicable [147].

2.6.6.5 Metal-link/chelation process

A partial explanation of this immobilization method seems to be the formation of covalent bonds between the gelatinous hydrous metal oxides used as support materials and suitable ligands contributed by proteins and carbohydrates present on the cell surface [148]. Hydrous titanium (IV) and zirconium (IV) oxides seem to have minimal effects on the activity of enzymes immobilized to these supports, and yeast cells immobilized in this way have remained viable, according to measurements of their external invertase activity in the periplastic space [149]. The cells also appeared to be quite firmly attached to the surface of the metal oxide. Cells of *Arthrobacter globiformis* have also been covalently bound to silica gel after activation with chromium (III) chloride and such immobilized cells were capable of steroid transformation. Cells immobilized on transition-metal-activated inorganic supports appeared to be operationally stable [148].

2.6.7 Inhibition bacterial sensor array

The main problem of using chemical and biosensors for detection of any toxic chemicals which considered as environmental pollutants is the requirements of specific receptors for every analyte of interest. Advances in synthetic chemistry and biochemistry allow these requirements, to be fulfilled though it is not easy and appeared to be the most expensive part of sensor development. An alternative approach lies in the development of inhibition sensors which utilize enzymes, cells, microorganisms as bioreceptors whose function can be inhibited by pollutants. Such reactions are not specific, e.g. bioreceptors could be inhibited simultaneously by different analytes, so that a single sensor can not differentiate the analytes. This can be done using a sensor array approach in which each sensor is affected differently by different analytes. Such a

sensor array equipped with the appropriate data processing system such as an artificial neural network (ANN) is capable of differentiating responses to several analytes. Our recent research, proved the concept of such inhibition sensor array using bacteria as sensing elements. Series of optical and electrochemical measurements of two types of bacteria (*E.coli* and *Deinococcus radiodurance*) allowed discrimination of two types of pollution, i.e. heavy metals (Ni,Cd) and radionuclides which emit γ -radiation [150]. There are many previous studies focused on using bacteria as sensing elements for different analytes detection and different sample sources based on optical and electrochemical transducers which are summarized in Table (2-1) as bacterial biosensors for detection of different toxic chemicals and pollutants.

Table 2-1. Bacterial biosensors for different pollutants detection.

Analyte	Bacterial type Biosensor	Transducer type	Sample	Reference
Zinc, copper, cadmium, and nickel	<i>Pseudomonas fluorescens</i> 10586s pUCD607 with the lux insertion on a Plasmid	Optical	Soil	[151]
Zinc, copper, cadmium, nickel, lead, iron, and aluminium	<i>Chlorella vulgaris</i> strain CCAP 211/12	Electrochemical	Waste	[152]
Zinc, cobalt, and Copper	<i>Pseudomonas</i> sp. B4251, <i>Bacillus cereus</i> B4368, and <i>Escherichia coli</i> 1257	Electrochemical	Water	[153]
Organophosphates, urea, and ethanol	<i>Flavobacterium</i> sp., <i>Bacillus</i> sp., <i>Saccharomyces Ellipsoideus</i>	Potentiometric	Laboratory Isolate	[154]
Mercury,lead,znic,cadmium atrazine, simazine,DDVP,hexane,octane pentane, pyrene,toluene and ethanol.	<i>E.coli</i> k12 <i>Shewanella oneidensis</i> <i>Methylococcus capsulatus</i> (<i>Bath</i>) and <i>Methylosinus trichosporium</i> (<i>OB3b</i>)	Electrochemical	Laboratory Isolate	This work

2.6.8 Electrochemical sensors based on immobilized bacteria cell

The examples which are given in the previous table are important as a further step towards the development of bacteria-based inhibition sensor array, but it is still far away from real sensor development. Dealing with liquid bacteria samples is not the way forward because of natural variations in bacterial concentration even in laboratory samples not to mention “real” samples taken for analysis. The problem of having a reliable reference for such measurements is a very difficult one. It would be much more useful for real sensor development to use bacteria immobilized on the electrode surface. Changes in biological parameters, including the cells number or cells size, can be studied and monitored in the electrical properties of the bio-cells, i.e. with a bio-cell sensor. A typical biosensor based whole cell consists of an anode and cathode, separated with an electrolyte solution, where the cathode electrode is coated with a cell-culture [155]. The current that easily passed through the aqueous electrolyte solutions can be affected by less conductive bacteria or cells which contain the lipid bilayer of the bacteria cells' membrane acting as an insulator. These measurements can be performed on two or three electrode systems, with working electrodes coated with cell cultures. The applied external electrical field catalyses the live bacteria (that had a lipid layer) accumulating on the working electrode, creating an isolation layer coating the electrode, the conductivity decreasing as a result of this effect. Different artefacts, such as some toxic chemicals and radiation, may affect the functioning of cells (increasing or reducing the number of viable bacteria) that appear as conductivity decreases or increases [156]. Therefore, comparing the results of electrochemical tests performed on a fresh cell culture and after exposure to the artefact can provide information on the concentration of pollutants or radiation dose. In the current project, this idea was explored using bacteria. The three electrodes electrochemical set up is more stable than the two electrodes. Firstly, it contains an additional reference electrode having a stable electrochemical potential invariant of applied voltage and chemical composition of the

solution; the potentials of other two electrodes are measured in respect to a reference electrode [157].

Two parallel plate electrodes are indicated as the working and counter electrodes, the third reference electrode was placed close to the working electrode. The electrical potentials of both working and counter electrodes are measured in respect to the reference electrode having a constant potential in electrolytes solutions. Typically Ag/AgCl reference electrodes are used in such measurements. Working and counter electrodes are typically made of metal or carbon. The working electrode is coated with the investigated substance, in this project cell-culture. Gold-coated glass slides seem to be the most common for working electrodes, since the chemistry of modification of gold is well established for coating gold with different biomaterials. Counter electrodes should be chemically inert; such as platinum or gold which is commonly used for this purpose. However, even chemically inert metals, such as Au and Pt, show instability of surface potential during electrochemical reactions, when a current flowing between electrodes is accompanied with chemical ion exchange electrode reactions. In this case, the role of the reference electrode is crucial for performing accurate electrochemical measurements that are typically carried out using potentiostat. In some cases, however, when electrochemical reactions are not essential, simple measurements can be performed in a two-electrode system without using reference electrode and potentiostat. These simple electrochemical measurements are used in order to establish the correlation between electrical properties (conductivity, capacitance, current or resistance) of liquid bacteria samples and live bacterial counts, after that studying the effect of γ -radiation and heavy metal ions on bacteria. The use bacteria in suspension were essential for preliminary *in-vitro* study of the effect of pollutants. However, it is of limited use in biosensors. Immobilized bacteria are much more promising for such applications. The measurements have to be taken twice, first on freshly immobilized bacteria, then on on bacteria exposed to pollutants. Electrochemical measurements were successfully used for studying electrical properties of cells deposited on metal

electrodes and showed great prospects in using such cell-based sensors for detection of various analytes [25, 26]. In the previous study, the principles of cell-sensors were extended further to more complex organisms, such as *E. coli*, and another type of bacteria, *D. radiodurans*, which is known for its high resistance to γ -radiation [150].

2.7 Bacteria as sensing elements and pollutants re-mediators

Different types of microorganisms (bacteria) were utilised as sensor elements in this study for detection of a large number of toxic chemicals, depending on if they were highly resistant or sensitive to these pollutants. The types of bacteria which can resist or tolerate some of environmental pollutants which are in general classified as gram negative, may be due to the presence of an extra membrane layer. Atypical example of such species is *S. oneidensis* known as a highly resistant and tolerant bacteria to different pollutants. On the other hand, highly sensitive Gram negative bacteria such as *E. coli* which is considered to be sensitive to the pollutants while *Methylococcus capsulatus* (Bath) and *Methylosinus trichosporium* (OB3b) may be highly sensitive to some pollutants, for instance heavy metals and pesticides and highly resistant to others such as petrochemical. In this study HgCl_2 , PbCl_2 , ZnCl_2 and CdCl_2 were used to study the effect of heavy metal ions on *E. coli*, *Mc. capsulatus* (Bath) & *Ms. trichosporium* and *S. oneidensis* samples. In the current project this approach will be developed further using simple electrochemical measurements on electrodes with immobilized bacteria, for extended range of analytes including heavy metals, pesticides and petrochemicals. The selection of bacteria can serve the purpose since *E. coli* is predominantly affected by heavy metals, while *S. oneidensis* requires them as nutrient and Methanotrophic bacteria thrive in the presence of some hydrocarbons. The desirable outcome of this PhD project will be the development of a sensor array prototype capable of differentiating the above pollutants. Such an inhibition sensor array may not be sensitive enough for all environmental pollutants, however, they can be used for quick preliminary detection

(screening) of water samples utilizing ANN subsequently these suspected samples could be transferred to conventional laboratory for further analysis.

2.7.1 General description of bacteria

Bacteria are typically between 0.5 μm and 5 μm in size, displaying different shapes, including spherical cocci, rod-shaped bacilli, and spiral-shaped spirilla or spirochetes, among others. Unlike eukaryotic cells, most bacteria are encapsulated by a cell wall which is present on the outside of the cytoplasmic membrane. The cell wall comprises mainly peptidoglycan, a negatively charged polymer matrix comprising of cross-linked chains of amino sugars, namely, *N*-acetylglucosamine and *N*-acetylmuramic acid. Bacteria can be classified as either Gram positive or Gram negative depending upon the architecture and thickness of the cell wall. Gram-positive bacteria retain the violet Gram stain due to their thick peptidoglycan layer on the outside of the cell membrane. In contrast, Gram-negative bacteria do not take up the stain, as their thinner peptidoglycan layer is sandwiched between two cell membranes. The outer lipid membrane of Gram-negative bacteria also contains lipopolysaccharides (LPS), which act as endotoxins and elicit a strong immune response in humans, as well as various proteins, including porins. The thick peptidoglycan wall surrounding Gram-positive bacteria contains extra components such as lipids, surface proteins, and glycoproteins. Pathogenic Gram-negative bacteria include *Escherichia coli*, *Salmonella*, *Shigella*, *Legionella*, *Haemophilis influenzae*, *Neisseria gonorrhoeae*, and *Neisseria meningitides*. Examples of pathogenic Gram-positive bacteria include *Streptococcus*, *Staphylococcus*, *Bacillus*, and *Clostridium* [158].

Bacteria comprise a large domain of prokaryotic microorganisms. Typically, a few micrometres in length, bacteria have a wide range of shapes, ranging from spheres to rods and spirals [159]. They were among the first life forms to appear on Earth, and are present in most habitats on the planet, including soil, acidic hot springs, radioactive waste, water, and deep in the Earth's shell, as well as in organic matter and the live

bodies of plants and animals, providing outstanding examples of mutualism in the digestive tracts of humans [160]. There are typically 40 million bacterial cells in a gram of soil and a million bacterial cells in a millilitre of fresh water. In all, there are approximately 5×10^{30} bacteria living on our planet [161, 162], forming a biomass that exceeds that of all plants and animals. Bacteria are vital in recycling nutrients, with many steps in nutrient cycles depending on these organisms, such as the fixation of nitrogen from the atmosphere and putrefaction [163]. In biological communities surrounding hydrothermal vents and cold seeps, bacteria provides the nutrients needed to sustain life by converting dissolved compounds such as hydrogen sulphide and methane. Most bacteria have not been characterised, and only about half of the phyla of bacteria have species that can be grown in the laboratory. Bacterial cells are about one tenth the sizes of eukaryotic cells and are typically 0.5-5.0 μm in length. However, a few species are up to half a millimetre long and are visible by the naked eye [164], for example, *Epulopiscium fishelsoni* reaches 0.7 mm [165]. Among the smallest bacteria are members of the genus *Mycoplasma*, which are parasitic organism in animal cell and measure only 0.3 μm , as small as the largest viruses. Some bacteria may be even smaller [166].

Most bacterial species are either spherical, called cocci or rod-shaped, called bacilli. The bacterial cell are surrounded by a lipid membrane, or cell membrane, which encloses the contents of the cell and acts as a barrier to hold nutrients, proteins and other essential components of the cytoplasm within the cell. As they are prokaryotes, bacteria do not tend to have membrane-bound organelles in their cytoplasm and thus contains few large intracellular structures. They consequently lack a true nucleus, mitochondria, chloroplasts and other organelles present in eukaryotic cells, such as the Golgi apparatus and endoplasmic reticulum [167]. Bacteria were once seen as simple bags of cytoplasm, but elements such as prokaryotic cytoskeleton [168] and the localization of proteins to specific locations within the cytoplasm have been found to show levels of complexity. These sub-cellular compartments have been called "bacterial hyper structures". Micro-

compartments such as carboxysomes supply a further level of organization, which are compartments within bacteria that are surrounded by polyhedral protein shells, rather than by lipid membranes. These "polyhedral organelles" restrict and compartmentalize bacterial metabolism, a function performed by the membrane-bound organelles in eukaryotes.

Many important biochemical reactions, such as energy generation, occur by concentration gradients across membranes. The general lack of internal membranes in bacteria means reactions such as electron transport occur across the cell membrane between the cytoplasm and the periplasmic space. However, in many photosynthetic bacteria the plasma membrane is highly folded and fills most of the cell with layers of light-gathering membrane. These light-gathering complexes may even form lipid-enclosed structures called chlorosomes in green sulphur bacteria [169]. Other proteins import nutrients across the cell membrane, or expel undesired molecules from the cytoplasm.

Bacteria do not have a membrane-bound nucleus, and their genetic material is typically a single circular chromosome located in the cytoplasm in an irregularly-shaped body, called the nucleoid. The nucleoid contains the chromosome, with associated proteins and RNA. The order Planctomycetes are an exception to the general absence of internal membranes in bacteria because they have a double membrane around their nucleoids and contain other membrane-bound cellular structures. Like all living organisms, bacteria contain ribosomes for the production of proteins, but the structure of the bacterial ribosome is different from those of eukaryotes and Archaea. Some bacteria produce intracellular nutrient storage granules, such as glycogen, polyphosphate, and sulfur or poly hydroxyalcanoates. These granules enable bacteria to store compounds for later use [170]. One of bacterial phyla, named photosynthetic cyanobacteria, are able to produce internal gas vesicles, which they use to regulate their buoyancy, allowing them to move up or down into water layers with different light intensities and nutrient levels and split H_2O and make O_2 .

2.7.2 Bacterial cell wall structure

In most bacteria a rough external layer, the cell wall, protects the delicate protoplast from mechanical damage and osmotic lysis; it also determines a cell's shape. Additionally, the cell wall acts as a molecular filter, a permeability barrier that excludes various molecules. It also plays an active role in regulating the transport of ions and molecules. The cell walls of different species may differ greatly in thickness, structure and composition. There are broadly speaking two different types of cell wall in bacteria, whether a given cell has one or the other type of wall can generally be determined by the cells reaction to certain dyes, these two types called Gram-positive and Gram-negative. The names originate from the reaction of cells to the Gram stain (red stain), a test long-employed for the classification of bacterial species. Gram-positive bacteria (are a class of bacteria that take up the crystal violet stain used in the gram staining method of bacterial differentiation), which possess a thick cell wall (about 30-100 nm) and it generally has a simple, uniform appearance under the electron microscope. Some 40-80% of the wall is made of a tough, complex polymer, peptidoglycan. Essentially, peptidoglycan consists of linear hetero polysaccharide chains and teichoic acids [171]. In contrast, Gram-negative bacteria (are a class of bacteria that do not retain the crystal violet stain (stained red) used in the Gram staining method of bacterial differentiation), which it have a relatively thin cell wall (20-30 nm) with a distinctly layered appearance under the electron microscope. The inner layer nearest the cytoplasmic membrane is widely believed to consist of a few layers of peptidoglycan (15 nm thick) surrounded by a second lipid membrane, containing lipopolysaccharides and lipoproteins. Most bacteria have the Gram-negative cell wall, and only the *Firmicutes* and *Actinobacteria* (which are known as the low G+C and high G+C Gram-positive bacteria, respectively) have the alternative Gram-positive arrangement [172]. These differences in structure can produce differences in antibiotic susceptibility. Therefore, the lipid membrane reaction for gram stain helped the researcher to distinguish between the bacteria. The simple structure of a bacteria cell is shown in Figure (2-13).

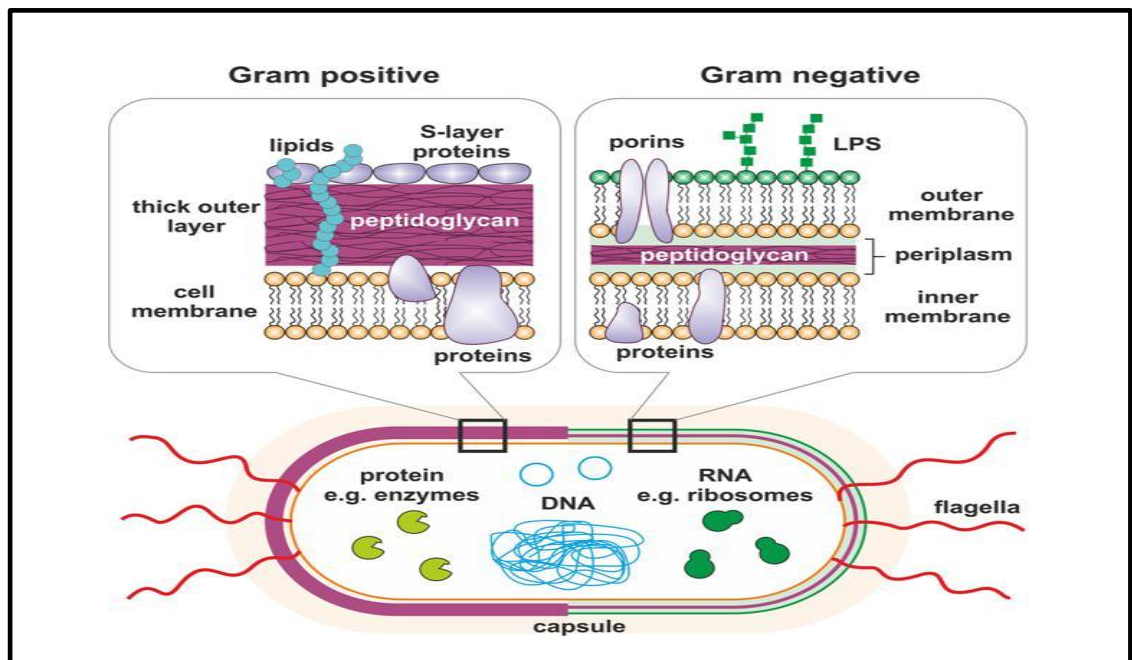


Figure 2-13: The schematic structural image of a typical Gram-positive and Gram-negative bacteria cell [173].

The lipid membrane is a thin polar membrane consisting of two layers of lipid molecules. These membranes are flat sheets that form a continuous barrier around cells. The cell membrane of almost all living organisms and many viruses are covered by a lipid, as are the membranes surrounding the cell nucleus and other sub-cellular structures. The lipid layer is the barrier that keeps ions, proteins and other molecules where they are needed and prevents them from diffusing into areas where they should not be. Lipid layers are ideally suited to this role because, even though they are only a few nanometres in width, they are impermeable to water-soluble (hydrophilic) molecules and are particularly impermeable to ions, which allow cells to regulate salt concentrations and pH by pumping ions across their membranes using proteins called ion pumps. In many bacteria there are fine, hair like proteinaceous filaments extending from the cell surface; these filaments can be divided into three main types: flagella, fimbriae and pili. Sex pili (singular: pilus) are elongated or hair-like proteinaceous structures which project from a cell's surface; they are found specifically on those

Gram-negative cells which have the ability to transfer DNA to other cells by conjugation, a process in which the pili themselves play an essential role. The various types of pili differ in size and shape: for example, some are long, thin and flexible, while others are short, rigid and nail-like, the type of pilus correlates with the physical condition under which conjugation can take place.

2.7.3 Growth of bacteria

Bacteria cell growth involves a coordinated increase in the mass of its constituent parts; it is not simply an increase in total mass, since this could be due, for example, to the accumulation of a storage compound within the cell. Usually, growth leads to the division of a cell into two similar or identical cells. Thus, growth and reproduction are closely linked in bacteria, and the term growth is generally used to cover both processes. Bacteria grow only if their environment is suitable; if it's not optimal, growth may occur at a lower rate or not at all or the bacteria may die, depending on species and condition. Essential requirements for growth include, (i) a supply of suitable nutrients; (ii) a source of energy; (iii) water; (iv) an appropriate temperature; (v) an appropriate pH; (vi) appropriate levels (or the absence) of oxygen. Consider the growth of bacteria on a solid medium of one common type of solid medium widely used in bacteriological laboratories, which is a jelly like substance (an agar gel) containing nutrients and other ingredients. Suppose that a single bacterial cell is placed on the surface of such a medium and given everything necessary for growth and division. The cell grows, division continues, the progeny of the original cell eventually reach such immense numbers that they form a compact heap of the cells that is usually visible to the naked eye; this mass of cells is called a colony. In addition, either bacterium can move freely through a liquid medium by diffusion or, in motile species, by active movement; thus, as cells grow and divide, the progeny are commonly dispersed throughout the medium. Usually, as the concentration of cells increases, the medium becomes increasingly turbid (cloudy), so that each bacterial species need specific medium and particular environmental conditions for pure growth [174]. This study utilized three kinds of bacteria to scan a wide range of environmental pollution.

2.8 Types of Bacteria used as sensing elements in this work

2.8.1 *Escherichia coli* K-12 strain

E. coli K-12 is a Gram-negative, rod-shaped bacterium commonly found in the intestine of warm-blooded organisms (endotherms). Most of *E. coli* strains are non-pathogenic, but some of them can cause serious food poisoning in human e.g. *E. coli* O157 and several kinds of disease in animals, which are occasionally responsible for product recalls due to food contamination [175]. The non-pathogenic strains are part of the normal flora of the gut, and can benefit their hosts by producing vitamin K2, and by preventing the establishment of pathogenic bacteria within the intestine. This work aims at the development of novel sensing technologies based on different types of bacteria as inhibition sensing array for detection of petrochemicals, pesticides and heavy metals. *E. coli* belongs to the Gram-negative bacteria, and was selected for this task. Also, it is facultative anaerobic, rod shape. As mentioned in previous sections, there are hundreds of different strains of *E. coli*: some are harmless; others cause serious illness. A non-pathogenic strain of *E. coli* (K12) normally present in the intestinal tract in humans and animals was used in this study. Figure (2-14) shows the *E. coli* bacteria cells and their colonies.

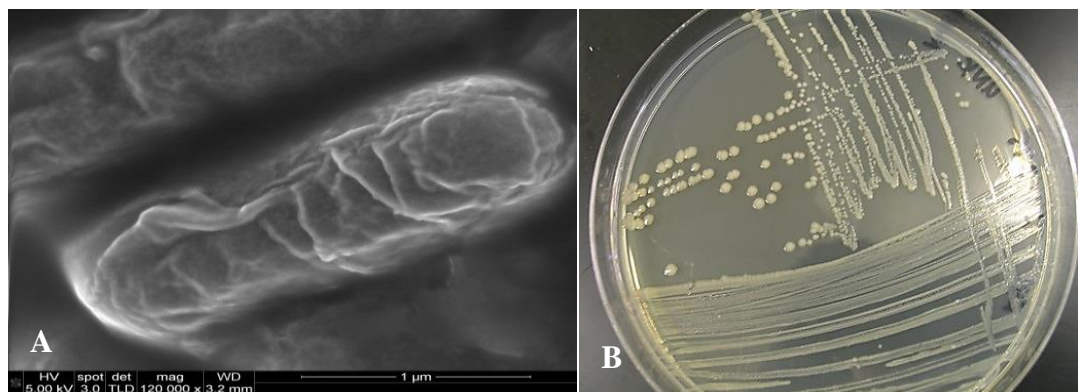


Figure 2-14: (A) SEM image of *E. coli* (K12 strain) Gram-Negative bacteria cells (B); their culture colonies.

2.8.2 *Shewanella oneidensis* MR-1 strain

Shewanella oneidensis MR-1 a facultative anaerobe classified as a gamma proteobacterium, can utilize numerous inorganic compounds as electron acceptors (e.g., oxygen, nitrate, and metals). *Shewanella oneidensis* MR-1 (formerly *Alteromonas putrefaciens* and *Shewanella putrefaciens*) best known for its respiratory versatility, including the ability to reduce metal oxides and radionuclides. Like many other members of the *Shewanella* genus, it can also grow aerobically or use any of a broad variety of organic (fumarate, trimethyl-amine oxide, dimethyl sulfoxide, and glycine) and inorganic (nitrate, elemental sulphur, thiosulfate, and sulphite) compounds as terminal electron acceptors in the absence of O₂. This strain was originally isolated from anaerobic sediments of Oneida Lake in New York through the selective enrichment of bacteria that could respire Mn (IV) [176]. Members of the *Shewanella* genus are frequently isolated from redox-stratified freshwater and marine environments, where they are proposed to play an important role in the geochemical cycling of nitrogen [177], metals [178] and sulphur [179]. Figure (2-15). Shows the SEM image of *S.oneidensis* (MR-1 strain) Gram-Negative bacteria cell (A), and their colonies (B)

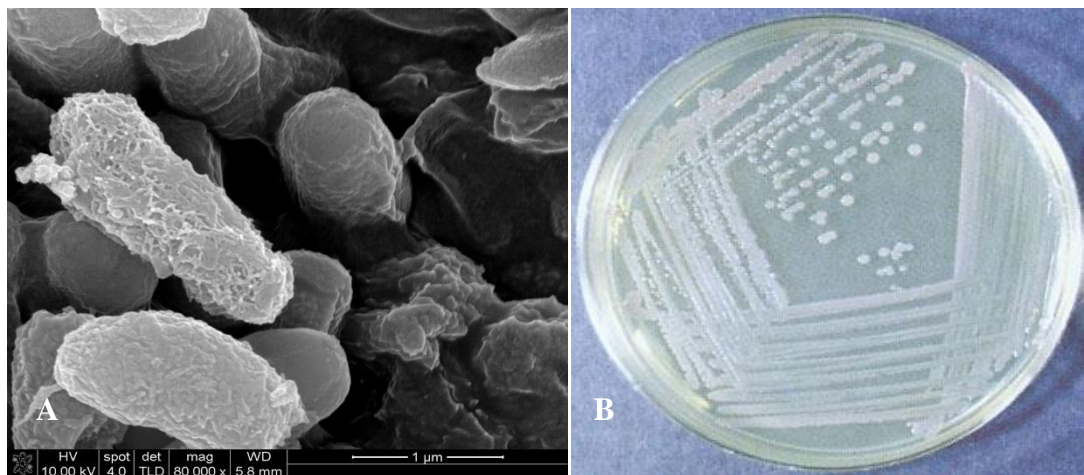


Figure 2-15: (A) SEM image of *S.oneidensis* (MR-1 strain) Gram-Negative bacteria cell (B); their culture colonies.

2.8.3 Methanotrophic bacteria

Methane-utilizing bacteria (methanotrophs) are a diverse group of gram-negative bacteria that are related to other members of the Proteobacteria. These bacteria are classified into three groups based on the pathways used for assimilation of formaldehyde, the major source of cell carbon, and other physiological and morphological features. The type I and type X methanotrophs are found within the gamma subdivision of the Proteobacteria and employ the ribulose monophosphate pathway for formaldehyde assimilation, whereas type II methanotrophs, which employ the serine pathway for formaldehyde assimilation, form a coherent cluster within the beta subdivision of the Proteobacteria. Methanotrophic bacteria are ubiquitous. The growth of type II bacteria appears to be favored in environments that contain relatively high levels of methane, low levels of dissolved oxygen, and limiting concentrations of combined nitrogen and/or copper. Type I methanotrophs appear to be dominant in environments in which methane is limiting and combined nitrogen and copper levels are relatively high. These bacteria serve as biofilters for the oxidation of methane produced in anaerobic environments, and when oxygen is present in soil, atmospheric methane is oxidized. A limited number of methanotrophs have the genetic capacity to synthesize a soluble methane monooxygenase which catalyzes the rapid oxidation of environmental pollutants including trichloroethylene. [180]. (See Figure 2-16)

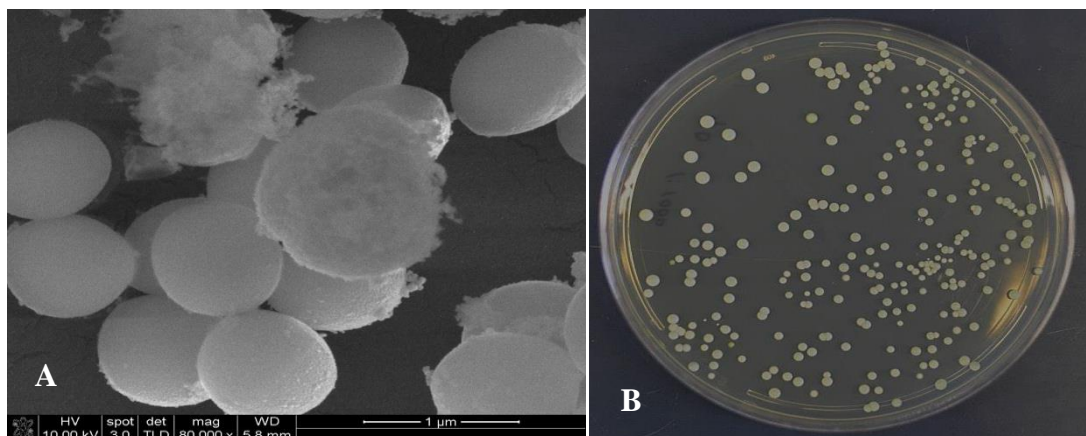


Figure 2-16: (A) SEM image of *Mc. capsulatus* (Bath strain) Gram-Negative bacteria cell (B); their culture colonies.

References

1. Wanekaya, A. K., Chen, W., & Mulchandani, A. (2008). Recent biosensing developments in environmental security. *Journal of Environmental Monitoring*, 10(6), 703-712.
2. Faragó, I., Georgiev, K., & Havasi, Á. (Eds.). (2006). *Advances in Air Pollution Modeling for Environmental Security: Proceedings of the NATO Advanced Research Workshop Advances in Air Pollution Modeling for Environmental Security*, Borovetz, Bulgaria, 8-12 May 2004 (Vol. 54). Springer Science & Business Media.
3. Ribeiro, A. R., Nunes, O. C., Pereira, M. F., & Silva, A. M. (2015). An overview on the advanced oxidation processes applied for the treatment of water pollutants defined in the recently launched Directive 2013/39/EU. *Environment international*, 75, 33-51.
4. Manahan, S. (2017). *Environmental chemistry*. CRC press.
5. Kumar, A., Bisht, B. S., Joshi, V. D., & Dhewa, T. (2011). Review on bioremediation of polluted environment:: A management tool. *International journal of environmental sciences*, 1(6), 1079.
6. Förstner, U., & Wittmann, G. T. (2012). *Metal pollution in the aquatic environment*. Springer Science & Business Media.
7. Erftemeijer, P. L., Riegl, B., Hoeksema, B. W., & Todd, P. A. (2012). Environmental impacts of dredging and other sediment disturbances on corals: a review. *Marine pollution bulletin*, 64(9), 1737-1765.
8. Rodriguez-Mozaz, S., de Alda, M. J. L., Marco, M. P., & Barceló, D. (2005). Biosensors for environmental monitoring: A global perspective. *Talanta*, 65(2), 291-297.
9. Crini, G., Lichtfouse, E., Wilson, L. D., & Morin-Crini, N. (2018). Adsorption-Oriented Processes Using Conventional and Non-conventional Adsorbents for Wastewater Treatment. In *Green Adsorbents for Pollutant Removal* (pp. 23-71). Springer, Cham.

10. Deblonde, T., Cossu-Leguille, C., & Hartemann, P. (2011). Emerging pollutants in wastewater: a review of the literature. *International journal of hygiene and environmental health*, 214(6), 442-448.
11. Rodriguez-Mozaz, S., de Alda, M. J. L., & Barcelo, D. (2006). Biosensors as useful tools for environmental analysis and monitoring. *Analytical and bioanalytical chemistry*, 386(4), 1025-1041.
12. Ronkainen, N. J., Halsall, H. B., & Heineman, W. R. (2010). Electrochemical biosensors. *Chemical Society Reviews*, 39(5), 1747-1763.
13. Mir, M., Homs, A., & Samitier, J. (2009). Integrated electrochemical DNA biosensors for lab-on-a-chip devices. *Electrophoresis*, 30(19), 3386-3397.
14. Pérez-López, B., & Merkoçi, A. (2011). Nanomaterials based biosensors for food analysis applications. *Trends in Food Science & Technology*, 22(11), 625-639.
15. Min, D., Cheng, L., Zhang, F., Huang, X. N., Li, D. B., Liu, D. F., & Yu, H. Q. (2017). Enhancing extracellular electron transfer of *Shewanella oneidensis* MR-1 through coupling improved flavin synthesis and metal-reducing conduit for pollutant degradation. *Environmental science & technology*, 51(9), 5082-5089.
16. Bretschger, O., Obraztsova, A., Sturm, C.A., Chang, I.S., Gorby, Y.A., Reed, S.B., Culley, D.E., Reardon, C.L., Barua, S., Romine, M.F. & Zhou, J. (2007). Current production and metal oxide reduction by *Shewanella oneidensis* MR-1 wild type and mutants. *Applied and Environmental Microbiology*, 73(21), 7003-7012.
17. Su, L., Jia, W., Hou, C., & Lei, Y. (2011). Microbial biosensors: a review. *Biosensors and Bioelectronics*, 26(5), 1788-1799.
18. Eltzov, E., & Marks, R. S. (2011). Whole-cell aquatic biosensors. *Analytical and bioanalytical chemistry*, 400(4), 895-913.
19. Hill, M. K. (2010). *Understanding environmental pollution*. Cambridge University Press.
20. Margot, J., Rossi, L., Barry, D. A., & Holliger, C. (2015). A review of the fate of micropollutants in wastewater treatment plants. *Wiley Interdisciplinary Reviews: Water*, 2(5), 457-487.

21. Holloway, A. F., Nabok, A., Hashim, A. A., & Penders, J. (2010). The use of calixarene thin films in the sensor array for VOCs detection and olfactory navigation. *Sensors & Transducers*, 113(2), 71.
22. Grieshaber, D., MacKenzie, R., Voeroes, J., & Reimhult, E. (2008). Electrochemical biosensors-sensor principles and architectures. *Sensors*, 8(3), 1400-1458.
23. Heidelberg, J. F., Paulsen, I. T., Nelson, K. E., Gaidos, E. J., Nelson, W. C., Read, T. D & Clayton, R. A. (2002). Genome sequence of the dissimilatory metal ion-reducing bacterium *Shewanella oneidensis*. *Nature biotechnology*, 20(11), 1118.
24. Wang, X., Gao, N., & Zhou, Q. (2013). Concentration responses of toxicity sensor with *Shewanella oneidensis* MR-1 growing in bioelectrochemical systems. *Biosensors and Bioelectronics*, 43, 264-267.
25. Al-Shanawa, M., Nabok, A., Hashim, A., Smith, T., & Forder, S. (2013). Detection of γ -radiation and heavy metals using electrochemical bacterial-based sensor. In *Journal of Physics: Conference Series* (Vol. 450, No. 1, p. 012025). IOP Publishing.
26. Al-Shanawa, M., Nabok, A., Hashim, A., Smith, T., & Forder, S. (2014). Optical Study of the Effect of Gamma Radiation and Heavy Metals on Microorganisms (Bacteria). *BioNanoScience*, 4(2), 180-188.
27. Xie, Y., Fan, J., Zhu, W., Amombo, E., Lou, Y., Chen, L., & Fu, J. (2016). Effect of heavy metals pollution on soil microbial diversity and bermudagrass genetic variation. *Frontiers in plant science*, 7, 755.
28. Jaishankar, M., Tseten, T., Anbalagan, N., Mathew, B. B., & Beeregowda, K. N. (2014). Toxicity, mechanism and health effects of some heavy metals. *Interdisciplinary toxicology*, 7(2), 60-72.
29. Tchounwou, P. B., Yedjou, C. G., Patlolla, A. K., & Sutton, D. J. (2012). Heavy metal toxicity and the environment. In *Molecular, clinical and environmental toxicology* (pp. 133-164). Springer, Basel.
30. Manios, T., Stentiford, E. I., & Millner, P. (2002). The effect of heavy metals on the total protein concentration of *Typha latifolia* plants, growing in a substrate

- containing sewage sludge compost and watered with metaliferus wastewater. *Journal of Environmental Science and Health, Part A*, 37(8), 1441-1451.
31. Förstner, U., & Wittmann, G. T. (2012). *Metal pollution in the aquatic environment*. Springer Science & Business Media.
 32. Smith, M. T., Guyton, K. Z., Gibbons, C. F., Fritz, J. M., Portier, C. J., Rusyn, I & Hecht, S. S. (2016). Key characteristics of carcinogens as a basis for organizing data on mechanisms of carcinogenesis. *Environmental Health Perspectives (Online)*, 124(6), 713.
 33. Walter, I., Martinez, F., & Cala, V. (2006). Heavy metal speciation and phytotoxic effects of three representative sewage sludges for agricultural uses. *Environmental pollution*, 139(3), 507-514.
 34. Duffus, J. H. (2002). " Heavy metals" a meaningless term?(IUPAC Technical Report). *Pure and applied chemistry*, 74(5), 793-807.
 35. Nagajyoti, P. C., Lee, K. D., & Sreekanth, T. V. M. (2010). Heavy metals, occurrence and toxicity for plants: a review. *Environmental chemistry letters*, 8(3), 199-216.
 36. Lima, I., Moreira, S. M., Rendon-Von Osten, J., Soares, A. M., & Guilhermino, L. (2007). Biochemical responses of the marine mussel *Mytilus galloprovincialis* to petrochemical environmental contamination along the North-western coast of Portugal. *Chemosphere*, 66(7), 1230-1242.
 37. Ofunne, G. C. (2008). A closer look at crude oil. *African Rev*, 34-39.
 38. Thangaraj, K., Kapley, A., & Purohit, H. J. (2008). Characterization of diverse *Acinetobacter* isolates for utilization of multiple aromatic compounds. *Bioresource technology*, 99(7), 2488-2494.
 39. Morelli, I. S., Del Panno, M. T., De Antoni, G. L., & Paineira, M. T. (2005). Laboratory study on the bioremediation of petrochemical sludge-contaminated soil. *International biodeterioration & biodegradation*, 55(4), 271-278.

40. Fritsche, W., & Hofrichter, M. (2005). Aerobic degradation of recalcitrant organic compounds by microorganisms. *Environmental Biotechnology Concepts and Applications*.
41. Behera, K. K., Alam, A., Vats, S., Sharma, H. P., & Sharma, V. (2012). Organic farming history and techniques. In *Agroecology and strategies for climate change* (pp. 287-328). Springer, Dordrecht.
42. Pimentel, D. (1995). Amounts of pesticides reaching target pests: environmental impacts and ethics. *Journal of Agricultural and environmental Ethics*, 8(1), 17-29.
43. Tilman, D., Cassman, K. G., Matson, P. A., Naylor, R., & Polasky, S. (2002). Agricultural sustainability and intensive production practices. *Nature*, 418(6898), 671.
44. Chandler, D., Bailey, A. S., Tatchell, G. M., Davidson, G., Greaves, J., & Grant, W. P. (2011). The development, regulation and use of biopesticides for integrated pest management. *Philosophical Transactions of the Royal Society B: Biological Sciences*, 366(1573), 1987-1998.
45. Boada, L. D., Zumbado, M., Henríquez-Hernández, L. A., Almeida-González, M., Álvarez-León, E. E., Serra-Majem, L., & Luzardo, O. P. (2012). Complex organochlorine pesticide mixtures as determinant factor for breast cancer risk: a population-based case-control study in the Canary Islands (Spain). *Environmental Health*, 11(1), 28.
46. Frank, R., Clegg, B. S., & Patni, N. K. (1991). Dissipation of cyanazine and metolachlor on a clay loam soil, Ontario, Canada, 1987-1990. *Archives of Environmental Contamination and Toxicology*, 21(2), 253-262.
47. Wu, M., Quirindongo, M., Sass, J., & Wetzler, A. (2010). Still poisoning the well. Natural Resources Defense Council, Washington, DC.
48. Bethsass, J., & Colangelo, A. (2013). European Union bans atrazine, while the United States negotiates continued use. *International journal of occupational and environmental health*.

49. Kamrin, M. A. (1997). Pesticide profiles: toxicity, environmental impact, and fate. CRC press.
50. Manahan, S. E. (2005). Green Chemistry and the Ten Commandments of Sustainability; ChemChar Research. Inc.: Columbia, MO.
51. Edwards, D. (2006). Reregistration Eligibility Decision (RED) for Propiconazole. Agency, USEP (Ed.).
52. Aktar, W., Sengupta, D., & Chowdhury, A. (2009). Impact of pesticides use in agriculture: their benefits and hazards. *Interdisciplinary toxicology*, 2(1), 1-12.
53. Okazaki, S., Nakagawa, H., Fukuda, K., Asakura, S., Kiuchi, H., Shigemori, T., & Takahashi, S. (2000). Re-activation of an amperometric organophosphate pesticide biosensor by 2-pyridinealdoxime methochloride. *Sensors and Actuators B: Chemical*, 66(1-3), 131-134.
54. Wasi, S., Tabrez, S., & Ahmad, M. (2013). Toxicological effects of major environmental pollutants: an overview. *Environmental monitoring and assessment*, 185(3), 2585-2593.
55. Flora, S. J., & Agrawal, S. (2017). Arsenic, cadmium, and lead. In *Reproductive and developmental toxicology* (pp. 537-566). Academic Press.
56. Bielicka, A., Bojanowska, I., & Wisniewski, A. (2005). Two Faces of Chromium-Pollutant and Bioelement. *Polish Journal of Environmental Studies*, 14(1).
57. Vincent, J. B. (2010). Chromium: celebrating 50 years as an essential element?. *Dalton Transactions*, 39(16), 3787-3794.
58. Chen, G., Liu, P., Pattar, G. R., Tackett, L., Bhonagiri, P., Strawbridge, A. B., & Elmendorf, J. S. (2006). Chromium activates glucose transporter 4 trafficking and enhances insulin-stimulated glucose transport in 3T3-L1 adipocytes via a cholesterol-dependent mechanism. *Molecular Endocrinology*, 20(4), 857-870.
59. Ahamed, M., & Siddiqui, M. K. J. (2007). Environmental lead toxicity and nutritional factors. *Clinical Nutrition*, 26(4), 400-408.
60. Nava-Ruiz, C., Méndez-Armenta, M., & Ríos, C. (2012). Lead neurotoxicity: effects on brain nitric oxide synthase. *Journal of molecular histology*, 43(5), 553-563.

61. Rice, K. M., Walker Jr, E. M., Wu, M., Gillette, C., & Blough, E. R. (2014). Environmental mercury and its toxic effects. *Journal of preventive medicine and public health*, 47(2), 74.
62. Nriagu, J. (2007). Zinc toxicity in humans. *Encyclopedia of Environmental Health; Nriagu, J., Ed.; Elsevier BV: Amsterdam, NL, The Netherlands*, 1-7.
63. Mahurpawar, M. (2015). Effects of heavy metals on human health. *Int. J. Res. Granthaalayah*, 1(7).
64. Barceloux, D. G., & Barceloux, D. (1999). Nickel. *Journal of Toxicology: Clinical Toxicology*, 37(2), 239-258.
65. Alvarez, A., Saez, J. M., Costa, J. S. D., Colin, V. L., Fuentes, M. S., Cuozzo, S. A., & Amoroso, M. J. (2017). Actinobacteria: current research and perspectives for bioremediation of pesticides and heavy metals. *Chemosphere*, 166, 41-62.
66. Popović, N. T., Strunjak-Perović, I., Klobučar, R. S., Barišić, J., Babić, S., Jadan, M., & Car, I. (2015). Impact of treated wastewater on organismic biosensors at various levels of biological organization. *Science of the Total Environment*, 538, 23-37.
67. Wake, H. (2005). Oil refineries: a review of their ecological impacts on the aquatic environment. *Estuarine, Coastal and Shelf Science*, 62(1), 131-140.
68. Neff, J.M., Ostazeski, S., Gardiner, W., Stejskal, I. (2000). Effects of weathering on the toxicity of three offshore Australian crude oils and a diesel fuel to marine animals. *Environ. Toxicol. Chem.* 19, 1809–1821.
69. Meador, J.P. (2003). Bioaccumulation of PAHs in marine invertebrates. In: Douben, P.E.T. (Ed.), *PAHs: An Ecotoxicological Perspective*. Wiley, Chichester, England, pp. 147–171.
70. Altenburger, R., Segner, H., Van dar Oost, R. (2003). Biomarkers and PAHs – prospects for the assessment of exposure and effects in aquatic systems. In: Douben, P.E.T. (Ed.), *PAHs: An Ecotoxicological Perspective*. Wiley, Chichester, England, pp. 147–171.

71. Buonocore, G., Perrone, S., & Tataranno, M. L. (2010, August). Oxygen toxicity: chemistry and biology of reactive oxygen species. In *Seminars in Fetal and Neonatal Medicine* (Vol. 15, No. 4, pp. 186-190).
72. Ozben, T. (2007). Oxidative stress and apoptosis: impact on cancer therapy. *Journal of pharmaceutical sciences*, 96(9), 2181-2196.
73. Mittler, R. (2002). Oxidative stress, antioxidants and stress tolerance. *Trends in plant science*, 7(9), 405-410.
74. Cooke, M. S., Evans, M. D., Dizdaroglu, M., & Lunec, J. (2003). Oxidative DNA damage: mechanisms, mutation, and disease. *The FASEB Journal*, 17(10), 1195-1214.
75. Collins, A., & Harrington, V. (2002). Repair of oxidative DNA damage: assessing its contribution to cancer prevention. *Mutagenesis*, 17(6), 489-493.
76. Mehrpour, O., Karrari, P., Zamani, N., Tsatsakis, A. M., & Abdollahi, M. (2014). Occupational exposure to pesticides and consequences on male semen and fertility: a review. *Toxicology letters*, 230(2), 146-156.
77. Matthews, G. (2008). *Pesticide application methods*. John Wiley & Sons.
78. Pimentel, D., & Burgess, M. (2014). Environmental and economic costs of the application of pesticides primarily in the United States. In *Integrated pest management* (pp. 47-71). Springer, Dordrecht.
79. Iyer, P., & Makris, S. (2010). Developmental and reproductive toxicology of pesticides. In *Hayes' Handbook of Pesticide Toxicology* (pp. 381-440). Academic Press.
80. Meeker, J. D. (2010). Exposure to environmental endocrine disrupting compounds and men's health. *Maturitas*, 66(3), 236-241.
81. Nicolopoulou-Stamati, P., Maipas, S., Kotampasi, C., Stamatis, P., & Hens, L. (2016). Chemical pesticides and human health: the urgent need for a new concept in agriculture. *Frontiers in public health*, 4, 148.
82. Hernandez, A. F., & Tsatsakis, A. M. (2017). Human exposure to chemical mixtures: challenges for the integration of toxicology with epidemiology data in risk assessment. *Food and Chemical Toxicology*, 103, 188-193.

83. McKinlay, R., Plant, J. A., Bell, J. N. B., & Voulvoulis, N. (2008). Endocrine disrupting pesticides: implications for risk assessment. *Environment international*, 34(2), 168-183.
84. Jayaraj, R., Megha, P., & Sreedev, P. (2016). Organochlorine pesticides, their toxic effects on living organisms and their fate in the environment. *Interdisciplinary toxicology*, 9(3-4), 90-100.
85. Mostafalou, S., & Abdollahi, M. (2017). Pesticides: an update of human exposure and toxicity. *Archives of toxicology*, 91(2), 549-599.
86. Bersier, P. M., Howell, J., & Bruntlett, C. (1994). Tutorial review. Advanced electroanalytical techniques versus atomic absorption spectrometry, inductively coupled plasma atomic emission spectrometry and inductively coupled plasma mass spectrometry in environmental analysis. *Analyst*, 119(2), 219-232.
87. Gałuszka, A., Migaszewski, Z., & Namieśnik, J. (2013). The 12 principles of green analytical chemistry and the SIGNIFICANCE mnemonic of green analytical practices. *TrAC Trends in Analytical Chemistry*, 50, 78-84.
88. Ure, A. M., & Davidson, C. M. (Eds.). (2008). *Chemical speciation in the environment*. John Wiley & Sons.
89. Lajunen, L. (2007). *Spectrochemical analysis by atomic absorption and emission*. Royal Society of Chemistry.
90. Lagalante, A. F. (2004). Atomic absorption spectroscopy: A tutorial review. *Applied Spectroscopy Reviews*, 34(3), 173-189.
91. Sanz-Medel, A., & Pereiro, R. (2014). *Atomic Absorption Spectrometry: An Introduction*. Momentum Press.
92. Koirtiyohann, S. R. (1991). "A HISTORY OF ATOMIC ABSORPTION SPECTROMETRY". *Analytical Chemistry*. 63 (21): 1024A–1031A.
93. Welz, B., & Sperling, M. (2008). *Atomic absorption spectrometry*. John Wiley & Sons.
94. Skoog, D. A., Holler, F. J., & Crouch, S. R. (2017). *Principles of instrumental analysis*. Cengage learning.

95. Pröfrock, D., & Prange, A. (2012). Inductively coupled plasma-mass spectrometry (ICP-MS) for quantitative analysis in environmental and life sciences: a review of challenges, solutions, and trends. *Applied spectroscopy*, 66(8), 843-868.
96. Davis, A. C., Wu, P., Zhang, X., Hou, X., & Jones, B. T. (2006). Determination of cadmium in biological samples. *Applied Spectroscopy Reviews*, 41(1), 35-75.
97. McMahon, G. (2008). *Analytical instrumentation: a guide to laboratory, portable and miniaturized instruments*. John Wiley & Sons.
98. Moore, G. L. (2012). *Introduction to inductively coupled plasma atomic emission spectrometry* (3).
99. Rao, R. N., & Talluri, M. K. (2007). An overview of recent applications of inductively coupled plasma-mass spectrometry (ICP-MS) in determination of inorganic impurities in drugs and pharmaceuticals. *Journal of pharmaceutical and biomedical analysis*, 43(1), 1-13.
100. Matusiewicz, H., & Ślachciński, M. (2010). In situ vapor generation inductively coupled plasma spectrometry for determination of iodine using a triple-mode microflow ultrasonic nebulizer after alkaline solubilization. *Analytical Methods*, 2(10), 1592-1598.
101. Wong, J. W., Zhang, K., Hayward, D. G., Krynitsky, A. J., Schenck, F. J., Wittenberg, J. B. & Yang, P. (2019). Determination of. *Analysis of Pesticides in Food and Environmental Samples*, 175.
102. Robert, I. Grob & Eugene, F. Barry.(2004) *Modern Practice of Gas Chromatography* (Fourth Edition .), ISBN: 0-471-22983-0.
103. Czaplicki, S. (2013). Chromatography in bioactivity analysis of compounds. In *Column chromatography*. IntechOpen.
104. Amine, A., Mohammadi, H., Bourais, I., & Palleschi, G. (2006). Enzyme inhibition-based biosensors for food safety and environmental monitoring. *Biosensors and Bioelectronics*, 21(8), 1405-1423.
105. Turdean, G. L. (2011). Design and development of biosensors for the detection of heavy metal toxicity. *International Journal of Electrochemistry*, 2011.

106. Grieshaber, D., MacKenzie, R., Voeroes, J., & Reimhult, E. (2008). Electrochemical biosensors-sensor principles and architectures. *Sensors*, 8(3), 1400-1458.
107. Thévenot, D. R., Toth, K., Durst, R. A., & Wilson, G. S. (2001). Electrochemical biosensors: recommended definitions and classification. *Biosensors and Bioelectronics*, 16(1), 121-131.
108. Prodromidis, M. I., & Karayannis, M. I. (2002). Enzyme based amperometric biosensors for food analysis. *Electroanalysis*, 14(4), 241.
109. Fanget, S., Hentz, S., Puget, P., Arcamone, J., Matheron, M., Colinet, E. D., & Roukes, M. L. (2011). Gas sensors based on gravimetric detection—A review. *Sensors and Actuators B: Chemical*, 160(1), 804-821.
110. Hansen, L. H., & Sørensen, S. J. (2001). The use of whole-cell biosensors to detect and quantify compounds or conditions affecting biological systems. *Microbial ecology*, 42(4), 483-494.
111. Ahmed, A., Rushworth, J. V., Hirst, N. A., & Millner, P. A. (2014). Biosensors for whole-cell bacterial detection. *Clinical microbiology reviews*, 27(3), 631-646.
112. Melamed, S., Elad, T., & Belkin, S. (2012). Microbial sensor cell arrays. *Current opinion in biotechnology*, 23(1), 2-8.
113. Van Dyk, T. K., DeRose, E. J., & Gonye, G. E. (2001). LuxArray, a high-density, genomewide transcription analysis of *Escherichia coli* using bioluminescent reporter strains. *Journal of bacteriology*, 183(19), 5496-5505.
114. Bereza-Malcolm, L. T., Mann, G., & Franks, A. E. (2014). Environmental sensing of heavy metals through whole cell microbial biosensors: a synthetic biology approach. *ACS synthetic biology*, 4(5), 535-546.
115. Gui, Q., Lawson, T., Shan, S., Yan, L., & Liu, Y. (2017). The application of whole cell-based biosensors for use in environmental analysis and in medical diagnostics. *Sensors*, 17(7), 1623.
116. Sassolas, A. Leca-Bouvier, B. D. & Blum, L. J. (2008). DNA Biosensors and Microarrays, *Chemical Reviews*, 108(1), 109-139. doi:10.1021/cr0684467.

117. Nowicka, A. M. Kowalczyk, A. Stojek Z. & Hepel, M. (2010). Nanogravimetric and Voltammetric DNA-Hybridization Biosensors for Studies of DNA Damage by Common Toxicants and Pollutants, *Biophysical Chemistry*,146(1), 42-53. doi:10.1016/j.bpc.2009.10.003.
118. Pumera, M., Sanchez, S., Ichinose, I., & Tang, J. (2007). Electrochemical nanobiosensors. *Sensors and Actuators B: Chemical*, 123(2), 1195-1205.
119. Ellington, A. D. & Szostak, J. W. (1990). In Vitro Selection of RNA Molecules that Bind Specific Ligands,” *Nature*, 346(6287), 818-822. doi:10.1038/346818a0.
120. Hamula, C. L. A. Guthrie, J. W. Zhang, H. Li, X. F. & Le, X. C. (2011). Selection and Analytical Applications of Aptamers, *Trends in Analytical Chemistry*, 30(10), 1587-1597. doi:10.1016/j.trac.2011.08.006.
121. Song, K. M., Lee, S., & Ban, C. (2012). Aptamers and their biological applications. *Sensors*, 12(1), 612-631.
122. Sassolas, L. J. Blum & Leca-Bouvier, B. D. (2011). Optical Detection Systems Using Immobilized Aptamers,” *Bio-sensors and Bioelectronics*, 26(9), 3725-3736. doi:10.1016/j.bios.2011.02.031.
123. He, J. Liu, Y. Fan, M. & Liu, X. (2011). Isolation and Identification of the DNA Aptamer Target to Acetamiprid,” *Journal of Agricultural and Food Chemistry*, 59,(5),1582-1586. doi:10.1021/jf104189g.
124. Wang, L., Wang, M., Shi, F., Liu, Z., & Su, X. (2017). Aptamer based fluorescence biosensor for protein kinase activity detection and inhibitor screening. *Sensors and Actuators B: Chemical*, 252, 209-214.
125. Sampson, T. (2003). Aptamers and SELEX: the technology. *World Patent Information*, 25(2), 123-129.
126. Stoltenburg, R., Reinemann, C., & Strehlitz, B. (2007). SELEX—a (r) evolutionary method to generate high-affinity nucleic acid ligands. *Biomolecular engineering*, 24(4), 381-403.
127. Gopinath, S. C. B. (2007). Methods developed for SELEX. *Analytical and bioanalytical chemistry*, 387(1), 171-182.

128. Dwivedi, H. P., Smiley, R. D., & Jaykus, L. A. (2010). Selection and characterization of DNA aptamers with binding selectivity to *Campylobacter jejuni* using whole-cell SELEX. *Applied microbiology and biotechnology*, 87(6), 2323-2334.
129. Shieh, K. R. (2016). *Computational studies of de novo motif discovery in aptamerselections* (Doctoral dissertation, Yeshiva University).
130. Song, S., Wang, L., Li, J., Fan, C., & Zhao, J. (2008). Aptamer-based biosensors. *TrAC Trends in Analytical Chemistry*, 27(2), 108-117.
131. D'souza, S. F. (2001). Microbial biosensors. *Biosensors and Bioelectronics*, 16(6), 337-353.
132. Chönhoff, M. (2003). Self-assembled polyelectrolyte multilayers. *Current opinion in colloid & interface science*, 8(1), 86-95.
133. Serpe, M. J., Yarmey, K. A., Nolan, C. M., & Lyon, L. A. (2005). Doxorubicin uptake and release from microgel thin films. *Biomacromolecules*, 6(1), 408-413.
134. Ramakrishna, S. V., & Prakasham, R. S. (1999). Microbial fermentations with immobilized cells. *Current Science*, 87-100.
135. Mallick, N. (2002). Biotechnological potential of immobilized algae for wastewater N, P and metal removal: a review. *Biometals*, 15(4), 377-390.
136. Moreno-Garrido, I. (2008). Microalgae immobilization: current techniques and uses. *Bioresource technology*, 99(10), 3949-3964.
137. Navarro, J. M., & Durand, G. (1977). Modification of yeast metabolism by immobilization onto porous glass. *European journal of applied microbiology and biotechnology*, 4(4), 243-254.
138. Messing, R. A., & Oppermann, R. A. (1979). Pore dimensions for accumulating biomass. I. Microbes that reproduce by fission or by budding. *Biotechnology and Bioengineering*, 21(1), 49-58.
139. Górecka, E., & Jastrzębska, M. (2011). Immobilization Techniques and Biopolymer Carriers—A Review. *Biotechnol. Food Sci.*, 75, 27-34.

140. Stolarzewicz, I., Białecka-Florjańczyk, E., Majewska, E., & Krzyczkowska, J. (2011). Immobilization of yeast on polymeric supports. *Chemical and biochemical engineering quarterly*, 25(1), 135-144.
141. Park, J. K., & Chang, H. N. (2000). Microencapsulation of microbial cells. *Biotechnology advances*, 18(4), 303-319.
142. Song, S. H., Choi, S. S., Park, K., & Yoo, Y. J. (2005). Novel hybrid immobilization of microorganisms and its applications to biological denitrification. *Enzyme and Microbial Technology*, 37(6), 567-573.
143. Lozinsky, V. I., & Plieva, F. M. (1998). Poly (vinyl alcohol) cryogels employed as matrices for cell immobilization. 3. Overview of recent research and developments. *Enzyme and microbial technology*, 23(3-4), 227-242.
144. Klein, J., & Ziehr, H. (1990). Immobilization of microbial cells by adsorption. *Journal of biotechnology*, 16(1-2), 1-15.
145. Kozlyak, E. I., Solomon, Z. G., Yakimov, M. M., & Fadyushina, T. V. (1993). The sorption of *Pseudomonas fluorescens* 16n2 cells on various adsorbents. *Prikl. Biokhim. Mikrobiol*, 29(1), 138-143.
146. Kilonzo, P., & Bergougou, M. (2012). Surface modifications for controlled and optimized cell immobilization by adsorption: applications in fibrous bed bioreactors containing recombinant cells. *J. Microbial Biochem. Technol*, 4, 22-30.
147. Martins, S. C. S., Martins, C. M., Fiúza, L. M. C. G., & Santaella, S. T. (2013). Immobilization of microbial cells: A promising tool for treatment of toxic pollutants in industrial wastewater. *African Journal of Biotechnology*, 12(28).
148. Woodward, J. (1988). Methods of immobilization of microbial cells. *Journal of microbiological Methods*, 8(1-2), 91-102.
149. Chróst, R. J. (1991). Environmental control of the synthesis and activity of aquatic microbial ectoenzymes. In *Microbial enzymes in aquatic environments* (29-59). Springer, New York, NY.

150. Al-Shanawa, M., (2015). Detection of Environmental Pollution (Radionuclides and Heavy Metals) Using Microorganisms. Sheffield Hallam University, PhD thesis, , 42-60.
151. McGrath, Steve P., et al. "Assessment of the toxicity of metals in soils amended with sewage sludge using a chemical speciation technique and a lux-based biosensor." *Environmental Toxicology and Chemistry* 18.4 (1999): 659-663.
152. Berezhetsky, A. L., Durrieu, C., Nguyen-Ngoc, H., Chovelon, J. M., Dzyadevych, S. V., & Tran-Minh, C. (2007). Conductometric biosensor based on whole-cell microalgae for assessment of heavy metals in wastewater. *Biopolymers and cell*, 23(6), 511-518.
153. Gruzina, T. G., Zadorozhnyaya, A. M., Gutnik, G. A., Vember, V. V., Ulberg, Z. R., Kanyuk, N. I., & Starodub, N. F. (2007). A bacterial multisensor for determination of the contents of heavy metals in water. *Journal of Water Chemistry and Technology*, 29(1), 50-53.
154. Saxena, S. (2015). Immobilisation and Biosensors. In *Applied Microbiology* (pp. 179-190). Springer, New Delhi.
155. Desmet, C., Marquette, C. A., Blum, L. J., & Doumèche, B. (2016). Paper electrodes for bioelectrochemistry: Biosensors and biofuel cells. *Biosensors and Bioelectronics*, 76, 145-163.
156. Barrera-Díaz, C. E., Lugo-Lugo, V., & Bilyeu, B. (2012). A review of chemical, electrochemical and biological methods for aqueous Cr (VI) reduction. *Journal of hazardous materials*, 223, 1-12.
157. Ianeselli, L., Greci, G., Callegari, C., Tormen, M., & Casalis, L. (2014). Development of stable and reproducible biosensors based on electrochemical impedance spectroscopy: Three-electrode versus two-electrode setup. *Biosensors and Bioelectronics*, 55, 1-6.
158. Ahmed, A., Rushworth, J. V., Hirst, N. A., & Millner, P. A. (2014). Biosensors for whole-cell bacterial detection. *Clinical microbiology reviews*, 27(3), 631-646.

159. Young, K. D. (2006). The selective value of bacterial shape. *Microbiol. Mol. Biol. Rev.*, 70(3), 660-703.
160. Knoll, A. H. (2015). *Life on a Young Planet: The First Three Billion Years of Evolution on Earth-Updated Edition* (Vol. 35). Princeton University Press.
161. Konhauser, K. O. (2009). *Introduction to geomicrobiology*. John Wiley & Sons.
162. Whitman, W. B., Coleman, D. C., & Wiebe, W. J. (1998). Prokaryotes: the unseen majority. *Proceedings of the National Academy of Sciences*, 95(12), 6578-6583.
163. Rappe, M. S., & Giovannoni, S. J. (2003). The uncultured microbial majority. *Annual Reviews in Microbiology*, 57(1), 369-394.
164. Vellai, T., & Vida, G. (1999). The origin of eukaryotes: the difference between prokaryotic and eukaryotic cells. *Proceedings of the Royal Society of London. Series B: Biological Sciences*, 266(1428), 1571-1577.
165. Velimirov, B. (2001). Nanobacteria, Ultramicrobacteria and Starvation Forms: A Search for the Smallest Metabolizing Bacterium. *Microbes and Environments*, 16(2), 67-77.
166. Robertson, J., Gomersall, M., & Gill, P. (1975). *Mycoplasma hominis*: growth, reproduction, and isolation of small viable cells. *Journal of bacteriology*, 124(2), 1007-1018.
167. Kaiser, D. (2004). Signaling in myxobacteria. *Annu. Rev. Microbiol.*, 58, 75-98.
168. Shih, Y. L., & Rothfield, L. (2006). The bacterial cytoskeleton. *Microbiology and Molecular Biology Reviews*, 70(3), 729-754.
169. Harold, F. M. (1972). Conservation and transformation of energy by bacterial membranes. *Bacteriological Reviews*, 36(2), 172.
170. Kadouri, D., Jurkevitch, E., Okon, Y., & Castro-Sowinski, S. (2005). Ecological and agricultural significance of bacterial polyhydroxyalkanoates. *Critical reviews in microbiology*, 31(2), 55-67.
171. Black, J. G. (2008). *Microbiology: principles and explorations*. John Wiley & Sons.

172. Engelhardt, H., & Peters, J. (1998). Structural research on surface layers: a focus on stability, surface layer homology domains, and surface layer–cell wall interactions. *Journal of structural biology*, 124(2), 276-302.
173. Ahmed, A., Rushworth, J. V., Hirst, N. A., & Millner, P. A. (2014). Biosensors for whole-cell bacterial detection. *Clinical microbiology reviews*, 27(3), 631-646.
174. Cooper, S. (2006). Bacterial growth and division. *Reviews in Cell Biology and Molecular Medicine*.
175. Hudault, S., Guignot, J., & Servin, A. L. (2001). *Escherichia coli* strains colonising the gastrointestinal tract protect germfree mice against *Salmonella typhimurium* infection. *Gut*, 49(1), 47-55.
176. Myers, C. H & Nealson, K. H. (1988). Bacterial manganese reduction and growth with manganese oxide as the sole electron acceptor. *Science*, 240(4857), 1319-1321.
177. Brettar, I., Christen, R., & Höfle, M. G. (2002). *Shewanella denitrificans* sp. nov., a vigorously denitrifying bacterium isolated from the oxic-anoxic interface of the Gotland Deep in the central Baltic Sea. *International journal of systematic and evolutionary microbiology*, 52(6), 2211-2217.
178. Nealson, K. H., & Scott, J. (2006). Ecophysiology of the genus *Shewanella*. In *The prokaryotes*, 1133-1151. Springer New York.
179. Gralnick, J. A., Vali, H., Lies, D. P., & Newman, D. K. (2006). Extracellular respiration of dimethyl sulfoxide by *Shewanella oneidensis* strain MR-1. *Proceedings of the National Academy of Sciences of the United States of America*, 103(12), 4669-4674.
180. Hanson, R. S., & Hanson, T. E. (1996). Methanotrophic bacteria. *Microbiological reviews*, 60(2), 439-471.

CHAPTER 3 EXPERIMENTAL METHODOLOGY

This chapter describes with more details a number of experimental techniques, such as fluorescence microscopy, flow cytometry, and optical density (OD₆₀₀) which were utilized in this study for the purpose of counting the percentage of live and dead bacteria and then studying the effect of environmental pollution on bacterial concentration. The development of sensor array devices for detection of heavy metals, pesticides and petrochemical pollutions is the desirable outcome of this work. In addition, to the above mentioned optical techniques, scanning electron microscopy (SEM) and atom forces microscopy (AFM) will be described as well. Also, the use of simple DC and AC electrochemical measurements e.g. cyclic voltammogram (CV) and electrochemical impedance spectroscopy (EIS) for studying the effect of these pollutants on bacterial suspension and immobilized bacteria will be described.

3.1 Experimental equipment used

3.1.1 Optical methods

The effect of the above pollutants on the bacterial cultures was examined using three different optical experimental techniques: fluorescence microscopy, UV-visible spectrophotometry, and flow cytometry. A Becton-Dickinson FACSCalibur flow cytometer was used to characterise bacteria after staining them with the BacLight live/dead bacterial viability kit (Molecular Probes). Fluorescence microscopy of bacterial suspension and bacteria immobilized on the screen printed gold electrodes was performed with an Olympus-BX60 instrument using the BacLight kit for staining bacteria. Optical density of bacterial cultures was measured at 600 nm with a 6715 UV/Vis spectrophotometer (Jenway).

3.1.1.1 Fluorescence microscopy using Olympus-BX60 instrument

The most common imaging technique used to study the morphological structures of different materials including organic films and biological objects is optical microscopy. The limitations in resolution of optical microscopy due to the diffraction limit and aberrations in optical elements do not allow observing objects in sub-micron dimensions. Alternative modern microscopic techniques, such as electron microscopy and scanning probe microscopy, offer much better resolution down to 10 nanometers (nm). However, they can be invasive due to the use of high vacuum or direct contact of nano-probes and thus not suitable for biological objects. In this respect, non-invasive optical microscopy is advantageous for studying biological objects. Recent advances of optical microscopy, such as near field optical microscopy, managed to overcome the diffraction limit. The use of modern image-processing software can also enhance the performance of optical instrumentation, such as interfacial force microscope (IFM). Another problem in optical microscopy is the lack of contrast of some objects, such as organic and biological thin films. This problem can be solved using polarised light in dark-field microscopy as shown in Figure (3-1A,B), or staining the material with light absorbing or fluorescent dyes [1]. The biological cells are typical example of non-contrast objects, and the most common way to increase it is to stain the cell culture with selective dyes for example (BacLightTM Bacterial Viability Kit, for microscopy and flow cytometry) [2]. Therefore, the fluorescence dyes that used in this study is BacLight bacterial viability kit contain two dyes the first one is SYTO 9 green fluorescence DNA dye, and the other is red fluorescence DNA (propidium iodide) dye. Those dyes have different physical and biological effect in their spectrum and permeability into the living bacteria cell membrane. In short, bacteria with intact cell membranes stain fluorescent green (live cell), whereas bacteria with damaged membranes stain fluorescent red (dead cell) depends on the charge [3]. Typical dark- field images of bacteria stained with BacLight are given in Chapter 4. The background remains virtually non-fluorescent. The ratio of (excitation/emission) wavelength about (480/500 nm) for SYTO9 stain

which show green spot, and (490/635 nm) for propidium iodide enabling to see the red spots which refers to the dead cells.

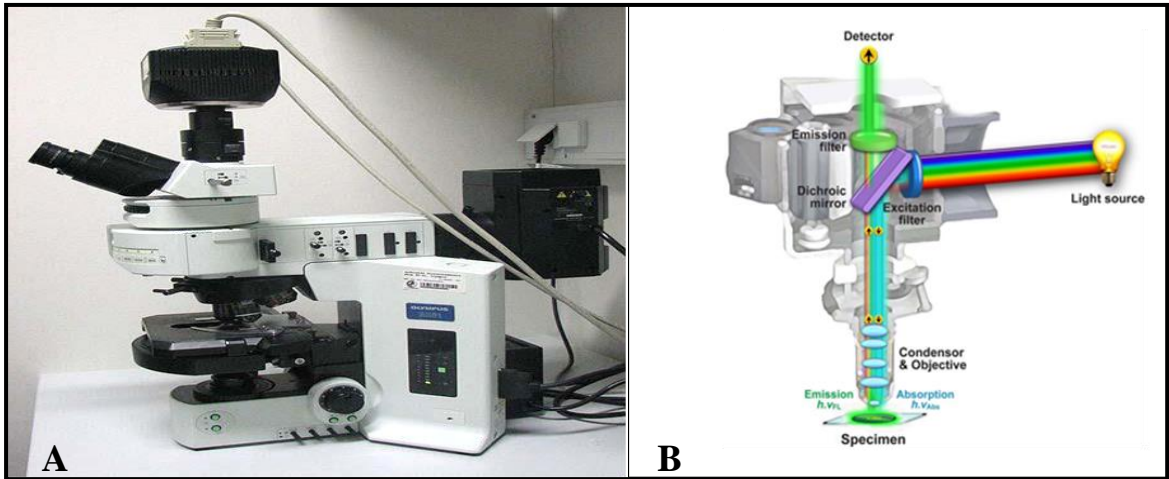


Figure 3-1: (A) Fluorescence microscope Olympus-BX60, (B); its schematic diagram

3.1.1.2 Optical density measurements using 6715 UV/Vis spectrophotometer

One of the most common methods of detecting optical density of cell culture at 600 nm is (OD_{600}) which used to determinate the cells density [4]. A linear relationship exists between the number or density of cells) and the absorption rate at 600 nm as in Figure (3-2A,B).

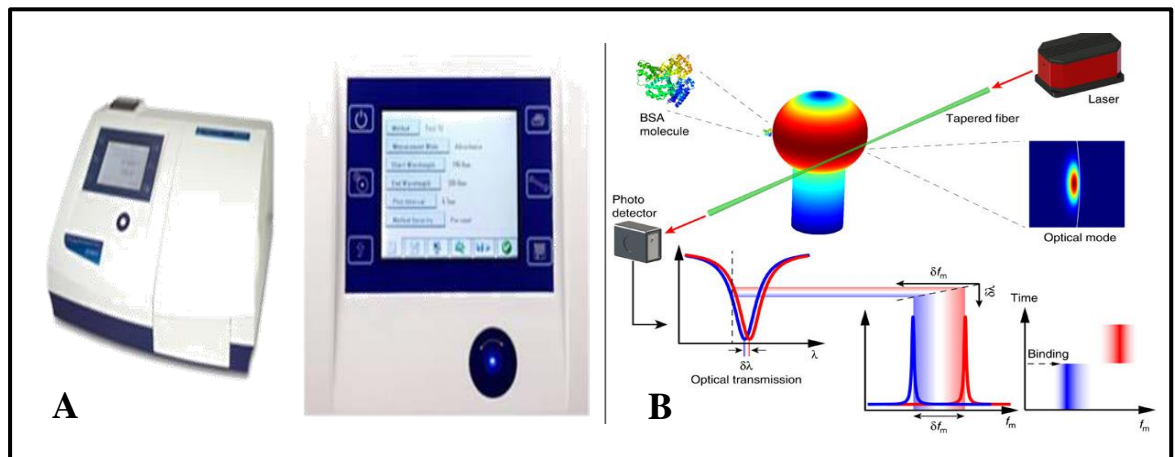


Figure 3-2: (A) 6715 UV/Vis spectrophotometer (B); Schematic of a typical optical density device imaging process.

The calibrate OD₆₀₀ measurements in concentration units (cell/ml) the calibration has to be performed using an independent technique such as optical microscopy [5]. The feature single wavelength allows simple absorbance (Abs) or transmission (T %) measurements at a single wavelength defined by user. However, when light hits bacteria, the light may be scattered and/or absorbed [6]. Because bacteria are usually transparent the (OD₆₀₀) of a bacteria liquid culture is mostly due to light scattering. The (OD₆₀₀) outcome represents the amount of light passed through a sample relative to a reference. In this study, the optical density (OD₆₀₀) was studied and plotted as a function of time exposed to pollutants. The concept of OD₆₀₀ device is based on the principle of light scattering. When measuring light scattering, it is important to consider the wavelength of light used, so that the light absorption is minimal for most bacterial cultures. A wavelength of around 600 nm is a good choice, and it is the middle of visible range. So the measured absorbance in such samples is due to light scattering, and not the result of molecular absorption and OD₆₀₀ gives true account of viable bacteria assuming that dead bacteria are not motile and sediment [7].

3.1.1.3 Flow cytometry using Becton-Dickinson FACSCalibur

Quantification of the total counting of bacterial numbers is a basic and essential task in several areas of microbiology. During the last two decades, the direct counting methods that use fluorochrome stains and fluorescence microscopy have become increasingly popular because most naturally occurring bacteria cannot be enumerated accurately as a colony-forming unit (CFU) by culturing on agar media. Advances in fluorescent dye technology and flow cytometry now allow the application of this rapid, automated technique to such studies.

Flow cytometry has become increasingly popular because it offers the advantage over microscopy in rapid, easy, and accurate bacteria enumeration [8]. This increasing popularity is also due to the recent development of low-cost compact flow cytometers. In this work flow cytometry was used to count bacterial cells of different types: i.e.

E. coli, *S. oneidensis* and *Mc capsulatus* (Bath). To verify the accuracy and the precision of this technique, total bacteria counts made by flow cytometry were compared with those obtained using fluorescence microscopy. The results of this study showed that flow cytometry was a reliable technique for counting a mixture of bacteria in samples from aquatic ecosystems.

Flow cytometry has been described as automated microscopy that has the advantages of automation, objectivity and speed (flow cytometers can analyse thousands of cells per second). To achieve this flow cytometers quantitatively measure the optical characteristics of cells (or other particles) as they are presented in single file in front of a focused light beam. In order to present cells in single file they are introduced, in the flow cell, into a fast flowing fluid stream termed the sheath flow.

The basis of the flow is a jet of isotonic sheath fluid (approximately 100 µm in diameter) into which samples are injected at a controlled rate, typically between 10 and 60 ml/min. The light source used to illuminate samples is either a high-pressure mercury vapour lamp or an assortment of lasers. As particles pass through the light beam the following three parameters are measured using photomultiplier tubes as shown in Figure (3-3A,B); these are forward light scattering (also called FALS or FSC), side scattering (also called 90° LS SALS or SSC) and fluorescence (FL).

The amount of light scattered forward and at right angles by any particle tends to increase with the bacterial cell size or numbers. In addition, the cell refraction ability is related to surface properties and internal structure, and these also affect FSC and SSC. Natural fluorescence (auto-fluorescence) is emitted by cellular components such as flavin nucleotides, pyridine and photosynthetic pigments. A typical flow cytometer measures fluorescence in three wavelength ranges. Light of defined wavelengths is channelled to particular detectors, for example detector FL1 will typically measure green fluorescence, FL2 orange fluorescence and FL3 red fluorescence. All these information referred to Shapiro (1995) [9], and Robinson (1997) [10].

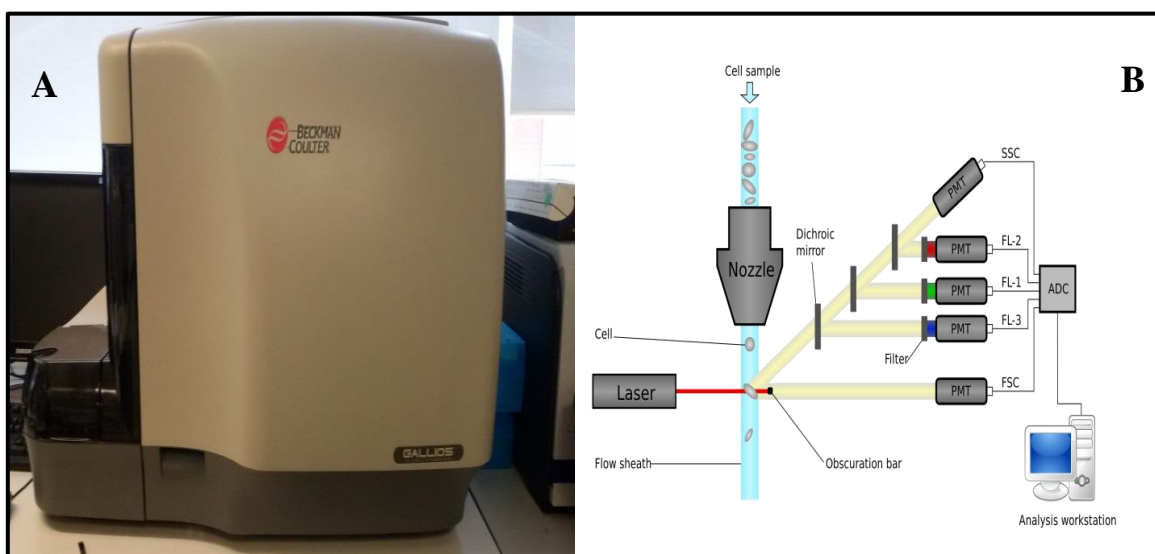


Figure 3-3: (A) Flow cytometry instrument (B); Schematic diagram of flow cytometry measurements.

3.1.1.4 Scanning Electron Microscopy using FEI-Nova SEM

Scanning electron microscopy is one of the traditional and well-established methods in surface science. The SEM operates in a vacuum, with a high energy electron beam (typically from 5 to 20 keV) focused into a spot of several tens of nanometers in diameter (or fractions of nanometers in modern high-resolution instruments) [11]. Because of a very short wavelength of the electrons used (for example, electrons with an energy of 100 eV have a wavelength $\lambda_e =$ equal to 0.12 nm), the resolution of SEM is limited by the beam diameter and image distortions, (astigmatism) introduced by the focusing system. A complex electromagnetic system provides both the formation of the electron beam and its scanning over the sample (see Figure 3-4). The electrons that are reflected (backscattered) from the surface, or the emitted secondary electrons, are collected with a sensitive detector to provide imaging of the studied surfaces. SEM can be used to study samples of different nature and morphologies, practically without any limitations. Ideally, the samples for SEM study should be conductive to avoid electrical charging of the sample with an electron beam which causes image distortion. Therefore, the samples of insulating materials for SEM study are recommended to coat (decorate)

with thin of carbon or gold film which reproduces the surface profile. Another possible drawback of SEM lies in the film damage caused by high energy electrons, which is particularly important for organic film study. The interpretation of SEM images of composite samples may not always be straightforward. This is especially true for secondary electron images, which represent a combination of both the surface and the work function profiles [11]. In scanning electron microscopy (SEM), beams of electrons are focused by the electromagnetic lenses on the sample with energy up to 40 KeV in high vacuum chamber and scanned with parallel lines. Consequently, the reflected signals backscattered or secondary electrons are collected to estimate the sample morphology and provide an image. [12]. Up to date, SEM is widely used in several fields, for instance in semiconductor manufacturing, medical and material science research. Figure (3-4 A,B) shows the SEM scheme and operation with the instrument image. An SEM instrument contains on electron source which is the electron gun, two magnetic or condenser lenses, scanning coils which facilitates the deviation of electron beam in x and y dimensions, objective lens and detectors for backscattered and secondary electrons[13]. The scanning electron microscope FEI-Nova SEM has been used in this research.

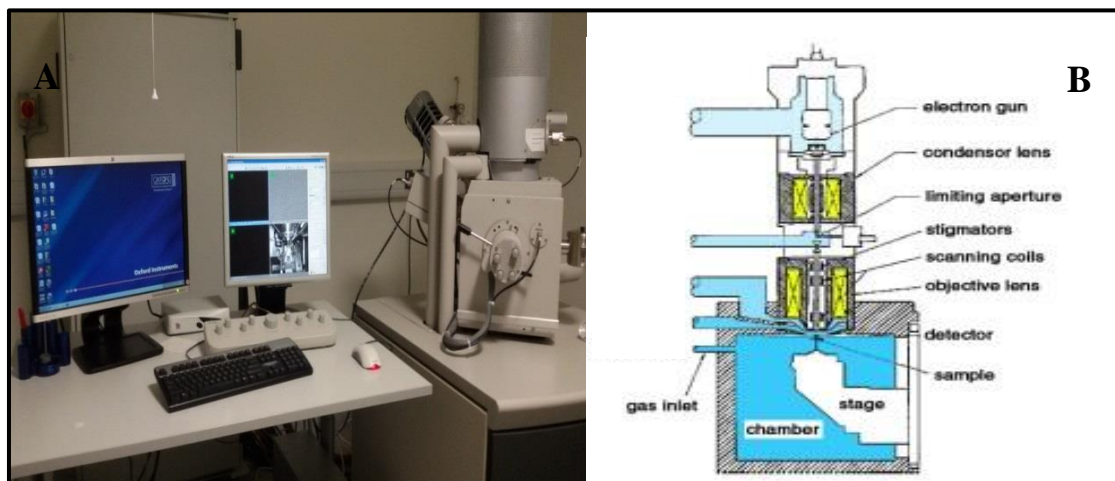


Figure 3-4: (A) Scanning Electron Microscope FEI-Nova (B); Schematic diagram of a typical SEM.

3.1.1.5 Atomic Force Microscopy using Nanoscope IIIa Brucker AFM

Atomic force microscopy (AFM) is a scanning probe technique widely used in research and industrial applications for visualizing surfaces at the nanoscale as well as measuring surface physical properties. Even though electron microscopy techniques like transmission electron microscopy (TEM) or scanning electron microscopy (SEM) can be utilized for similar surface investigations, the high vacuum environment and specific sample preparation required, prevents the real time imaging and in-situ monitoring of biological systems.

AFM, with its ability to obtain high resolution images under ambient (air or fluid) conditions, therefore, has been used to follow kinetic processes in many systems ranging from polymeric and crystalline materials [14], to cellular membranes and biomolecules [15]. Atomic force microscopy (AFM) is a high-resolution scanning microscopy with a verified nanometer resolution. Gerd Binnig and Heinrich Rohrer were developed both SEM and AFM in the early 1980s at IBM Research - Zurich, an achievement that earned them the Nobel Prize in Physics in 1986. The first atomic force microscope was available in the market in 1989.

AFM includes a cantilever with a sharp tip which is used to scan the film surface. This probe follows the surface profile and the information recorded using a laser as shown in Figure (3-5A), and Figure (3-5B) shows the AFM principles operation [16].

The topographic image of the surface can be acquired by recording the deflection of the cantilever, which results from the difference of interaction force between cantilever tip and the sample surface [17]. AFM can operate in three different modes: contact mode, noncontact mode, and tapping mode [11]. Figure (3-5B) shows the dependence of the interaction force on the distance between the tip and the sample surface. At larger distances from the surface, the attraction force is dominating, while the repulsion force starts to dominate at smaller distances (in the range of a few angstroms). The basic idea of AFM is slightly different from SEM, Although the main unit is the same [X,Y,Z

piezo-ceramic positioner], the principle of registration of vertical movement of the tip, which is usually made of Si_3N_4 by CVD, on a flexible cantilever, is optical.

The laser beam reflected from the cantilever is detected with the position sensitive photodiode. This construction is universal, and is adopted by the majority of scanning nanoprobe instruments [11]. In the contact mode, the tip is brought into close contact with the sample surface, so that the force between the tip and the sample becomes repulsive. The deflection of the cantilever caused by this force is registered with a photodiode. The signal is compared to the predefined value of deflection (force), and the DC feedback system generates a certain voltage applied to the Z-part of the piezo-ceramic to keep the value of deflection (force) constant. This DC voltage therefore, measures the surface roughness. The vertical resolution of the AFM contact mode is in the range of 10^{-2} nm, while the lateral resolution can reach the values less than 1 nm, depending mostly on the tip radius [11]. The disadvantage of contact mode is that it can damage both the sample and the tip. Comparison of AFM tapping and contact modes shows clearly the advantage of the former for this particular application.

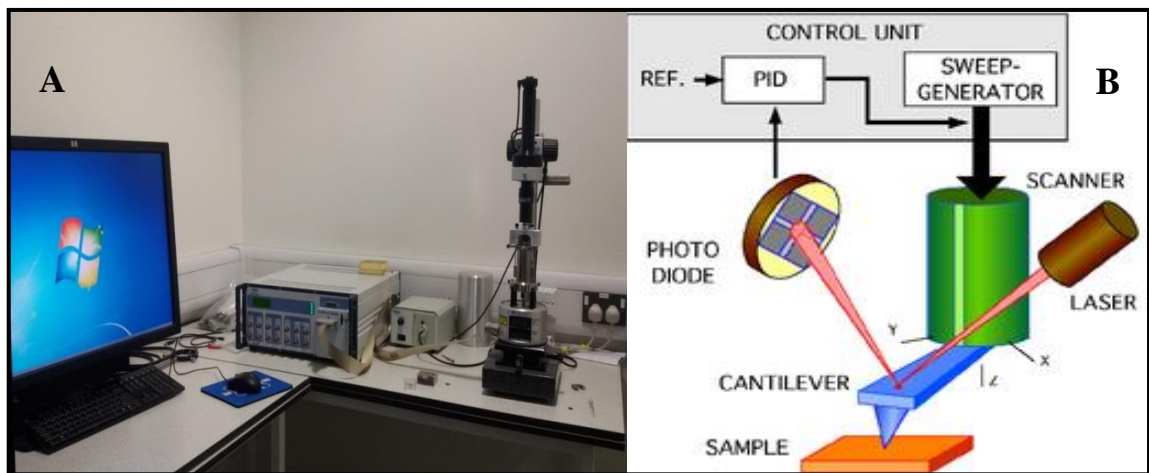


Figure 3-5: (A) Atomic force microscope Nanoscope IIIa (Brucker) (B); Schematic diagram of a typical atomic force microscope.

3.2 Electrochemical DC and AC methods for biosensing approaches

Electrochemical sensors can be classified by their operational principles, e.g. amperometric, conductometric (impedimetric), and potentiometric, which are based, respectively, on measurements of electric current, conductivity in DC measurements or general impedance in AC measurements, and voltage (potential). Different biological reactions and processes can be monitored using their electrochemical characteristics; this approach is not invasive and is relatively cheap. The parameters and metabolic activity of cells and microorganisms can be studied and monitored using their electrochemical properties. Cell growth, cell activity, changes in cell composition, numbers, shapes or cell locations are only some examples of characteristics can be detected by microelectrode cell sensors. The electrochemical properties of a biological sample reflect actual physical properties of the cell membrane.

3.2.1 DC electrochemical measurements

DC measurement is a very reliable technique for investigating the electrical properties of a liquid bacteria suspension. If a DC potential is applied across the electrodes, a current may flow under certain conditions. Thus, it is important to consider the addition of a resistive path in parallel with the capacitive in the electrical model of this surface. This resistor can be non-linear with the applied voltage. The flow of a current through this metal-electrolyte interface requires the net movement of a charge in response to an electric field due to the applied voltage.

The conductivity of metals and semiconductors is due to electrons (holes in semiconductors are missing electrons) while electrolytes conduct the current due to ions. Therefore the processes of discharging ions must take place at the interface between metal as semiconductor and electrolyte, for example, in the case of a simple system of two metal electrodes dipped into NaCl aqueous solution and connected to a battery (see Figure 3-6) the following electrochemical reactions are taking place:

$2H^+ + 2e^- \rightarrow H_2 \uparrow$ and $Na^+ + e^- \rightarrow Na \uparrow$ on cathode, $O^{2-} \rightarrow 2e^- + O_2 \uparrow$ and $2Cl^- \rightarrow 2e^- + Cl_2 \uparrow$ on anode.

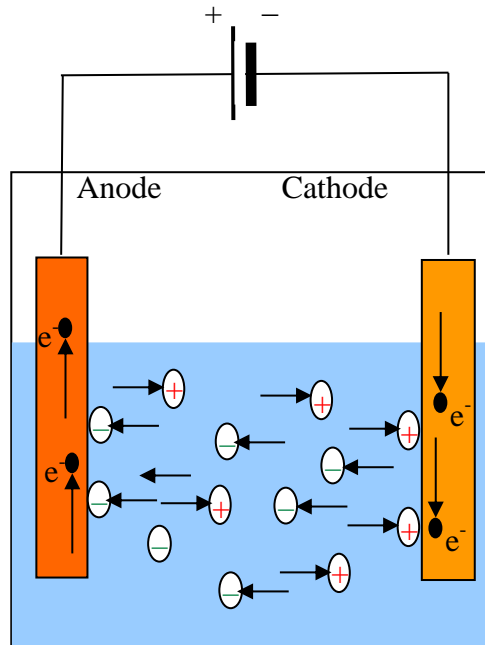


Figure 3-6: Charges exchange on metal electrodes in contact with electrolyte

In reality, the reactions are more complex: highly reactive Na will most likely react with water to form $NaOH$ near cathode, while O_2 and Cl_2 gas may cause the corrosion of anode by forming metal oxides and metal chlorides, respectively; alternatively Cl_2 may react with water to form HCl near the anode.

As a result of such charge exchange processes electrical double layers will form on the surface of both electrodes. For example on the cathode, the negative electron charge on the surface of metal will be counterbalanced by positive ions in solution, as shown in Figure 3-7. Because the concentration of ions in solution is much lower than concentration of electrons in metals, the space charge of ions will be extended (by few microns) into solution.

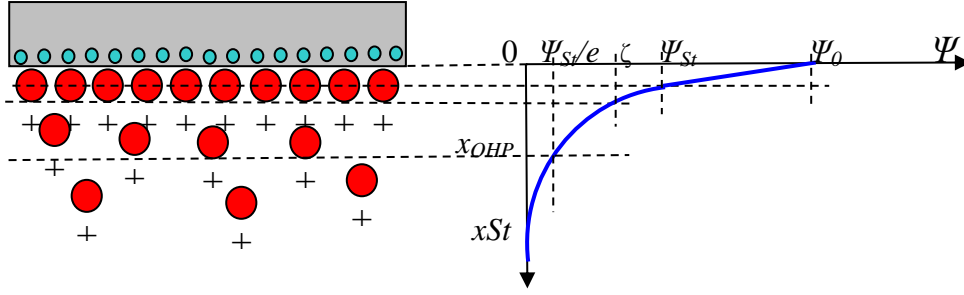


Figure 3-7: Electrical double layer (EDL) at metal-electrolyte interface and the resulting distribution of surface potential in EDL.

The diagram of an EDL in Figure 3-7 is schematic and in reality both cations and anions in the electrolyte are solvated by polar water molecules. The main feature of an EDL is however represented correctly, with an actual double-layer called the Helmholtz layer at the very surface and an extended diffusion layer called as Gouy-Chapman layer. According to the Sterns model [18] the resulted surface potential distribution is described by a linear potential drop within the Helmholtz layer between 0 and outer Helmholtz plane (x_{OHP}) also called as Stern plane

$$\Psi = \Psi_0 \left(1 - \frac{x}{x_{OHP}} \right) \quad (3.1)$$

and an exponential dependence within the Gouy-Chapman layer beyond the Stern plane

$$\Psi = \Psi_{st} \exp\left(-\frac{x - x_{OHP}}{\delta}\right). \quad (3.2)$$

The potential ζ at shear plane (boundary of diffuse layer) is known as ζ -potential or electrokinetic potential. ($x > x_{OHP}$). Because Stern and shear planes are very close $\zeta \approx \Psi_{st}$. Another characteristic parameter, e.g. Debye length (δ), is introduced at the point of Ψ_{st}/e . The Debye length depends on the ion concentration C in solution as $\delta \approx 1/\sqrt{C}$, and typically is in the nanometres range. ζ -potential and thus the voltage

drop on a particular metal-electrolyte contact depend on many parameters. There include the surface potential of the metal, electrolyte contents, concentrations of chemicals present, pH, and temperature. Passing current through the contact may alter the chemical composition and concentrations in the vicinity of the electrode and therefore affect the potential drop at the contact. Such instability of the contacts' potentials should be taken into account during electrical measurements in electrolytic cells. The simplest electrochemical cell shown in Figure (3-8a) consists of two electrodes traditionally called as working electrode (WE) and counter electrode (CE). The working electrode is usually the electrode being studied, i.e. the electrochemical processes on this electrode which could be functionalised with biological receptors, such as enzymes, are of interest. The distribution of the electric potential in this system in Figure (3-8b) exhibits potential drops at both electrodes as well as a potential drop in the electrolyte in the middle. Since both contact potentials are not stable the electrical measurements in two-electrode system have some uncertainty. In order to eliminate the instability of one of the electrode (typically WE), its potential is recorded against the third reference electrode which a stable potential.

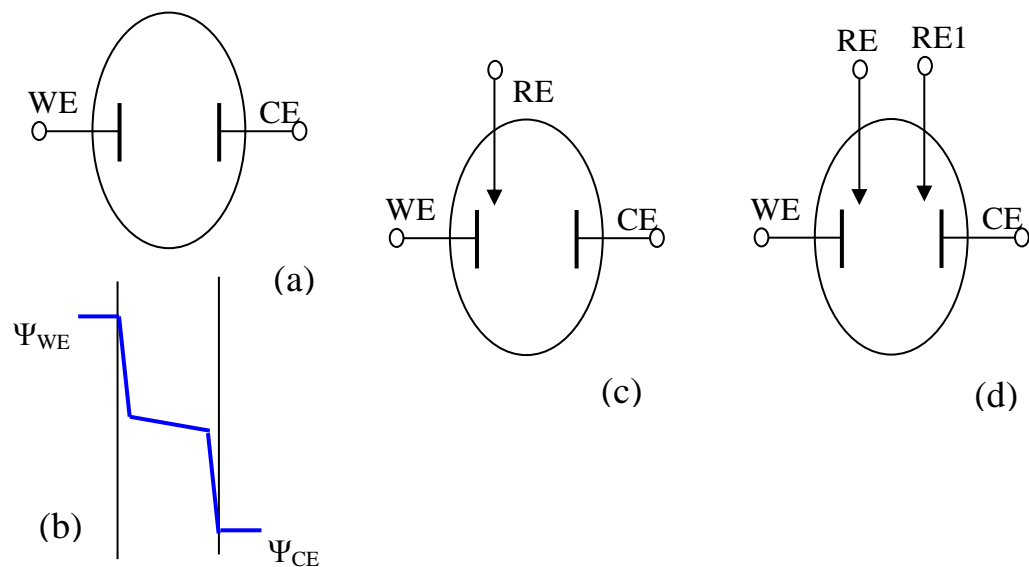


Figure 3-8: Two-electrode system (a) and potential distribution in it (b); three-electrode (c) and four-electrode systems (d).

as shown in Figure (3-8c). The construction of the RE is such that potential is invariant of the electrolyte content. One of the most popular RE designs is Ag/AgCl electrode which consists of an Ag wire in contact with the saturated AgCl solution encapsulated into a glass probe connected to the cell via porous glass tip. Such three-electrode systems are very common and widely accepted in electrochemistry. If, however, the stability of potentials of both WE and CE are of concern, a second reference electrode (RE1) coupled to CE can be introduced in four-electrode cell as shown in Figure (3-8d). One more condition should be obeyed when using reference electrodes in three- or four-electrode systems, the electric current should not pass between WE and RE (or CE and RE1). The circuit design for basic DC electrical measurements of current voltage characteristics in three-electrode cell, called voltammetry, is shown in Figure (3-9a). The current is passed between WE and CE and recorded with the amperometer while the voltage at WE is measured against the RE. Usually such measurements are carried out using a potentiostat (see Figure 3-9b) which automatically provide such functionality. The potentiostat allows operating in different modes, for example, cyclic voltammetry during which the current is recorded during scanning over the predefined voltage range.

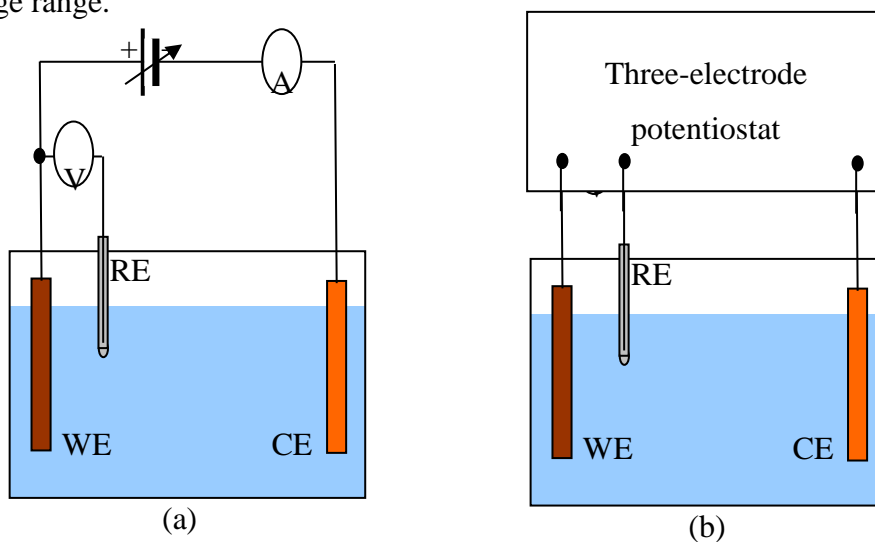


Figure 3-9: Circuit for voltammetry in three-electrode cell (a), the same circuit with potentiostat (b).

Let's discuss the processes of electric charge exchange on electrodes in more detail. The electroactive chemicals which take part in the electric charge exchange could exist in either reduced (Red) or oxidized (Ox) forms, thus the charge exchange reaction on electrodes can be described as: $Ox + ze^- \leftrightarrow Red$, where z is the number of electrons discharged at the electrode. According to Faraday's law the electric current between two electrodes immersed in an electrolyte consists of two components, i.e. cathode (or reduction) current I_c and anode (or oxidation) current I_a which is given by Faraday law:

$$I = I_c + I_a = zFk_c C_{ox} - zFk_a C_{red}, \quad (3.3)$$

in which F is Faraday constant, C_{ox} and C_{red} are concentrations of Ox and Red components, respectively, while k_c and k_a are, respectively, cathode and anode reactions rates which in turn depend on respective electrodes' potentials:

$$k_c = k_0 \exp\left[-\alpha zF \frac{(E - E_0)}{RT}\right]; \text{ and } k_a = k_0 \exp\left[(1 - \alpha)zF \frac{(E - E_0)}{RT}\right]; \quad (3.4)$$

where k_0 and E_0 are, respectively, standard rate constant and standard redox potential, R is gas (or Redberger) constant and T is temperature. Assuming that $I_c = I_a$ in equilibrium, the ratio of concentrations of Ox and Red components is given by Nernst's equation:

$$\frac{C_{Ox}}{C_{Red}} = \exp\left[\frac{zF(E - E_0)}{RT}\right] \quad (3.5)$$

Current-voltage characteristics of electrolytic cell are usually recorded by scanning the applied voltage from negative (cathode) to positive (anode) potentials and back; such characteristics are called as cyclic voltammograms (CV) in electrochemistry. Typical CV characteristics of redox reaction are shown schematically in Figure (3-10). The peak current corresponding to the oxidation process is observed on the forward pass, while almost symmetrical negative current peak associated with the reduction process appears on the reverse pass.

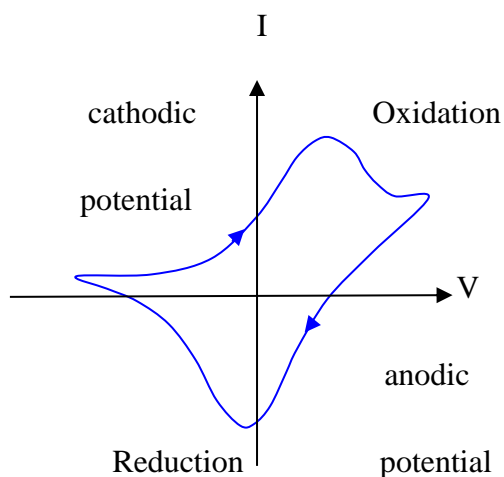


Figure 3-10: Typical cyclic voltammogram of redox reaction.

As has been mentioned previously, the most common and therefore accurate measurements are taken in three-electrode systems using a potentiostat. Typically, the voltage on the plot corresponds to the voltage of working electrode measured against the reference electrode. The current values from peaks may deviate from zero value due to so-called non-Faradaic processes not related to charge exchange, i.e. polarization of electrodes, adsorption and desorption of molecules on electrodes and corresponding redistribution of electrical charges in the system.

The most common approach is based on measurements of cyclic voltammograms (CV) in three-electrode electrochemical cell as described in previous (3.3.1) section. The first electrochemical sensor, known as Clark's oxygen electrode, was developed by L.C. Clark in 1956 [19]. As shown schematically in Figure (3-11), it is constructed on a bases of Ag/AgCl electrode with inserted Pt wire acting as a catalytic working electrode; the electrode is separated from the investigated volume by an oxygen-permeable membrane. An amperometer connecting Ag/AgCl and Pt electrodes registers a current caused by oxygen reduction on the Pt electrode acting as a cathode:

$$O_2 + 4e^- + 2H_2O \rightarrow 4OH^-.$$

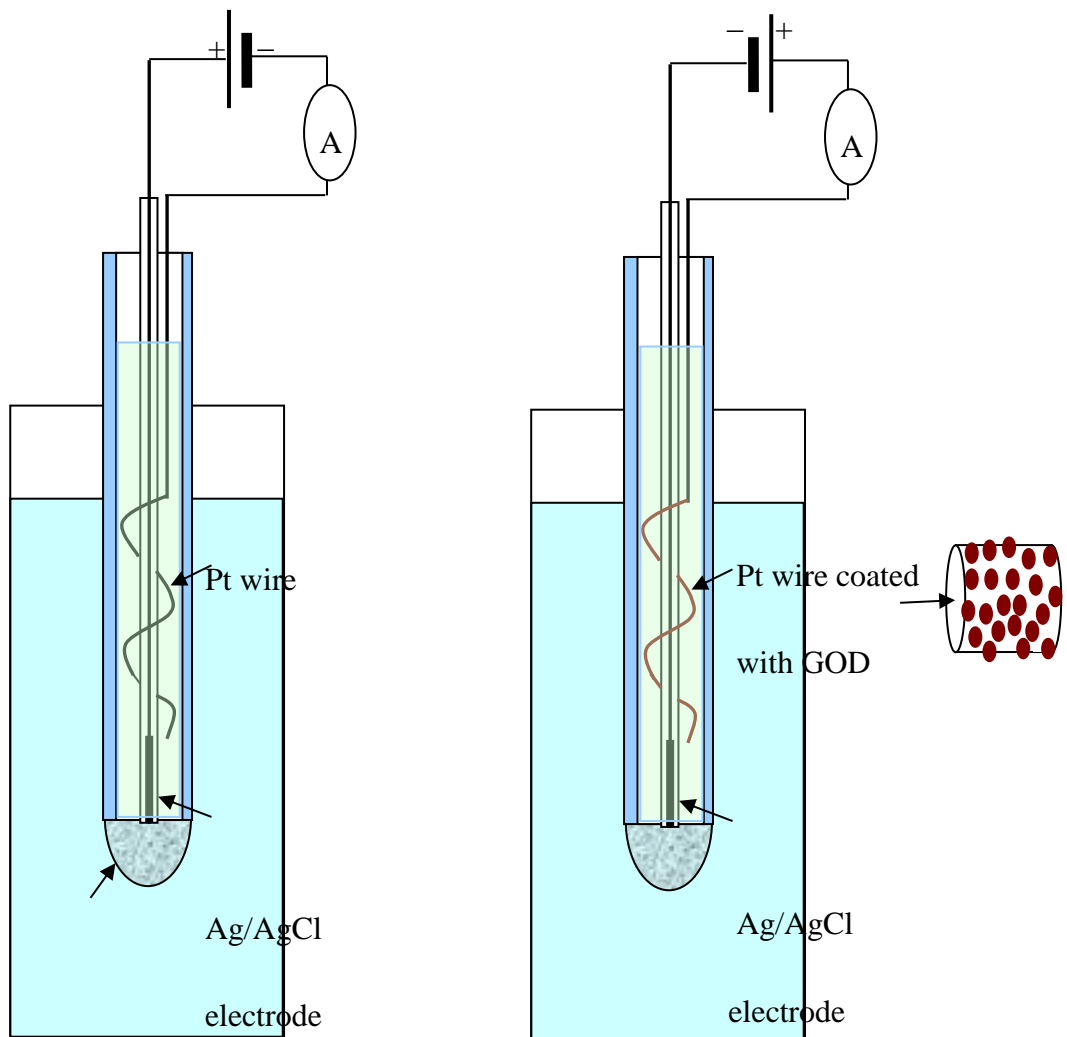


Figure 3-11: Clark oxygen electrode (a), Glucose sensor (b).

Further modification of Clark electrode by coating it with the enzyme glucose-oxidase (GOD) lead to development of glucose sensor. Enzymes are folded proteins which can capture selectively some small molecules (known as substrata) and catalyze their decomposition. In this case, glucose-oxidase catalyses decomposition of glucose with one of the side products being hydrogen peroxide;



Hydrogen peroxide is further reduced to oxygen ($2H_2O_2 \rightarrow O_2 + 2H_2O$) which can be detected with the Clark electrode.

Also H_2O_2 can be directly detected with Clark electrode, but this time the Pt electrode has to be set at anode potential of 0.68V, and the current was due to the following electrochemical anode reaction: $H_2O_2 \rightarrow O_2 + 4e^- + 2H^+$.

Later, the glucose sensor as well as other enzyme sensors, have been developed further in using direct amperometry on electrodes with entrapped enzymes [20]. Different enzyme reactions can be utilised for sensor development; in addition to decomposition of glucose by glucose-oxidase, other typical enzyme/substratum pairs are: cholinesterase/choline, urease/urea, lactase/lactose, alcohol dehydrogenase converting alcohols to aldehydes or ketones, etc. It is interesting that glucose sensors are the most common on the biosensing market because of the unique stability of glucose-oxidase. But due to diabetes being an increasingly common and controllable condition, so long as blood glucose is known.

These days the most common approach in enzyme amperometric sensing is based on the use of mediators as alternative oxidising agents [21]. Mediators are typically redox pairs, i.e. chemicals having distinctive oxidized and reduced states with corresponding peaks on CV. Such mediated enzyme electrochemical reaction is shown schematically in Figure (3-12):

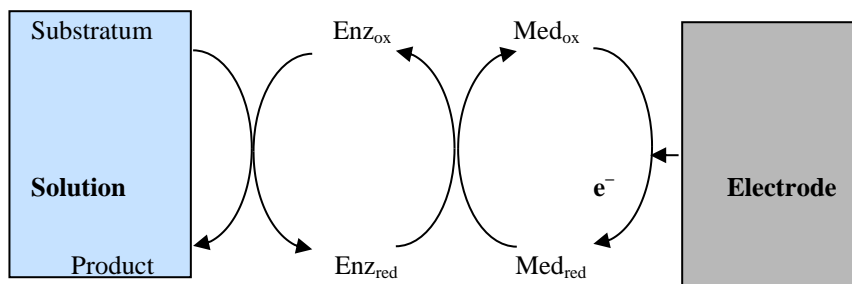


Figure 3-12: The scheme of mediated enzyme reaction.

Typical examples of such mediated enzyme sensors are: sensor for glucose utilising enzyme glucose oxidase and ferrocene (as mediator) [22], sensors for fructose using the enzyme fructose dehydrogenase and mediator ferricyanide [23], sensor for morphine based on the enzyme morphine dehydrogenase and mediator phenazine methasulfate [24].

These days, the design of amperometric enzyme sensors is mostly based on standard screen-printed three-electrode assemblies produced commercially, for example by DropSens. Typical electrode materials are gold, platinum, and carbon and the assembly typically has a solid Ag/AgCl electrode on board. Portable plug-and-play DropSens potentiostats allows various types of measurements including CV. Immobilization of active enzymes on the surface of electrodes can be achieved by different means. In addition to traditional methods of enzyme encapsulation into a porous matrix such as glutaraldehyde/BSA mixture [25] or hydrogels [26] the method of electrostatic self-assembly proved to be successful [27]. Deposition of alternating layers of enzyme urease or cholinesterase and the polycation PAH proved to be successful and provided good stability of enzymes samples could be kept in the fridge for few weeks as well as good permeation of substrata into the matrix [11].

3.2.1.1 Cyclic voltammetry using μ STAT 4000 (DropSens)

Cyclic voltammetry is the most common technique used for acquiring versatile information on the redox processes and the kinetics of heterogeneous electron-transfer reactions, and adsorption processes. It is often the first experiment performed in an electrochemical analytical study and usually used to learn the electrochemical properties of an analyte in solution [28].

μ STAT 4000 is a portable multi potentiostat/galvanostat from DropSens for use with electrochemical sensors or electrochemical cells. The instrument contains a microprocessor which controls up to four independent electrochemical nodes; each one is able to apply potential or current to the electrodes and measure the current or

potential response. Each node is used with electrochemical sensors or electrochemical cells with three electrodes: working electrode, reference electrode and auxiliary electrode. With μ Stat 4000 you can perform up to four different electrochemical techniques at the same time, or carry out the study using the same electrochemical technique in several nodes but selecting different parameters to record. Also, μ STAT 4000 can be used in multichannel mode, with up to four working electrodes sharing one auxiliary electrode and one reference electrode. μ STAT 4000 can be connected to a PC via Bluetooth or by means of a USB cable [29].

Cyclic voltammetry has proven to be a convenient and relatively fast method of screening electro-catalysts, while *in situ* cyclic voltammetry has been widely used for evaluating electrode preparation procedures and characterizing electrode changes during fuel cell durability testing. However, the limitation of cyclic voltammetry is that it mainly provides qualitative and quantitative information, so the thorough investigation of electrochemical reactions is often always associated with other electro analytical methods. Cyclic voltammetry is an important and very frequently utilized electrochemical technique because it offers a wealth of experimental information and insights into the kinetic and thermodynamic details of many chemical systems. It was first reported in 1938, and then described theoretically by Randles in 1948 [28]. Cyclic voltammetry measurement is accomplished with a two- or three-electrode arrangement, whereby the potential relative to some reference electrode is scanned at a working electrode while the resulting current flowing through a counter electrode is monitored as it shown in Figure (3-13A,B). It is rarely used for quantitative determination, but it is ideally suited for a quick search of redox couples, for understanding reaction intermediates, and for obtaining stability in reaction products [30].

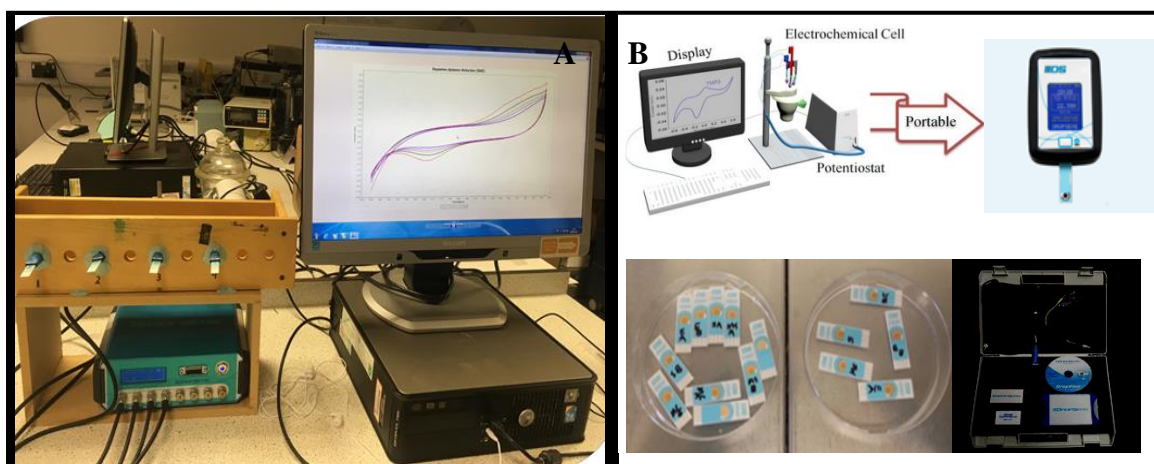


Figure 3-13: (A) Four-channel cyclic voltammetry experimental set-up based on μ STAT 4000 potentiostat (B); Typical voltammogram on PC screen, portable fixed-voltage potentiostat and screen-printed three electrode assemblies.

3.2.1.2 Cyclic voltammogram analysis

In cyclic voltammetry, the electrode potential changes linearly versus time. This ramping is known as the experiment's test rate (V/s). The voltage is applied between the electrodes and the current is measured between the working electrode and the counter-electrode. The data are most often plotted as current (I) against voltage (V). Cyclic voltammetry (CV) has become a broadly used electro analytical technique in many areas of chemistry. It is widely used to study a diversity of redox processes, to achieve stability of reaction products, the presence of intermediates in oxidation-reduction reactions, reaction and electron transfer kinetics [28], and the reversibility of a reaction [30].

The curve resulting from a particular set of cyclic voltammetry measurements is known as a cyclic voltammogram. A typical cyclic voltammogram recorded for a reversible redox system is shown in Figure (3-14A). The characteristics of the peaks in a cyclic voltammogram can be used to acquire qualitative information about the relative rates of reaction and reactant diffusion in a given electrochemical system. In Figure (3-14B), it can be observed that when the potential of the working electrode is more positive than

that of a redox couple, the corresponding reactants may be oxidized and produce an anodic current. The peak current occurs when the potential reaches a value at which all the electrochemically active reactants at the electrode surface are completely consumed. When the potential is controlled at this value, the mass transport rate from the bulk to the electrode surface reaches a maximum, driven by the largest concentration gradient between them. After this peak, the current will decline because the double-layer thickness increases, resulting in a less steep concentration gradient for the active reactant. On the reverse voltage scan, as the working electrode potential becomes more negative than the reduction potential of a redox couple, reduction may occur and cause a cathodic current. A cyclic voltammogram can have several cathodic and anodic peaks due to intrinsic reaction mechanisms.

The important parameters in a cyclic voltammogram are the peak potential and peak currents. If the electron-transfer process is fast as compared to other processes (such as diffusion), the reaction is regarded as electrochemically reversible, and the peak separation due to the potential scan rate.

Therefore, the reversibility of an electrochemical reaction is always a relative term, related to the potential scan rate. A reaction that is reversible at low-scan rates may become quasi reversible or even irreversible at high-scan rates. In these cases, the anodic peak potential becomes more positive and the cathodic peak potential becomes more negative. This occurs because the current takes more time to respond to the applied voltage than in the reversible case. The separation of the two peaks also becomes larger than in the reversible case, as shown in Figure (3-14B). Therefore, cyclic voltammetry can be used to elucidate the kinetics of electrochemical reactions taking place at electrode surfaces. From the sweep-rate-dependent peak amplitudes, and the widths and potentials of the peaks in the voltammogram, information can be obtained about adsorption, desorption, diffusion, and coupled homogeneous electrochemical reaction mechanisms. If the rate of the electron-transfer is slow in

comparison to other processes (such as diffusion) the electrochemical reactions will be quasi-reversible or irreversible rather than completely reversible [29].

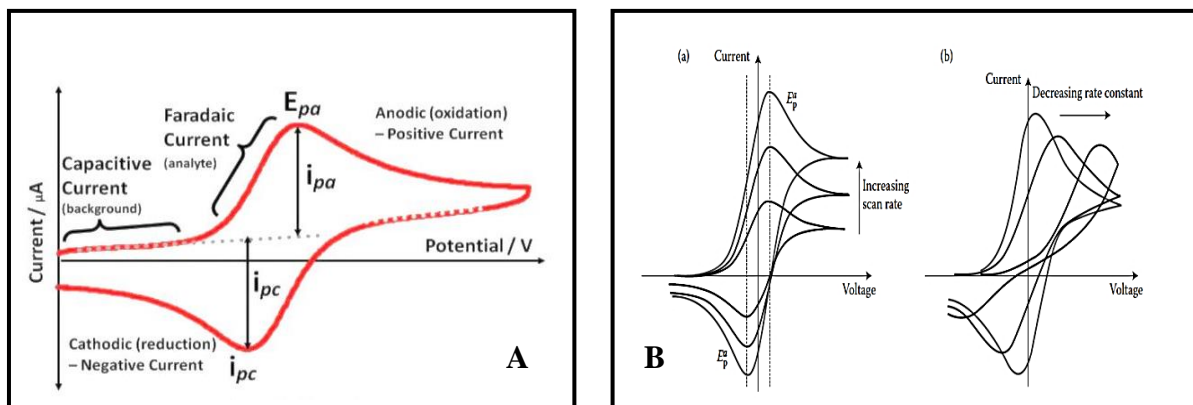


Figure 3-14: (A) Typical cyclic voltammogram; (B) The effects of scan rate (a) electron transfer rate (b) on cyclic voltammogram.

3.2.2 AC electrochemical measurements

Today, AC electrochemical measurement might be one of the most powerful and sensitive technologies, for examining the surface electrical properties of an electrode and its coatings which used for determining surface area of the electrode and analyte reaction. These techniques fall into two general categories. The first type uses a surface-limited chemical reaction to quantify the surface area of the electrode. In contrast, the second type measures a physical characteristic that is proportional to the surface area.

3.2.2.1 Electrochemical Impedance Spectroscopy using PARSTAT 4000A

The PARSTAT 4000 teamed with the VersaStudio software package, comprises a simple-to-use, flexible, and extremely powerful system for performing a wide range of electrochemical testing. The PARSTAT 4000 is a potentiostat/galvanostat with frequency response analyzer (FRA) combined in a single unit. It is controlled from any

suitably equipped PC using the VersaStudio electrochemistry software package. The usefulness of impedance spectroscopy lies in the ability to distinguish the dielectric and electrical properties of individual contributions of components under investigation. Electrochemical impedance involves the analysis of resistive and capacitive (or inductive) elements responses to the small amplitude sinusoidal excitation signal response [31].

Impedance spectroscopy has been widely used for detection of a variety of analytes from small molecules, such as toxins, to large protein molecules and even larger objects such as viruses and bacteria [32].

The detection principle of impedance spectroscopy (IS) lies in recording the changes of impedance caused by different phenomena: (i), binding of target molecules to receptors antibodies, DNA, proteins, whole cells, bacteria and other bio-recognition elements immobilized on the surface of the electrodes [33] (ii), changes in the conductivity of the medium caused by the growth of bacteria [34] (iii), due to suspension of target molecules in the aqueous medium [35], or (iv), capturing bacterial cells on the surface of electrodes using dielectrophoresis (DEP) [36], or (v), changes in the ionic concentration of the medium caused by the activity of enzyme used as labels for the signal amplification [37].

Generally impedance measurements are divided into two categories: Faradaic and non-Faradaic [38]. Faradaic measurements require the presence of a redox probe providing electron-ion exchange at the electrodes, while non-Faradsic measurements can be performed in the absence of a redox probe. Traditionally, macro-sized metal rods or wires were used as electrodes immersed in the medium to measure the impedance [39], shown in Figure (3-15 A,B). In attempt to miniaturize the IS sensors and improve their sensitivity, micro-electrodes have been considered as potential candidates to combine with traditional detection systems. Microelectrodes favor a greater rate of reactant supply while macro electrodes cause greater depletion of reactants and require lower

concentrations of electro-active ions to form double layer as compared to macro electrodes [40].

As a result, microelectrodes can perform impedance measurement even in solutions of low conductivity, where macro electrodes may not be sensitive. Among microelectrodes, interdigitated array microelectrodes (IDAM) present promising advantages in terms of low ohmic drop, fast establishment of steady-state, rapid reaction kinetics, and increased signal-to-noise ratio [41]. IDAM consist of a series of parallel microband electrodes in which alternating microbands are connected together, forming a set of interdigitating electrode fingers. Due to proximity of cathodic and anodic electrodes, minute amounts of ionic species can be efficiently cycled between the electrodes resulting in very large (>0.98) collection efficiencies, giving the IDAM an advantage in detecting small amounts of generated electrode products [42]. IS using IDAM is illustrated in Figure (3-15 A,B).

Additionally, IDAM eliminates the need for a reference electrode because of small amplitudes of AC signal and provides simple means for obtaining a steady-state current response, which is comparatively simpler to detect in comparison to three or four electrode systems [43]. Impedance spectroscopy is one of the principal electrical/electrochemical transductions methods providing the means of label-free, real-time, and non-invasive detection of different analytes for a wide range of applications in biological and biomedical areas.

The following examples clearly show the great potential of impedance spectroscopy which still is not fully explored [44]. Electrochemical impedance spectroscopy is being applied for detection of the concentration of cells adhered on surfaces and present in solution. This method has been extensively used in microbiology for detection, quantification, and identification of bacteria, including micro-machined devices for cell counting or cell differentiation. It has also been used for selective capturing of bacterial cells, antibodies, aptamers, or bacteriophages [45]. Another common application of

impedance spectroscopy is the monitoring of bacterial growth; this technique allows distinguishing between viable and dead bacteria cells. A novel impedance biosensor for bacterial cell detection is constructed by immobilizing antibodies that are specific to the target bacterial cells on an electrode surface. The presence of intact cell membranes on the electrodes determines the current and thus the sensor signal. In this method, the impedance is recorded as a function of the interrogating frequency, and thus having the name of electrical/electrochemical impedance spectroscopy (EIS) [46].

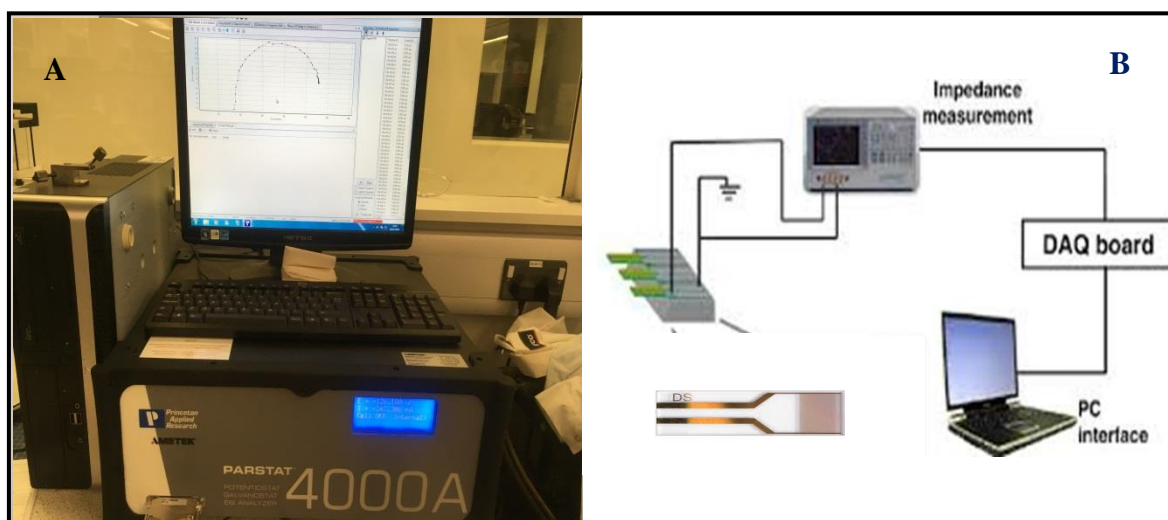


Figure 3-15: (A) PARSTAT 4000A impedance analyzer instrument; (B) Schematic diagram of impedance measurements, and DropSens interdigitated electrode used.

3.2.2.2 Electrochemical impedance analysis

The conductometric electrochemical sensors are based on measurements of conductivity or resistivity of electrolyte solutions containing some active organic or bio-molecules acting as receptors. Since electrochemical DC measurements involve ion-exchange processes on electrodes described in the previous section (3.2.2.1). Conductometry is usually associated with AC measurements of electrical impedance; this method is often referred to impedimetry. These measurements are usually performed in a two-electrode configuration using very small amplitudes of AC voltage in order to avoid any electrochemical processes on the electrodes. The electrodes are functionalised with

molecular receptors capable of binding analyte molecules; these could be antibody-antigen pairs. Alternatively, the active chemicals may exist in solution. The design of electrodes and cells can vary widely. However, these days commercially produced interdigitated metal (gold or platinum) electrodes are the most common. An interdigitated electrode design is schematically shown in Figure (3-16).

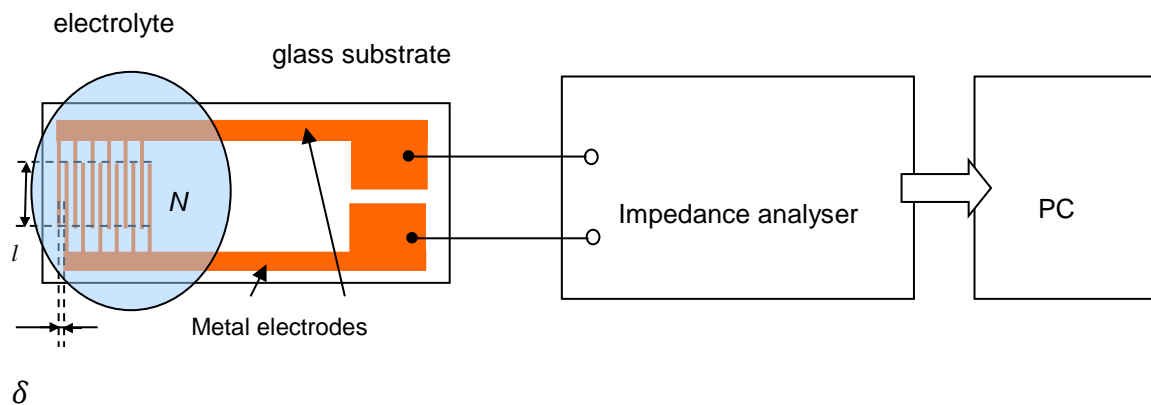


Figure 3-16: Design of interdigitated electrodes and the scheme of AC measurements.

Depending on the manufacturer, the number of fringes N is varied from tens to hundreds, the distance between fringes (δ) is from single to tens of microns, and the overlap (l) is typically of few millimetres. Such design allows increasing significantly the effective area between electrodes (A): $A = l \times \delta \times (2N - 1)$ For example, DropSens produce platinum or gold interdigitated electrode assemblies having 50 or 100 fringes with the spacing of $5\mu\text{m}$ or $10\mu\text{m}$. The AC impedance measurements are usually carried out using impedance analysers operating over a wide frequency range from fractions of Hz up to hundreds of MHz. The dependences of impedance (Z) versus frequency (f) called as impedance spectrum is recorded at small amplitudes of AC voltage, typically 100mV, with or without DC off-set. The impedance spectrum obtained can be presented in different ways. For example as spectra of real (Z') and imaginary (Z'') parts of impedance known as a Nyquist plot. Alternatively, the spectrum

can be presented as spectrum of parallel conductance (G_p) vs capacitance (C_p), or spectrum of the magnitude of Z and phase angle ($\tan\theta$). The results obtained are analysed using dedicated software, which allows fitting the data to the equivalent circuit model and evaluate its parameters.

Typical equivalent circuits explaining the majority of experimental features of impedance measurements in metal-electrolyte-metal systems shown in Figure (3-11) splits in two parts: (i), the electrolyte solution which is described by the resistance of solution (R_S), and (ii), a double layer near the metal electrodes, which represents polarisation of the capacitance of a double layer C_{DL} in parallel with resistor (R_{DL}). An addition, a constant phase element Z_w is associated with the diffusion of chemicals in the vicinity of the double layer; at frequencies higher than 10Hz this element can be neglected (see Fig. 3-17 a,b).

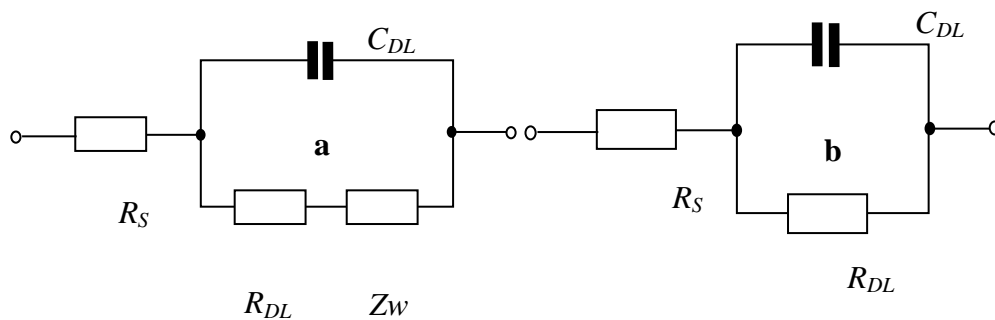


Figure 3-17: Equivalent circuit for impedance measurement in metal-electrolyte-metal system (a), simplified equivalent circuit (b).

It was assumed that two electrodes are identical, thus elements related to double layers on two electrodes can be combined be in one parallel circuit.

The impedance of the simplified circuit can be calculated as

$$Z = Z' - jZ''; Z' = \frac{R_{DL}}{1 + \omega^2 R_{DL}^2 C_{DL}^2} + R_S; Z'' = \frac{\omega R_{DL}^2 C_{DL}}{1 + \omega^2 R_{DL}^2 C_{DL}^2}, \quad (3.6)$$

At low frequencies ($\omega \rightarrow 0$) $Z' = R_{DL} + R_S$ and $Z'' = 0$, while at high frequencies ($\omega \rightarrow \infty$) $Z' = R_S$ and $Z'' = 0$.

The reciprocal of impedance is admittance (i.e., admittance is the current-to-voltage ratio). Impedance is represented as a complex quantity Z and the term 'complex impedance' and real part is the resistance R , and the imaginary part is the reactance X . The reactance and impedance of a capacitor are respectively, where ω is the angular frequency of the sinusoidal signal and j phase indicates. (see Appendix-B).

The results of impedance spectra measurements are often presented as the dependence of Z'' vs Z' known as a Nyquist plot (see schematic graph in Figure 3-18 a,b).

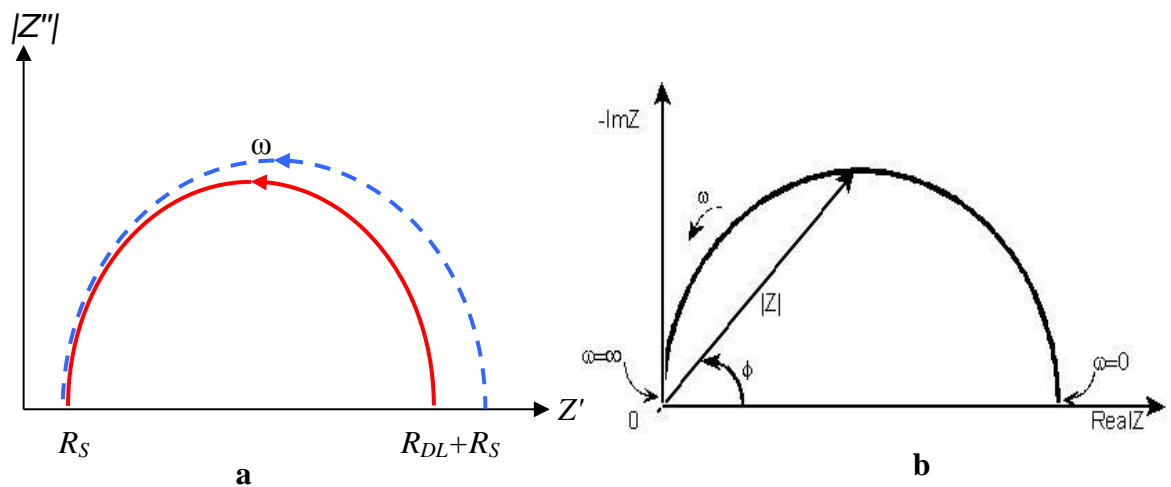


Figure 3-18: Nyquist plot Z'' vs Z' ; Dotted line indicate the outcome of binding analyte to receptor (a) schematic graph of the affinity (b).

Typically, the affinity of reactions, i.e. binding the analyte to receptor immobilized on the surface of interdigitated electrodes, causes changes in the Nyquist plot as shown

schematically in Figure 3-18 (a,b). The conductometric sensor response can be easily quantified by the parameter R_{DL} which can be easily extracted from data using appropriate data fitting software,

Alternatively, Z can be presented by parallel conductivity (or resistivity) and G_p (R_p) and capacitance C_p .

$$Z = \frac{R_p}{1 + \omega^2 R_p^2 C_p^2} - j \frac{\omega R_p^2 C_p}{1 + \omega^2 R_p^2 C_p^2}, \quad (3.7)$$

Both representations are very close. For example, at low frequencies ($\omega \rightarrow 0$)

$$G_p = \frac{1}{R_{DL} + R_S}, \text{ and } C_p = C_{DL} \frac{R_{DL}^2}{(R_{DL} + R_S)^2}, \text{ while at high frequencies } (\omega \rightarrow \infty)$$

$$G_p \rightarrow \infty \text{ and } C_p = C_{DL}.$$

One more possibility is to present the results as spectra of $|Z|$ and $\tan\theta$ which can be easily worked out from eq (3.7). The critical cases are: $|Z| = R_{DL} + R_S$ and $\tan\theta = 0$ when $\omega \rightarrow 0$, $|Z| = 0$ and $\tan\theta = 0$ when $\omega \rightarrow \infty$. The choice of representation of the experimental results and their analysis depends on the particular application.

Therefore, electrochemical methods (both DC and AC) are very common in bio-sensing due to several advantages mainly high sensitivity, low-cost, and simplicity of use. Amperometric sensors based on DC measurements, e.g. CV, are typically associated with enzyme sensors, while conductometric sensors based on AC measurements can be utilised for detection of affinity reactions such as immune reactions.

References

1. Lemmer, P., Gunkel, M., Baddeley, D., Kaufmann, R., Urich, A., Weiland, Y., & Cremer, C. (2008). SPDM: light microscopy with single-molecule resolution at the nanoscale. *Applied Physics B*, 93(1), 1-12.
2. Spring, K. R., & Davidson, M. W. (2008). *Introduction to fluorescence microscopy*. Nikon Microscopy U.
3. Kaprelyants, A. S., & Kell, D. B. (1992). Rapid assessment of bacterial viability and vitality by rhodamine 123 and flow cytometry. *Journal of Applied Bacteriology*, 72(5), 410-422.
4. Yu, W., Dodds, W. K., Banks, M. K., Skalsky, J., & Strauss, E. A. (1995). Optimal staining and sample storage time for direct microscopic enumeration of total and active bacteria in soil with two fluorescent dyes. *Applied and Environmental Microbiology*, 61(9), 3367-3372.
5. Schwedt, G. (1997). *The essential guide to analytical chemistry*. John Wiley & Sons Inc.
6. Lin, H. L., Lin, C. C., Lin, Y. J., Lin, H. C., Shih, C. M., Chen, C. R., & Kuo, T. C. (2010). Revisiting with a relative-density calibration approach the determination of growth rates of microorganisms by use of optical density data from liquid cultures. *Applied and environmental microbiology*, 76(5), 1683-1685.
7. Lecoœur, H. (2002). Nuclear apoptosis detection by flow cytometry: influence of endogenous endonucleases. *Experimental cell research*, 277(1), 1-14.
8. Marie, D., Partensky, F., Jacquet, S., & Vaulot, D. (1997). Enumeration and cell cycle analysis of natural populations of marine picoplankton by flow cytometry using the nucleic acid stain SYBR Green I. *Applied and Environmental Microbiology*, 63(1), 186-193.
9. Shapiro, H. M., & Darzynkiewicz, Z. (1995). *Practical Flow Cytometry* (3rd edn). *Trends in Cell Biology*, 5(9), 372.
10. Robinson, J. P. (Ed.). (1997). *Current protocols in cytometry*. Wiley.
11. Nabok, A. (2005). *Organic and Inorganic Nanostructures* (Artech House Memos and Sensors Library). Artech House Publishers Hardcover: 286 pages.
12. Bogner, A., Jouneau, P. H., Thollet, G., Basset, D., & Gauthier, C. (2007). A history of scanning electron microscopy developments: towards "wet-STEM" imaging. *Micron*, 38(4), 390-401.
13. Egerton, R. F. (2006). *Physical principles of electron microscopy: an introduction to TEM, SEM, and AEM*. Springer Science & Business Media.
14. Ulčinas, A., Butler, M. F., Heppenstall-Butler, M., Singleton, S., & Miles, M. J. (2007). Direct observation of spherulitic growth stages of CaCO₃ in a poly (acrylic acid)-chitosan system: In situ SPM study. *Journal of Crystal Growth*, 307(2), 378-385.
15. Berquand, A., Mingeot-Leclercq, M. P., & Dufrene, Y. F. (2004). Real-time imaging of drug-membrane interactions by atomic force microscopy. *Biochimica et Biophysica Acta (BBA)-Biomembranes*, 1664(2), 198-205.
16. Lang, K. M., Hite, D. A., Simmonds, R. W., McDermott, R., Pappas, D. P., & Martinis, J. M. (2004). Conducting atomic force microscopy for nanoscale tunnel barrier characterization. *Review of scientific instruments*, 75(8), 2726-2731.

17. Lee, J. L., & Gilmore, I. S. (2009). The application of multivariate data analysis techniques in surface analysis. *Surface Analysis-The Principal Techniques*, 2nd Edition, 563-612.
18. Stern, O. Z. (1924). Schematic of double layer in a liquid at contact with a negatively-charged solid. *Electrochem*, 30, 508-516.
19. Clark, L. C. (1956). Jr: Monitor and control of blood and tissue oxygen tensions. *Trans. Am. Soc. Artificial Internal Organs*, 2, 41.
20. Hicks, G. P., & Updike, S. J. (1966). The preparation and characterization of lyophilized polyacrylamide enzyme gels for chemical analysis. *Analytical chemistry*, 38(6), 726-730.
21. Kress-Rogers, E. (1996). *Handbook of biosensors and electronic noses: medicine, food, and the environment*. CRC Press.
22. Cass, A. E., Davis, G., Francis, G. D., Hill, H. A. O., Aston, W. J., Higgins, I. J., & Turner, A. P. (1984). Ferrocene-mediated enzyme electrode for amperometric determination of glucose. *Analytical chemistry*, 56(4), 667-671.
23. Stredansky, M., Pizzariello, A., Stredanska, S., & Miertu, S. (1999). Determination of D-fructose in foodstuffs by an improved amperometric biosensor based on a solid binding matrix. *Analytical Communications*, 36(2), 57-61.
24. Holt, P. J., Stephens, L. G., Bruce, N. C., & Lowe, C. R. (1995). An amperometric opiate assay. *Biosensors and Bioelectronics*, 10(6-7), 517-526.
25. Albareda-Sirvent, M., Merkoci, A., & Alegret, S. (2000). Configurations used in the design of screen-printed enzymatic biosensors. A review. *Sensors and Actuators B: Chemical*, 69(1-2), 153-163.
26. Safdar, M., Sproß, J., & Jänis, J. (2014). Microscale immobilized enzyme reactors in proteomics: latest developments. *Journal of Chromatography A*, 1324, 1-10.
27. Cai, K., Hu, Y., Jandt, K. D., & Wang, Y. (2008). Surface modification of titanium thin film with chitosan via electrostatic self-assembly technique and its influence on osteoblast growth behavior. *Journal of Materials Science: Materials in Medicine*, 19(2), 499.
28. Bard, Allen J.; Larry R. Faulkner. (2000), *Electrochemical methods: Fundamentals and applications*, (2 ed.), Wiley.
29. Sekhar, P. K., & Kysar, J. S. (2017). An electrochemical ammonia sensor on paper substrate. *Journal of The Electrochemical Society*, 164(4), B113-B117.
30. DuVall, Stacy DuVall; McCreery, Richard, (1999), Control of catechol and hydroquinone electron-transfer kinetics on native and modified glassy carbon electrodes", *Anal. Chem.* 71: pp. 4594-4602.
31. Guan, J. G., Miao, Y. Q., & Zhang, Q. J. (2004). Impedimetric biosensors. *Journal of bioscience and bioengineering*, 97(4), 219-226.
32. Ahmed, A., Rushworth, J. V., Wright, J. D., & Millner, P. A. (2013). Novel impedimetric immunosensor for detection of pathogenic bacteria *Streptococcus pyogenes* in human saliva. *Analytical chemistry*, 85(24), 12118-12125.
33. Yang, L., & Li, Y. (2005). AFM and impedance spectroscopy characterization of the immobilization of antibodies on indium–tin oxide electrode through self-assembled monolayer of epoxysilane and their capture of *Escherichia coli* O157: H7. *Biosensors and Bioelectronics*, 20(7), 1407-1416.

34. Yang, L., & Li, Y. (2006). Detection of viable *Salmonella* spp using microelectrode-based capacitance measurement coupled with immunomagnetic separation. *Journal of Microbiological Methods*, 64(1), 9-16.
35. Varshney, M., & Li, Y. (2007). Interdigitated array microelectrode based impedance biosensor coupled with magnetic nanoparticle–antibody conjugates for detection of *Escherichia coli* O157: H7 in food samples. *Biosensors and Bioelectronics*, 22(11), 2408-2414.
36. Aldaeus, F., Lin, Y., Roeraade, J., & Amberg, G. (2005). Superpositioned dielectrophoresis for enhanced trapping efficiency. *Electrophoresis*, 26(22), 4252-4259.
37. Ruan, C., Yang, L., & Li, Y. (2002). Immunobiosensor chips for detection of *Escherichia coli* O157: H7 using electrochemical impedance spectroscopy. *Analytical Chemistry*, 74(18), 4814-4820.
38. Yang, L., Li, Y., & Erf, G. F. (2004). Interdigitated Array Microelectrode-Based Electrochemical Impedance Immunosensor for Detection of *Escherichia coli* O157: H7. *Analytical Chemistry*, 76(4), 1107-1113.
39. Bontidean, I., Berggren, C., Johansson, G., Csöregi, E., Mattiasson, B., Lloyd, J.R., Jakeman, K.J. & Brown, N.L., (1998). Detection of heavy metal ions at femtomolar levels using protein-based biosensors. *Analytical Chemistry*, 70(19), pp.4162-4169.
40. Min, J., & Baeumner, A. J. (2004). Characterization and optimization of interdigitated ultramicroelectrode arrays as electrochemical biosensor transducers. *Electroanalysis*, 16(9), 724-729.
41. Maruyama, K., Ohkawa, H., Ogawa, S., Ueda, A., Niwa, O., & Suzuki, K. (2006). Fabrication and characterization of a nanometer-sized optical fiber electrode based on selective chemical etching for scanning electrochemical/optical microscopy. *Analytical chemistry*, 78(6), 1904-1912.
42. Thomas, J. H., Kim, S. K., Hesketh, P. J., Halsall, H. B., & Heineman, W. R. (2004). Bead-based electrochemical immunoassay for bacteriophage MS2. *Analytical chemistry*, 76(10), 2700-2707.
43. Liu, D., Perdue, R. K., Sun, L., & Crooks, R. M. (2004). Immobilization of DNA onto poly (dimethylsiloxane) surfaces and application to a microelectrochemical enzyme-amplified DNA hybridization assay. *Langmuir*, 20(14), 5905-5910.
44. Blanke, H., Bohlen, O., Buller, S., De Doncker, R. W., Fricke, B., Hammouche, A., & Sauer, D. U. (2005). Impedance measurements on lead–acid batteries for state-of-charge, state-of-health and cranking capability prognosis in electric and hybrid electric vehicles. *Journal of power Sources*, 144(2), 418-425.
45. Lisdat, F., & Schäfer, D. (2008). The use of electrochemical impedance spectroscopy for biosensing. *Analytical and bioanalytical chemistry*, 391(5), 1555.
46. Yang, L., & Bashir, R. (2008). Electrical/electrochemical impedance for rapid detection of foodborne pathogenic bacteria. *Biotechnology advances*, 26(2), 135-150.

CHAPTER 4 Optical and electrochemical detection of toxic pollutants: data obtained on bacterial suspensions

This chapter covers in more detail the experimental procedure of bacterial growth in culture media and focused on the optical and electrochemical data of effect three types of environmental pollutants i.e. heavy metals (Hg^{2+} , Pb^{2+} , Zn^{2+} and Cd^{2+}), pesticides (atrazine, simazine and DDVP) and petrochemicals (hexane, pentane, pyrene, toluene, octane and ethanol), on three types of bacterial isolates which are *E. coli* K12, *S. oneidensis* MR-1, and the methanotrophic bacteria (*Mc. capsulatus* Bath or *Ms. trichosporium* OB3b). The effects of these toxic chemicals on the optical and electrochemical properties of bacteria in suspensions are measured.

4.1 Bacterial culture conditions

Three diverse bacterial strains were selected for this work: (i), the model Gram negative *E. coli* K12, known to be sensitive to various types of pollutants including heavy metals, pesticides, and hydrocarbons [1] (ii), *S. oneidensis* MR-1, a Gram-negative bacterium known to tolerate and interact with heavy metals [2], and (iii), methanotrophic bacteria (*Mc. capsulatus* Bath and *Ms. trichosporium* OB3b) which are Gram-negative bacteria that grow on methane and are also able to co-oxidise a range of other hydrocarbons and hydrophobic organic molecules [3,4]. *E. coli* cultures were grown at 37 °C for 16 h in LB broth and LB agar [5], *S. oniedensis* cultures were grown at 30 °C for 24 h in the same medium [6]., while methanotrophs bacteria (*Mc. capsulatus* Bath or *Ms. trichosporium* OB3b) were grown at 30 °C for 2 weeks in flask cultures in nitrate mineral salts (NMS) medium and on NMS agar plates, using methane as the carbon source, as described previously [7].

4.2 Preparation of analyte samples

The samples of Hg^{2+} , Pb^{2+} , Zn^{2+} , Cd^{2+} , atrazine, simazine, DDVP, hexane, pentane, pyrene, toluene, octane and ethanol (all from Sigma-Aldrich) were prepared at concentrations of 0.1, 1, 10, 100 mM by consecutive dilution of 1 M stock solutions in

deionised water. The stock solutions of hydrocarbons were prepared in a 40% (v:v) ethanol: water mixture. Liquid bacterial culture samples were mixed with these solutions in 1:1 ratio and incubated for 2 hr at (22-25) °C.

4.3 Optical Measurements of bacteria suspension samples

The numbers of live and dead bacteria were determined with fluorescence microscopy and OD₆₀₀ similarly to that described in [8] and earlier in Chapter 3. Live and dead bacteria appeared under microscope as green and red cells, respectively. Typical fluorescence microscopy images are shown in Figure (4-1) for *E. coli*, Figure (4-2) for *Ms. trichosporium* OB3b and Figure (4-3) for *S. oneidensis*, respectively.

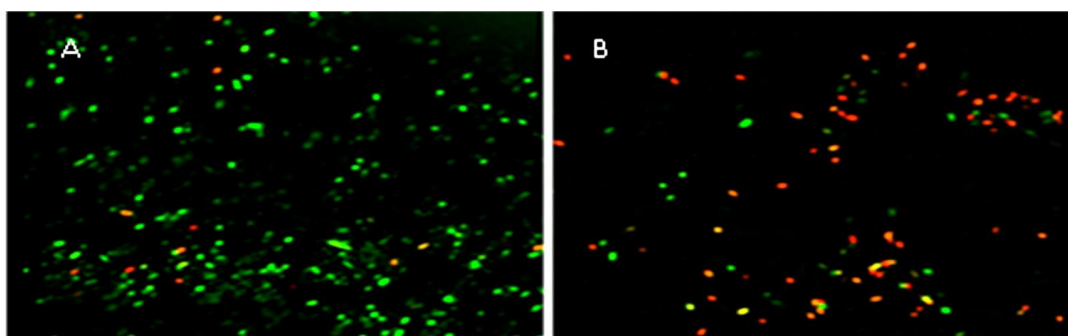


Figure 4-1: Fluorescence microscopy images of *E. coli* before (A) and after (B) treatment with HgCl₂ (1 M) for 2 hr.

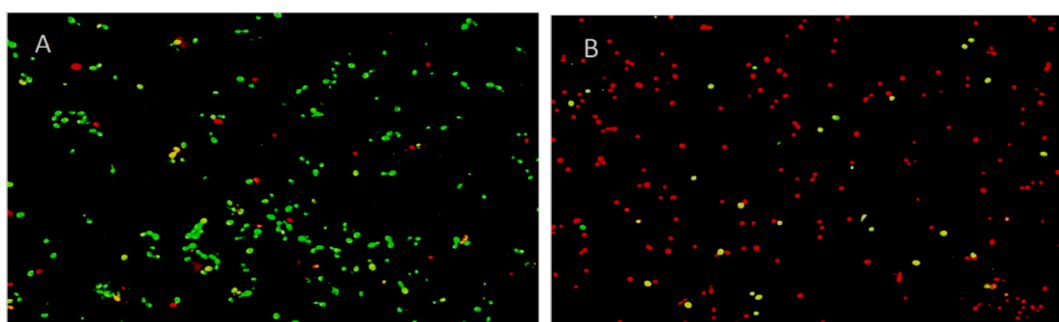


Figure 4-2: Fluorescence microscopy images of *Ms. trichosporium* (OB3b) before (A) and after (B) treatment with HgCl₂ (1 M) for 2 hr.

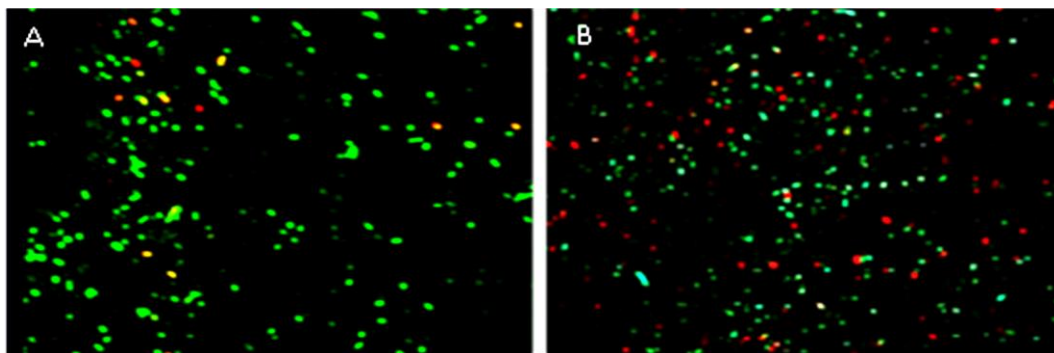


Figure 4-3: Fluorescence microscopy images of *S. oneidensis* before (A) and after (B) treatment with HgCl₂ salt (1M) for 2 hr.

It is clear that the exposure to HgCl₂, (simazine, and octane which will be shown in appendix-A1,2) reduces the number of live (green) bacteria and increases the dead ones (red), though *S. oneidensis* are much less affected than *E. coli* and *Ms. trichosporium* (OB3b). A similar though even more pronounced pattern was observed in flow cytometry experiments where bacteria were stained with the same L7012 Live/Dead Bacterial Viability Kit. The results in Figure 4-4, show live and dead bacteria as blue (live) and orange (dead) dots respectively. Increase in the dead *E. coli* bacteria count after exposure to HgCl₂ salt, (simazine, and octane which will be shown in appendix-A1,2) is visually apparent. Analysis of Figure 4-4A(b) yields the percentage of live *E. coli* cells as 23.88% and 76.12% for dead cells. In addition, dead *E. coli* bacteria appear mostly in the bottom-left quadrant of the graph in Figure 4-4A(b) indicating that increase in the bacterial size is most-likely due to the damage of cell membranes. In contrast, *S. oneidensis* bacteria were affected much less, the percentages of live and dead bacteria after exposure to 1M HgCl₂ solution were 83.36% and 16.64%, respectively. Again, dead bacteria appeared slightly enlarged since they were shifted to the bottom-left in Figure 4-4 B (b). Figure 4-4 C (a , b) shows flow cytometry results for *Ms. trichosporium* (OB3b), where the percentage was 43.57% for live bacteria and 56.43% for dead bacteria.

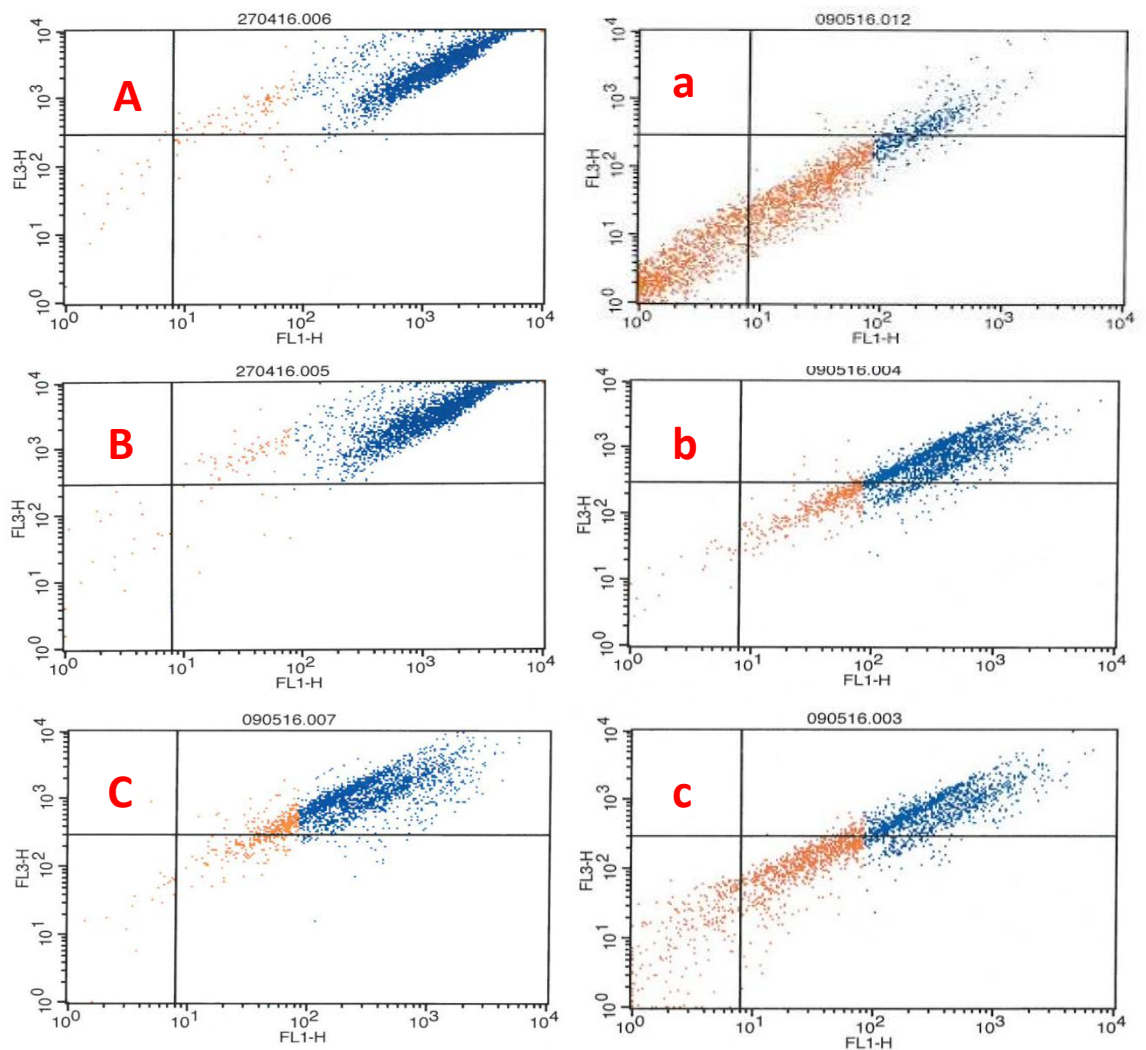


Figure 4-4: Flow cytometry results for *E. coli* Bacteria (A) , *S. oneidensis* (B) and *Ms. trichosporium* (OB3b) (C) ; graphs (a) and (b) were obtained, respectively, before and after treatment with HgCl_2 (1M) for 2 hr.

The result of optical density measurements of all bacteria species and the effect of their treatment with HgCl_2 , simazine, and octane prepared at different concentrations are shown in Table 4-1. The bacterial density was assessed and presented as absorbance by losses of light intensity in the middle of visible range (600nm) as a result of light scattering on the bacteria. The reduction in optical density upon increasing the HgCl_2 concentration was much more pronounced for *E. coli* and *Ms. trichosporium* (OB3b) than that for *S. oneidensis*.

Table 4-1: The results of OD600 for all bacteria samples after exposure to HgCl₂ for 2 hr.

Bacteria	HgCl ₂ concentration						STD(n=3)
	Before treatment	0.1mM	1 mM	10 mM	100 mM	1M	
<i>E. coli</i>	0.813	0.773	0.712	0.637	0.416	0.356	±0.02
<i>S. oneidensis</i>	0.827	0.869	0.861	0.793	0.832	0.753	±0.01
<i>Ms. trichosporium</i> <i>OB3b</i>	0.754	0.728	0.679	0.626	0.554	0.431	±0.03

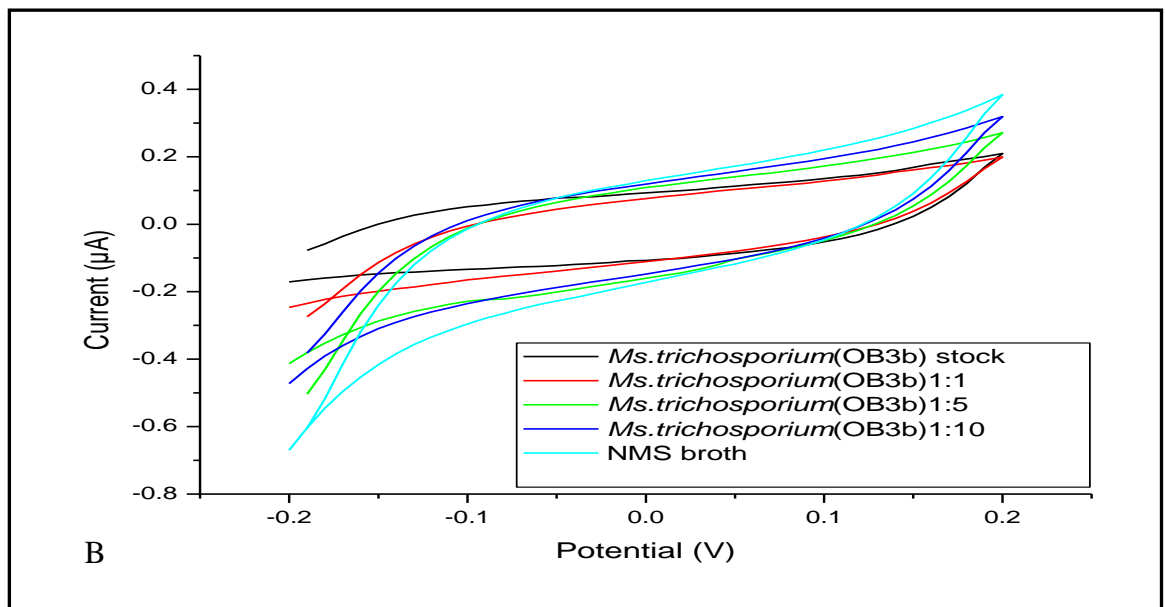
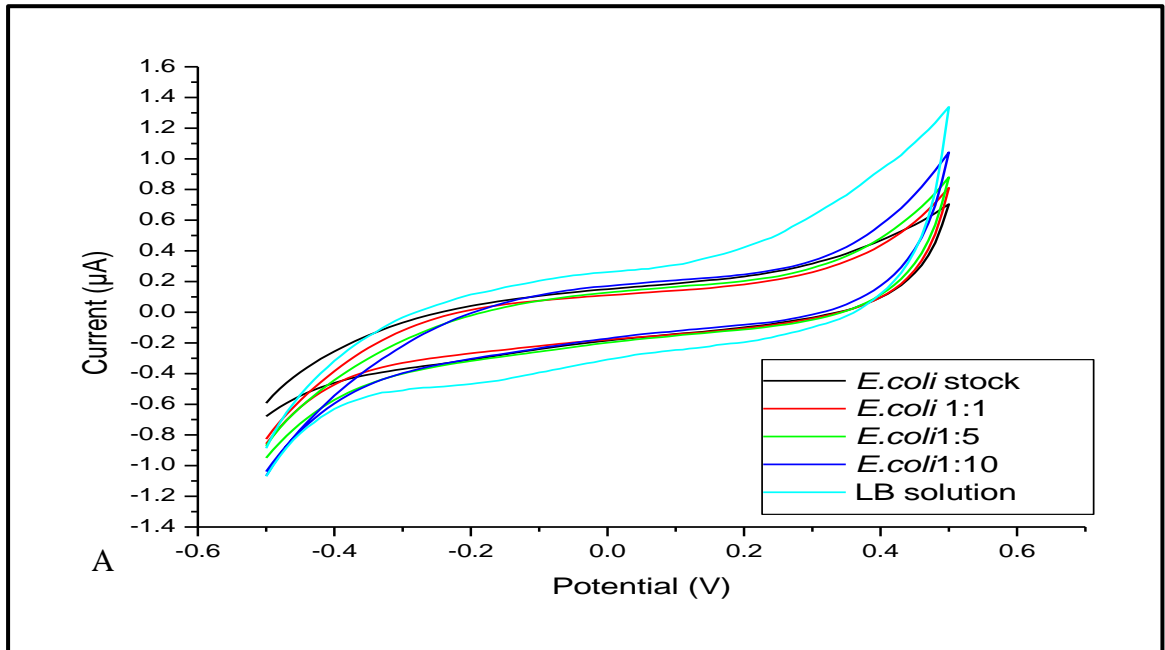
Among the three optical methods used, flow cytometry appeared to be the most reliable and not affected by different motility of *E. coli*, *Ms. trichosporium* (OB3b) and *S. oneidensis*. It is known that dead *E.coli* and *Ms. trichosporium* (OB3b) bacteria are not motile and tend to sediment which may affect the results of static fluorescent microscopy and optical density measurements. Nevertheless, the results of optical testing of bacterial samples provided a background for further study using much simpler electrochemical methods.

4.4 Electrochemical measurements on bacterial suspension samples

4.4.1 CV measurements

All CV electrochemical measurements were carried out on a DropSTAT4000P potentiostat instrument (from DropSens) controlled by Autolab software using DropSens screen printed gold electrodes (SPGEs). These electrodes have a conventional three electrode configuration with gold working electrode (4-mm diameter disk) and counter electrode (16 mm×1.5 mm curved line), and the potentials were ± 0.2 and ±0.5, at a scan rate of 100mV/s recorded against Ag/AgCl (16 mm×1.5 mm straight line) pseudo-reference electrode. Typical cyclic voltammograms for *E. coli*,

Ms. trichosporium (OB3b) and *S. oneidensis* of different cell densities (i.e. dilutions with nutrient broth) are shown in Figure (4-5 A, B ,C).



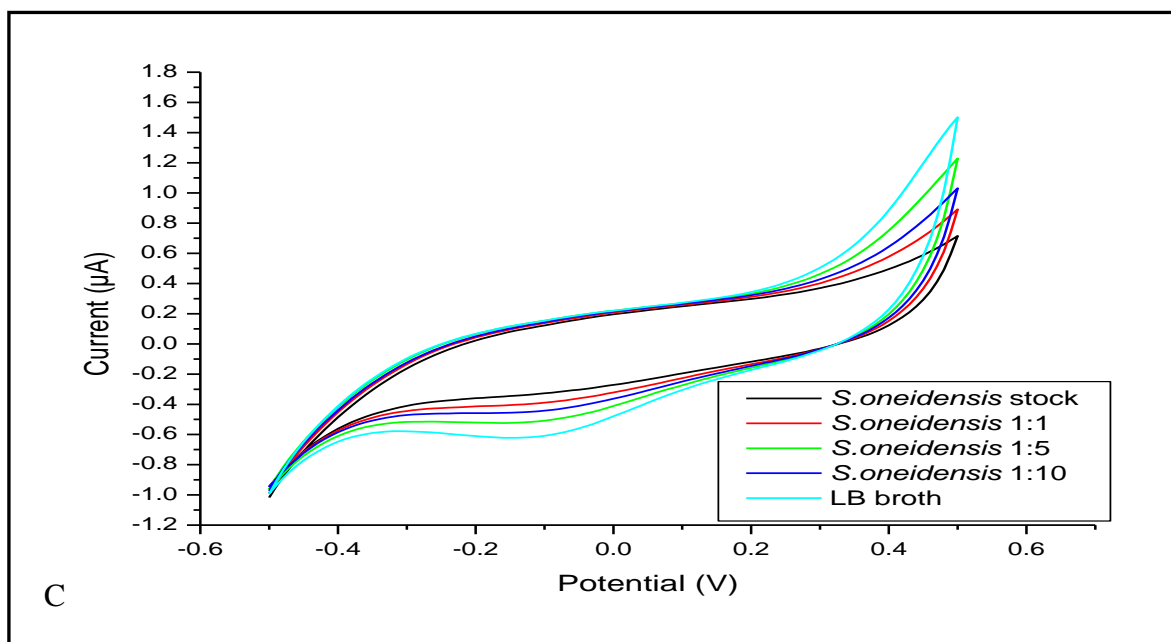
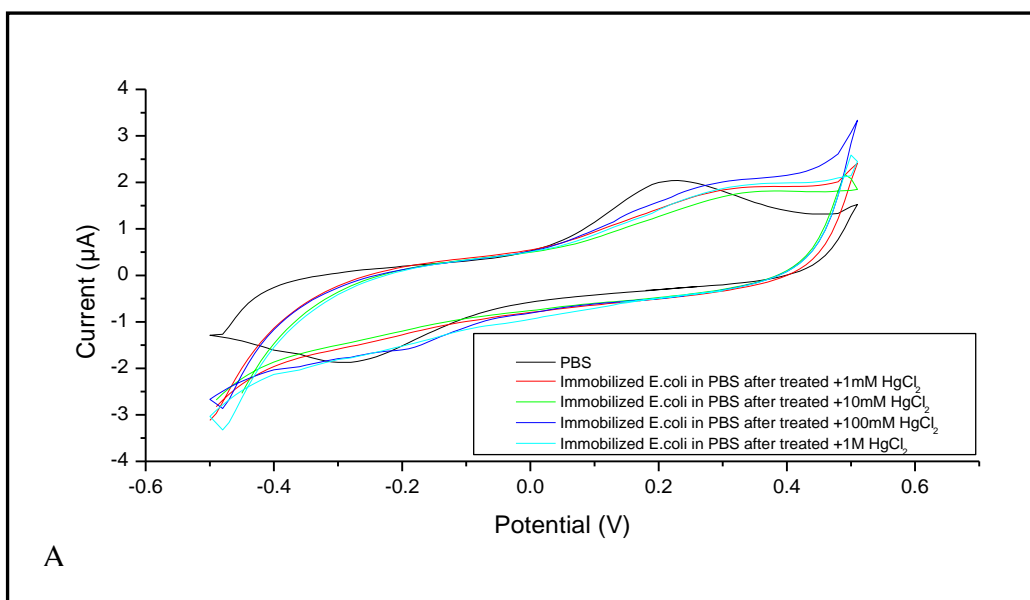


Figure 4-5: Cyclic voltammogram recorded on *E. coli* (A), *Ms. trichosporium* (OB3b) (B) and *S. oneidensis* (C) of different dilutions (1:1, 1:5, 1:10 and stock solutions); CV curves for clear broth are shown on all the graphs.

Generally, the CV graphs in Figure (4-5) are almost featureless for all bacterial species in the selected voltage range from -0.5V to +0.5V which was chosen deliberately in order to avoid electrochemical reactions on the electrodes. A slight increase in the anode current at -0.2V indicates the beginning of hydrogen reduction. The values of cathode current at -0.5V appear to decrease with the increase in bacteria concentration (or dilution ratio 1:10, 1:5, 1:2, 1:1) with the largest current shown for clear LB broth and the lowest for undiluted bacterial stock suspension. This indicates that the bacteria adsorbed onto the surface of gold electrodes and act as an insulating layer, reducing the current. These data are very important since they establish a correlation between the values of cathode current and bacterial cell density in the LB broth.

The next step was to study the effect of Hg^{2+} ions, simazine, and octane on CV characteristics of *S. oneidensis*, *Ms. trichosporium* (OB3b) and *E. coli* bacteria. A series of CV measurements were carried out on liquid samples of bacterial suspensions in LB broth which was mixed in 1:1 ratio with different concentrations of HgCl_2 , simazine, and octane and kept for 2 hours in (22-25) $^{\circ}\text{C}$ prior to CV measurements. The results of these measurements in Figure (4-6) show substantial increase in cathode current (I_c) for *E. coli* samples (Figure 4-6A) upon increasing the concentration of HgCl_2 , simazine, and octane. This effect was much less pronounced for *S. oneidensis* samples (Figure 4-6B). In addition, oxidation and reduction peaks appeared on CV curves for *S. oneidensis* and *Ms. trichosporium* (OB3b) samples in (Figure 4-6A,C) which are definitely related to electrochemical reactions associated with the presence of HgCl_2 and octane. The anodic peak increases with the increase in HgCl_2 concentration. However, such electrochemical reactions do not appear with *E. coli* samples in (Figure 4-6B). It is known that HgCl_2 and octane act as cofactors for *S. oneidensis* and *Ms. trichosporium* (OB3b) bacterial cell growth [9].



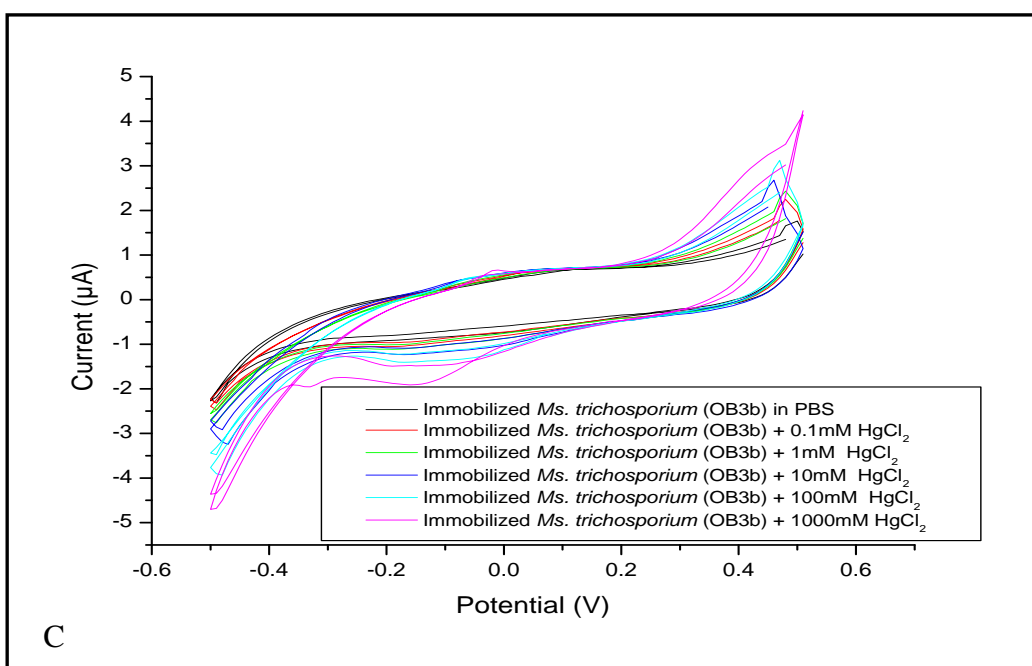
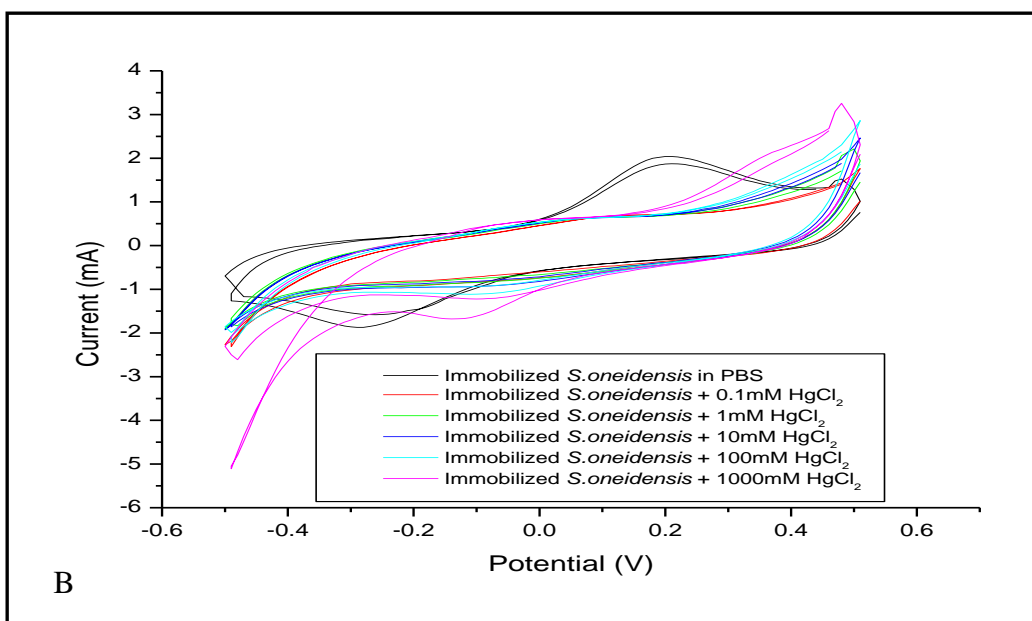


Figure 4-6: Cyclic voltammogram of *E.coli* (A) *S. oneidensis* (B) and *Ms. trichosporium* (OB3b) (C) bacteria solutions in nutrient broth which treated with different concentration of HgCl_2 .

When analysing the effect of heavy metal salts on CV characteristics of liquid bacterial culture samples the effect of extra Hg^{2+} and Cl^- ions on conductivity of liquid medium has to be taken into account. In order to find out the true effect of heavy metal ions on the bacteria, the values of anode current (I_A) of bacterial samples has to be normalized by the reference current I_{ref} of the LB broth diluted 1:1 with particular concentration of HgCl_2 . The values of relative changes of anode current $\Delta I_A/I_{A0} = (I_A - I_{A0})/I_{A0}$ at -0.5V of *S. oneidensis*, *Ms. trichosporium* OB3b and *E. coli* bacteria are plotted in Figure 4-7 against the concentration of HgCl_2 .

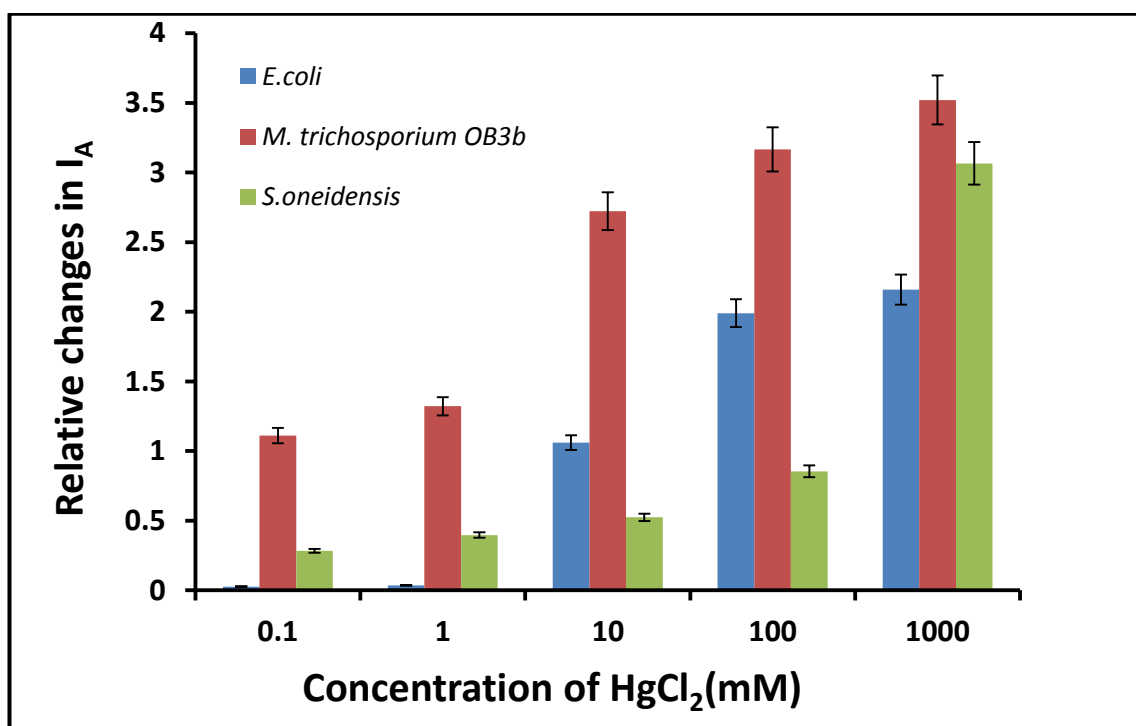


Figure 4-7: The dependence of relative changes in cathode current at -0.5 V for *S. oneidensis*, *M. trichosporium* OB3b and *E. coli* on the concentration of HgCl_2 .

The effects of HgCl_2 on *S. oneidensis*, *trichosporium* OB3b and *E. coli* are completely different: $\Delta I_A/I_{ref}$ goes up with the increase in HgCl_2 concentration for *E. coli* and *M. trichosporium* OB3b which means that *E. coli* and *M. trichosporium* OB3b bacteria are

inhibited by Hg^{2+} ions becoming less electrically resisting, while $\Delta I_A/I_{ref}$ is almost flat at low concentrations of HgCl_2 and slightly increases at high concentration of 1M. This means that *S. oneidensis* are practically not affected by HgCl_2 low concentrations but inhibited at high concentrations. This is a very promising result showing a possibility of pattern recognition of heavy metals using the two bacteria.

4.4.2 Electrochemical Impedance Spectroscopy measurement

Impedance spectra were measured using an impedance analyzer (2000A) and gold interdigitated electrodes (from DropSens), 5 μm dimension for bands/gaps are available with reference number (G-IDEAU5) and the overlapping length is 6.76 mm. The AC voltage amplitude was 5 mV with the frequency varied from 100 mHz to 100 kHz; no DC bias was applied. Similarly to the CVs, the impedance spectra measurements were carried out on electrodes coated with bacterial suspension which were treated with solutions containing different concentrations of pollutants. Typical results are shown as Nyquist plots in Figure (4-8).

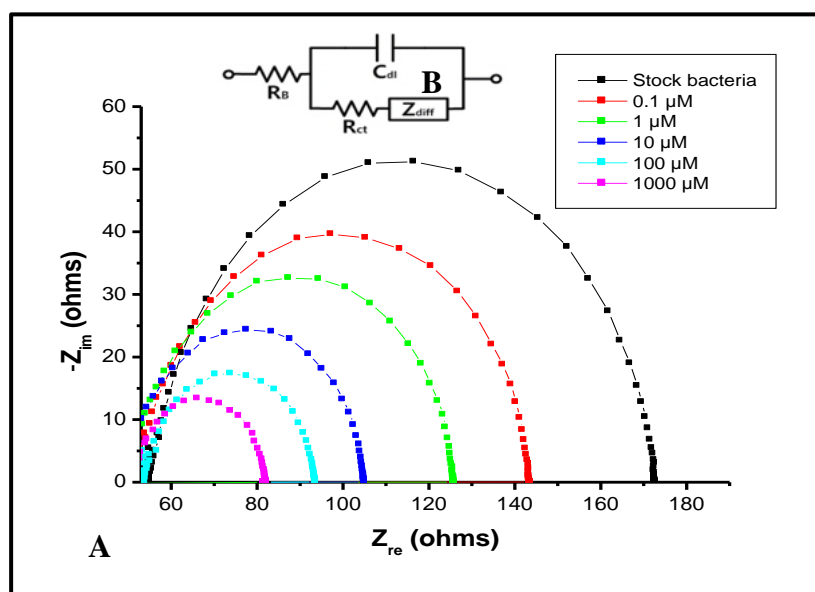


Figure 4-8: The Nyquist plots ($-Z_{im}$ vs Z_{re}) for interdigitated electrodes with *E. coli* bacteria suspension treated with Hg^{2+} ions of different concentrations (A); equivalent circuit (B).

The analysis of impedance spectra using an equivalent circuit model (shown as inset in Figure 4-8) was carried out according to the simplified circuit model impedance when the diffusion impedance Z_{diff} is neglected [10]. Study of the inhibition effect of toxic pollutants on optical and electrochemical properties of bacteria in suspension from proved the principle of pollution detection, from a practical point of view, the use of bacteria immobilized on the surface electrodes is much more promising for such sensor development.

A decrease in impedance was observed with increasing Hg^{2+} concentration, as evidenced by the decreasing height and diameter of the semi-circular Nyquist traces, which correspond to decreased capacitance and resistance of the sensor surface respectively. R_s (solution resistance), R_{dl} (double layer resistance) are presented in Table 4-2. Good stability of the sensor was observed as the solution resistance was nearly constant at all stages of biosensor construction and testing; while R_{dl} decrease due to treat the bacteria with Hg^{2+} ions.

Table 4-2: Values for the EIS parameters obtained from fitting the Nyquist plots shown in Figure 4-8 to the equivalent circuit model.

Analyte	R_s (Ω)	R_{dl} (Ω)
Bacteria suspension	54.903	172.63
0.1 $\mu M Hg^{2+}$	50.529	143.75
1 $\mu M Hg^{2+}$	48.726	125.82
10 $\mu M Hg^{2+}$	48.038	105.14
100 $\mu M Hg^{2+}$	53.414	93.666
1000 $\mu M Hg^{2+}$	51.053	81.606

References

1. Lăzăroaie, M. M. 2010. Multiple responses of gram-positive and gram-negative bacteria to mixture of hydrocarbons. *Brazilian Journal of Microbiology*, 41(3), 649-667.
2. Ramírez-Díaz, M. I., Díaz-Pérez, C., Vargas, E., Riveros-Rosas, H., Campos-García, J., & Cervantes, C. 2008. Mechanisms of bacterial resistance to chromium compounds. *Biometals*, 21(3), 321-332.
3. Smith, T. J., & Dalton, H. 2004. Biocatalysis by methane monooxygenase and its implications for the petroleum industry. *Petroleum Biotechnology, Developments and Perspectives*, 177-192.
4. Han, J. I., Lontoh, S., & Semrau, J. D. 1999. Degradation of chlorinated and brominated hydrocarbons by *Methylobacterium album* BG8. *Archives of microbiology*, 172(6), 393-400.
5. Sezonov, G., Joseleau-Petit, D., & D'Ari, R. 2007. *Escherichia coli* physiology in Luria-Bertani broth. *Journal of bacteriology*, 189(23), 8746-8749.
6. Gorby, Y. A., Yanina, S., McLean, J. S., Rosso, K. M., Moyles, D., Dohnalkova, A. & Culley, D. E. 2006. Electrically conductive bacterial nanowires produced by *Shewanella oneidensis* strain MR-1 and other microorganisms. *Proceedings of the National Academy of Sciences*, 103(30), 11358-11363.
7. Smith, T. J., & Murrell, J. C. 2011. Mutagenesis of soluble methane monooxygenase. In *Methods in enzymology* (Vol. 495, pp. 135-147). Academic Press.
8. Al-Shanawa, M. Nabok, A. Hashim, A. Smith, T. Forder, S.(2013). Sensors & their applications XVII, J. Phys. Conf. Ser. 450 (012025). <http://dx.doi.org/10.1088/1742-6596/450/1/012025>.
9. Hanson, R. S., Tsien, H. C., Tsuji, K., Brusseau, G. A., & Wackett, L. P. (1990). Biodegradation of low-molecular-weight halogenated hydrocarbons by methanotrophic bacteria. *FEMS microbiology reviews*, 7(3-4), 273-278.
10. Macdonald, J. R. (1992). Impedance spectroscopy. *Annals of biomedical engineering*, 20(3), 289-305.

CHAPTER 5 Optical and electrochemical detection of toxic pollutants: data obtained on immobilized bacteria

The results given in the previous chapter are important as a preliminary step towards the development of bacteria-based inhibition sensor array, but it is still far away from real sensor development. Dealing with liquid bacterial samples is not the way forward because of natural variations of bacteria concentration even in laboratory samples not to mention “real” samples taken for analysis. This chapter will focus on the problem of having a reliable reference for such measurements. It would be much more useful for sensor array development to use bacteria immobilized on the electrode surface.

5.1 Bacterial immobilization process

Three selected types of bacteria e.g. *E. coli*, *Mc. capsulatus* Bath and *S. oneidensis* were immobilized on the surface of the screen-printed gold electrodes modified with poly L-lysine (PLI) [1, 2], This was achieved by incubating samples in 1:1000 mixture on Dropsens electrodes (Figure 5-1 a,b) of PLI (0.1 mg/ml) with deionized water for 1 h at 37 °C. Then bacteria were immobilized by dropping stock suspensions of *E. coli*, *Mc. capsulatus* Bath and *S. oneidensis* on the modified electrodes, keeping it there for 1 h, then washing out non-bound bacteria with PBS as illustrated in Figure (5-1c). The electrodes with immobilized bacteria could be kept at 4°C for 24 hours without compromising bacterial activity.

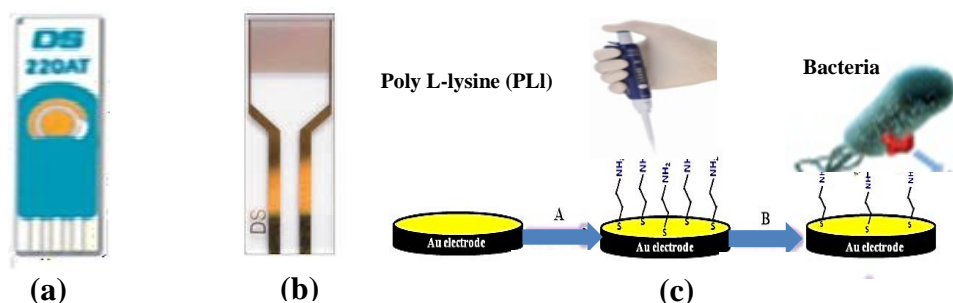


Figure 5-1: DropSens three-electrode assembly (a), DropSens interdigitated electrodes (b), Schematic diagram of bacteria immobilization procedure (c).

5.2 Preparation of analyte solutions

The inhibition effects on the above mentioned bacteria was studied by exposing them to the following chemicals (pollutants): HgCl₂, PbCl₂, ZnCl₂ and CdCl₂, atrazine, simazine, DDVP, hexane, pentane, octane, ethanol, toluene and pyrene. Solutions of different concentrations (0.1, 1, 10, 100, and 1000 μM) were prepared by multiple dilution of 1 mM stock solution of each analyte dissolved in deionised water. 40% ethanol solution in water was used for dissolving the hydrocarbons, including toluene and pyrene. The samples of immobilized bacteria were treated by immersing them into the required solutions of the above chemicals for 2 hours.

5.3 Optical and SEM characterization of immobilized bacteria

5.3.1 Fluorescent microscopy study of immobilized bacteria

In this section we deployed fluorescent microscopy for characterization of bacteria immobilized on the surface of screen printed gold electrode. Fluorescence microscopy images in Figures (5-2 and (5-3) show the effect of Pb²⁺ and Zn²⁺ ions on *S. oneidensis* bacteria immobilized on modified screen printed gold electrodes where live and dead bacteria appear as green and red spots, respectively. It is clear that the exposure to 1M solution of PbCl₂ , ZnCl₂ and CdCl₂ for 2 hours reduced the number of live bacteria (green spots) and increases the dead ones (red spots). Such experiments were carried out for all three types of bacteria and all analyte types used. The results of this study are presented in Figure (5-2) and Figure (5-3) and Table 5-1 as the numbers of live (green) and dead (red) bacteria on recorded images of identical dimensions.

5.3.2 SEM study of immobilized bacteria

For scanning electron microscopy (SEM) immobilized bacteria were fixed on double-sides carbon tape mounted on a sample holder and coated with a few-nanometer-thick

layer of carbon using a carbon evaporator (Edwards E306A; Edwards, United Kingdom). The samples were examined with a LEO1550VP field emission scanning electron microscope equipped with an Oxford INCA energy-dispersive X-ray spectrophotometer. The system was operated at 1 to 15 kV for high-resolution secondary electron imaging and elemental analysis (see Figure 5-4).

5.3.3 Fixation of immobilized bacteria samples for SEM measurements

Bacteria amended culture (1.5 mL) were pelleted by centrifugation ($11000 \times g$; 10 min; room temperature), and washed with 0.1 M sodium phosphate buffer (pH 7.4). The specimens were then fixed in 3% (v/v) glutaraldehyde in the same buffer overnight at room temperature and washed again in the same buffer. Secondary fixation was carried out in 1% (w/v) aqueous osmium tetroxide for 1 hour at room temperature followed by the same wash step. Fixed cells were dehydrated through a graded series of ethanol dehydration steps 75%, 95% and 100% (v/v), and then placed in a 50/50 (v/v) mixture of 100% ethanol and 100% hexamethyldisilazane for 30 min followed by 30 min in 100% hexamethyldisilazane [3].

5.3.4 AFM imaging of immobilized live bacteria

A drop of the bacterial suspension was deposited on the surface of the screen printed gold electrode and characterized by atomic force microscopy. The immobilized bacterial cells were imaged in 5500 AFM microscope outfitted with a 90 μm scanner in combination with an inverted Olympus IX81 light microscope. Silicon nitride cantilevers (0.1 N/m) were used to scan the sample in non-contact mode at a rate of 6–13 $\mu\text{m/s}$ at 512 or 256 points per line resolution. Images were processed on first-order flattening (Figure 5-5 A,B) [4].

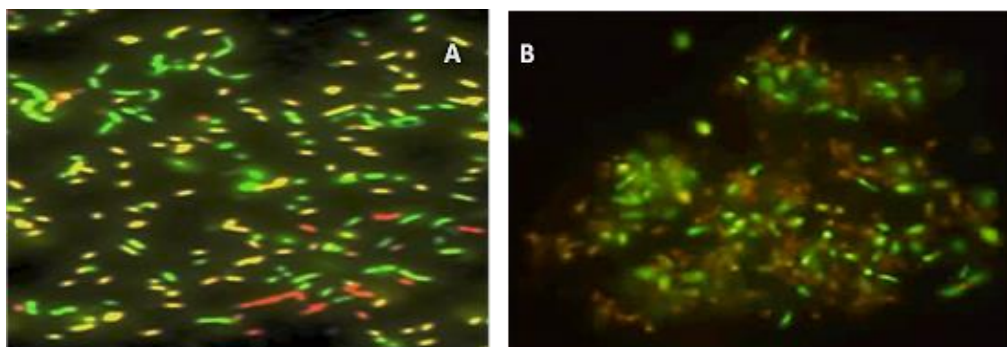


Figure 5-2: Fluorescence microscopy images of immobilized *S. oneidensis* bacteria before (A) and after (B) treatment with PbCl_2 (1 M) for 2 hours.

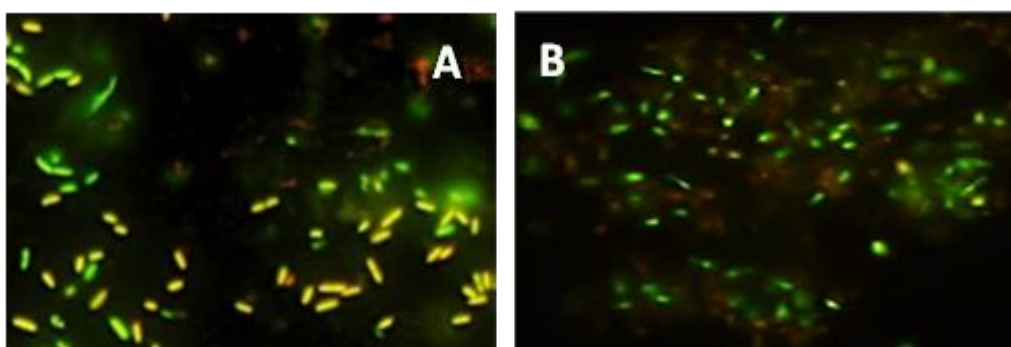


Figure 5-3: Fluorescence microscopy images of immobilized *S. oneidensis* before (A) and after (B) treatment with ZnCl_2 (1M) for 2 hours.

Table 5-1: The numbers of live and dead bacteria immobilized on microscopic images of modified screen printed gold electrodes obtained from fluorescence microscopy images for all three bacteria before and after treatment with 1M solutions of the three pollutants for 2 hours.

Types of Bacteria used	Types of Pollutants	Bacteria count			
		Before exposure		After exposure	
		Live	Dead	Live	Dead
<i>Escherichia coli</i>	HgCl ₂	93	20	21	65
<i>Shewanella oneidensis</i>	HgCl ₂	149	22	72	79
<i>Mc. capsulatus Bath</i>	HgCl ₂	43	13	16	57
<i>Escherichia coli</i>	Atrazine	81	25	18	64
<i>Shewanella oneidensis</i>	Atrazine	79	18	15	77
<i>Mc. capsulatus Bath</i>	Atrazine	62	17	19	51
<i>Escherichia coli</i>	Toluene	69	21	20	87
<i>Shewanella oneidensis</i>	Toluene	57	11	28	62
<i>Mc. capsulatus Bath</i>	Toluene	75	19	71	14

Analysis of fluorescence microscopy data in Table. (5-1) revealed that *E. coli* and *Mc. capsulatus Bath* were badly affected by large concentrations of Hg²⁺ ions, while *S. oneidensis* are less affected. The negative effect of atrazine is dramatic and more or less similar for all three bacteria. Toluene, however, did not affect *Mc. capsulatus Bath*; though it inhibited both *E. coli* and *S. oneidensis*. Such behaviour of immobilized bacteria is similar to those bacteria in solution.

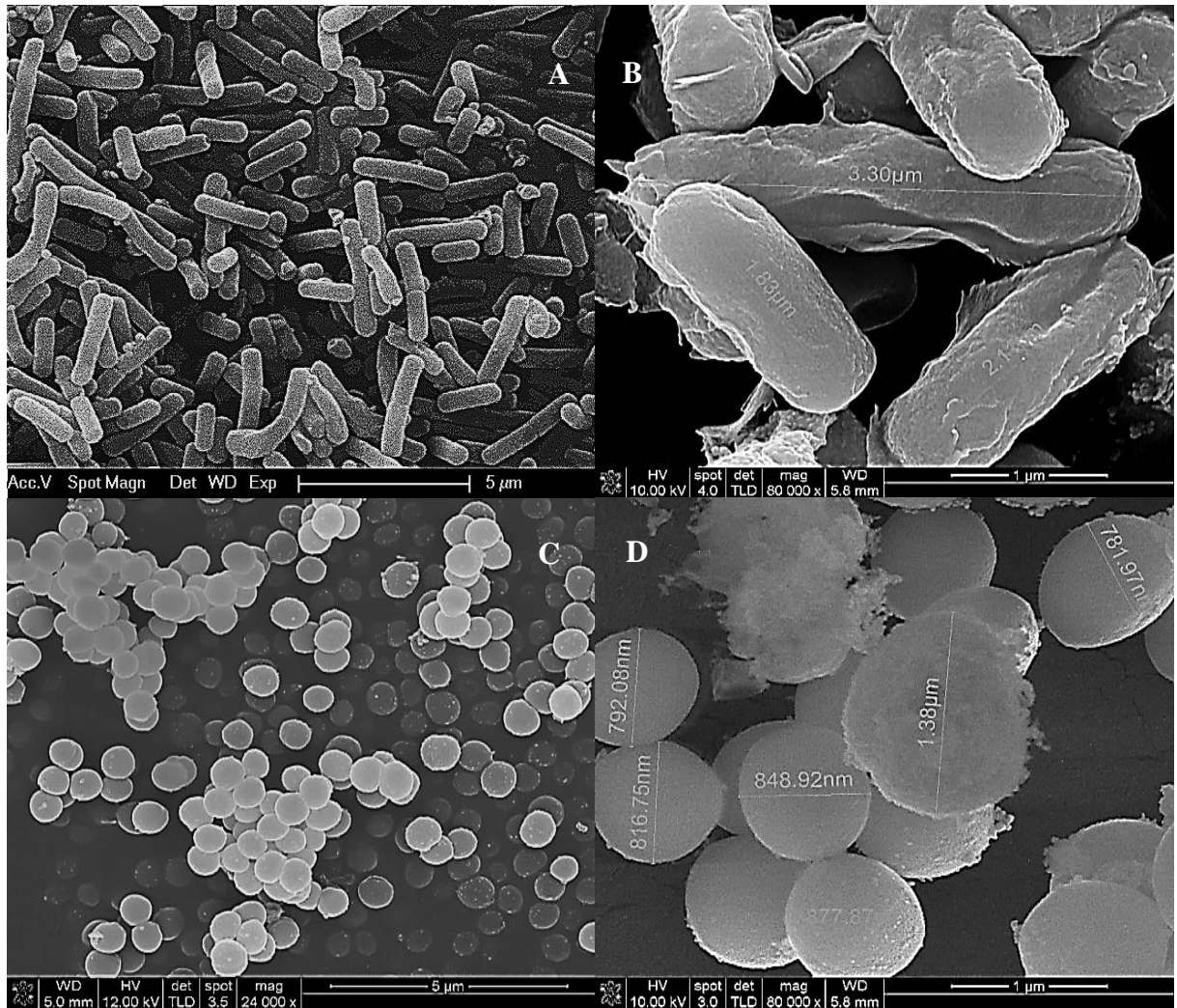


Figure 5-4: (A) SEM images of *E. coli* before treatment, (B) after treatment with ZnCl₂ (1M) (C), *Mc. capsulatus Bath* before treatment, (D) after treatment with ZnCl₂ (1M).

The direct evidence of cell enlargement was obtained from SEM study. SEM images in Figure (5-4) show the enlargement of *E. coli* bacteria (Figure 5-4B) and rupture of *Mc. capsulatus Bath* bacteria cells (Figure. 5-4D) caused by exposure to high concentration (1M) of ZnCl₂. These observations are similar to previously reported SEM studies of bacteria [5,6].

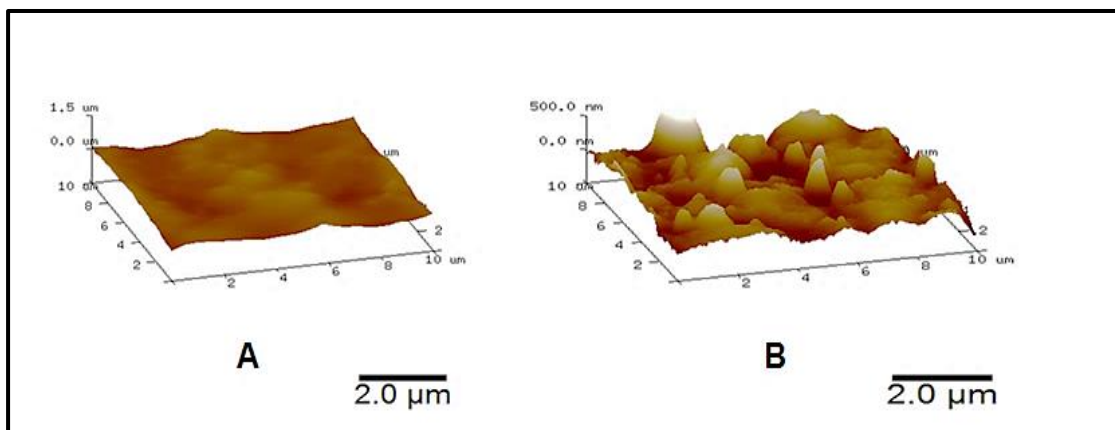


Figure 5-5: AFM images of modified SPGE before (A) and after (B) immobilized *E. coli* bacteria with poly -L-lysine.

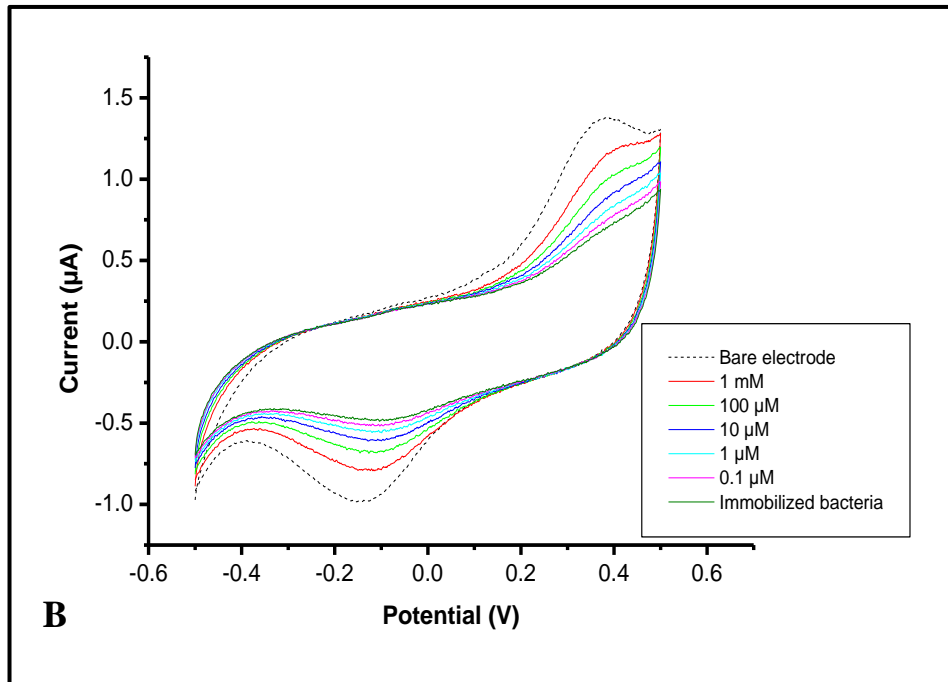
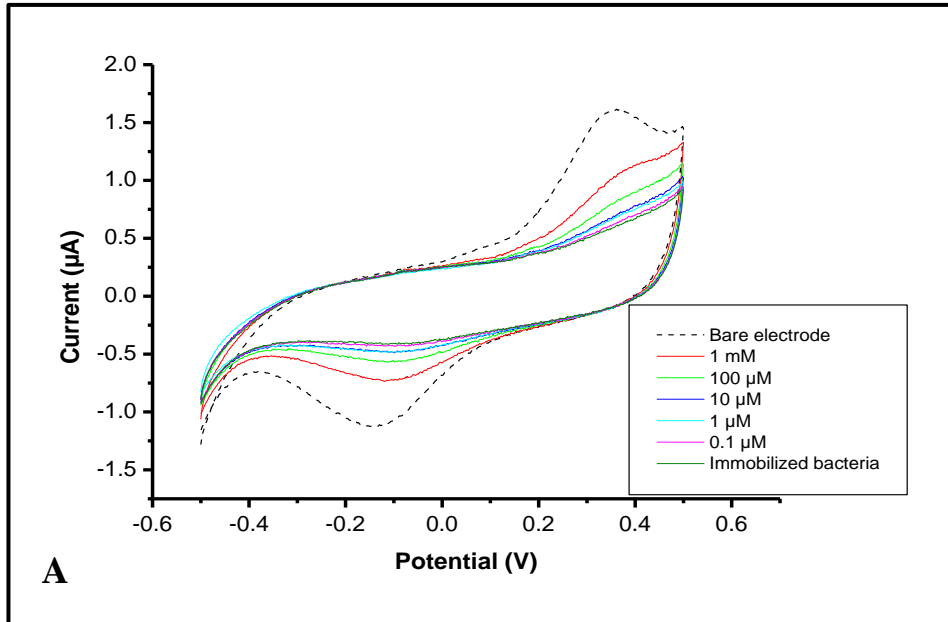
In contrast, *S. oneidensis* bacteria were affected much less by ZnCl_2 than the other bacterial strains and appeared slightly elongated. Similar elongation has been observed in *S. aureus* due to exposure to high salt concentration as a specific response to other stress conditions [7]. Also, a significant increase in bacteria length was found in *S. oneidensis* exposed to UV radiation [8].

5.4 Electrochemical measurements of immobilized bacteria samples

5.4.1 Cyclic voltammograms (CVs) measurement

The effect of HgCl_2 , atrazine, and toluene on all three bacteria, in immobilized bacteria using cyclic voltammograms (CVs) was studied. Typical series of CVs recorded on *E. coli*, *S. oneidensis*, and *Mc. capsulatus* Bath samples are shown in Figure (5-6). The graphs of CV in Figure (5-6) show a characteristic peak of anodic current at about 0.3V and peak of cathodic current between -0.1V and -0.2V which are most likely correspond to oxidation and reduction reaction of PBS buffer. The current peak values which are maximal on bare electrodes in PBS reduced substantially on the electrodes with immobilized bacteria which act as an insulating layer reducing both anodic and cathodic currents. Exposure of bacteria to toxic chemicals probably causes damage to bacteria

cell wall thus affecting their insulating properties which is why the peak currents are rising with the increase in pollutants concentrations.(see Appendix - A3)



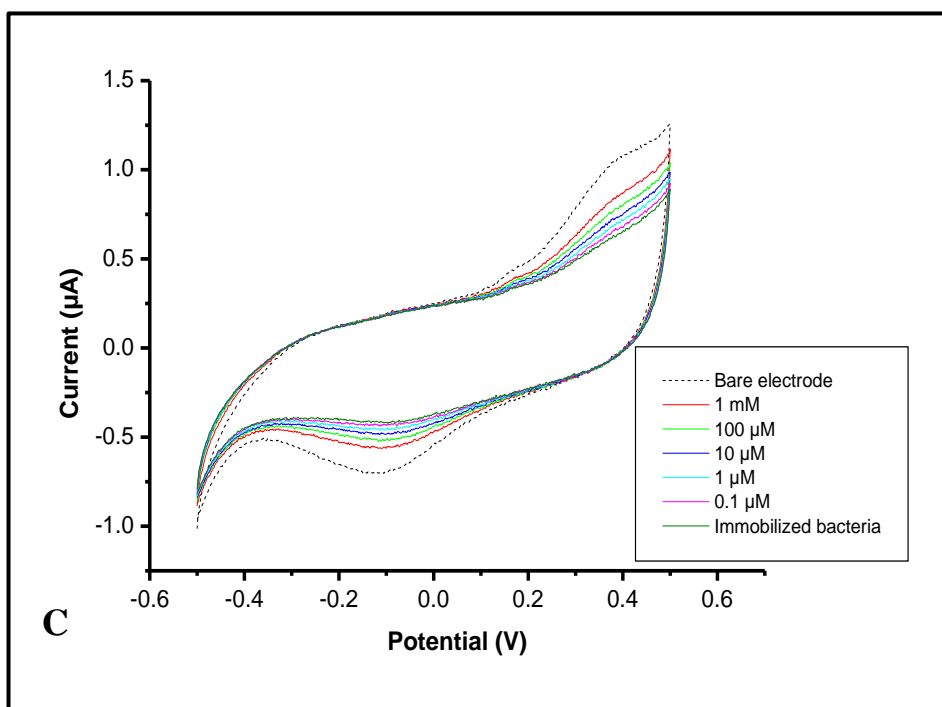


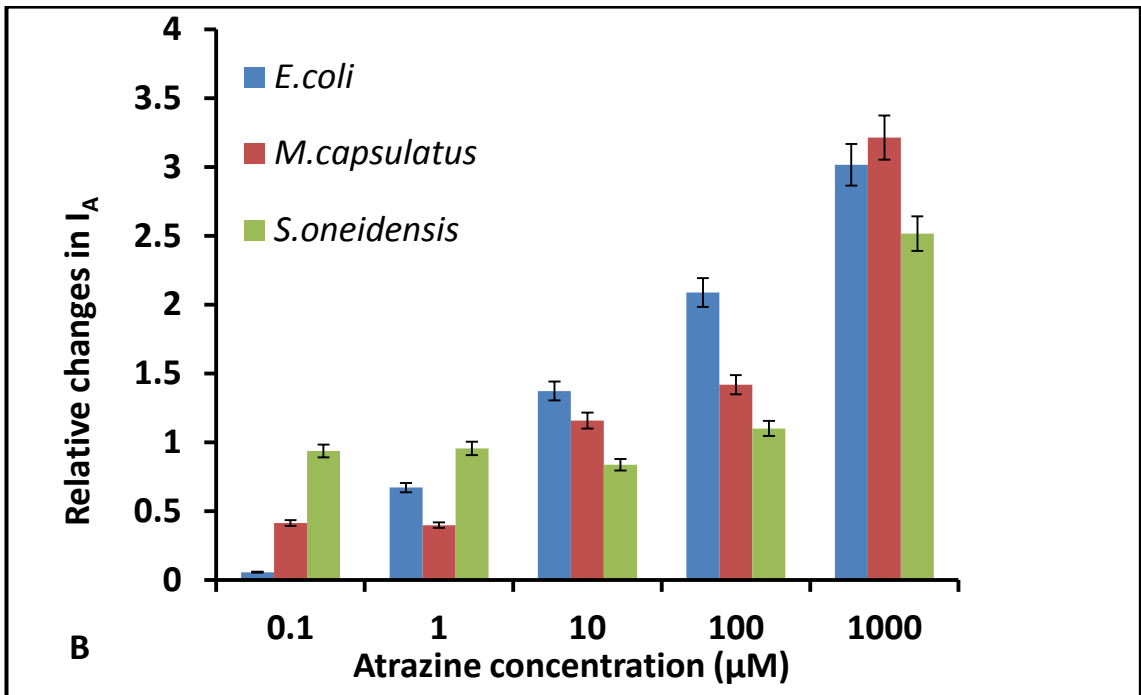
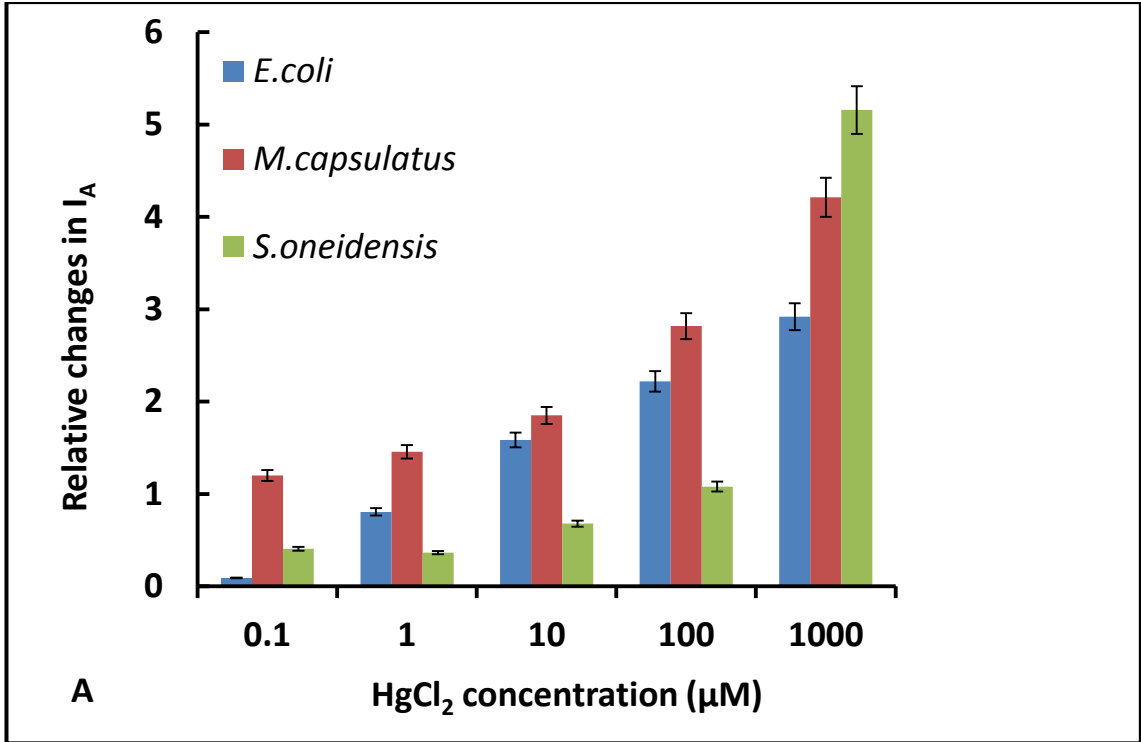
Figure 5-6: Cyclic voltammograms in the selected voltage range from (-0.5 V to +0.5 V) and scan rate at 100mV/s, for: immobilized *E.coli* treated with toluene from 0.1 µM-1mM concentration (A), immobilized *Mc. capsulatus* Bath treated with atrazine from 0.1 µM-1mM concentration (B), and immobilized *S. oneidensis* treated with HgCl₂ from 0.1 µM-1mM concentration (C).

In Figure (5-6A,B,C) the CV cycles appear to shift upwards upon increasing the pollutants concentration from 0 (untreated bacteria) to 0.1 mM, 1mM, 10 mM, 100 mM, and 1M. The characteristic parameter in this study, e.g. the value of anodic current at +0.5 V increases with the increase in pollutant concentration for all three bacteria in both liquid and immobilized forms. This means that the electrical conductivity is controlled by bacteria adsorbed on the surface of the surface of screen printed gold electrodes and acting as insulating layer which reducing the current. The correlation between bacterial concentration and the electric current (or conductivity) values is very important for further study of the effect of pollutants, and such measurements were

always carried out first [9]. The presence of pollutants (Hg^{2+} ions, atrazine, and toluene in our case) causes damage to the bacterial cells, and therefore bacteria became less insulating, in-turn leading to an increase in the anodic current, which is observed in Figure 5-6 (A,B,C).

Similar analysis could have been carried out using cathodic peaks, however the use of anodic peaks is sufficient for this study. To analyze the effect of pollutants on electrical properties of immobilized bacteria, the values of anodic current (I_A) at +0.5V from CV measurements were normalized to the currents values of uncoated electrodes in PBS with the addition of a particular pollution of particular concentrations (I_{A0}) to construct the values of relative changes of anodic current . $\Delta I_A/I_{A0} = (I_A - I_{A0})/I_{A0}$ For example, for *S. oneidensis* bacteria treated with 1mM solution of PbCl_2 (Figure 5-6 C), the reference was recorded on uncoated electrodes in PBS containing 1mM PbCl_2 .

The relative changes in anodic current are presented in Figure (5-7) for all three bacteria studied as concentration dependences of the three pollutants. As one can see the effects of HgCl_2 , atrazine, and toluene on *S. oneidensis*, *Mc. capsulatus Bath* and *E. coli* are completely different. *E. coli* appeared to be affected by HgCl_2 , atrazine, and toluene even at low concentrations since the $\Delta I_A/I_{A0}$ values increase monotonically in Figures 5-7 (A), 5-7 (B), and 5-7 (C), respectively. This means that *E. coli* is equally inhibited by all three pollutants and becoming less electrically resisting. In contrast, *S. oneidensis* is almost unaffected by HgCl_2 at low concentrations of all pollutants up to 10mM, and then $\Delta I_A/I_{A0}$ started to increase at high concentrations of 100mM and 1M.



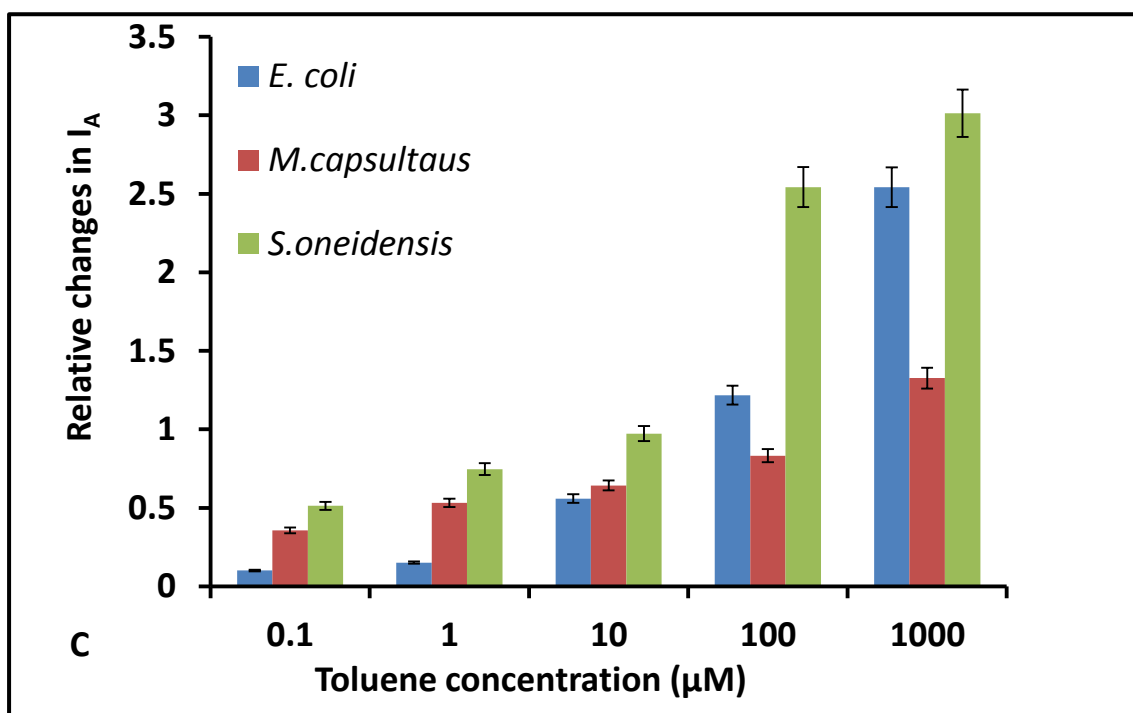


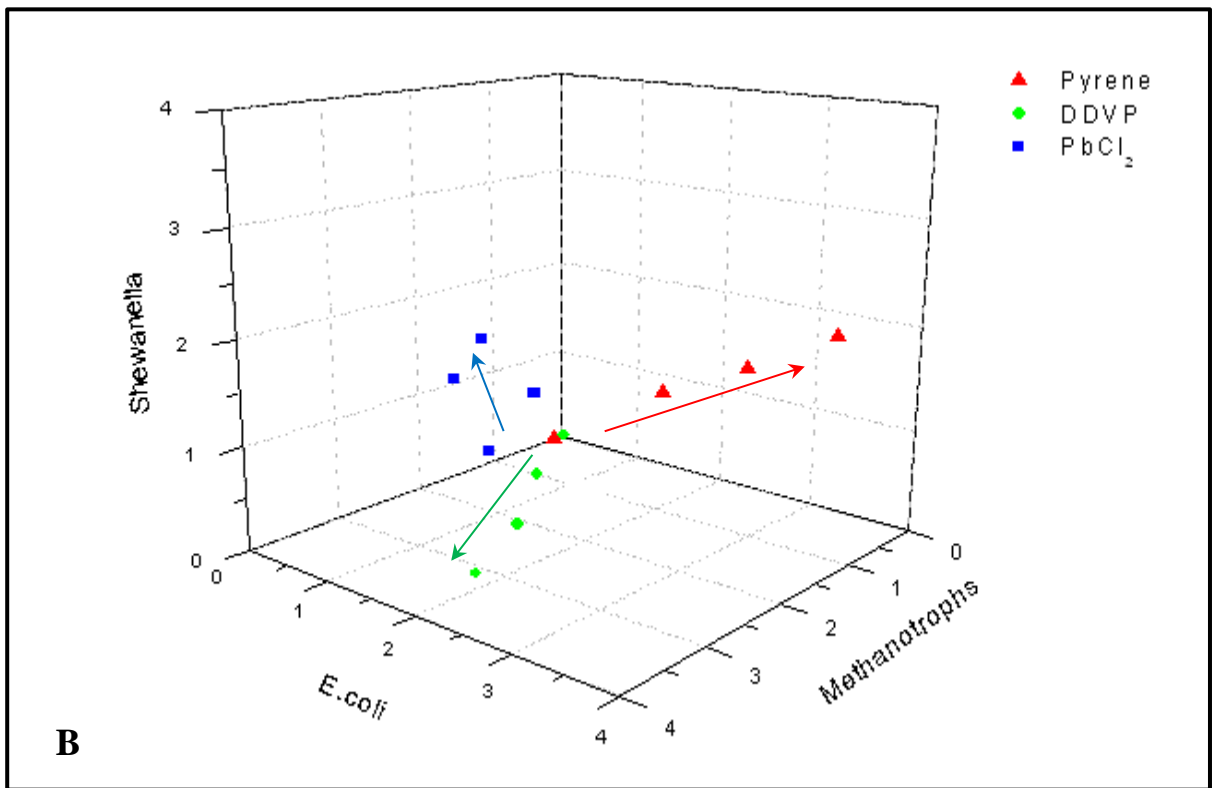
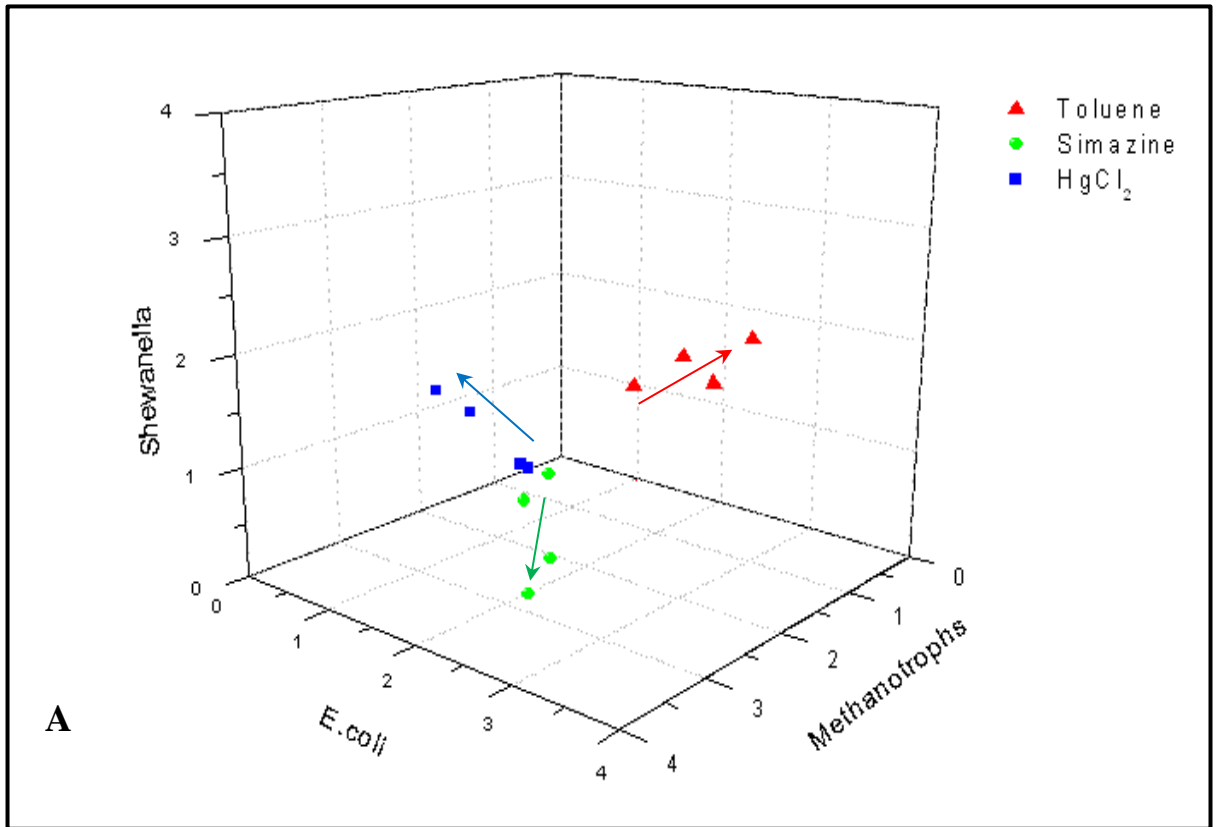
Figure 5-7: Comparison of relative changes of anodic current (I_A) at +0.5V of all three types immobilized bacteria samples on modified electrodes exposure to HgCl_2 (A), Atrazine (B), and Toluene (C).

Such behaviour of immobilized *E. coli* and *S. oneidensis* bacteria is similar to those free in liquid as reported in our previous study. *M. capsulatus* (Bath) respond to HgCl_2 (Figure 5-7A) and atrazine (Figure 5-7B) similarly to the other two bacteria studied though the changes in $\Delta I_A/I_{A0}$ are more pronounced at high concentrations, particularly for atrazine. However, *M. capsulatus* (Bath) bacteria are not affected by toluene (see Figure 5-7C) even at high concentration; moreover an overall trend to small decrease in $\Delta I_A/I_{A0}$ is observed. Such behavior was expected since *M. capsulatus* (Bath) consume some hydrocarbons [10]. (see Appendix - A3 for more results of another immobilized bacteria)

5.5 Sensor array data analysis

5.5.1 Identification of water pollutants using pseudo 3D plots of sensor responses

All the data obtained from the sensor array containing three electrodes functionalized by three different types of bacteria, namely *E. coli*, *S. oneidensis*, and *M. capsulatus*, treated by 12 different pollutants, e.g. heavy metal ions (Hg^{2+} , Pb^{2+} , and Cd^{2+}), pesticides (atrazine, simazine, and DDVP) and petrochemicals (hexane, octane, pentane, ethanol, pyrene and toluene) at concentrations of 0.1, 1, 10, 100, 1000 μM were analysed using pseudo-3D plots of sensor responses in Figure 5-8 (A, B, C). In Figure 5-8A the experimental points for toluene, simazine and HgCl_2 are well separated up to their concentrations of 100 μM . Similarly, in Figure 5-8B, the data for pyrene, DDVP and PbCl_2 are well separated up to their concentrations of 100 μM . Also octane, atrazine and CdCl_2 show similar pattern in Figure 5-8C. An attempt of pattern recognition has been done by presenting the relative responses of the three channels, e.g. three bacteria (*E. coli*, *M. capsulatus* (Bath) and *Shewanella oneidensis*) immobilized on three screen-printed electrodes, to the three pollutants (HgCl_2 , atrazine, and toluene) in a pseudo-3D plot in Figure 5-8(A, B, C). It can be also noticed that heavy metal ions (Hg^{2+} , Pb^{2+} , and Cd^{2+}) give responses mostly in the "north-west" section of respective 3D graphs, while pesticides (atrazine, simazine, and DDVP) appeared in the "south", "south-west" sections, and petrochemicals (hexane, octane, pentane, ethanol, pyrene and toluene) lie mostly in the "north-east" sections. This is a clear indication that pattern recognition principles can be applied for identification of toxic pollutants using different types of bacteria. The concentration of these pollutants could be evaluated too using the appropriate calibration and data extrapolation.



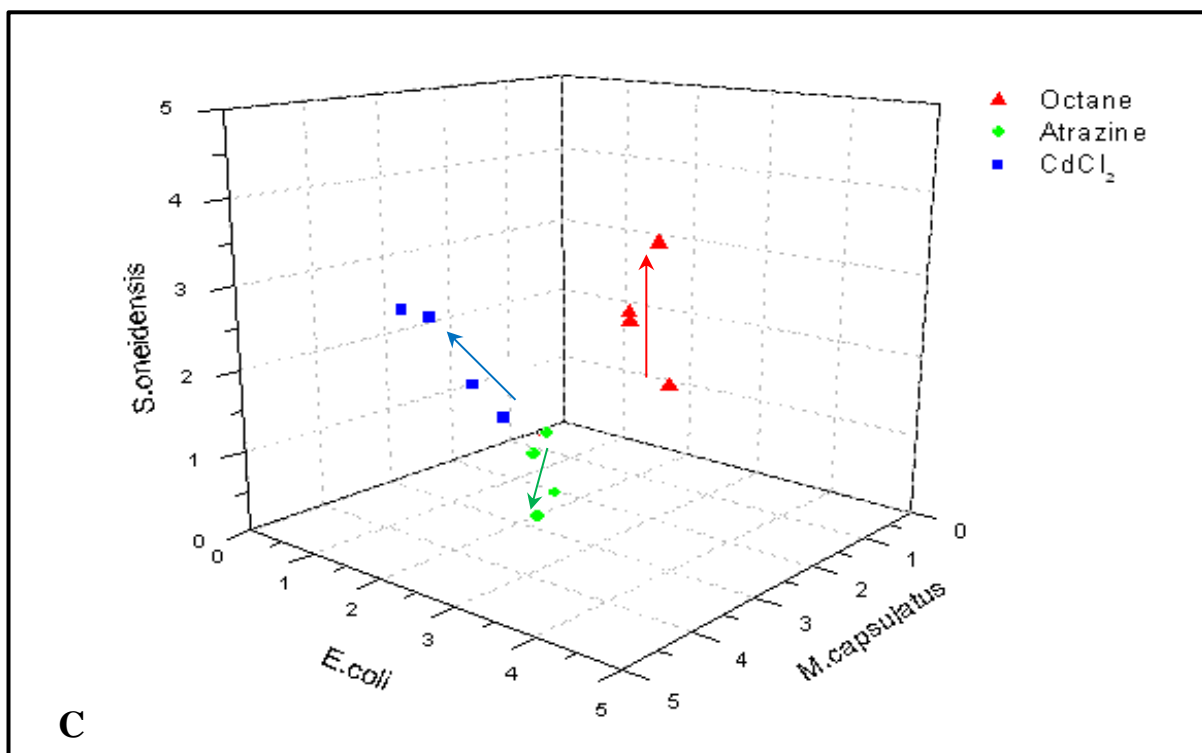


Figure 5-8: 3D plot of relative changes I_A/I_{ref} in anodic current for *E. coli*, *M. capsulatus*, and *S. oneidensis* caused by different pollutants. Arrows show the direction of the pollutants' concentration increase from 0.1 mM to 100 mM.

5.5.2 Electrochemical Impedance Spectroscopy (EIS) measurements

Impedance spectra were measured using an impedance analyzer (4000A) and gold interdigitated electrodes (from DropSens), 5 μm dimension for bands/gaps are available with reference number (G-IDEAU5) and the overlapping length is 6.76 mm. The AC voltage amplitude was 5 mV with the frequency varied from 100 mHz to 100 kHz; no DC bias was applied. Similarly to CVs, the impedance spectra measurements were carried out on electrodes modified with immobilized bacteria which treated with solutions containing different concentrations of pollutants. A typical example of data is shown as Nyquist plots in Figure (5-9) for immobilized *E. coli* treated with different concentrations of pyrene. (see Appendix-A4 figures 1,2).

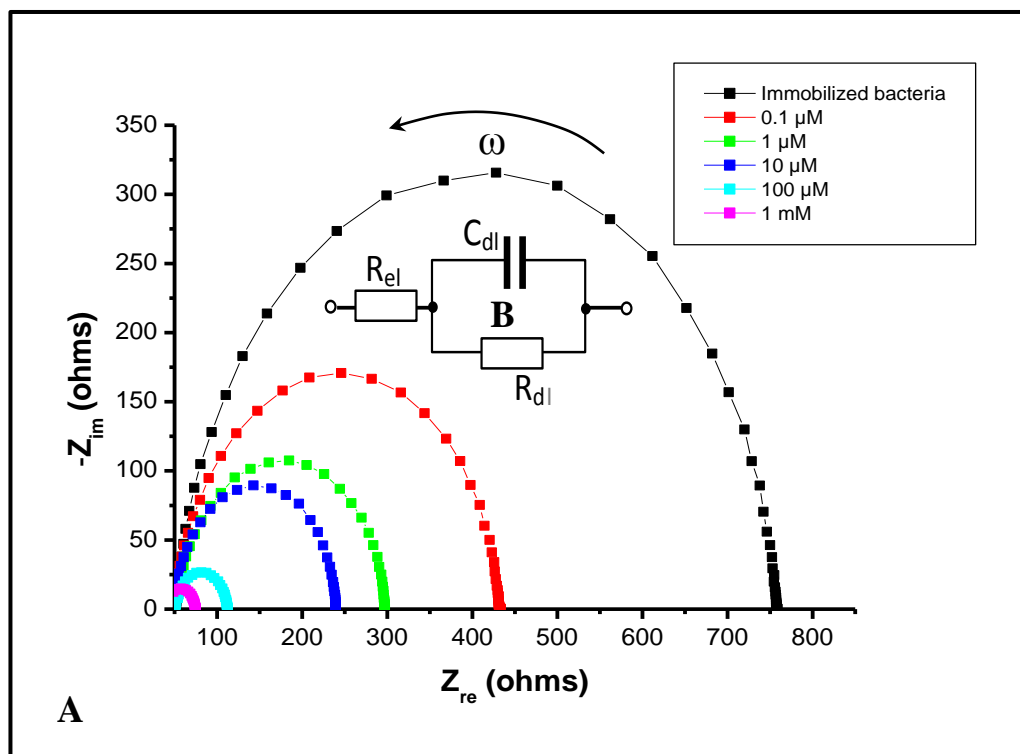


Figure 5-9: The Nyquist plots ($-Z_{im}$ vs Z_{re}) for interdigitated electrodes modified with immobilized *E.coli* bacteria treated with pyrene of different concentrations (A); equivalent circuit (B).

The EIS data are presented as Nyquist plots in Figure 5-9. The analysis of impedance spectra using an equivalent circuit model shown as inset in Figure (5-9 B) was carried out according to the simplified circuit model impedance (when the diffusion impedance Z_{diff} is neglected) [10]. A decrease in impedance was observed with increasing Hg^{2+} concentration, as evidenced by the decreasing height and diameter of the semi-circular Nyquist traces, which correspond to decreased capacitance and resistance of the sensor surface respectively. R_s (solution resistance), R_{dl} (double layer resistance) are presented in Table 5-1. Good stability of the sensor was observed as the solution resistance was nearly constant at all stages of biosensor construction and testing. Whilst the R_{dl} values decreased upon addition of Hg^{2+} , showing a clear trend. The effect of analyte to a

biosensor surface causes an increase in impedance, and this has been widely reported [11].

Table 5-1: Values for the EIS parameters obtained from fitting the Nyquist plots shown in Figure 5-9 to the equivalent circuit model.

Analyte	R_s (Ω)	R_{dl} (Ω)
Immobilized bacteria	50.986	758.47
0.1 μM Hg^{2+}	49.366	433.25
1 μM Hg^{2+}	48.205	297.08
10 μM Hg^{2+}	45.510	239.33
100 μM Hg^{2+}	43.311	112.17
1000 μM Hg^{2+}	40.412	74.777

5.6 Discussion of the optical and electrochemical measurement results

The observed effects of the above pollutants on the three selected bacteria are somehow expected. In general terms, different chemicals of both organic and inorganic origin may affect microorganisms in two possible ways, e.g. acting as either catalyzers enhancing bacterial metabolism or as inhibitors having an opposite effect of reducing bacteria metabolism and even damaging bacteria membranes and causing their death. In our case, *E. coli* is obviously inhibited by the pollutants used. This results in the reduction of live bacteria count which was confirmed by the optical study. Consequently, the increased number of damaged or dead bacteria reduces their insulating properties, thus causing an increase in both anodic and cathodic currents as well as the reduction in resistance (R_s) is very small and (R_{dl}) is much effected in impedance spectroscopy. *Shewanella oneidensis* bacteria are known to be tolerant to heavy metals at low concentration, which may have even be growth stimulating, and which can be used in water treatment [12]. High concentrations of heavy metals are damaging. This explains the observed tolerance of *S. oneidensis* to heavy metals at low concentrations, while

other pollutants are still acting as inhibitors. *M. capsulatus* (Bath), in contrast, are known by their ability to use some organic chemicals (hydrocarbons, alcohols) as a food source [13], and therefore are used in sewage treatment [14]. In other words, *M. capsulatus* bacteria are stimulated by some petrochemicals, while heavy metals and pesticides still act as inhibitors. Optical and electrochemical study of both *S. oneidensis* and *M. capsulatus* (Bath) showed the characteristic changes, respectively, in the live bacterial concentration and anodic current in line with their expected catalytic-inhibition patterns. Combining the above three types of bacteria in a sensor array was logical and therefore enabled the array to identify the type of pollutants. This could be achieved using optical methods with flow cytometry being perhaps the most suitable method for this task.

However, very simple electrochemical measurements of anodic current could do a similar job at substantially reduced cost. Modified screen-printed electrodes with immobilized bacteria can be prepared in advance and kept active for few weeks when stored at 4 °C. Such electrical tests can be used for quick preliminary analysis of water samples. The samples indicating a presence of certain pollutants can be passed to specialized laboratories for further more detailed and accurate testing. The overall cost and time of analysis would be substantially reduced as a result. The sensor stability depends on the activity of the immobilized bacteria. We found that bacteria were still alive and active after 24 hours storing in the refrigerator at 4 °C. After 48 hours the live bacterial concentration reduced slightly (10-15%), and after 72 hours reduced further to over 50%. Therefore, we can conclude, that currently the sensors stability is limited to 24 hours. Ideally, electrodes with freshly immobilized bacteria have to be used for sensing.

References

1. Suo, Z., Avci, R., Yang, X., Pascual, D. W. Efficient immobilization and patterning of live bacterial cells. *Langmuir*, (2008). 24(8), 4161-4167.
2. Lonergan, N. E., Britt, L. D., & Sullivan, C. J. (2014). Immobilizing live *Escherichia coli* for AFM studies of surface dynamics. *Ultramicroscopy*, 137, 30-39.
3. Eswayah, A. S., Smith, T. J., Scheinost, A. C., Hondow, N., & Gardiner, P. H. (2017). Microbial transformations of selenite by methane-oxidizing bacteria. *Applied microbiology and biotechnology*, 101(17), 6713-6724.
4. Kailas, L., Ratcliffe, E. C., Hayhurst, E. J., Walker, M. G., Foster, S. J., & Hobbs, J. K. (2009). Immobilizing live bacteria for AFM imaging of cellular processes. *Ultramicroscopy*, 109(7), 775-780.
5. Aono, R., Kobayashi, H., & Horikoshi, K. (1994). Effects of organic solvents on growth of *Escherichia coli* K-12. *Bioscience, biotechnology, and biochemistry*, 58(11), 2009-2014.
6. Aono, R., & Kobayashi, H. (1997). Cell surface properties of organic solvent-tolerant mutants of *Escherichia coli* K-12. *Applied and environmental microbiology*, 63(9), 3637-3642.
7. Vijaranakul, U., Nadakavukaren, M. J., De Jonge, B. L., Wilkinson, B. J., & Jayaswal, R. K. (1995). Increased cell size and shortened peptidoglycan interpeptide bridge of NaCl-stressed *Staphylococcus aureus* and their reversal by glycine betaine. *Journal of bacteriology*, 177(17), 5116-5121.
8. Qiu, X., Sundin, G. W., Wu, L., Zhou, J., & Tiedje, J. M. (2005). Comparative analysis of differentially expressed genes in *Shewanella oneidensis* MR-1 following exposure to UVC, UVB, and UVA radiation. *Journal of bacteriology*, 187(10), 3556-3564.
9. Al-Shanawa, M., Nabok, A., Hashim, A., Smith, T., Forder, S. Sensors & their applications XVII, J. Phys. Conf. Ser. 450 (012025) (2013) <http://dx.doi.org/10.1088/1742-6596/450/1/012025>.
10. Leak, D. J.; Dalton, H. Growth yields of methanotrophs. *Applied microbiology and Biotechnology*, (1986). 23(6), 470-476.
11. Rushworth, J. V., Ahmed, A., Griffiths, H. H., Pollock, N. M., Hooper, N. M., & Millner, P. A. (2014). A label-free electrical impedimetric biosensor for the specific detection of Alzheimer's amyloid-beta oligomers. *Biosensors and bioelectronics*, 56, 83-90.
12. Du, Z.; Li, H., Gu, T. A state of the art review on microbial fuel cells: a promising technology for wastewater treatment and bioenergy. *Biotechnology advances*, (2007). 25(5), 464-482.
13. Hanson, R. S.; Hanson, T. E. Methanotrophic bacteria. *Microbiological reviews*, (1996). 60(2), 439-471.
13. Kampman, C.; Hendrickx, T. L.; Luesken, F. A.; van Alen, T. A.; den Camp, H. J. O.; Jetten, M. S.; Temmink, H. Enrichment of denitrifying methanotrophic bacteria for application after direct low-temperature anaerobic sewage treatment. *Journal of hazardous materials*, (2012). 227, 164-171.

CHAPTER 6 Analysis of Environmental Pollutants using Artificial Neural (ANN) Network Algorithm

6.1 Statistical analysis of sensor array data

The experimental data obtained by CV measurements in Chapter 5, shows distinct patterns of sensor responses to certain pollutants in water. According to the literature, such data patterns can be treated by various pattern recognition algorithms including principal component analysis [1], partial least squares [2], multiple correspondence analysis [3], multiple linear regression [4], and artificial neural networks [5]. Shaffer et al.(1999), demonstrated that among the above methods, the neural network based algorithms have the highest accuracy in classifying sets of data obtained from chemical and biological sensor arrays [6].

Artificial neural networks (ANNs) also performed very well in solving overlapping signal distributions or difficult non-linear quantifications [7]. A variety of applications that deployed ANNs as a tool for multi-component analysis have been reported, particularly in chemical sensing and biosensing. Examples of such applications are: the determination of pesticides using enzyme sensors and immunosensors [8, 9], the classification of neurotoxins [10], the analysis of ethanol-glucose mixtures [11] and the quantification of metals and inorganic pollutants in groundwater [12]. These complex analytical systems are sometimes defined as an ‘electronic tongue’ due to their capability to recognise both the quantitative and qualitative composition of solutions by mimicking the concept of human sensing [13]. Previous studies [17, 18, 19, 20, 21, 22 and 23] have been established that ANN based algorithm has a high accuracy in classifying experimental data obtained from enzyme sensor arrays.

6.2 The concept of artificial neural network

Much more accurate recognition of pollutants was achieved with the use of an artificial neural network (ANN) programme written using Neural Network Toolbox, version 4.0

within MATLAB 6.1 (Mathworks, Natick, MA). The ANN model shown in Figure 6.1 is a simple general example of ANN which consists of three layers: (i), the input layer of the responses of three sensing channels containing different bacteria; (ii), the hidden layer containing of a number of neurons corresponding to the number of pollutants studied (in this example it is 7); and (iii), the output layer representing a binary code (in this case a 3-digit code) which identifies the type of pollutants. The concept of artificial neural network has been inspired from examining the central nervous system of humans. The artificial neural network consists of simple computational units called neurons, which represent the processing elements in the network. Neurons are connected together using weighted links which pass signals between them. The weights of these links express the importance of its input, i.e. it is the long-term memory that the net uses to learn. Learning or training a neural network means finding the right values of weights. Each neuron accepts multi-inputs, computes a new activation level then produces a single output which could be transmitted to other neurons. The input signal to a neuron can be simple facts or outputs of other neurons while the output signal can be either an input to other neurons or a final solution to the problem.

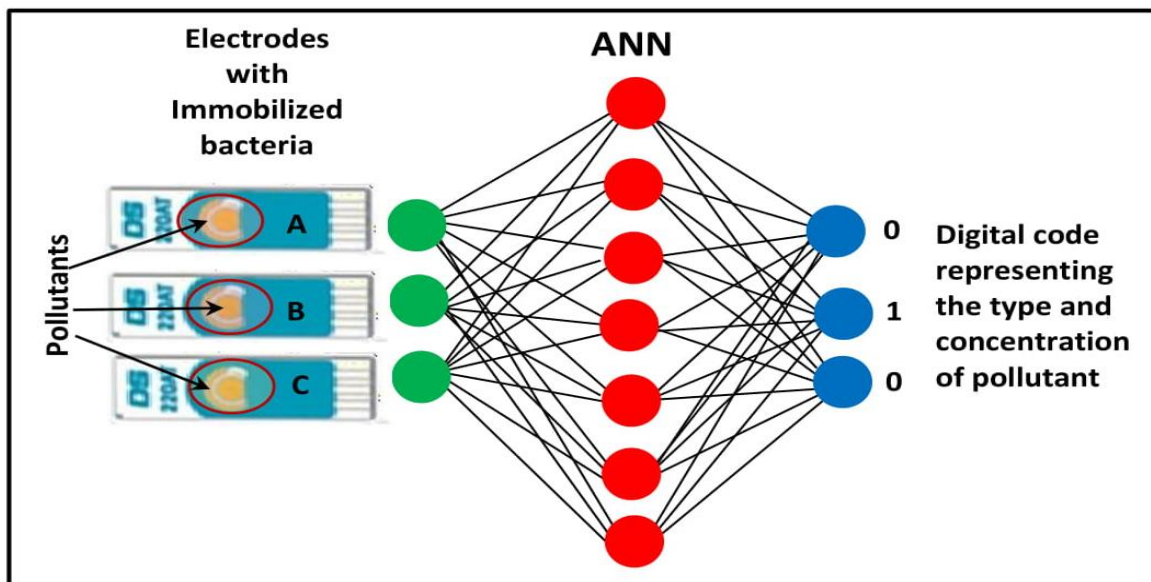


Figure 6-1: Schematic diagram of ANN.

Commonly, ANN consists of simple processing elements or ‘neurons’ grouped together to form three types of layers known as input, hidden, and output layers (see the example in Figure 6-1). The neurons are linked with each other in a particular configuration, so that the output from neurons of one layer becomes the input to the neurons in the next layer. In each neuron, the input signal (x_i) is multiplied by a weight factor (w_i). The weighted input signals are added together and transferred to an activation function (F) that generates an output signal (y_{neu}) of a neuron. The activation function can have any form, from a pure linear dependence to an elaborate exponential function, like the hyperbolic tangent (tan-sigmoid) function which was used in our case:

$$F_{\text{tan-sigmoid}}(S) = [\exp(S) - \exp(-S)] / [\exp(S) + \exp(-S)], \quad (6.1)$$

where S is the sum of p weighted input signals

$$S = \sum_{i=1}^p w_i x_i \quad (6.2)$$

ANN typically requires a large set of data and long training times. Generally, in trained networks particular input leads to a specific target output. During training, the weights of the network are iteratively adjusted to minimize the average squared error between the network outputs (a) and the target outputs (t), normally known as mean square error (MSE):

$$\text{MSE} = \frac{1}{n} \sum_{i=1}^n (e_i)^2 = \frac{1}{n} \sum_{i=1}^n (t_i - a_i)^2, \quad (6.3)$$

where n is the total number of the network inputs.

The weights of the network are optimised by several different training algorithms, such as Levenberg-Marquardt [6], resilient backpropagation [8,11], scaled conjugate gradient [9] and Bayesian regularization [7] algorithms.

6.3 The design strategy of ANN for data analysis of bacteria sensor array

The ANN used in this work for data analysis of the developed inhibition bacteria biosensor array was built using MATLAB software (version 6.1, Mathworks, Natick, MA) using the supplied functions and algorithms in MATLAB Neural Network Toolbox (version 4.0, Mathworks, Natick, MA). The strategy of the ANN design is outlined at the diagram in Figure 6-2

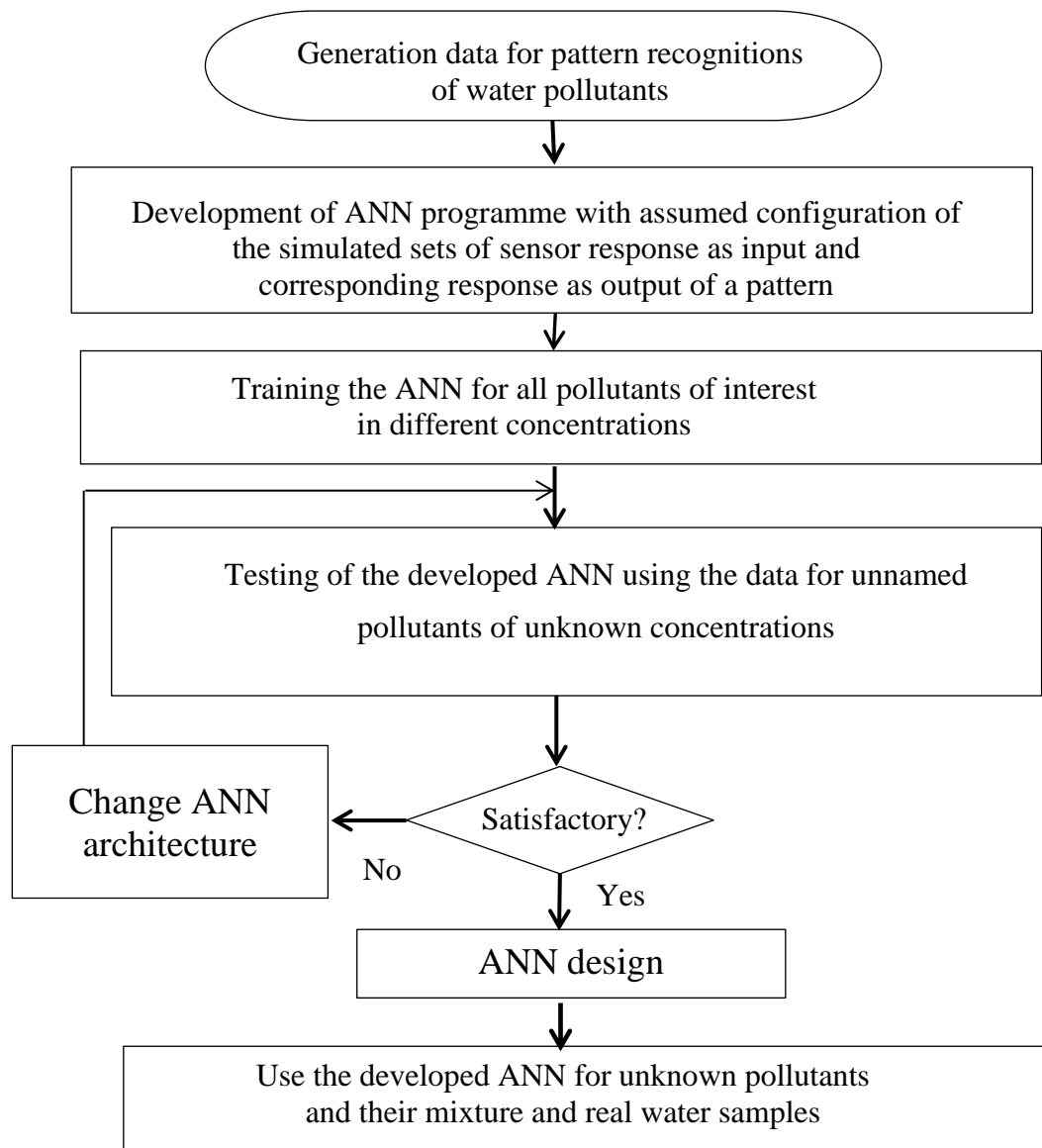


Figure 6-2: The strategy of ANN development for water pollutants identification

It starts with collecting the set of experimental data which contains the values of responses of all channels to all pollutants studied in all concentrations used. The second stage is the development of the ANN itself by selecting the required numbers of neurons in the input, hidden, and output layers. Then the designed ANN has to be “trained”. The training process required feeding the training data set, which is a table of all sensor responses to all pollutants in known concentrations, and the desired output, i.e. the binary code corresponding to particular pollutant and its concentration. The data are fed many times (up to 10^5 - 10^6 times) and results in tuning link weights between the neurons. The MSE value is calculated after each iteration; and when the MSE reaches the target value the training is terminated. After that, the ANN is ready for testing.

The testing is carried out by a single feeding the testing data set, e.g. the responses of all sensors to particular pollutants in known concentrations (though different from those used in training). The results of the test show whether the ANN system works properly; if both the type of pollutant and its concentration are identified correctly, then ANN is working properly, if not, some changes have to be made in the program.

In the final step of ANN testing the pollutants of unknown concentrations have to be used either separately or in their mixture. A properly designed and trained ANN should be able to identify pollutants and to evaluate their concentrations.

6.4 The ANN design

The ANN design used in this project is shown in Figure 6-3. It consists of three neuron layers: (i), the input layer containing three neurons corresponding to the relative sensor responses of each bacteria, e.g. *E.coli*, *M. capsulatus*, and *S. oneidensis* (see Chapter.5); (ii), the hidden layer consisting of 12 neurons corresponding to 3 heavy metals (Hg^{2+} , Pb^{2+} , Cd^{2+}), 3 pesticides (atrazine, simazine, DDVP) and 6 petrochemicals (hexane, octane, pentane, toluene, pyrene, and ethanol); and (iii), the output layer consisting of 6 neurons representing a 6-digit binary code which combines the type of pollutant and its

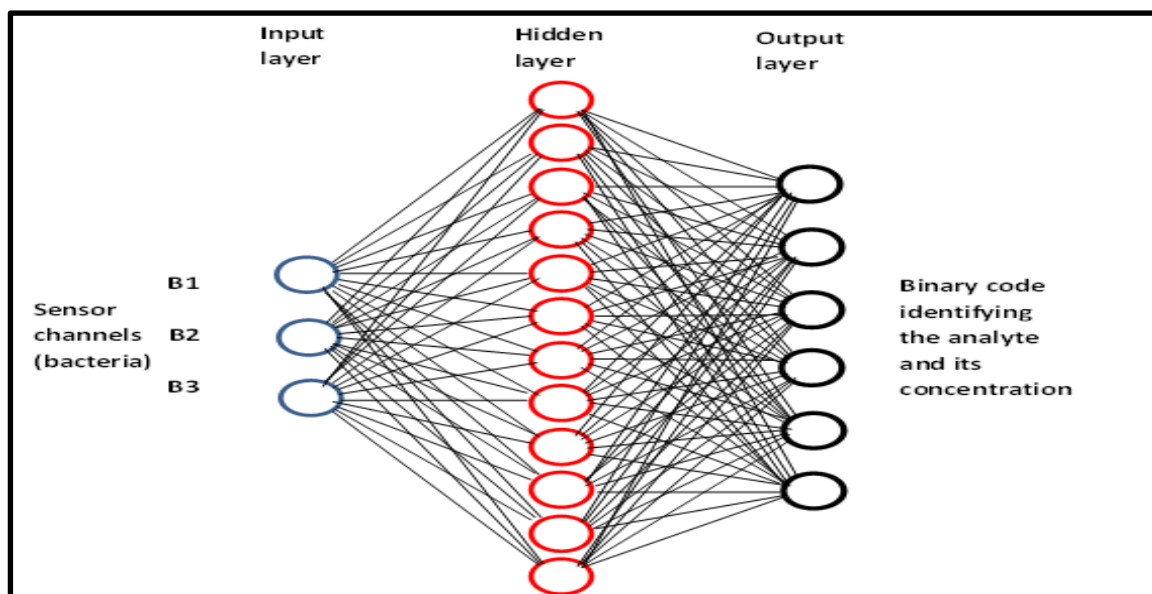


Figure 6-3: The ANN design used in the work for data analysis of bacteria sensor array.

concentration. The concentration is split into 5 bands, e.g. $0.1\mu\text{M}$, $1\mu\text{M}$, $10\mu\text{M}$, $100\mu\text{M}$, and 1 mM ; and the ANN rounds the concentration to the nearest lower band. A hyperbolic tangent was used as the activation function for the hidden neurons. The actual ANN MatLab code is given in Appendix C.

6.5 ANN training

The training data shown in Table 6-1 were presented as Excel files consisting of three significant parts: the concentration of analytes (C) in μM , the relative responses of the three bacteria, and the 6-digit binary code corresponding to the type of pollutant and its concentration. For example, the code (000001) corresponds to Hg^{2+} in concentration of $0.1\mu\text{M}$, while (001101) corresponds to Cd^{2+} in concentration of $10\mu\text{M}$, etc.

Table 6-1: Data set for ANN training.

C μM	Input values			Output values						
	<i>E. coli</i>	<i>M. capsulatus</i>	<i>S. oneidensis</i>	Binary code					target analyte	
0.1	0.0941	0.2011	0.0566	0	0	0	0	0	1	Hg²⁺
1	0.8061	0.6568	1.0651	0	0	0	0	1	0	
10	0.5862	1.5508	1.0790	0	0	0	0	1	1	
100	1.2180	1.4181	1.7796	0	0	0	1	0	0	
1000	1.9207	0.2134	2.1583	0	0	0	1	0	1	
0.1	0.1015	0.3573	0.5132	0	0	0	1	1	0	Pb²⁺
1	0.1513	0.5321	0.7467	0	0	0	1	1	1	
10	0.5591	1.6432	0.9733	0	0	1	0	0	0	
100	1.2180	1.8324	2.5427	0	0	1	0	0	1	
1000	2.5423	2.3265	3.0132	0	0	1	0	1	0	
0.1	0.3242	0.3423	0.1098	0	0	1	0	1	1	Cd²⁺
1	0.5342	0.7621	1.2765	0	0	1	1	0	0	
10	0.7454	1.2310	1.6546	0	0	1	1	0	1	
100	1.6454	1.5231	1.9342	0	0	1	1	1	0	
1000	2.5534	0.8702	2.3287	0	0	1	1	1	1	
0.1	0.0557	0.0123	0.0357	0	1	0	0	0	0	Atrazine
1	0.6705	1.0168	0.0551	0	1	0	0	0	1	
10	0.3716	2.1568	0.0359	0	1	0	0	1	0	
100	1.0880	3.4181	0.1996	0	1	0	0	1	1	
1000	2.0158	4.2134	2.5153	0	1	0	1	0	0	
0.1	0.2623	0.1034	0.1078	0	1	0	1	0	1	Simazine
1	0.8423	1.3765	0.2094	0	1	0	1	1	0	
10	1.6433	2.5473	0.4988	0	1	0	1	1	1	
100	2.1653	3.0231	0.9199	0	1	1	0	0	0	
1000	3.5432	4.7843	3.0742	0	1	1	0	0	1	
0.1	0.2045	0.5342	0.0357	0	1	1	0	1	0	DDVP
1	0.6548	1.2856	0.0551	0	1	1	0	1	1	
10	1.7231	2.1234	0.0359	0	1	1	1	0	0	
100	2.3075	3.0562	0.1996	0	1	1	1	0	1	
1000	3.2415	4.5324	2.5153	0	1	1	1	1	0	
0.1	0.0266	1.0912	0.4366	0	1	1	1	1	1	Hexane
1	0.0351	1.1861	0.5931	1	0	0	0	0	0	
10	1.0598	2.5862	0.8109	1	0	0	0	0	1	
100	2.9896	3.2180	0.9488	1	0	0	0	1	0	
1000	3.1583	4.9207	5.1583	1	0	0	0	1	1	
0.1	0.0266	1.1099	0.2834	1	0	0	1	0	0	Octane
1	0.0351	1.3209	0.3965	1	0	0	1	0	1	
10	1.0598	2.7213	0.5234	1	0	0	1	1	0	
100	1.9896	3.1653	0.8534	1	0	0	1	1	1	

1000	2.1583	3.5202	3.0652	1	0	1	0	0	0	
0.1	0.5432	1.1974	0.3144	1	0	1	0	0	1	Pentane
1	0.8453	1.5342	0.5462	1	0	1	0	1	0	
10	1.3541	2.8653	0.7451	1	0	1	0	1	1	
100	2.2761	3.6452	0.8953	1	0	1	1	0	0	
1000	3.4532	4.2756	4.3523	1	0	1	1	0	1	
0.1	0.0350	1.32091	0.3965	1	0	1	1	1	0	Toluene
1	1.0598	2.72134	0.5234	1	0	1	1	1	1	
10	1.9896	3.16532	0.8534	1	1	0	0	0	0	
100	2.1583	3.52016	3.0652	1	1	0	0	0	1	
1000	0.0912	1.20111	0.4065	1	1	0	0	1	0	
0.1	0.2965	0.99123	0.7365	1	1	0	0	1	1	Pyrene
1	0.9050	1.1860	0.4931	1	1	0	1	0	0	
10	2.0598	1.2861	0.6108	1	1	0	1	0	1	
100	2.9896	1.0180	1.5487	1	1	0	1	1	0	
1000	4.1583	0.9206	5.1583	1	1	0	1	1	1	
0.1	0.1015	0.3573	0.5132	1	1	1	0	0	0	Ethanol
1	0.1513	0.5321	0.7467	1	1	1	0	0	1	
10	0.5591	1.6432	0.9733	1	1	1	0	1	0	
100	1.2180	1.8324	2.5426	1	1	1	0	1	1	
1000	2.5423	2.3265	3.0132	1	1	1	1	0	0	

The training was carried out using Multilayer Perceptron Back Propagation Algorithm (MLP BPA) [15]. The neuron link weights are consequently tuned utilizing the *purelin* function for expanding the precision of the output. The error is ascertained as the contrast between the objective output and the system output. During the calculation the weights and biases of the system are modified to minimize the LMSE (Least Mean Square Error).

The ANN training procedure exploited the Levenberg-Marquardt algorithm to optimize the weights of neurons in a hidden layer. This algorithm appeared to be the fastest method for the network training using the limited experimental data of this study. A hyperbolic tangent was used as the activation function for the hidden neurons and a log-sigmoid function was used for the output neurons. The training was performed for 250000 epochs (e.g. 250,000 repetitions of data feeding) with the mean square error (MSE) goal set to 10^{-10} . Figure 6-4 shows the saturation of MSE at about 250,000 epochs, which indicates the completion of the ANN training.

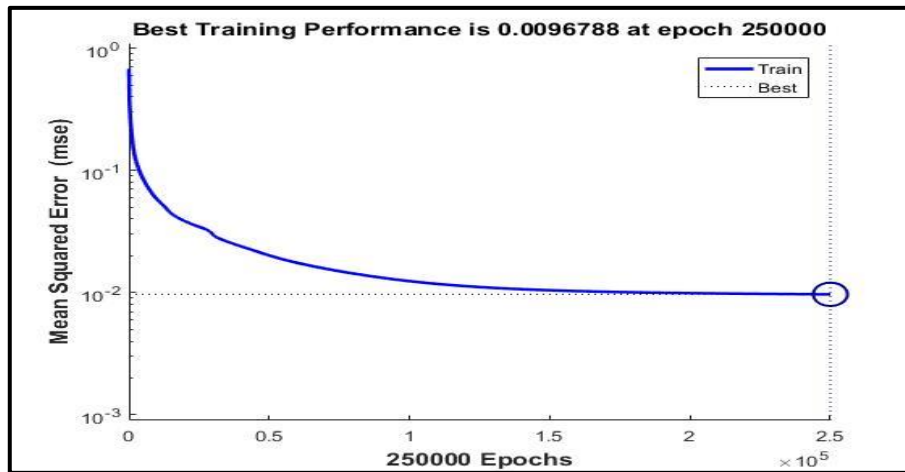


Figure 6-4: ANN training: Reduction of MSE during the 250,000 epochs of data feeding.

6.6 ANN testing (simulation)

After the training, the ANN programme was tested by feeding the data obtained from the bacterial sensor array for PBS solutions spiked with a particular concentration of pollutants randomly selected within the 1 μM - 100 μM concentration ranges. Both the input testing data and the outcomes of pollutants classification are shown in Table 6-2.

Table 6-2: The results of ANN identification of pollutants and estimation their concentration.

Input values			Output values							
<i>E. coli</i>	<i>M. capsulatus</i>	<i>S. oneidensis</i>	Binary code					Pollutant	Concentration (μM)	
									Obtained	Actual
0.09417	0.58032	0.06211	0	0	0	0	1	0	1	0.66
0.46138	1.48214	1.08641	0	0	0	0	1	1	10	1.3
1.19823	1.37532	1.65302	0	0	0	1	0	0	100	66
0.09023	0.45121	0.67656	0	0	0	1	1	1	1	1.25
0.48352	1.56176	0.87403	0	0	1	0	0	0	10	22
1.21501	1.71608	2.47263	0	0	1	0	0	1	100	83
0.54321	0.59745	1.31435	0	0	1	1	0	0	1	1.37
0.76232	1.13421	1.54623	0	0	1	1	0	1	10	26
1.55412	1.66534	1.82152	0	0	1	1	1	0	100	76
0.55657	1.01232	0.01566	0	1	0	0	0	1	1	1.45
0.30508	2.09684	0.08508	0	1	0	0	1	0	10	24

Input values			Output values								
1.06593	2.95676	0.97593	0	1	0	0	1	1		100	71
0.76231	1.20342	0.18784	0	1	0	1	1	0	simazine	1	1.61
1.54231	2.47652	0.36941	0	1	0	1	1	1		10	12.5
2.14325	2.89732	0.89876	0	1	1	0	0	0		100	87
0.50453	1.13423	0.05566	0	1	1	0	1	1	DDVP	1	1.1
1.65483	2.08563	0.02508	0	1	1	1	0	0		10	13.8
2.26314	2.87342	0.09593	0	1	1	1	0	1		100	99
0.03290	1.24231	0.49265	1	0	0	0	0	0	hexane	1	1.2
1.04398	2.72134	0.56021	1	0	0	0	0	1		10	32
2.89296	2.36532	0.75134	1	0	0	0	1	0		100	83
0.02965	1.299123	0.27365	1	0	0	1	0	1	octane	1	1.22
0.95120	2.61860	0.41931	1	0	0	1	1	0		10	17
2.00623	2.92861	0.65108	1	0	0	1	1	1		100	77
0.71525	1.47123	0.51132	1	0	1	0	1	0	pentane	1	1.6
1.29723	2.68243	0.74167	1	0	1	0	1	1		10	18
2.26211	2.85412	0.97133	1	0	1	1	1	0		100	89
0.90123	2.51252	0.46326	1	0	1	1	1	1	toluene	1	1.2
2.03251	2.85421	0.59131	1	1	0	0	0	0		10	11
1.98589	2.85862	2.87109	1	1	0	0	0	1		100	93
0.80173	1.01099	0.38134	1	1	0	1	0	0	pyrene	1	1.4
2.01351	1.13209	0.53965	1	1	0	1	0	1		10	11.6
2.90598	1.07213	1.43312	1	1	0	1	1	0		100	83
0.15432	0.51974	0.63144	1	1	1	0	0	1	ethanol	1	1.5
0.48453	1.53342	0.54762	1	1	1	0	1	0		10	12.1
1.31541	1.81653	2.65021	1	1	1	0	1	1		100	97

The ANN outcome is a 6-digit code representing the type of pollutant and its concentration rounded to the nearest quantized concentration value. Despite the limited amount of data for ANN training, the programme managed to identify the pollutants correctly. The comparison of values in the last two columns representing, respectively, the obtained and actual concentrations of pollutants showed that the concentration was estimated correctly. For example, the sample spiked with 1.45 μM of atrazine was identified by a binary code 010001 which corresponds to atrazine in concentration of 1 μM ; the sample spiked with 0.66 μM of HgCl_2 was identified by a code 000001 corresponding to Hg^{2+} in concentration of 1 μM ; the sample spiked with 83 μM of pyrene was identified by a code 110110 as pyrene in concentration of 100 μM .

The precision of the network model was evaluated using 36 randomly selected experimental data points. This test shows that 91 % of the test data was correctly classified, using the equation of True negatives / True negatives + False positives to include the calculation of that 91% precision [16]. Classified pollutants were then quantified using the optimized individual network algorithm. The results were reasonable since the network models were trained using a limited amount of data. A very good correlation between the target and the evaluated concentration of pollutants was observed with an acceptable average error of 10^{-10} . The successful classification and quantification of randomly selected data sets proves that the neural network models were able to process the information given and could be used to analyse unknown compounds or their mixtures, assuming that they belong to the group of 12 analytes used to build the models.

6.7 Summary

The use of ANN software for data processing allowed the more accurate identification of water pollutants, e.g. heavy metals, pesticides, and hydrocarbons as well as the estimation of their concentration in the range from 0.1 μM to 1mM.

The designed ANN programme is capable of identification of pollutants as well as the rough estimation of their concentration by rounding the output to the nearest quantized concentration value, e.g. 0.1 μM , 1 μM , 10 μM , 100 μM , and 1 mM. The ANN was trained by multiple feeding the experimental results, e.g. the responses of all three sensing channels to all 12 pollutants (Hg^{2+} , Pb^{2+} , Cd^{2+} , atrazine, simazine, DDVP, hexane, pentane, pyrene, toluene, octane and ethanol) in five concentrations (0.1 μM , 1 μM , 10 μM , 100 μM , and 1 mM). Despite a rather small amount of experimental data, the trained ANN was able to classify and quantify the pollutants with acceptable errors of less than 10 %.

The results obtained are very promising since simple electrochemical measurements of anodic current at +0.5V combined with ANN-based data processing allow both the identification of pollutants studied as well as rough estimation of their concentrations in the range from 0.1 μM to 1000 μM . This has emphasised the implementation of the artificial neural network algorithm as a tool for the analysis of the distinct pattern of sensor responses.

It has to be said that ANN approach in sensor array data processing is not ideal though better than the other statistical methods mentioned earlier in section 6-1. The main problem is that the ANN will only identify the analytes (pollutants in our case) which the ANN was trained on; the unknown chemicals could be either misdiagnosed, e.g. mixed up with some of the known analytes and the concentration could be wrong. That is why the analysis of “real samples” was always problematic because of a background of a number of chemicals which the ANN was not trained on.

Nevertheless, the ANN system combined with the bacteria sensor array could be successfully used for preliminary detection (screening) of water samples, in which the suspected samples containing particular pollutants in large concentrations are identified and passed to specialized laboratories for further testing.

References

1. Vlasov, Y. G., Legin, A. V., Rudnitskaya, A. M., D'amico, A., & Di Natale, C. (2000). «Electronic tongue»—new analytical tool for liquid analysis on the basis of non-specific sensors and methods of pattern recognition. *Sensors and Actuators B: Chemical*, 65(1-3), 235-236.
2. Mortensen, J., Legin, A., Ipatov, A., Rudnitskaya, A., Vlasov, Y., & Hjuler, K. (2000). A flow injection system based on chalcogenide glass sensors for the determination of heavy metals. *Analytica Chimica Acta*, 403(1-2), 273-277.
3. Evgen'ev, M. B., & Arkhipova, I. R. (2005). Penelope-like elements—a new class of retroelements: distribution, function and possible evolutionary significance. *Cytogenetic and genome research*, 110(1-4), 510-521.
4. Di Natale, C., Macagnano, A., Davide, F., D'amico, A., Legin, A., Vlasov, Y., & Selezenev, B. (1997). Multicomponent analysis on polluted waters by means of an electronic tongue. *Sensors and Actuators B: Chemical*, 44(1-3), 423-428.
5. Bachmann, T. T., Leca, B., Vilatte, F., Marty, J. L., Fournier, D., & Schmid, R. D. (2000). Improved multianalyte detection of organophosphates and carbamates with disposable multielectrode biosensors using recombinant mutants of *Drosophila* acetylcholinesterase and artificial neural networks. *Biosensors and Bioelectronics*, 15(3-4), 193-201.
6. Shaffer, R. E., & Rose-Pehrsson, S. L. (1999). Improved probabilistic neural network algorithm for chemical sensor array pattern recognition. *Analytical chemistry*, 71(19), 4263-4271.
7. Gutés, A., Céspedes, F., Alegret, S., & Del Valle, M. (2005). Determination of phenolic compounds by a polyphenol oxidase amperometric biosensor and artificial neural network analysis. *Biosensors and Bioelectronics*, 20(8), 1668-1673.
8. Bachmann, T. T., Leca, B., Vilatte, F., Marty, J. L., Fournier, D., & Schmid, R. D. (2000). Improved multianalyte detection of organophosphates and carbamates with disposable multielectrode biosensors using recombinant mutants of *Drosophila* acetylcholinesterase and artificial neural networks. *Biosensors and Bioelectronics*, 15(3-4), 193-201.
9. Reder, S., Dieterle, F., Jansen, H., Alcock, S., & Gauglitz, G. (2003). Multi-analyte assay for triazines using cross-reactive antibodies and neural networks. *Biosensors and bioelectronics*, 19(5), 447-455.

10. Gholmieh, G., Courellis, S., Fakheri, S., Cheung, E., Marmarelis, V., Baudry, M., & Berger, T. (2003). Detection and classification of neurotoxins using a novel short-term plasticity quantification method. *Biosensors and Bioelectronics*, 18(12), 1467-1478.
11. Lobanov, A. V., Borisov, I. A., Gordon, S. H., Greene, R. V., Leathers, T. D., & Reshetilov, A. N. (2001). Analysis of ethanol–glucose mixtures by two microbial sensors: application of chemometrics and artificial neural networks for data processing. *Biosensors and Bioelectronics*, 16(9-12), 1001-1007.
12. Rudnitskaya, A., Ehlert, A., Legin, A., Vlasov, Y., & Büttgenbach, S. (2001). Multisensor system on the basis of an array of non-specific chemical sensors and artificial neural networks for determination of inorganic pollutants in a model groundwater. *Talanta*, 55(2), 425-431.
13. Vlasov, Y. G., Legin, A. V., Rudnitskaya, A. M., D'amico, A., & Di Natale, C. (2000). «Electronic tongue»—new analytical tool for liquid analysis on the basis of non-specific sensors and methods of pattern recognition. *Sensors and Actuators B: Chemical*, 65(1-3), 235-236.
14. Shaffer, R. E., Rose-Pehrsson, S. L., & McGill, R. A. (1999). A comparison study of chemical sensor array pattern recognition algorithms. *Analytica Chimica Acta*, 384(3), 305-317.
15. Durairaj, M., & Revathi, V. (2015). Prediction Of Heart Disease Using Back Propagation MLP Algorithm. *International Journal Of Scientific & Technology Research*, 4(08).
16. Lalkhen, A. G., & McCluskey, A. (2008). Clinical tests: sensitivity and specificity. *Continuing Education in Anaesthesia Critical Care & Pain*, 8(6), 221-223.
17. Haron S. Planar waveguide enzyme sensors coated with nanocomposite membranes for water pollution monitoring, Thesis for the degree of Doctor of Philosophy, Sheffield Hallam university, 2005.
18. Arkhypova V. N., Dzyadevych S. V., Soldatkin A. P. et al. Multibiosensor based on enzyme inhibition analysis for determination of different toxic substances, *Talanta* 55 (2001) 919-927.
19. Starodub N. F., Kanjuk N. I., Kukla A. L. et al. Multi-enzymatic electrochemical sensor: field measurements and their optimisation, *Analytica Chimica Acta* 385 (1999) 461-466.

20. Kukla A. L., Kanjuk N. I., Starodub N. F. et al. Multienzyme electrochemical sensor array for determination of heavy metal ions, *Sensors and Actuators B* 57 (1999) 213-218.
21. Bachmann T. T., Leca B., Vilatte F. et al. Improved multianalyte detection of organophosphates and carbamates with disposable multielectrode biosensors using recombinant mutants of *Drosophila* acetylcholinesterase and artificial neural networks, *Biosensors and Bioelectronics* 15 (2000) 193-201.
22. Bachmann T. T. and Schmid R. D. A disposable multielectrode biosensor for rapid simultaneous detection of the insecticides paraoxon and carbofuran at high resolution, *Analytica Chimica Acta* 401 (1999) 95-103.
23. Tsargorodska, A. (2007). Research and development in optical biosensors for determination of toxic environmental pollutants. Sheffield Hallam University (United Kingdom).

CHAPTER 7 Detection of heavy metals using aptamer-based assays

As an alternative to the use of non-specific bio-receptors such as bacteria in inhibition sensor array format, highly specific receptors such as aptamers were used in current study, so this chapter describes the use of specific aptamers against Hg^{2+} and Pb^{2+} ions having electrochemically active labels of ferrocene and methylene blue, attached respectively, at 5' termini. The sensing mechanism of these aptamer probes is based on the changes in the DNA strand's conformation from the linear to a folded structure upon binding the metal ions, which in turn affects the electron transfer between the redox label and the metal electrode.

7.1 Experimental Methodology

7.1.1 Aptamers and other chemicals used

The following modified deoxyribonucleotides (P1 and P2) selected as specific aptamers for Hg^{2+} and Pb^{2+} ions, respectively, were purchased from Sangon-Biotech (China):

P1: Ferrocene-5'-**TTC TTT CTT CCC CTT GTT TGT T-3'**-SH [1].

P2: Methylene blue-5'-**CAA CGG TTG GTG TGG TTGG-3'**-SH [2].

The thiol groups (SH) at the C3 termini or prime were attached to provide strong and oriented binding of the aptamers to screen printed gold electrodes. The redox functional groups, e.g. ferrocene or methylene blue, were attached to C5 termini or prime in order to provide distinctive electrochemical properties, such as current peaks on CV characteristics associated with oxidation and reduction reactions.

The other chemicals used (all from Sigma Aldrich) were Hepes and phosphate binding buffers (HBB and PBB), also 1,4-dithiothreitol (DTT). Hepes binding buffer (HBB) was prepared by dissolving 50 mM Hepes sodium salt, 3 mM MgCl_2 , 120 mM NaCl, and 5 mM KCl in deionized Milli-Q water. The pH of the buffer was adjusted to 7.4. Similarly, phosphate binding buffer (PBB) was prepared by dissolving 10 mM Na_2HPO_4 , 1.76 mM KH_2PO_4 , 3 mM MgCl_2 , 2.7 mM KCl, and 137 mM NaCl. The pH

of the buffer was adjusted to 7.4. The addition of MgCl_2 to the buffers was essential to preserve the aptamer single DNA strand from self-coiling. For long-term storage, the 100 μM solutions of received aptamer was prepared in sterilized deionized water and stored at $-20\text{ }^\circ\text{C}$ in small aliquots in order to avoid repeated thaw-freeze cycles.

7.1.2 Immobilization of aptamers

The aptamers were immobilized on gold surface via thiol groups on the 3'-termini in the following procedure. Stock solution of the required aptamer was diluted to 1 μM with HBB or PBB supplemented with 1 mM of 1,4-dithiothreitol (DTT) and 3 mM of MgCl_2 . DTT causes the removal of the protecting group from the SH moiety and released the aptamers with free SH end groups that could then bind to the surface of screen printed gold electrode in the presence of Mg^{2+} aptamers are initially stretched. Before immobilization, the aptamers samples were activated by rapid (1 min) heating up to $95\text{ }^\circ\text{C}$ followed by 1 min cooling at ($4\text{ }^\circ\text{C}$) using a conventional thermocycler polymerase chain reaction unit (TECHNE PCR version TC-3000) as appeared in Figure 7-1. Immobilization was carried out by casting aptamers solution onto the screen printed gold electrode surface; the samples were then incubated for 4 h at room temperature in a humidity chamber. The unreacted aptamers were removed from the electrode surface by several rinses with non-folding buffer (HBB), then the screen printed gold electrode with immobilized aptamers were kept in HBB to prevent aptamers from coiling.

7.2 ICP-MS measurements

A PerkinElmer NexION™ 350X ICP mass spectrometer was used as a test method for the determination of Hg^{2+} and Pb^{2+} in the real water samples. The ICP-MS instrument was equipped with a PE-AS91 auto-sampler. Samples were introduced via a cross-flow nebulizer with a Scott-type spray chamber. The NexION™ 350X and auto-sampler and peristaltic pump are controlled by the NexION™ 350X Windows NT software and are fully automated.

7.3 Electrochemical measurements

Electrochemical measurements provide the means for rapid and portable detection of heavy metal ions [3]. All CV electrochemical measurements were carried out using a DropSTAT4000P potentiostat instrument (from DropSens) controlled by Autolab software and using DropSens screen printed gold electrodes (SPGEs). These electrodes have a conventional three electrode configuration with gold working electrode (4-mm diameter disk) and counter electrode (16 mm×1.5 mm curved line), and Ag/AgCl (16 mm×1.5 mm straight line) pseudo-reference electrode and scan rate 100 mV/s [4]. CV measurements were carried out on electrodes with the immobilized aptamers, first, in pure buffer solution (HBB or PBB), then in buffer solutions with the addition of either HgCl₂ or PbCl₂ salts at different concentrations starting from 1 ng/l up to 10 µg/l. Because the addition of heavy metal salts increases the conductivity of buffer solutions, control measurements were carried out in on electrodes without aptamers at each concentration of metal salts. These measurements provide a calibration which was later used for analysis of real samples of water taken from different natural resources in the area were tested using the same screen-printed electrodes with immobilized aptamers. The reference in this case was bottled drinking water. The aptamer/metal ion binding kinetics was studied by recording current in SPGEs at fixed potentials: (-0.2 V) for HgCl₂ of different concentrations and (-0.4V) for PbCl₂ of different concentrations. Impedance spectra were measured using an impedance spectroscope (4000A) and gold interdigitated electrodes (from Metrohm DropSens) containing 250 fringes on each side spaced by 5 µm; the overlapping length 6.76 mm. The AC voltage amplitude was 5 mV with the frequency varied from 100 mHz to 100 kHz; no DC bias was applied. Similarly to CVs, the impedance spectra measurements were carried out on electrodes both coated and non-coated with aptamers, in buffer solutions containing different concentrations of metal ions

7.4 Results and discussion

7.4.1 Design strategy of the apta-sensor

The strategy in this study (illustrated in Figure 7-2) was based on the principle that the aptamers could act as chelating factor for the analytes and undergo conformational changes that lead to changes in the electrochemical properties of aptamers containing the redox label. According to this model, in the absence of target analyte, the aptamer would remain unfolded with an extended conformation (the presence of MgCl_2 in the buffer is vital for that). However, upon addition of target analyte, the conformation of aptamer changes to a coiled oligonucleotide chain wrapping around the target, that would bring the probe closer to the electrode surface, resulting in increase in both cathodic and anodic currents due to the enhancement of the electron transfer between the electrode and the redox label. The increase in concentration of target analyte would increase the concentration of coiled aptamers on the surface and subsequently increase the electrochemical current. The screen printed gold electrodes activated with the anti- Hg^{2+} or anti- Pb^{2+} aptamers were prepared as described in the 7.1.2 section. These electrodes functionalized with Hg^{2+} and Pb^{2+} -specific aptamers after reactivated using PCR as appeared below in Figure 7-1, were used directly as apta-sensors or stored submerged in HBB at 4 °C or room temperature for several days without any decrease in sensitivity.

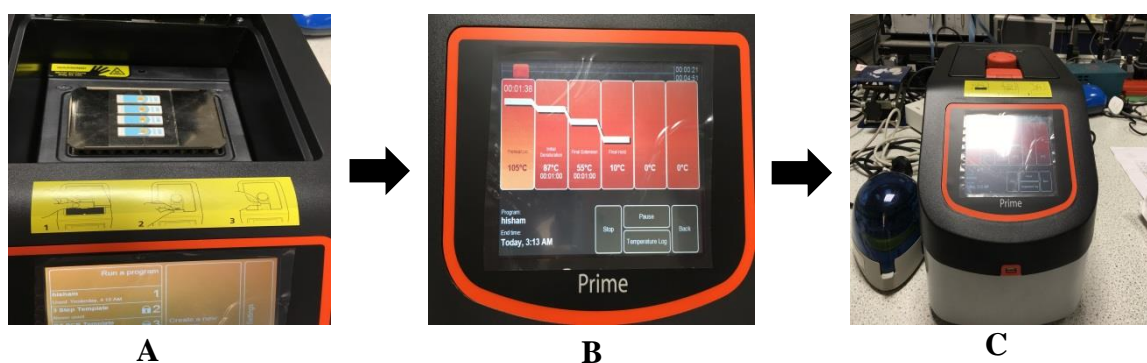


Figure 7-1: PCR activation process, (A) SPGEs functionalized with Hg^{2+} and Pb^{2+} specific aptamers, (B) heating up to 95 °C, and (C) cooling aptamers at (4 °C).

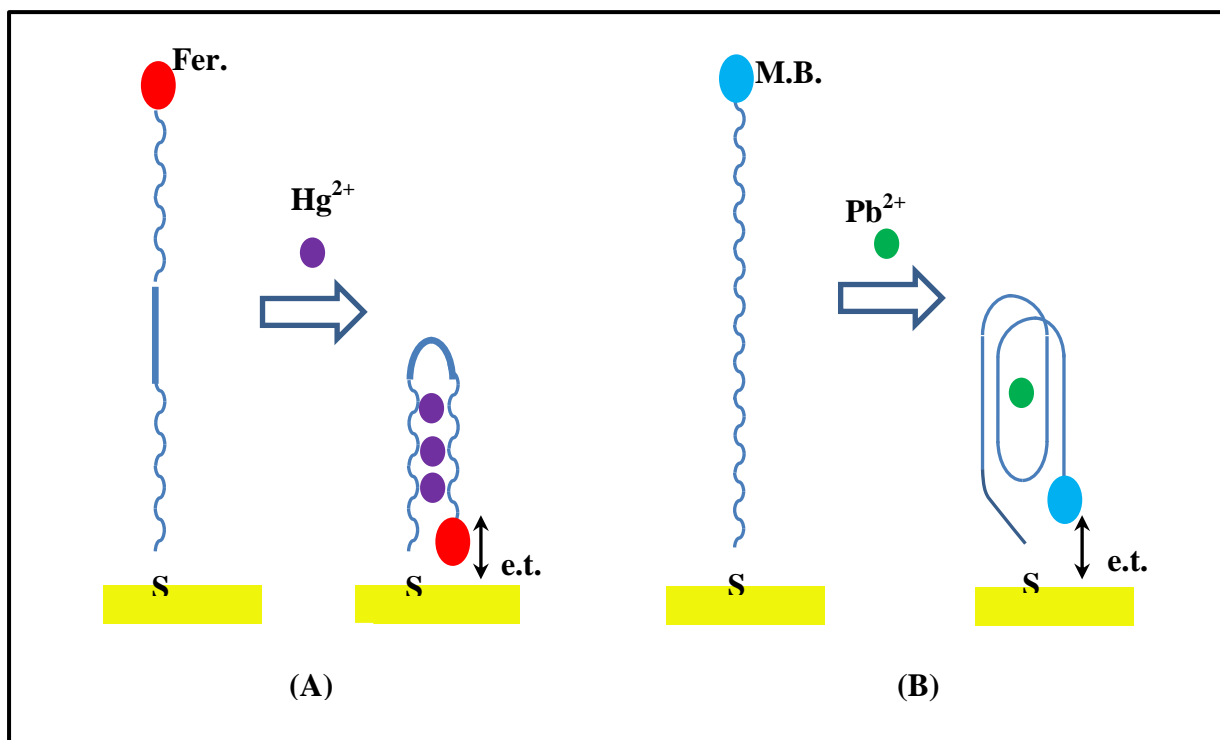
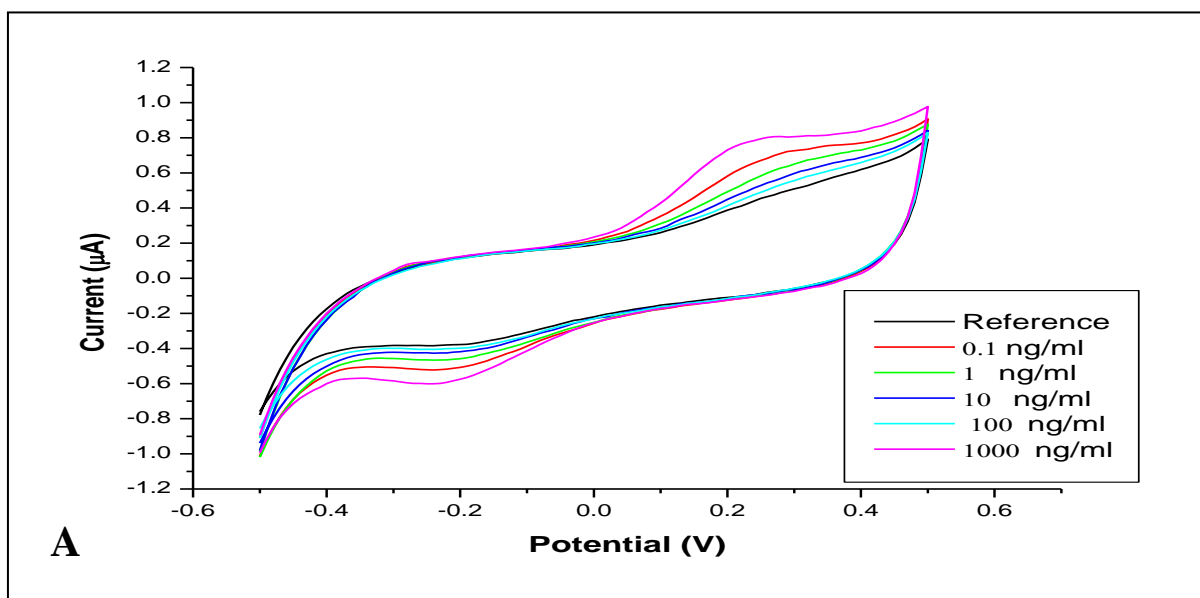


Figure 7-2: Schematic diagram of electrochemical detection of heavy metal ions Hg^{2+} (A) and Pb^{2+} (B) using redox-labelled aptamers.

7.4.2 Cyclic Electrochemical measurements

Typical cyclic voltammograms (CVs) recorded on electrodes with immobilized aptamers in PBB solution with added heavy metal salts in different concentrations are shown Figure 7-2(A,B). The anti- Hg^{2+} aptamer with ferrocene redox group showed well-resolved anodic and cathodic current peaks at about +0.2V and -0.2V, respectively, corresponding to oxidation and reduction of ferrocene (see Figure 7-2A). There is a clear correlation between the amplitudes of those two peaks and the concentrations of HgCl_2 in the buffer solution; the current goes up with the increase in Hg^{2+} ions contents as was explained in the schematic diagram in Figure (7-2). Similar results were observed for anti- Pb^{2+} aptamer with methylene blue redox label shown in Figure (7-2B), though the current peaks were not well-pronounced but rather appeared as shoulders at

potentials of about ± 0.2 V. Again, a correlation between the values of current and PbCl_2 salt concentration is apparent and proves the apta-sensing concept in Figure (7-2). In order to eliminate the effect of HgCl_2 and PbCl_2 salts on the conductivity of HBB solutions the control measurements were carried out on three-electrode assemblies without immobilized aptamers. These results are shown in Figure 7-4(A,B) and demonstrated no current peaks associated with redox groups, but just monotonous increase in anodic and cathodic currents above the respective potentials of about ± 0.4 V upon increasing the heavy metal salts concentrations. The main point is that the current increase at the voltages of ± 0.2 V was very small as compared to those on Figure (7-3).



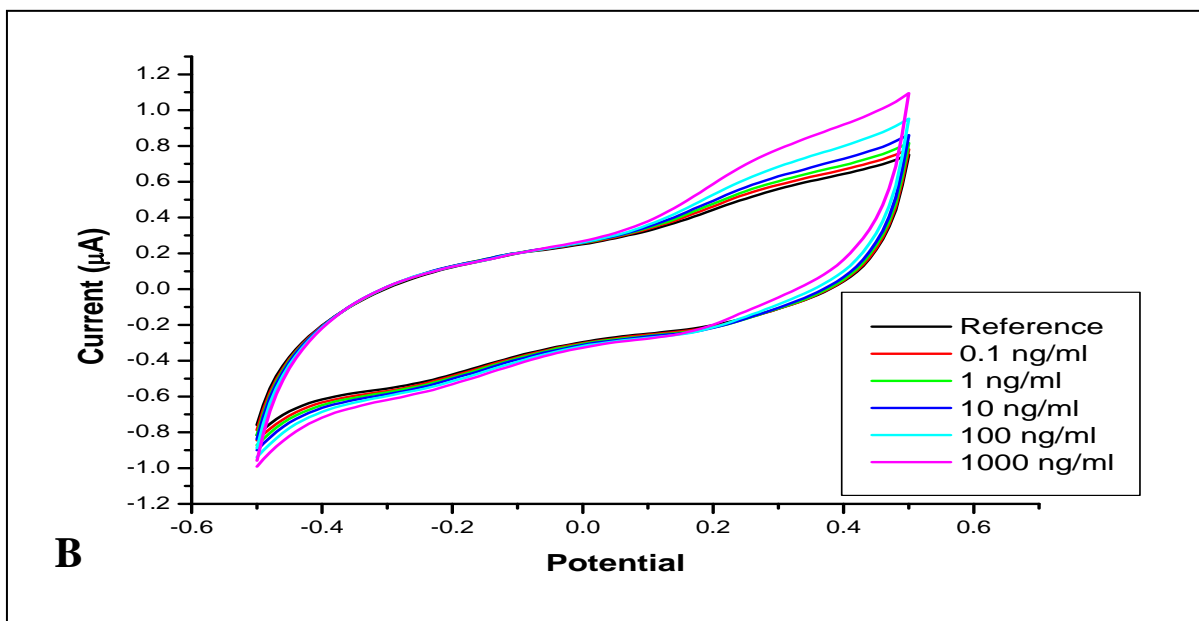
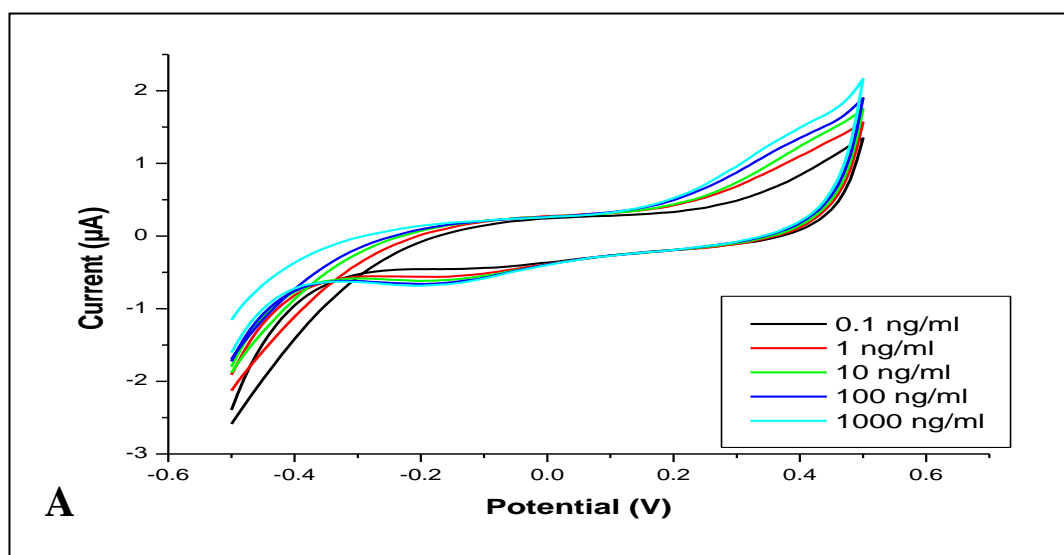


Figure 7-3: Cyclic voltammograms of screen-printed electrodes with immobilized anti Hg^{2+} (A) and anti- Pb^{2+} (B) aptamers in HBB solutions with different concentrations of HgCl_2 and PbCl_2 salts. The reference curves were recorded in pure HBB without heavy metal salts added.



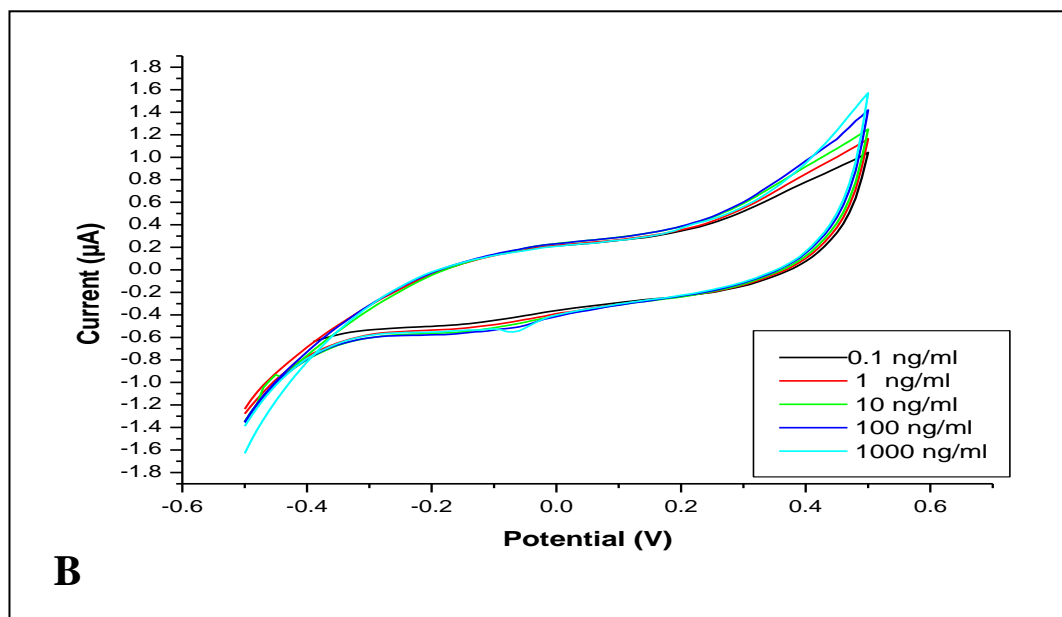


Figure 7-4: Cyclic voltammograms of screen-printed electrodes without immobilized aptamers in HBB solutions with different concentrations of HgCl_2 and PbCl_2 salts.

The dependence of the anodic current changes (at +0.2V) against the concentrations of heavy metals ions are shown in Figure 7-5(A,B). The background currents caused by the conductivity of HBB with added heavy metal salts was subtracted.

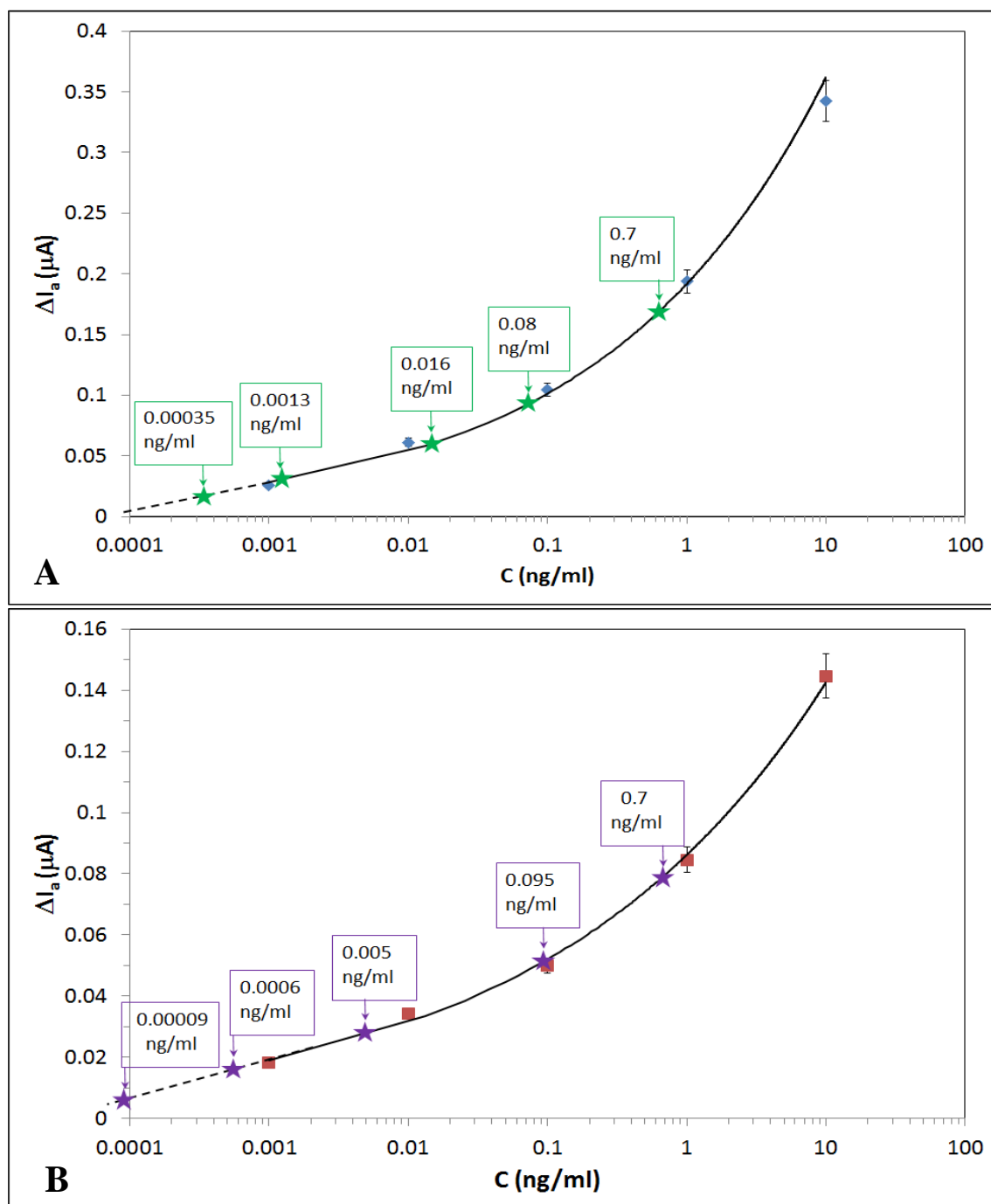


Figure 7-5: The concentration dependences of changes in anodic current at 0.2V upon binding of Hg²⁺ (A) and Pb²⁺ (B) ions to respective aptamers. Insets show the zoomed-in calibration curves with the data of five real water samples (marked as star points).

The cross-sensitivity tests were carried out by measuring CV curves on samples with immobilized anti-Hg and anti-Pb aptamers to other metal (e.g. Zn, Cu, Cd, and Pb or Hg) chloride salts. The results of such tests presented in Figure 7-6 showed no responses for non-complementary metals, which confirm high specificity of the aptamers used.

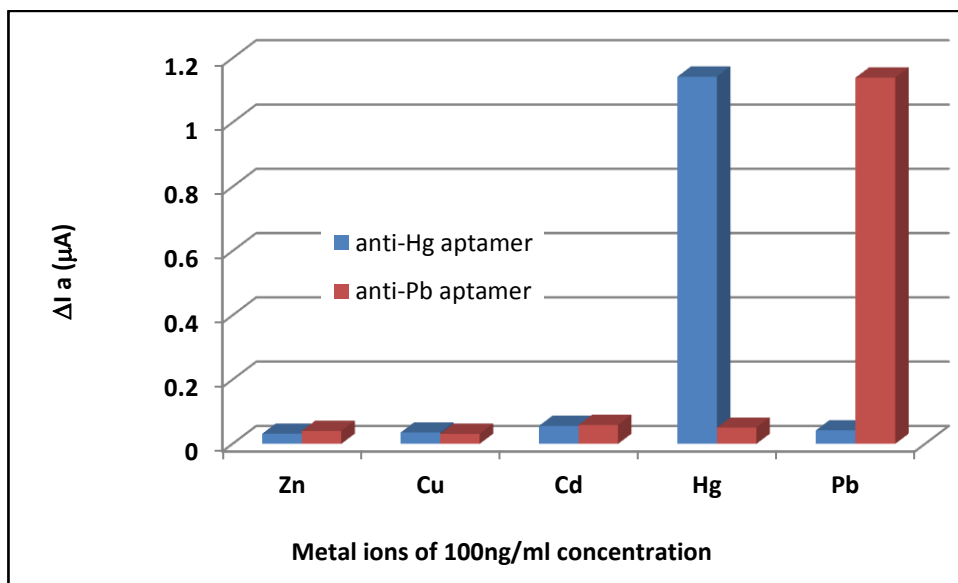


Figure 7-6: The cross-sensitivity tests: The CV responses of anti-Hg²⁺ aptamer (blue) and anti-Pb²⁺ aptamer (red) to Zn²⁺, Cu²⁺, Cd²⁺, Hg²⁺, and Pb²⁺ ions in 100 ng/ml concentrations.

Real samples of water were taken from different natural resources in the area were tested by CV measurements on screen-printed electrodes with immobilized anti-Hg²⁺ and anti-Pb aptamers. The results are lined up on the respective calibration graphs in Figure 7-5. For the sake of evaluation of Hg²⁺ and Pb²⁺ content in these samples the concentration dependences in Figure (7-6) were extrapolated to lower concentrations of Hg²⁺ and Pb²⁺ ions below the 0.01 ng/ml level. The estimated values for Hg²⁺ and Pb²⁺ contents are shown near respective data points. The obtained data for real samples of water are compared in Table 7-1 with the results of ICP-MS testing of the same water

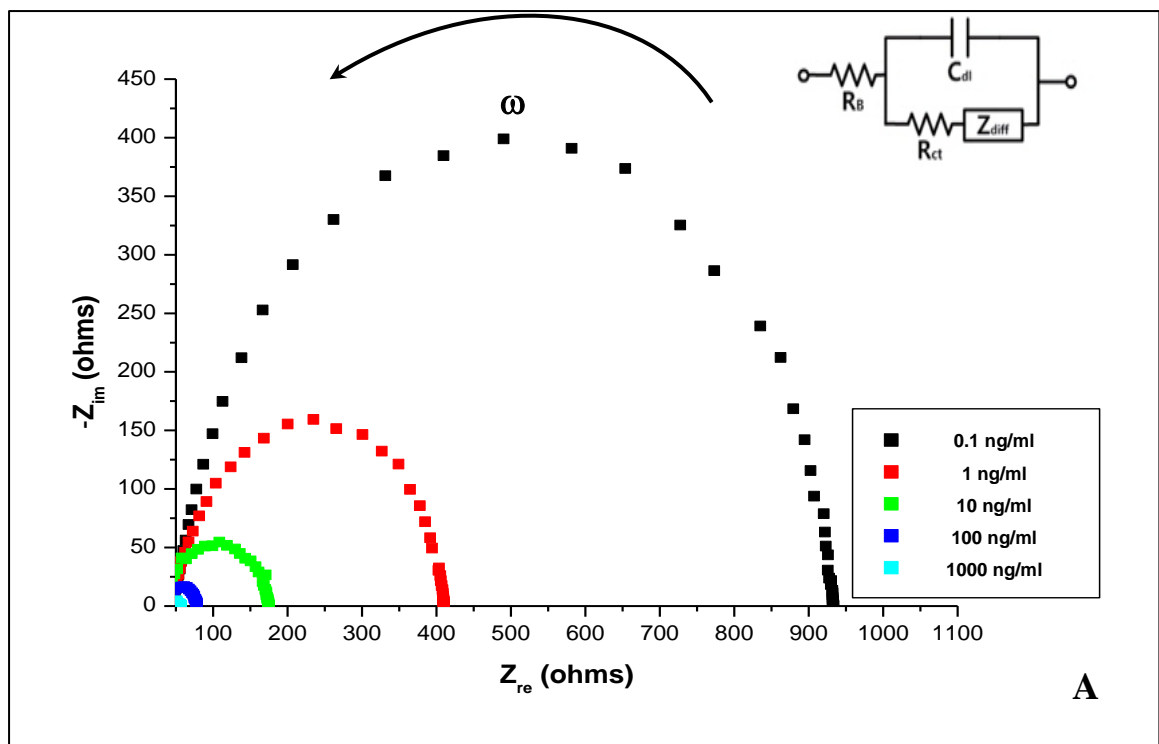
samples. The correlation between the two sets of data is present in terms of order of the concentration increase, however the ICP-MS values are typically from 3 to 10 times larger than those obtained with CVs. The semi-logarithmic calibration graphs of both sensors in Figure 7-6 (A,B), showed linear dependences on concentrations of respective ions. The studied concentration range was from 0.1 to 1000 ng/ml. The cross-sensitivity tests, e.g. exposures of anti-Hg²⁺ aptamer to Pb²⁺ and anti-Pb²⁺ aptamer to Hg²⁺, showed no responses which confirmed high specificity of aptamers. The data for real samples of water taken from different natural resources in the area are lined up on the above calibration graphs. For the sake of evaluation of these samples the concentration dependences were extrapolated to lower concentrations of Hg²⁺ and Pb²⁺ ions. The estimated values for Hg²⁺ and Pb²⁺ contents are shown near respective data points. The obtained data are compared in Table 7-1 with the results of ICP-MS testing of the same samples. Reasonable correlation was achieved for mercury ions, with CV data being in the same increasing order from samples 1 to 5 as ICP-MS data. Unfortunately, there is no correlation for lead ions; CV measurements showed much high values as compared to ICP-MS.

Table 7-1: ICP-MS testing results of real samples.

Sample number	Hg ²⁺ ions (ng/ml)		Pb ²⁺ ions (ng/ml)	
	CV results	ICP-MS result	CV results	ICP-MS result
Sample 1	0.00035	0.00170	0.00009	0.0001
Sample 2	0.00133	0.01062	0.00061	0.0088
Sample 3	0.01611	0.07831	0.00510	0.0349
Sample 4	0.08133	0.70311	0.09513	0.9600
Sample 5	0.71010	0.90013	0.70001	1.7000

7.4.3 Impedance spectroscopy measurements

The impedance spectroscopy scans were carried out on interdigitated electrodes with immobilized aptamers (as well as on bare electrodes) in HBB solutions containing heavy metal salts. Typical results are shown as Nyquist plots in Figure 7-7(A,B). As one can see, there is a major difference between these two graphs; in the presence of aptamers the Nyquist plots shift to the left (lower resistance) and reduces in radius with the increase in Hg^{2+} concentration, while in the absence of aptamers the plots remain almost unchanged with a small decrease in the $-Z_{im}$ values.



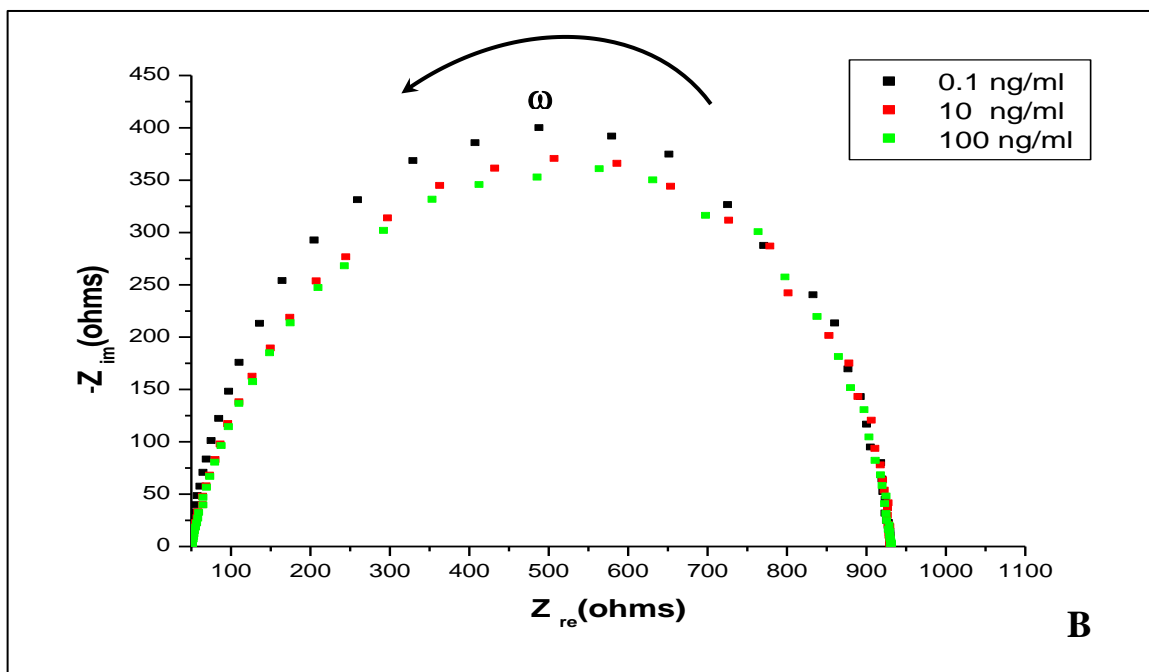


Figure 7-7: The Nyquist plots ($-Z_{im}$ vs Z_{re}) for interdigitated electrodes with immobilized anti- Hg^{2+} aptamers binding Hg^{2+} ions of different concentrations (A); the Nyquist plot for bare interdigitated electrodes in solutions with different concentrations of $HgCl_2$ (B).

Similar results were obtained for $PbCl_2$ (added in the appendix-A4 Fig.3). The analysis of impedance spectra using an equivalent circuit model (shown as inset in Figure 7-7A) was carried out. According to the simplified circuit model impedance (when the diffusion impedance Z_{diff} is neglected) [5], the real part of the impedance at critical points of the Nyquist plot is given as:

$$Z_{re} = R_b + R_{ct} \text{ at } \omega = 0 \text{ and } Z_{re} = R_b \text{ at } \omega = \infty,$$

where R_b is the bulk resistance of the electrolyte solution, R_{ct} and C_{dl} connected in parallel are, respectively, the charge transfer resistance and capacitance associated with an electrical charge double layer on the surface of gold electrodes.

A decrease in impedance was observed with increasing Hg^{2+} concentration, as evidenced by the decreasing height and diameter of the semi-circular Nyquist traces, which correspond to decreased capacitance and resistance of the sensor surface respectively. R_s (surface resistance), R_{dl} (double layer resistance) are presented in Table 7-2. Good stability of the sensor was observed as the solution resistance was partially constant at all stages of biosensor construction and testing. Whilst the R_{dl} values decreased upon addition of Hg^{2+} , showing a clear trend. The binding of aptamers to the analyte as a biosensor surface causes a decrease in impedance.

Table 7-2: Values for the EIS parameters obtained from fitting the Nyquist plots shown in Figure 7-7A to the equivalent circuit model.

Analyte	R_s (Ω)	R_{dl} (Ω)
0.1 ng/ml Hg^{2+}	38.026	932.5964
1 ng/ml Hg^{2+}	40.412	409.7153
10 ng/ml Hg^{2+}	42.970	174.7767
100 ng/ml Hg^{2+}	45.160	78.67283
1000 ng/ml Hg^{2+}	51.043	56.78813

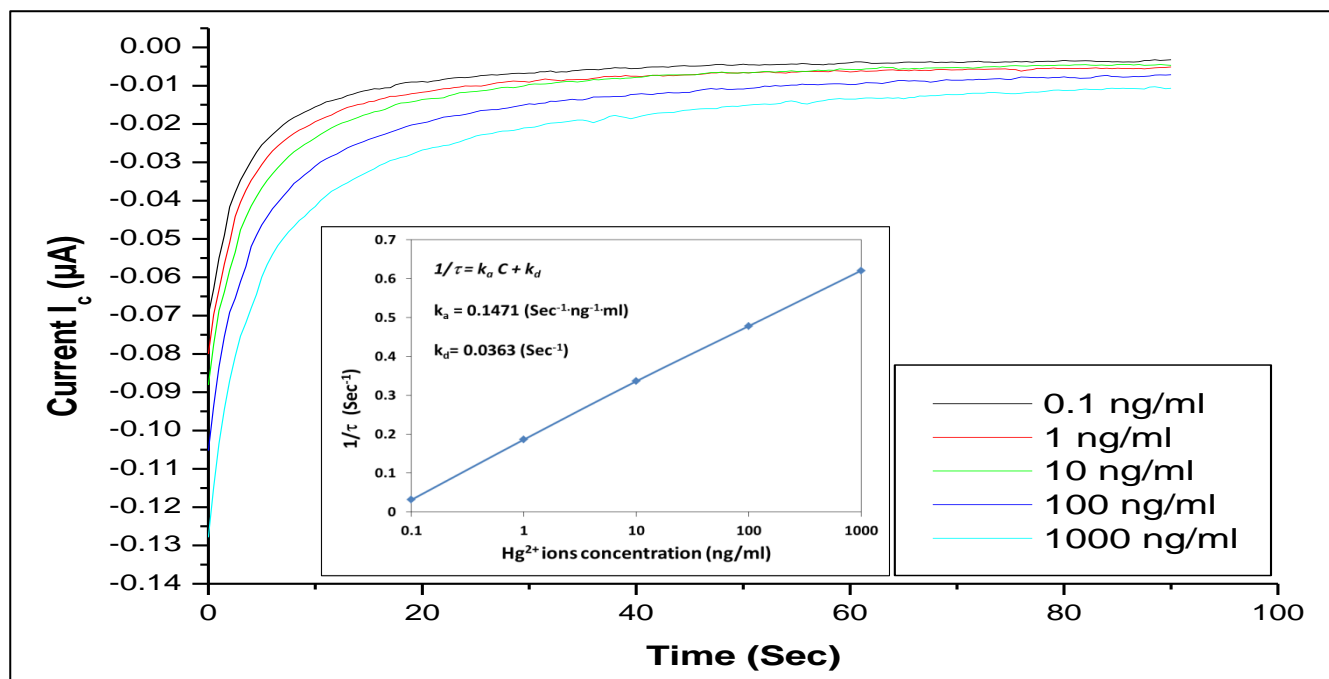


Figure 7-8: Typical kinetics for anti-Hg²⁺ aptamers binding Hg²⁺ ions of different concentrations. Inset shows the dependence of $1/\tau$ against the concentration of Hg²⁺ ions.

As one can see from Figure (7-7), the value of R_b is very small (typically in single Ohms), while R_{ct} is much larger (above 900 Ω at low concentrations of heavy metals) and decreases upon increasing concentration of Hg²⁺ ions most-likely due to the enhancement of the electron transfer between the ferrocene label and the electrode, very much in line with the scheme shown in Figure (7-2). At the same time, the increase of Hg²⁺ concentration without aptamers immobilized on the surface does not show any significant effect on the R_{ct} values which corresponds well to data in Figure (7-4). Similar results were observed for interdigitated electrodes with immobilized anti-Pb²⁺ aptamers in solutions containing PbCl₂. (see Appendix-A4 Fig.3 for Pb²⁺)

7.4.4 The kinetics of aptamers (Hg²⁺ and Pb²⁺) binding

The kinetics of Hg²⁺ and Pb²⁺ ions binding to specific aptamers were studied by recording the time dependencies of cathodic current (at -0.2V) of three-electrode assemblies with immobilized aptamers for different concentrations of both metals ions. Cathodic current was chosen because of smaller shift of the reduction peak upon binding Hg²⁺ ions. Typical time dependences for anti-Hg²⁺ aptamers are shown in Figure (7-8), for different concentrations of HgCl₂ salt varied from 0.01 ng/ml to 1 µg/ml. Then, the characteristic time constants (τ) were evaluated by fitting kinetics curves to rising exponential function. Following the Langmuir adsorption law, the reciprocal time constant ($1/\tau$) depends on the analyte adsorption and desorption rates (k_a and k_d) and the concentration (C) of analytes (in our case Hg²⁺ and Pb²⁺) as:

$$1/\tau = k_a C + k_d.$$

The values of k_a and k_d can be found, respectively, as the gradient and intercept from the linear dependence $1/\tau$ against C . Then both the association constant (K_A) and affinity constant (K_D) can be found as $K_A = k_a/k_d$ and $K_D = 1/K_A$ [6-8]. $1/\tau$ vs C dependence for Hg²⁺ ions was shown in Figure (7-8) as an inset. The values of k_a and k_d are calculated as: $k_a = 0.1471(\text{sec}^{-1}\cdot\text{ng}^{-1}\cdot\text{ml}) \times 271.52(\text{g}\cdot\text{mol}^{-1}) \times 10^3(\text{ml}\cdot\text{ng}^{-1}) \approx 3.94\cdot 10^4 (\text{sec}^{-1}\cdot\text{mol}^{-1})$ and $k_d = 0.0363 (\text{sec}^{-1})$, where 271.52 (g·mol⁻¹) is molecular weight of HgCl₂, and 10³ factor was used as conversion from ng/ml to µg/ml. Therefore $K_A = k_a/k_d = 1.1\cdot 10^6 (\text{mol}^{-1})$ and $K_D = 9.08\cdot 10^{-7}(\text{mol})$ for anti-Hg²⁺ aptamer. Similar values, e.g. $K_A = 1.2\cdot 10^6 (\text{mol}^{-1})$ and $K_D = 8.55\cdot 10^{-7}(\text{mol})$ were found for anti-Pb²⁺ aptamer. The obtained values correspond well to the aptamers affinity evaluated in the process of their synthesis [9, 10], and they are typical for highly specific binding of analytes to aptamers or antibodies. Similar analysis was carried out for binding kinetics of anti-Pb²⁺ aptamer, and quite similar values of $K_A = 1.2\cdot 10^6 (\text{mol}^{-1})$ and $K_D = 8.55\cdot 10^{-7}(\text{mol})$ were found. The obtained K_A and K_D values for both anti-Hg²⁺ and anti-Pb²⁺ aptamers correspond well to the aptamers affinity evaluated in the process of their synthesis [11, 12] and they are typical for highly specific binding reactions of analytes to aptamers or antibodies.

7.5 Discussion

The concept of electrochemical apta-sensor for heavy metal ions was proved, and the results obtained were encouraging. The selectivity and sensitivity of this apta-sensor to the heavy metals ions, e.g. Hg^{2+} and Pb^{2+} , is promising for development of novel, simple, and cost-effective electrochemical apta-sensors for rapid detection of heavy metals in water. A series of cyclic voltammogram and impedance spectroscopy measurements allowed the investigation of the mechanism of aptamer/heavy metal binding. The proposed model electrochemical apta-sensing based on changing the conformation of aptamer oligonucleotide chain from linear to the folded one, thus bringing the redox label closer to metal surface and increasing the electron charge transfer was proved. A simple detection of anodic (or cathodic) current at fixed voltage corresponding to oxidation (or reduction) peak potential is sufficient for detection of Hg^{2+} and Pb^{2+} in a wide range of concentrations down to 0.1 ng/ml (or 0.1 ppb). The detection of heavy metals in real water samples was attempted and was partially successful, however further work is required for developing methodology of real samples testing. The study of aptamer/target binding kinetics yielded the values for the association constant $K_A = 1.1 \cdot 10^{-6} (\text{mol}^{-1})$ and the affinity constant $K_D = 9.08 \cdot 10^{-7} (\text{mol})$ for aptamer/ Hg^{2+} binding; similar values of the association constant $K_A = 1.2 \cdot 10^{-6} (\text{mol}^{-1})$ and the affinity constant $K_D = 8.55 \cdot 10^{-7} (\text{mol})$ were found for aptamer/ Pb^{2+} binding. This study proved highly specific interaction between heavy metal ions and their specific aptamers. Further work could focus on development of the apta-sensor array for detection of other heavy metals (chromium, cadmium, arsenic, nickel, copper, silver, zinc, etc.) using simple DC electrochemical transducers. The different redox-labels can be used in future for simultaneous detection of different heavy metals and apply the possibility of using multiplexing aptamer arrays.

References

1. Y. Zhu, Y. Cai, Y. Zhu, L. Zheng, J. Ding, Y. Quan, B. Qi, Highly sensitive colorimetric sensor for Hg²⁺ detection based on cationic polymer/DNA interaction. *Biosensors and Bioelectronics*, 69, (2015) 174-178.
2. S. E. Wang, S. Si, Aptamer biosensing platform based on carbon nanotube long-range energy transfer for sensitive, selective and multicolor fluorescent heavy metal ion analysis. *Analytical Methods*, 5(12), (2013) 2947-2953.
3. L. Cui, J. Wu, H. Ju, Label-free signal-on aptasensor for sensitive electrochemical detection of arsenite. *Biosensors and Bioelectronics*, 79 (2016) 861-865.
4. A. Hayat, J. L. Marty, A. E. Radi, Novel Amperometric Hydrogen Peroxide Biosensor Based on Horseradish Peroxidase Azide Covalently Immobilized on Ethynyl-Modified Screen-Printed Carbon Electrode via Click Chemistry. *Electroanalysis*, 24(6) (2012) 1446-1452.
5. J. Macdonald, Ross. Impedance spectroscopy. *Annals of biomedical engineering*, 20(3) (1992) 289-305.
6. R. Karlsson, A. Michaelsson, L. Mattsson, Kinetic analysis of monoclonal antibody-antigen interactions with a new biosensor based analytical system. *Journal of immunological methods*, 145(1-2) (1991) 229-240.
7. Battaglioli, Gino, Hongcheng Liu, David L. Martin. Kinetic differences between the isoforms of glutamate decarboxylase: implications for the regulation of GABA synthesis. *Journal of neurochemistry* , 86(4) (2003) 879-887.
8. A. Nabok, A. Tsargorodskaya, M. K. Mustafa, I. Szekacs, N. F. Starodub, A. Szekacs. Detection of low molecular weight toxins using an optical phase method of ellipsometry. *Sensors and Actuators B: Chemical* , 154 (2) (2011) 232-237.
9. Y. Wang, Y. Zheng, F. Yang, X. Yang. Dual polarisation interferometry for real-time, label-free detection of interaction of mercury (II) with mercury-specific oligonucleotides. *Chemical Communications*, 48(23) (2012) 2873-2875.
10. H. N. Kim, W. X. Ren, J. S. Kim, J. Yoon. Fluorescent and colorimetric sensors for detection of lead, cadmium, and mercury ions. *Chemical Society Reviews*, 41(8) (2012) 3210-3244.
11. Wang, Y.; Zheng, Y.; Yang, F.; Yang, X. Dual polarisation interferometry for real-time, label-free detection of interaction of mercury (II) with mercury-specific oligonucleotides. *Chem. Comm* 2012,48, 2873-2875.
12. Kim, H. N.; Ren, W. X.; Kim, J. S.; Yoon, J. Fluorescent and colorimetric sensors for detection of lead, cadmium, and mercury ions. *Chem. Soci. Revi* 2012, 41, 3210-3244.

CHAPTER 8 Conclusion and future work

8.1 Thesis conclusion

The optical and electrochemical characteristics of both bacteria i.e. (bacteria in solution and immobilized bacteria) and the effect of toxic chemical pollutants i.e. heavy metal salts (HgCl_2 , PbCl_2 , ZnCl_2 and CdCl_2), pesticides (atrazine, simazine, DDVP), and petro-chemicals (hexane, octane, pentane, toluene, pyrene and ethanol) in water on all three bacteria types (*Escherichia coli*, *Methylococcus capsulatus* (Bath) or *Methylosinus trichosporium* (OB3b) and *Shewanella oneidensis*) and a possibility of exploiting the principles of pattern recognition for identification of these mentioned pollutants is the main goal of this thesis. This work concentrated on studying the effects of the above mentioned contaminants on living bacteria. The results were shown that many types of bacteria isolates have the ability to survive at high levels of environmental contamination. The types of bacteria strain that can resist above mentioned contaminants are in general classified as gram negative, a typical example of which is *S. oneidensis*, known for having the highest resistance to heavy metals and pesticides pollution. On the other hand, the highly sensitive types of bacteria, such as *E. coli*, are sensitive to the all of these pollutants. Also in this work Methanotrophic bacteria were used to study the effects of heavy metals, pesticides and petrochemical toxicity as bacteria in solution samples and immobilized bacteria. It was shown highly resistant to hydrocarbons and extremely sensitive to heavy metals and pesticides.

Characterisation of samples were carried out using a variety of experimental techniques, i.e. optical methods including optical density measurements, fluorescent microscopy and flow cytometry for studying light scattering in bacteria samples, also complementary methods such as SEM, AFM and electrochemical methods both DC and AC.

To study the effect of these pollutants, fluorescence microscopy measurements were carried out on samples of (*E. coli*, *Methylococcus capsulatus* (Bath) or *Methylosinus*

trichosporium (OB3b) and *S. oneidensis*) bacteria stained with two organic dyes: green and red, associated respectively with living and dead bacteria. The results showed a significant difference in images of bacteria before and after exposure to the pollutants. The numbers of live *E. coli* bacteria decreased exponentially with the increase in each pollutant concentration. On other hand, *S. oneidensis* which is a Gram-negative bacteria resisted the heavy metals at low concentration, and the concentration of live bacteria increase slightly. However, they were damaged at high concentration and the bacteria concentration gradually decreased. The method of fluorescence was illustrative, allowing direct observation of live and dead bacteria. However, this method did not provide correct bacteria counts because of the limited resolution of the analysis of microscopy images. An improved analysis was based on the calculation of total intensities of green and red fluorescence.

Optical density (OD₆₀₀) techniques have been used to estimate the bacteria cell's density as a function of exposure time and concentration of pollutants.

The same optical technique, namely fluorescence microscopy, was employed to study the effect of heavy metals, pesticides and petrochemical on immobilized bacteria. The effect of heavy metal salts (HgCl₂, PbCl₂, ZnCl₂ and CdCl₂), pesticides (atrazine, simazine, DDVP), and petro-chemicals (hexane, octane, pentane, toluene, pyrene and ethanol) appeared to be quite similar on bacteria in solution. Fluorescence microscopy seems to give the most reliable count of live bacteria concentrations. Therefore, the comparison of the inhibition effects of heavy metals, pesticides and petrochemical on (*E. coli*, *Methylococcus capsulatus* (Bath) or *Methylosinus trichosporium* (OB3b) and *S. oneidensis*) bacteria were carried out using true live and dead count of fluorescence microscopy. It showed clearly the possibility of pattern recognition of the three inhibition factors, e.g. heavy metals, pesticides and petrochemicals.

A simpler way of detecting pollutants was developed using the electrochemical properties of bacteria. The effect of heavy metals, pesticides and petrochemicals on electrochemical characteristics of microorganisms was studied.

The obtained data for DC and AC electrical study of three types of bacteria (*E. coli*, *Methylococcus capsulatus* (Bath) or *Methylosinus trichosporium* (OB3b) and *S. oneidensis*) correlated, as which did with the data of the optical study. The measurements of DC anodic and cathodic current were used for quantification of live bacteria concentrations, and thus the effect of heavy metals, pesticides and petrochemicals on bacteria. In addition, the AC characteristics, that included conductance and capacitance, were depicted as a function of pollutants exposure concentration. The AC capacitance increases when the bacteria concentration increases; in contrast AC conductance decreases. The capacitance and conductance were scanned for a wide range of frequencies; the big difference in the results of the three types of bacteria was very clearly related to the electrical properties change, which is related to the change in bacteria density or their concentration. The results at high frequency were very interesting, which encouraged us to utilize it to evaluate pollution levels.

The electrochemical technique was engaged to study the effect of heavy metals heavy metal salts (HgCl_2 , PbCl_2 , ZnCl_2 and CdCl_2), pesticides (atrazine, simazine, DDVP), and petro-chemicals (hexane, octane, pentane, toluene, pyrene and ethanol) on bacteria in solution and immobilized bacteria. The effect of above mentioned pollutants appeared to be comparable on (*E. coli*, *Methylococcus capsulatus* (Bath) or *Methylosinus trichosporium* (OB3b) and *S. oneidensis*) bacteria. AC and DC properties of electrochemical solutions that contained (*E. coli*, *Methylococcus capsulatus* (Bath) or *Methylosinus trichosporium* (OB3b) and *S. oneidensis*) bacteria were studied and the results were compared to immobilized bacteria and normalized to the results of samples not mixed with pollutants. Comparative results can be used to estimate pollutant concentration and the effect of each toxicant on bacteria.

Moreover, the difference in the responses of (*E. coli*, *Methylococcus capsulatus* (Bath) or *Methylosinus trichosporium* (OB3b) and *S. oneidensis*) bacteria to heavy metal salts (HgCl_2 , PbCl_2 , ZnCl_2 and CdCl_2), pesticides (atrazine, simazine, DDVP), and petro-chemicals

(hexane, octane, pentane, toluene, pyrene and ethanol) allows the application of the principle of pattern recognition for identification and quantification of pollutants. This work has proved the concept of a simple and cost effective electrical bacteria-based sensor and sensor array for preliminary assessment of the presence of toxins in water. This part of work has been achieved, through calculated and plot the pattern recognition of (live and dead) count for (*E. coli*, *Methylococcus capsulatus* (Bath) or *Methylosinus trichosporium* (OB3b) and *S. oneidensis*) bacteria, in addition the anodic and cathodic current subtract and AC conductance subtract, all of these calculations were done for heavy metal salts (HgCl_2 , PbCl_2 , ZnCl_2 and CdCl_2), pesticides (atrazine, simazine, DDVP), and petro-chemicals (hexane, octane, pentane, toluene, pyrene and ethanol) effect. Meanwhile, the electrical equivalent circuit of the bacteria cell sensor was estimated. The simplest idea for this circuit consists of surface resistance in parallel with surface capacitance, both in series with block resistance. The capacitance and conductance of equivalent circuits were calculated at low frequency (~ 0) and at high frequency ($\sim \infty$). For some tests, the theoretical results showed a clear identification with practical results. This identification in results confirms the validity of results obtained, whether practical or theoretical.

Also, this work involved development of an electrochemical biosensor for highly selective, and rapid detection of Hg^{2+} and Pb^{2+} ions using DNA-based specific aptamer probes labeled with ferrocene (or methylene blue) and thiol groups at their 5' and 3' termini, respectively. The concept of electrochemical apta-sensor for heavy metal ions was proved, and the results obtained were encouraging. The selectivity and sensitivity of this apta-sensor to heavy metals ions, e.g. Hg^{2+} and Pb^{2+} , is high and thus promising for development of novel, simple, and cost-effective electrochemical apta-sensors for rapid detection of heavy metals in water.

Aptamers were immobilized onto the surface of screen-printed gold electrodes via the SH groups, and then cyclic voltammetry and impedance spectra measurements were performed in buffer solutions with the addition of the HgCl_2 and PbCl_2 salts at different

concentrations. Changes in 3D conformation of aptamers caused by binding their respective targets, e.g. Hg^{2+} and Pb^{2+} ions, are accompanied by the increase in the electron-transfer between the redox label and the electrode, and thus the presence of the above ions can be detected electrochemically. The detection of Hg^{2+} and Pb^{2+} ions in a wide range of concentrations down to 0.1 ng/ml (or 0.1 ppb) was achieved. The study of the kinetics of aptamer/heavy metal ions binding gave the values of the affinity constants of around $9 \cdot 10^{-7}$ mol, which proved high specificity of the aptamers used.

Finally, the analysis of a large amount of experimental data was carried out using artificial neural network (ANN) programme for more accurate identification of pollutants as well as the estimation of their concentration. The results are encouraging for the development of a simple and cost-effective bio-sensing technology for preliminary in-field analysis (screening) of water samples for the presence of environmental pollutants. The use of ANN software for data processing allowed the more accurate identification of water pollutants, e.g. heavy metals, pesticides, and hydrocarbons as well as the estimation of their concentration in the range from 0.1 μM to 1mM.

8.2 Suggestion for future work

Since the current project was focused mostly on fundamental research aspects of environmental pollution detection, particularly on establishing novel detection principles using different types of bio-receptors, e.g. microorganisms (bacteria) and aptamers, further R&D work is required for development of sensor devices.

In terms of fundamental research, it will be of great interest to study in more detail the effect pollutants on bacteria cell membrane and cellular components using different methods, for instance confocal microscopy and AFM.

Further work is required in the development of bacteria sensor array devices which includes both the expansion of the array by adding new types of bacteria and widening

the range of analytes, particularly in pesticides and petro-chemicals. Detection of BETX and polycyclic aromatic hydrocarbons are of particular interest these days. Radioactive pollutants, such as depleted uranium, can also be included in the list of analytes; in that case *Deinococcus radiodurans* bacteria could be added to the sensor array.

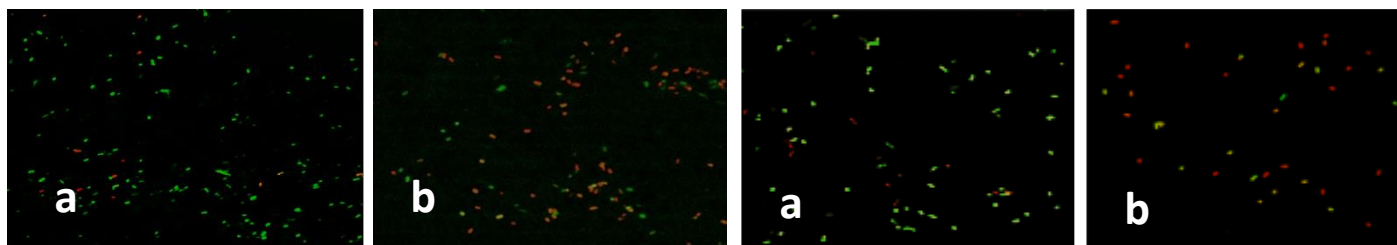
The improvement of the ANN data processing is also required mainly for more precise evaluation of pollutants' concentration. This could be achieved using two-stage ANN processing: identification of pollutants with the general ANN, and the evaluation of pollutants' concentration using several dedicated ANN for each pollutant. This work is currently underway.

So far, the *in-vitro* detection of pollutants was carried out in this project. In future the focus should be on pollutants detection in real samples of water using the developed bacteria sensor array. Complementary analytical techniques, such as Chromatography or Inductively Coupled Plasma Mass Spectrometry (ICP-MS) can be used to verify the results obtained with bacteria-sensor array. This work is also underway.

The use of aptamers for detection of environmental pollutants has great potential. An aptamer sensor array containing several channels which specifically detect particular analytes could be a very interesting future project. An alternative (to sensor array) approach could involve a range of aptamers for different pollutants having different labels. In that way, the sensor responses could be multiplexed in one sensor chip.

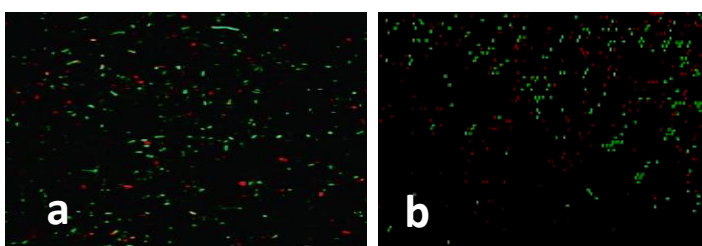
Another important problem to address is the remediation of environmental pollutants, which could be done with the use of suitable genetically modified bacteria. In future, the detection and remediation of pollutants could be combined together in one piece of equipment.

Appendix-A1: Fig. 1. Fluorescence microscopy images of different bacterial samples before (a) and after (b) treated with simazine in 1 M for 2 hours.



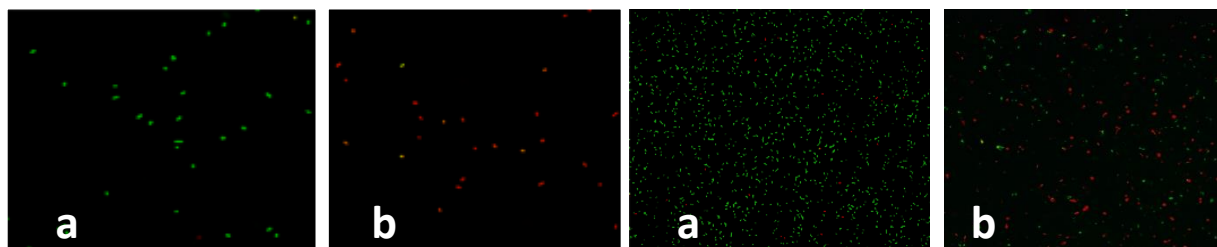
E.coli with simazine in 1M
a= before treatment, b= after treatment

M.capsulatus with simazine in 1M
a= before treatment, b= after treatment



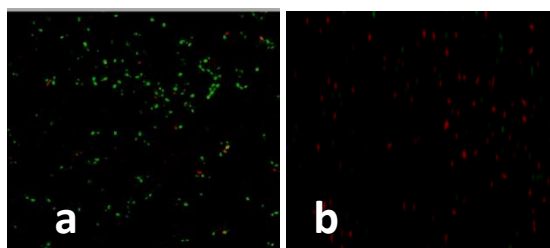
S.oneidensis with simazine in 1M
a= before treatment, b= after treatment

Appendix-A2: Fig. 2. Fluorescence microscopy images of different bacterial samples before (a) and after (b) treated with octane in 1M for 2 hours.



E.coli with octane in 1M
a= before treatment, b= after treatment

M. trichosporium with octane in 1M
a= before treatment, b= after treatment



S.oneidensis with octane in 1M
A= before treatment, B= after treatment

Appendix-A3: Figures (1-12) showed the cyclic voltammograms of different bacterial samples (bacteria suspension and immobilized bacteria after treated with different types of pollutants).

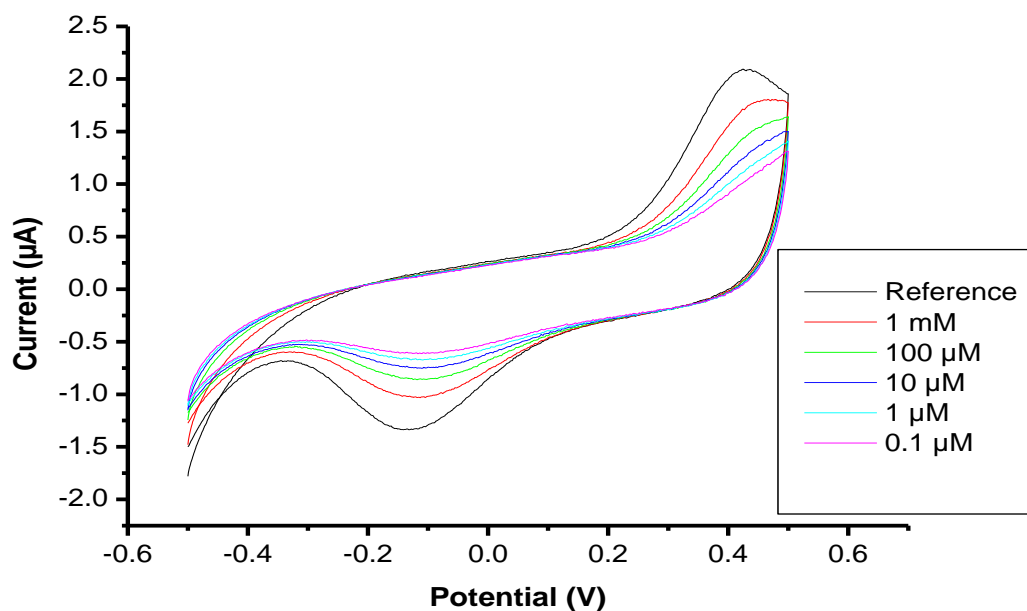


Fig.1: *E.coli* suspension with simazine in different concentrations.

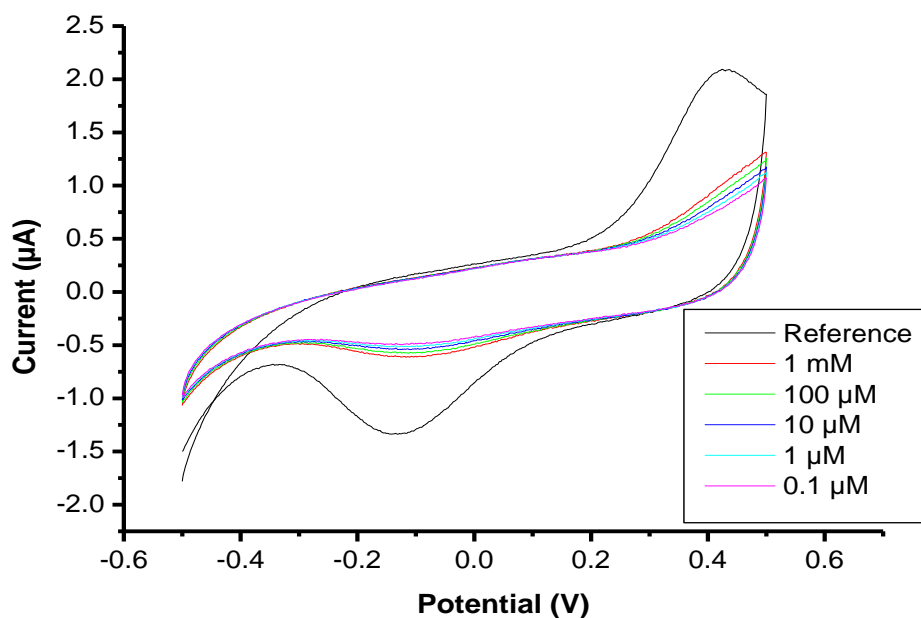


Fig.2: *M. capsulatus* suspension with octane in different concentrations.

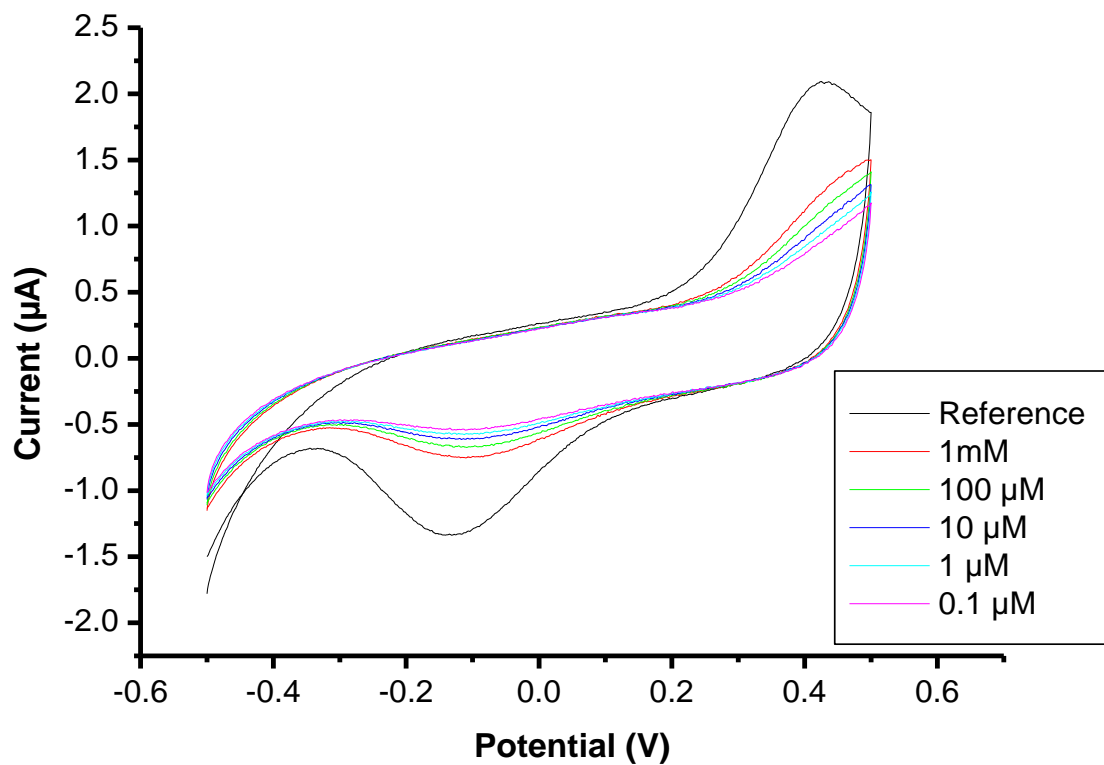


Fig.3: *S.oneidensis* suspension with toluene in different concentration.

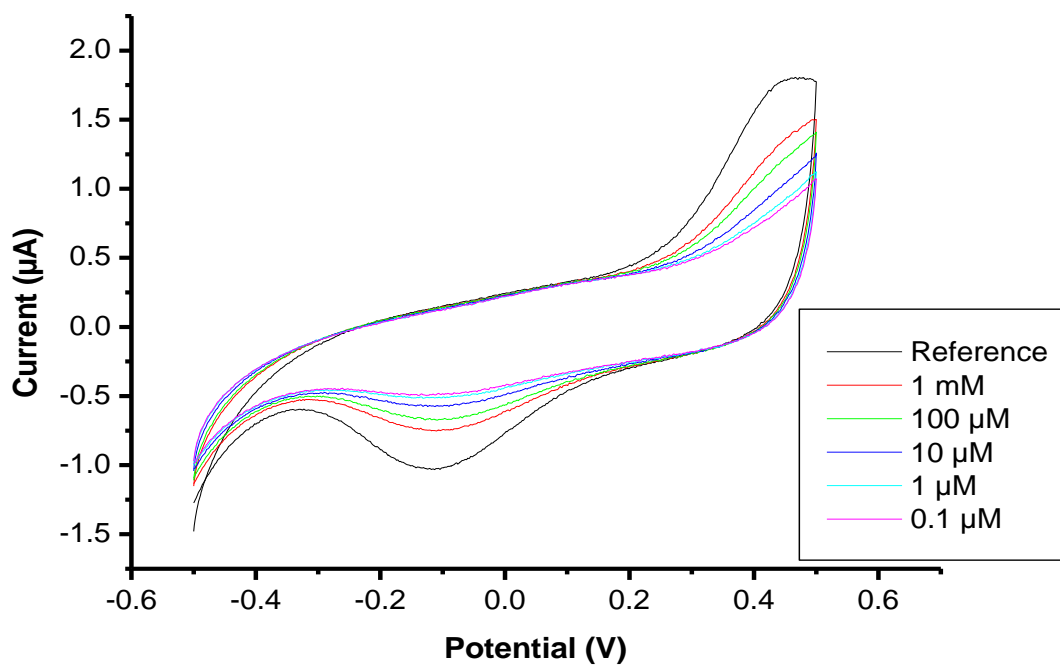


Fig.4: *M. trichosporum* suspension with $HgCl_2$ in different concentration.

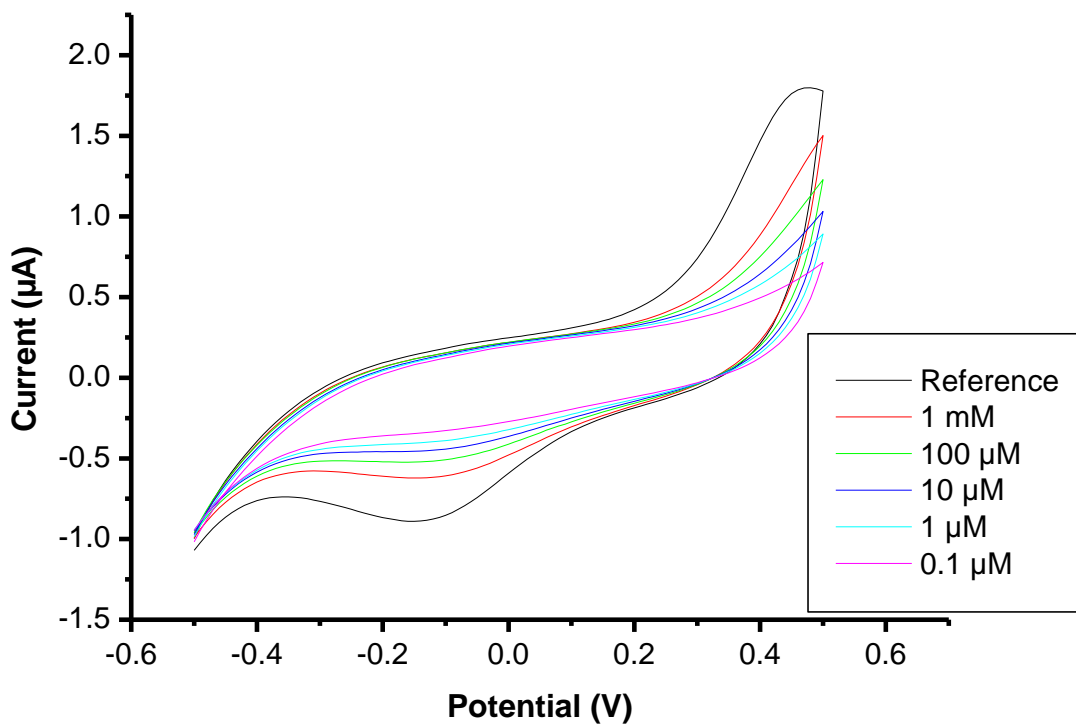


Fig.5: *E.coli* suspension with hexane in different concentrations.

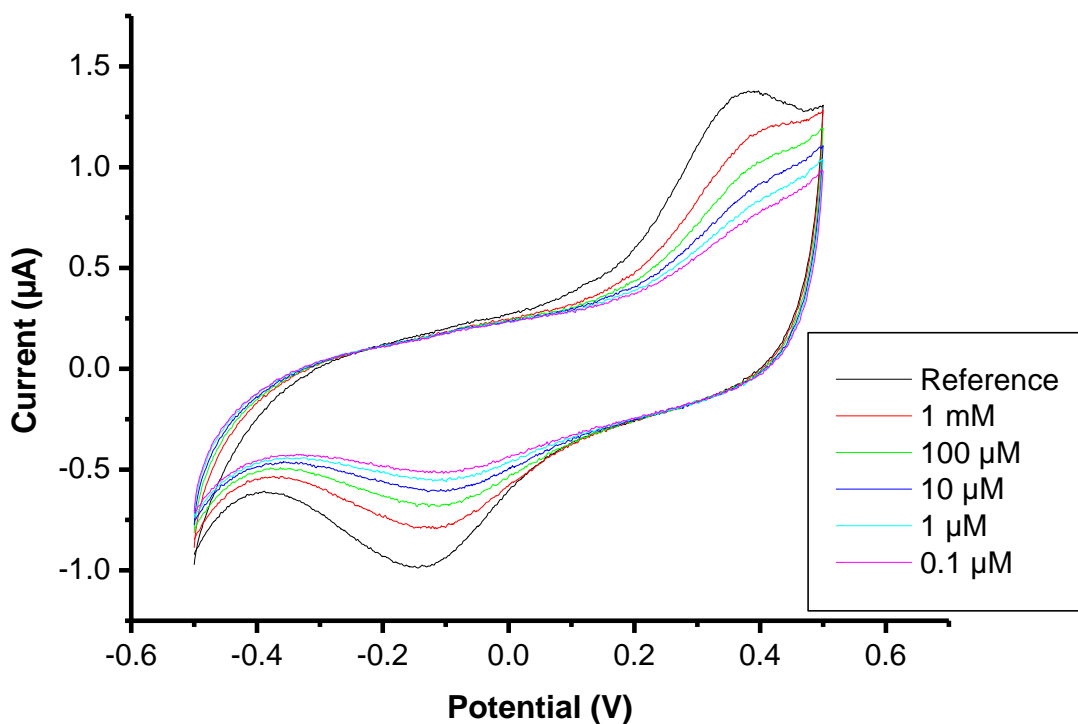


Fig.6: DDVP with immobilized *E.coli* in different concentration.

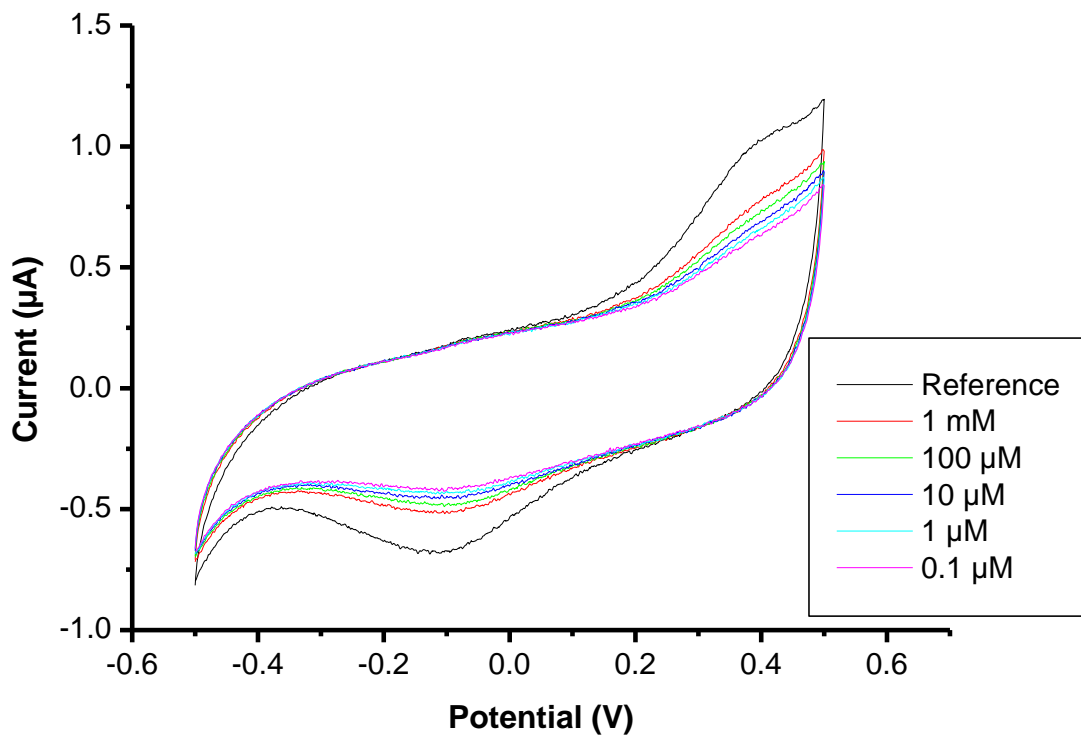


Fig.7: immobilized *M.trichomonus* with hexane in different concentrations.

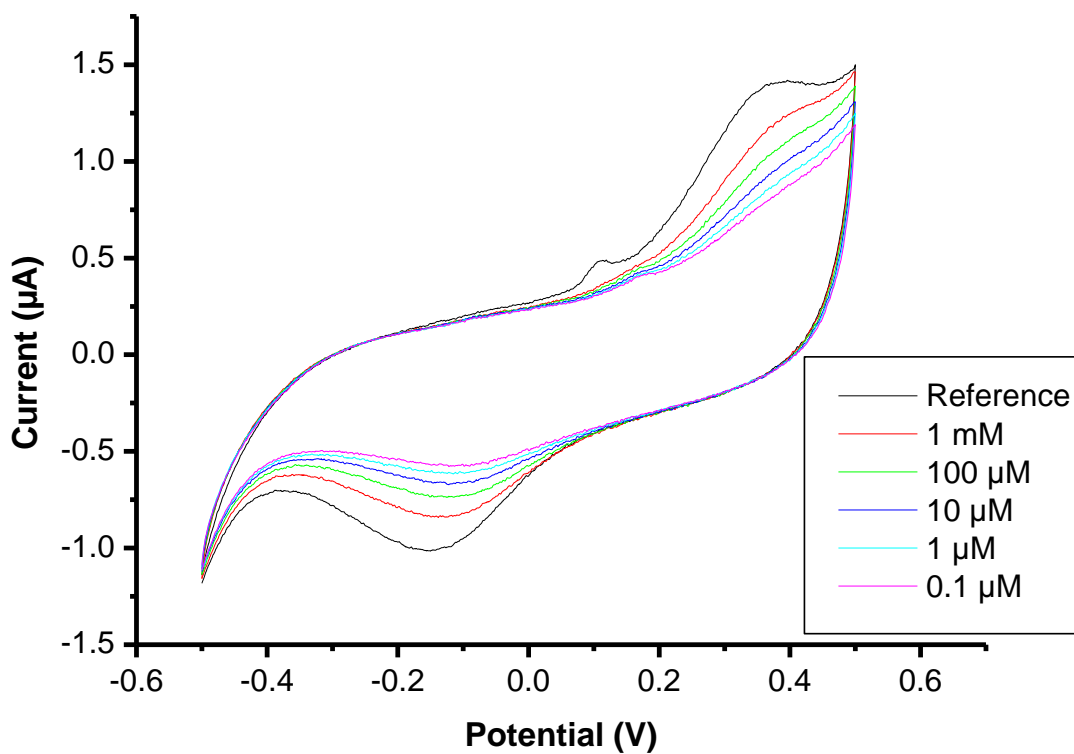


Fig.8: immobilized *E.coli* with Cd^{+2} in different concentrations.

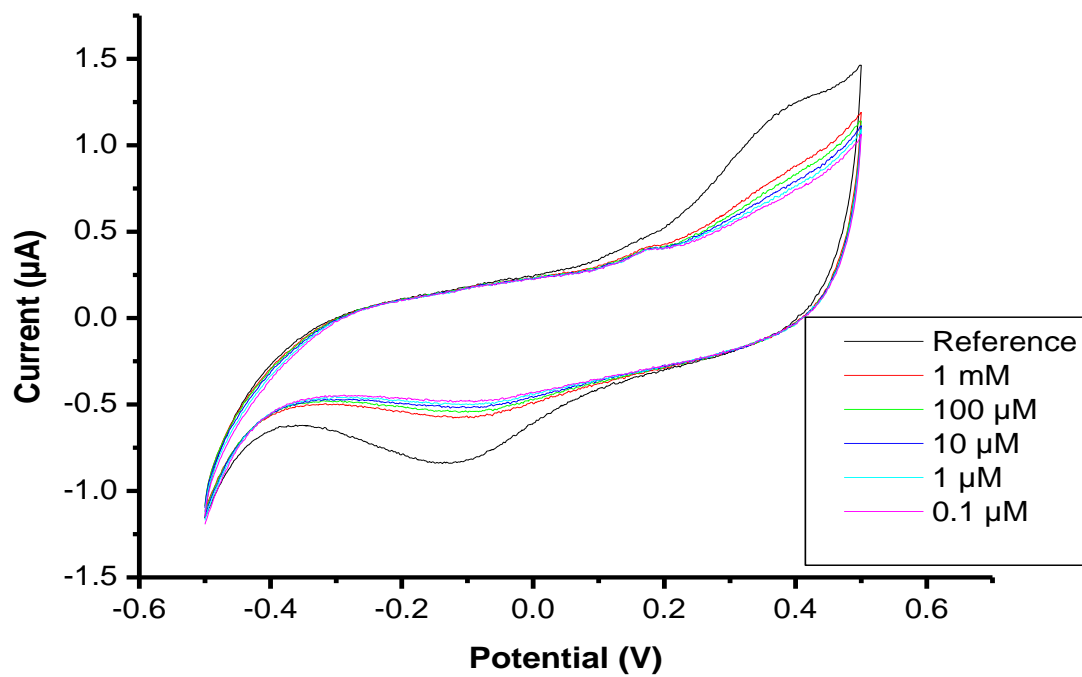


Fig.9: immobilized *S. oneidensis* with Cd^{2+} in different concentrations.

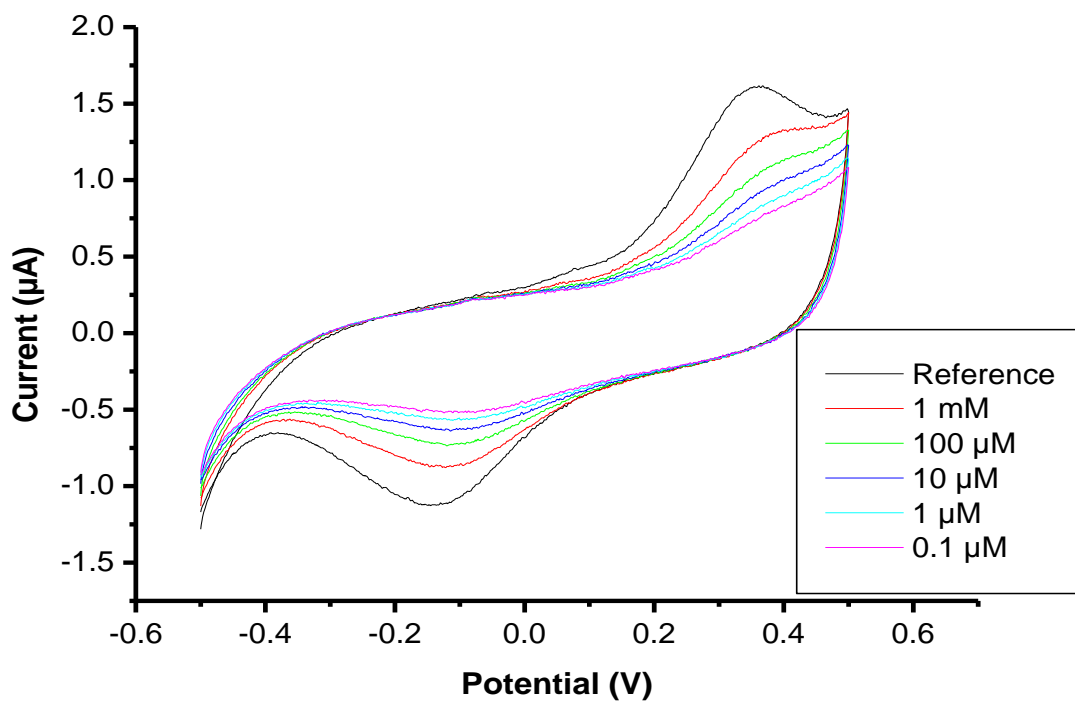


Fig10: immobilized *M. capsulatus* with Cd^{2+} in different concentrations.

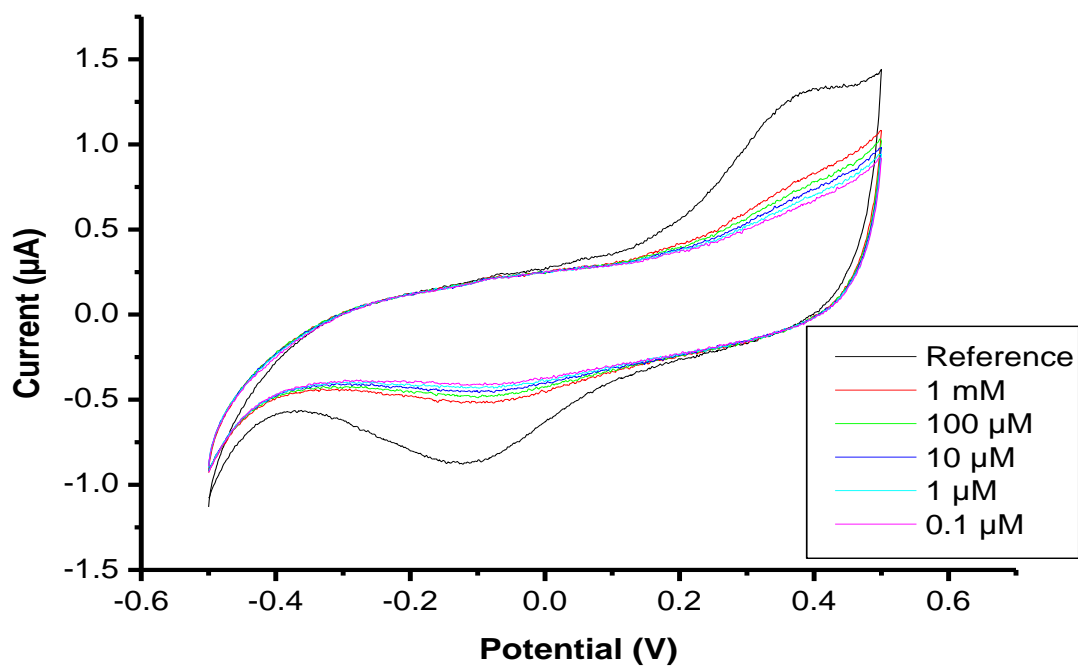


Fig.11: immobilized *S.oneidensis* with Zn⁺² in different concentrations.

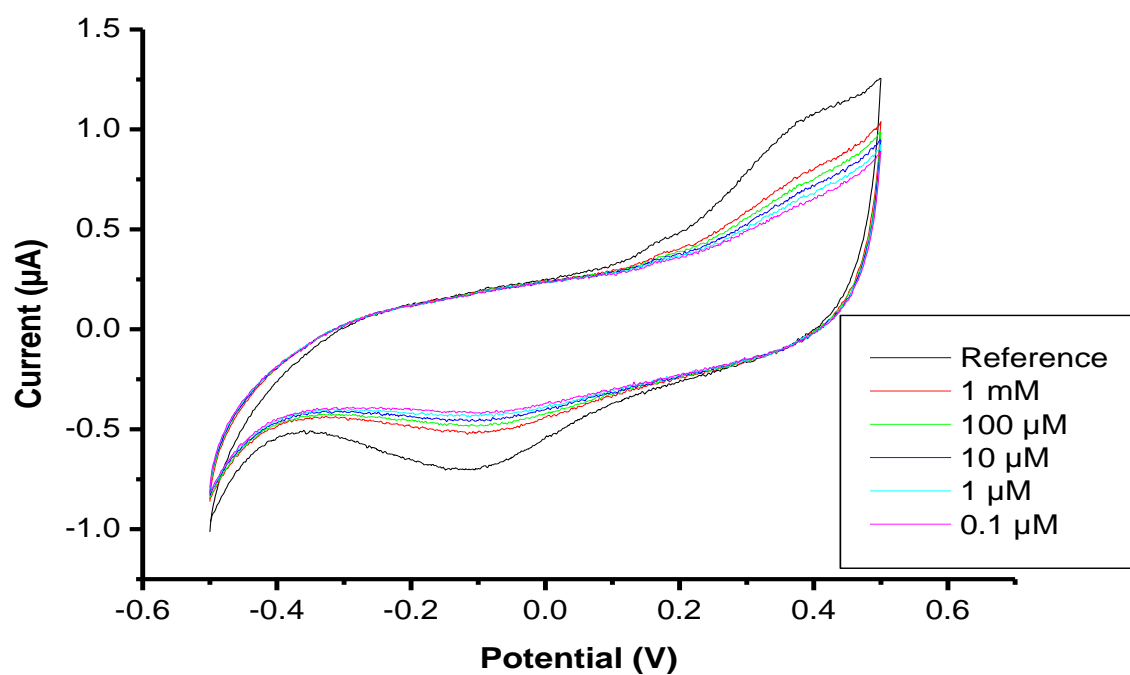


Fig.12: immobilized *S.oneidensis* with Pb⁺² in different concentrations.

Appendix -A4: Figures (1,2) showed the EIS of different of immobilized bacteria after treated with different types of pollutants. While Figure 3 for aptamer biniding Pb^{+2} .

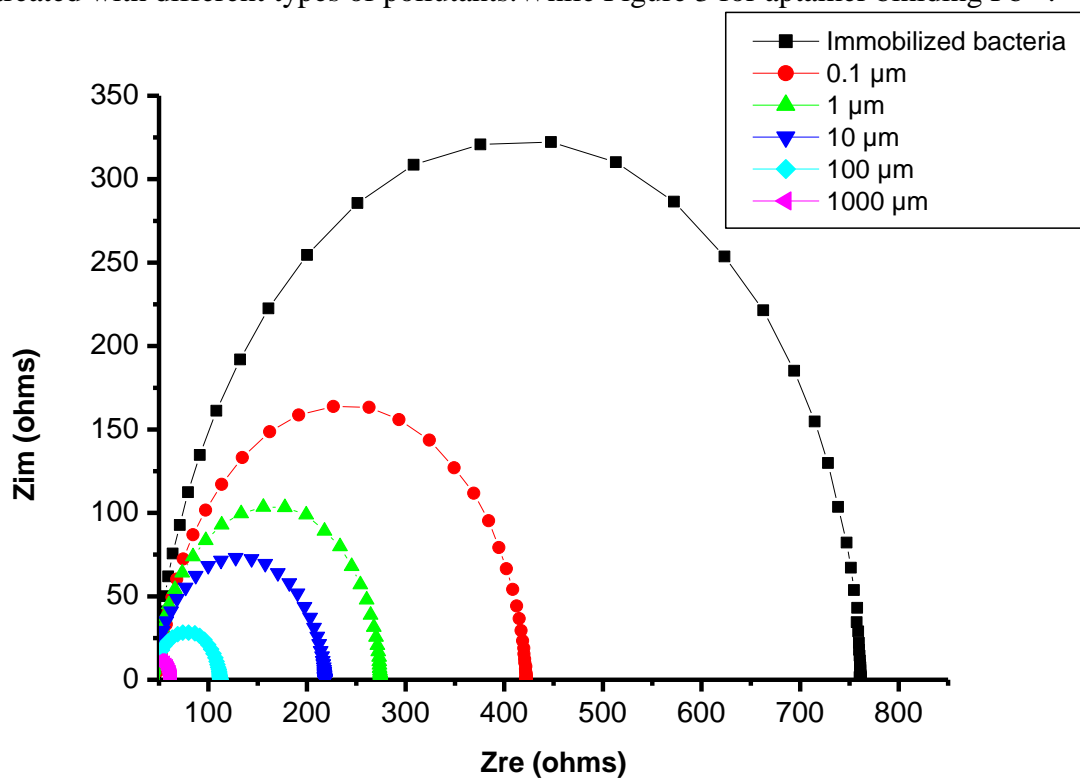


Fig. 1. The Nyquist plots (-Zim vs Zre) for interdigitated electrodes with immobilized *M.capsulatus* with DDVP in different concentrations.

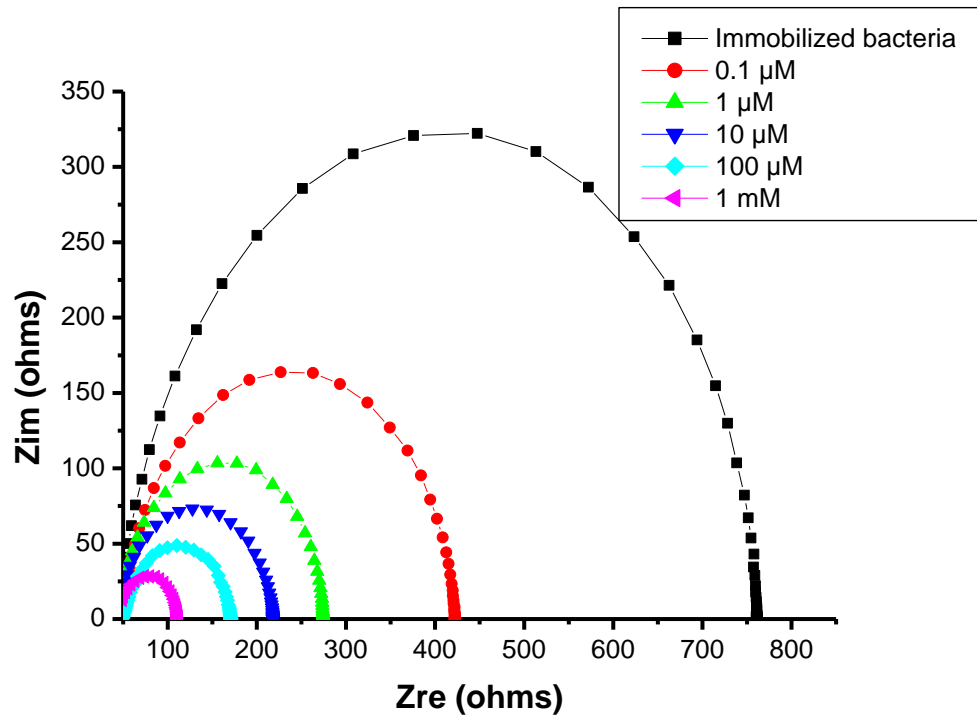


Fig. 2. The Nyquist plots ($-Z_{im}$ vs Z_{re}) for interdigitated electrodes with immobilized *S. oneidensis* with Pb^{2+} in different concentrations.

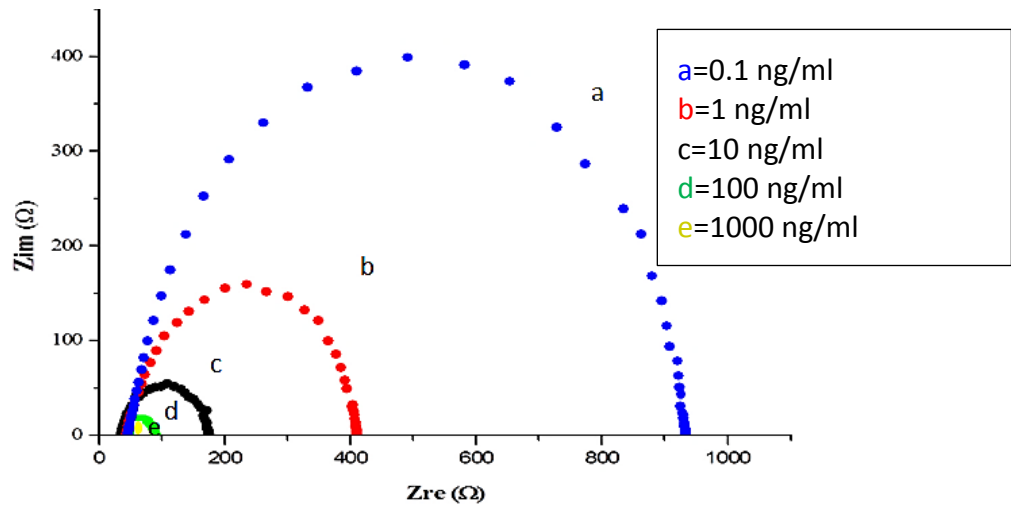
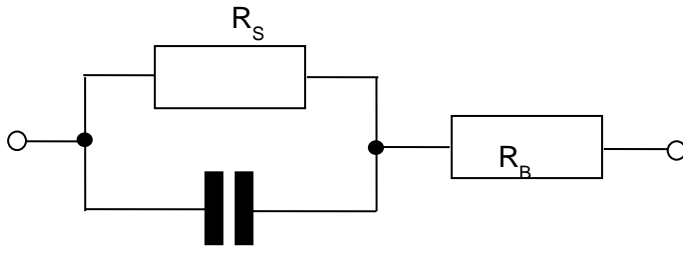


Fig. 3. The Nyquist plots ($-Z_{im}$ vs Z_{re}) for interdigitated electrodes with immobilized anti- Pb^{2+} aptamers binding Pb^{2+} ions of different concentrations.

Appendix -B Analysis of impedance spectroscopy measurements of bacteria samples

The data of impedance spectroscopy can be fitted into the following equivalent circuit:



Where R_S and C_S are associated, respectively, with the resistor and capacitance of bacteria layer adsorbed on the surface of metal electrodes, while R_B is the bulk resistance of bacteria sample.

$$\frac{1}{Z_S} = \frac{1}{R_S} + \frac{1}{-j \frac{1}{\omega C_S}} = \frac{1}{R_S} - j\omega C_S = \frac{1 + j\omega R_S C_S}{R_S};$$

$$Z_S = \frac{R_S}{1 + j\omega R_S C_S} = \frac{R_S - j\omega R_S C_S}{1 + \omega^2 R_S^2 C_S^2}; \quad Z = Z_S + R_B = \frac{R_S - j\omega R_S C_S}{1 + \omega^2 R_S^2 C_S^2} + R_B$$

after separating real and imaginary parts $Z = Z' + jZ''$

$$Z' = \frac{R_S}{1 + \omega^2 R_S^2 C_S^2} + R_B = \frac{R_S + R_B + \omega^2 R_B R_S^2 C_S^2}{1 + \omega^2 R_S^2 C_S^2}; \quad Z'' = -\frac{\omega R_S C_S}{1 + \omega^2 R_S^2 C_S^2}.$$

if $\omega = 0$, $Z' = R_S + R_B$; $Z'' = 0$.

if $\omega = \infty$, $Z' = R_B$; $Z'' = \frac{\omega R_S C_S}{\omega^2 R_S^2 C_S^2} = \frac{1}{\omega} = 0$.

at Z'' is maximal when $\frac{dZ''}{d\omega} = 0$

This gives $\omega^2 R_S^2 C_S^2 = 1$, therefore $C_S = \frac{1}{\omega_{\max} R_S} = \frac{1}{2\pi f_{\max} R_S}$;

Another representation of Z is $Z = \sqrt{(Z')^2 + (Z'')^2}$; $\tan\theta = \frac{Z''}{Z'}$.

$$Z = \frac{\sqrt{(R_S + R_B + \omega^2 R_B R_S^2 C_S^2)^2 + \omega^4 R_S^2 C_S^2}}{1 + \omega^2 R_S^2 C_S^2}; \quad \tan\theta = -\frac{\omega R_S C_S}{R_S + R_B(1 + \omega^2 R_S^2 C_S^2)}.$$

if $\omega = 0$, $Z = R_S + R_B$; $\tan\theta = 0$.

if $\omega = \infty$, $Z = \sqrt{R_B + 1} \approx R_B$; $\tan\theta = \frac{\omega R_S C_S}{\omega^2 R_B R_S^2 C_S^2} = \frac{1}{\omega R_B} = 0$.

Z can be also presented as a series connection of R and C: $Z = R - \frac{j}{\omega C}$.

$$\text{where } R = \frac{R_S}{1 + \omega^2 R_S^2 C_S^2} + R_B = \frac{R_S + R_B + \omega^2 R_B R_S^2 C_S^2}{1 + \omega^2 R_S^2 C_S^2};$$

and $\frac{1}{\omega C} = \frac{\omega R_S C_S}{1 + \omega^2 R_S^2 C_S^2}$; $\omega C = \frac{1 + \omega^2 R_S^2 C_S^2}{\omega R_S C_S}$; so that $C = \frac{1 + \omega^2 R_S^2 C_S^2}{\omega^2 R_S C_S}$.

if $\omega = 0$, $R = R_S + R_B$; $C = \infty$.

if $\omega = \infty$, $R = R_B$; $C = R_S C_S$.

Appendix C

Matlab code for ANN analysis of data of bacteria sensor array

The following code below has written and executed by using MATLAB.

```
targets=[0 0 0 0 0 1
          0 0 0 0 1 0
          0 0 0 0 1 1
          0 0 0 1 0 0
          0 0 0 1 0 1
          0 0 0 1 1 0
          0 0 0 1 1 1
          0 0 1 0 0 0
          0 0 1 0 0 1
          0 0 1 0 1 0
          0 0 1 0 1 1
          0 0 1 1 0 0
          0 0 1 1 0 1
          0 0 1 1 1 0
          0 0 1 1 1 1
          0 1 0 0 0 0
          0 1 0 0 0 1
          0 1 0 0 1 0
          0 1 0 0 1 1
          0 1 0 1 0 0
          0 1 0 1 0 1
          0 1 0 1 1 0
          0 1 0 1 1 1
          0 1 1 0 0 0
          0 1 1 0 0 1
          0 1 1 0 1 0
          0 1 1 0 1 1
          0 1 1 1 0 0
          0 1 1 1 0 1
          0 1 1 1 1 0
          0 1 1 1 1 1
          1 0 0 0 0 0
          1 0 0 0 0 1
          1 0 0 0 1 0
          1 0 0 0 1 1
          1 0 0 1 0 0]';
% create a feedforward network
net = feedforwardnet();

net.layers{1}.size = 60; % number of nodes in hidden layer
net.layers{2}.size = 6; % number of nodes in output layer

% initialize the network weights and biases
net = init(net);
```

```

% traingdm has momentum and train faster
net.trainFcn = 'traingdm';
% net.trainFcn = 'traingd';

%There are seven training parameters associated with traingd: epochs,
show,
%goal, time, min_grad, max_fail, and lr.

%net.trainParam.show = 10;           %show after specified iteration
net.trainParam.lr = 0.02;           % learning rate
%net.trainParam.mc = 0.05;           %momentum
net.trainParam.epochs = 250000;     %training iteration
%net.trainParam.goal = 1e-10;       %stopping goal

net.divideParam.trainRatio = 1; % training set [%]
net.divideParam.valRatio = 0; % validation set [%]
net.divideParam.testRatio = 0; % test set [%]

net.layers{1}.transferFcn = 'tansig';
net.layers{2}.transferFcn = 'tansig';

% Train
net = train(net,d,targets);
view(net);

a = sim(net,d);
a=a';
a=(a)

```